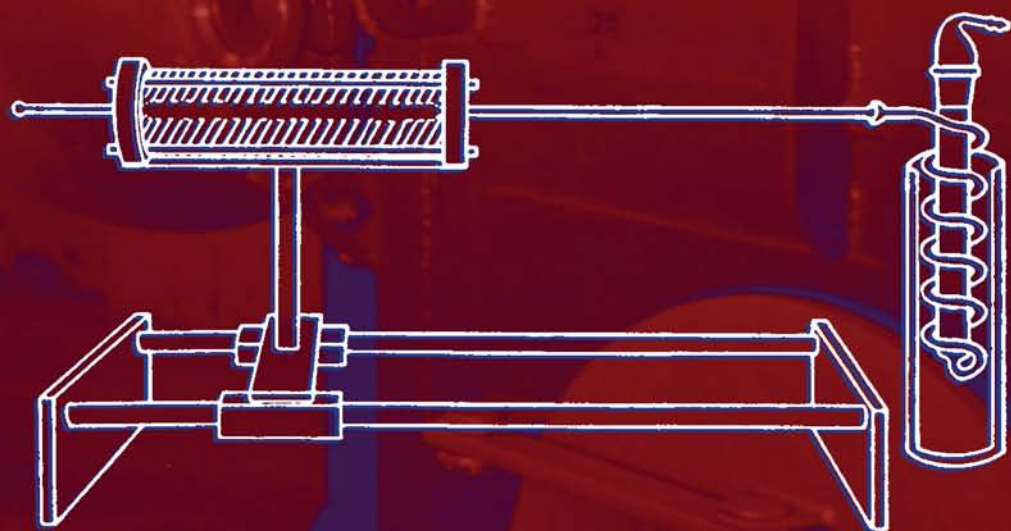


Applied Pyrolysis Handbook

SECOND EDITION



EDITED BY
THOMAS P. WAMPLER



CRC Press
Taylor & Francis Group

Applied Pyrolysis Handbook

SECOND EDITION

Applied Pyrolysis Handbook

SECOND EDITION

EDITED BY
THOMAS P. WAMPLER



CRC Press

Taylor & Francis Group

Boca Raton London New York

CRC Press is an imprint of the
Taylor & Francis Group, an informa business

CRC Press
Taylor & Francis Group
6000 Broken Sound Parkway NW, Suite 300
Boca Raton, FL 33487-2742

© 2007 by Taylor & Francis Group, LLC
CRC Press is an imprint of Taylor & Francis Group, an Informa business

No claim to original U.S. Government works
Printed in the United States of America on acid-free paper
10 9 8 7 6 5 4 3 2 1

International Standard Book Number-10: 1-57444-641-X (Hardcover)
International Standard Book Number-13: 978-1-57444-641-8 (Hardcover)

This book contains information obtained from authentic and highly regarded sources. Reprinted material is quoted with permission, and sources are indicated. A wide variety of references are listed. Reasonable efforts have been made to publish reliable data and information, but the author and the publisher cannot assume responsibility for the validity of all materials or for the consequences of their use.

No part of this book may be reprinted, reproduced, transmitted, or utilized in any form by any electronic, mechanical, or other means, now known or hereafter invented, including photocopying, microfilming, and recording, or in any information storage or retrieval system, without written permission from the publishers.

For permission to photocopy or use material electronically from this work, please access www.copyright.com (<http://www.copyright.com/>) or contact the Copyright Clearance Center, Inc. (CCC) 222 Rosewood Drive, Danvers, MA 01923, 978-750-8400. CCC is a not-for-profit organization that provides licenses and registration for a variety of users. For organizations that have been granted a photocopy license by the CCC, a separate system of payment has been arranged.

Trademark Notice: Product or corporate names may be trademarks or registered trademarks, and are used only for identification and explanation without intent to infringe.

Library of Congress Cataloging-in-Publication Data

Applied Pyrolysis handbook / edited by Thomas Wampler. -- 2nd ed.
p. cm.
Includes bibliographical references and index.
ISBN-13: 978-1-57444-641-8 (alk. paper)
ISBN-10: 1-57444-641-X (alk. paper)
1. Pyrolysis--Handbooks, manuals, etc. I. Wampler, Thomas P., 1948- II. Title.

TP156.P9A67 2006
543--dc22

2006023252

Visit the Taylor & Francis Web site at
<http://www.taylorandfrancis.com>
and the CRC Press Web site at
<http://www.crcpress.com>

Preface to the Second Edition

Analytical pyrolysis is the study of molecules by applying enough thermal energy to cause bond cleavage, and then analyzing the resulting fragments by gas chromatography, mass spectrometry, or infrared spectroscopy. Pyrolysis has been employed for the analysis of organic molecules for most of this century. It was initially connected with investigations of vapor-phase hydrocarbons and later became a routine technique for analyzing fuel sources and natural and synthetic polymers. Current applications include analysis of trace evidence samples in forensic laboratories, evaluation of new composite formulations, authentication and conservation of artworks, identification of microorganisms, and the study of complex biological and ecological systems. In the time since the first edition of this book, several significant changes have occurred in the field of analytical pyrolysis. First, the introduction of autosamplers for Py-gas chromatography-mass spectrometry (GC/MS) has made the technique more routine, more reproducible, and more acceptable for the analysis of complex solids. Second, the widespread availability of mass spectrometers as detectors for Py-GC has led to a better understanding of the degradation products and the processes that create them. Third, as mass spectrometry detectors have become more sensitive, the application of analytical pyrolysis to trace-level determinations has become routine, so that analysts may not only look at the matrix composition, but also investigate additives such as plasticizers, antioxidants, and stabilizers.

This book is intended to be a practical guide to the application of pyrolysis techniques to various samples and sample types. To that end, general and theoretical considerations, including instrumentation and degradation mechanisms, have been consolidated in the first two chapters. The balance of the book describes the use of pyrolysis as a tool in specific fields. Synthetic polymers, forensic materials, and other samples with a long history of analysis by pyrolysis are covered. In addition, we have been pleased to see some new areas of study, such as the analysis of surfactants, antiquities, and environmental materials, and these topics are presented as well.

The chapters examine the scope of work based on pyrolysis in particular fields of analysis and give specific examples of methods currently used for the examination of representative samples. This book is intended to serve as a starting point for analysts who are adding pyrolysis to their array of analytical techniques by providing concrete examples and suggesting additional reading.

I thank all of the authors for their contributions. With only a few exceptions, the authors of the chapters in the first edition agreed to update the chapters they wrote, adding recent examples and references. Each is actively involved in scientific pursuits, and the time that they have taken away from their busy schedules to contribute to this project was valuable and greatly appreciated.

Thomas P. Wampler

The Editor

Thomas P. Wampler has been actively engaged in the field of analytical pyrolysis for 25 years. He is director of science and technology at CDS Analytical, Inc., in Oxford, Pennsylvania. He is the author or coauthor of numerous professional papers on the use of analytical pyrolysis and other thermal sampling techniques. He received a B.S. degree (1970) in chemistry and a M.Ed. degree (1973) in natural science from the University of Delaware, Newark.

Contributors

Norbert S. Baer

Conservation Center
New York University
New York, New York

John M. Challinor

Chemistry Centre (WA)
East Perth, Western Australia

Randolph C. Galipo

University of South Carolina
Columbia, South Carolina

Karen Jansson

CDS Analytical, Inc.
Oxford, Pennsylvania

C.J. Maddock

Horizon Instruments Ltd.
Heathfield, East Sussex, England

Stephen L. Morgan

University of South Carolina
Columbia, South Carolina

T.O. Munson

Department of Math/Science
Concordia University
Portland, Oregon

Hajime Ohtani

Nagoya Institute of Technology
Nagoya, Japan

T.W. Ottley

Horizon Instruments Ltd.
Heathfield, East Sussex, England

Alexander Shedrinsky

Chemistry and Biochemistry
Department
Long Island University
Brooklyn, New York

Shin Tsuge

Nagoya University
Nagoya, Japan

Thomas P. Wampler

CDS Analytical, Inc.
Oxford, Pennsylvania

Bruce E. Watt

University of South Carolina
Columbia, South Carolina

Charles Zawodny

CDS Analytical, Inc.
Oxford, Pennsylvania

Contents

Chapter 1	Analytical Pyrolysis: An Overview	1
------------------	---	---

Thomas P. Wampler

Chapter 2	Instrumentation and Analysis.....	27
------------------	-----------------------------------	----

Thomas P. Wampler

Chapter 3	Pyrolysis Mass Spectrometry: Instrumentation, Techniques, and Applications	47
------------------	---	----

C.J. Maddock and T.W. Ottley

Chapter 4	Microstructure of Polyolefins	65
------------------	-------------------------------------	----

Shin Tsuge and Hajime Ohtani

Chapter 5	Degradation Mechanisms of Condensation Polymers: Polyesters and Polyamides	81
------------------	---	----

Hajime Ohtani and Shin Tsuge

Chapter 6	The Application of Analytical Pyrolysis to the Study of Cultural Materials.....	105
------------------	--	-----

Alexander Shedrinsky and Norbert S. Baer

Chapter 7	Environmental Applications of Pyrolysis	133
------------------	---	-----

T.O. Munson

Chapter 8	Examination of Forensic Evidence	175
------------------	--	-----

John M. Challinor

Chapter 9	Characterization of Microorganisms by Pyrolysis-GC, Pyrolysis-GC/MS, and Pyrolysis-MS	201
------------------	--	-----

Stephen L. Morgan, Bruce E. Watt, and Randolph C. Galipo

Chapter 10 Analytical Pyrolysis of Polar Macromolecules	233
<i>Charles Zawodny and Karen Jansson</i>	
Chapter 11 Characterization of Condensation Polymers by Pyrolysis-GC in the Presence of Organic Alkali	249
<i>Hajime Ohtani and Shin Tsuge</i>	
Chapter 12 Index of Sample Pyrograms	271
<i>Thomas P. Wampler</i>	
Index	285

1 Analytical Pyrolysis: An Overview

Thomas P. Wampler

CONTENTS

1.1	Introduction	1
1.2	Degradation Mechanisms	2
1.2.1	Random Scission	2
1.2.2	Side Group Scission	5
1.2.3	Monomer Reversion	6
1.2.4	Relative Bond Strengths	6
1.2.4.1	Polyolefins	7
1.2.4.2	Vinyl Polymers	8
1.2.4.3	Acrylates and Methacrylates	8
1.3	Examples and Applications	9
1.3.1	Forensic Materials	9
1.3.2	Fibers and Textiles	11
1.3.3	Paper, Ink, and Photocopies	13
1.3.4	Art Materials and Museum Pieces	16
1.3.5	Synthetic Polymers	18
1.3.6	Natural Materials and Biologicals	19
1.3.7	Paints and Coatings	22
1.3.8	Trace-Level Analyses	22
	References	24

1.1 INTRODUCTION

Pyrolysis, simply put, is the breaking apart of chemical bonds by the use of thermal energy only. Analytical pyrolysis is the technique of studying molecules either by observing their behavior during pyrolysis or by studying the resulting molecular fragments. The analysis of these processes and fragments tells us much about the nature and identity of the original larger molecule. The production of a variety of smaller molecules from some larger original molecule has fostered the use of pyrolysis as a sample preparation technique, extending the applicability of instrumentation designed for the analysis of gaseous species to solids, especially polymeric materials. As a result, gas chromatography, mass spectrometry, and Fourier-transform infrared

(FT-IR) spectrometry may be used routinely for the analysis of samples such as synthetic polymers, biopolymers, composites, and complex industrial materials.

The fragmentation that occurs during pyrolysis is analogous to the processes that occur during the production of a mass spectrum. Energy is put into the system, and as a result, the molecule breaks apart into stable fragments. If the energy parameters (temperature, heating rate, and time) are controlled in a reproducible way, the fragmentation is characteristic of the original molecule, based on the relative strengths of the bonds between its atoms. The same distribution of smaller molecules will be produced each time an identical sample is heated in the same manner, and the resulting fragments carry with them much information concerning the arrangement of the original macromolecule.

The application of pyrolysis techniques to the study of complex molecular systems covers a wide and diversified field. Several books have been published that present theoretical as well as practical aspects of the field, including a good introductory text by Irwin¹ and a compilation of gas chromatographic applications by Liebman and Levy.² A 1989 bibliography³ lists approximately 500 papers in areas as diverse as food and environmental and geochemical analysis, an excellent review by Blazs⁶⁴ lists over 150 papers just in the analysis of polymers, and the application to microorganisms has been examined by Morgan et al.⁵ This chapter will include only a few representational examples of the kinds of applications being pursued, with references for further reading. Specific areas of analysis are detailed in subsequent chapters.

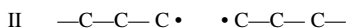
1.2 DEGRADATION MECHANISMS

The degradation of a molecule that occurs during pyrolysis is caused by the dissociation of a chemical bond and the production of free radicals. The general processes employed to explain the behavior of these molecules are based on free radical degradation mechanisms. The way in which a molecule fragments during pyrolysis and the identity of the fragments produced depend on the types of chemical bonds involved and the stability of the resulting smaller molecules. If the subject molecule is based on a carbon chain backbone, such as that found in many synthetic polymers, it may be expected that the chain will break apart in a fairly random fashion to produce smaller molecules chemically similar to the parent molecule. Some of the larger fragments produced will preserve intact structural information snipped out of the polymer chain, and the kinds and relative abundances of these specific smaller molecules give direct evidence of macromolecular structure. The traditional degradation mechanisms generally applied to explain the pyrolytic behavior of macromolecules will now be reviewed, followed by some general comments on degradation via free radicals.

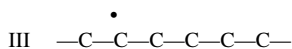
1.2.1 RANDOM SCISSION

Breaking apart a long-chain molecule such as the carbon backbone of a synthetic polymer into a distribution of smaller molecules is referred to as random scission. If all of the C—C bonds are of about the same strength, there is no reason for one to break more than another, and consequently, the polymer fragments to produce a

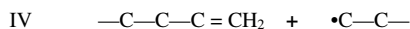
wide array of smaller molecules. The polyolefins are good examples of materials that behave in this manner. When poly(ethylene) (shown as structure I, with hydrogen atoms left off for simplicity) is heated sufficiently to cause pyrolysis, it breaks apart into hydrocarbons, which may contain any number of carbons, including methane, ethane, propane, etc.



Chain scission produces hydrocarbons with terminal free radicals (structure II), which may be stabilized in several ways. If the free radical abstracts a hydrogen atom from a neighboring molecule, it becomes a saturated end and creates another free radical in the neighboring molecule (structure III), which may stabilize in a number of ways. The most likely of these is beta scission, which accounts for most of the polymer backbone degradation by producing an unsaturated end and a new terminal free radical.



Beta scission



This process continues, producing hydrocarbon molecules that are saturated and have one terminal double bond or a double bond at each end. When analyzed by gas chromatography, the resulting pyrolysate looks like the bottom chromatogram in Figure 1.1. Each triplet of peaks represents the diene, alkene, and alkane containing a specific number of carbons and eluting in that order. The next set of three peaks contain one more carbon, etc. It is typical to see all chain lengths from methane to compounds containing 35 to 40 carbons, limited only by the upper temperature of the gas chromatography (GC) column.

When poly(propylene) is pyrolyzed, it behaves in much the same manner, producing a series of hydrocarbons that have methyl branches indicative of the structure of the original polymer. The center pyrogram in Figure 1.1 shows poly(propylene), revealing again a recurring pattern of peaks, with each group now containing three more carbons than the preceding group. Likewise, when a polymer made from a four-carbon monomer such as 1-butene is pyrolyzed, it produces yet another pattern of peaks, with oligomers differing by four carbons, as seen in the top pyrogram in Figure 1.1. The relationships of specific compounds produced in the pyrolysate to the original polymer structure have been extensively studied by Tsuge et al.,⁶ for example, in the case of poly(propylenes). The effects of temperature and heating rate have also been studied.⁷

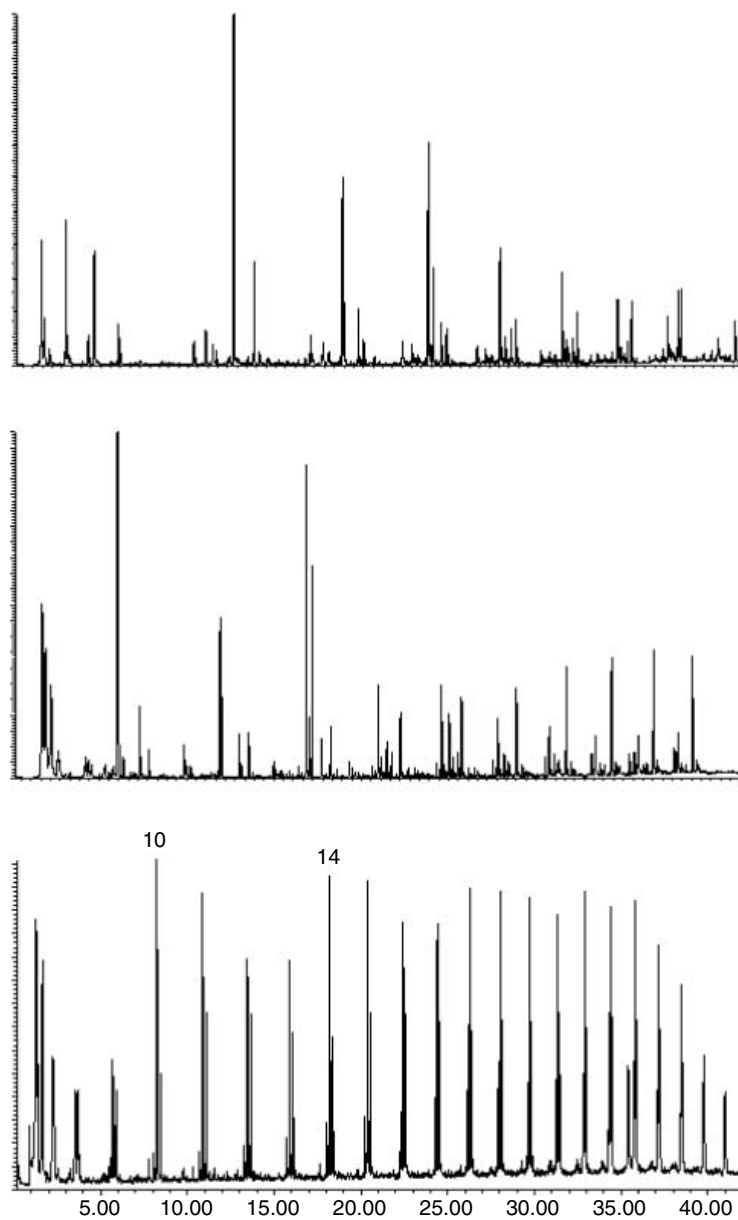


FIGURE 1.1 Pyrograms of poly(1-butene) (top), poly(propylene) (center), and poly(ethylene) (bottom).

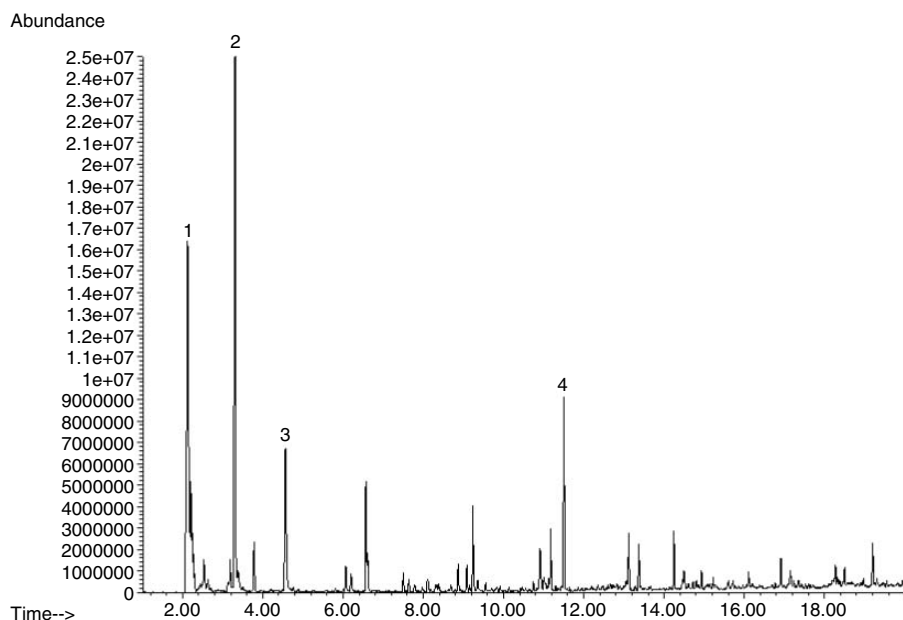
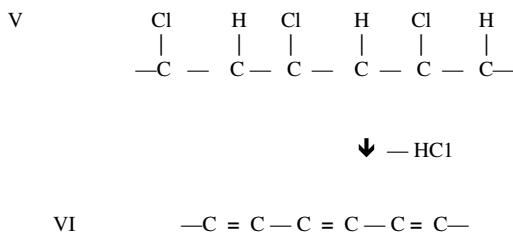


FIGURE 1.2 Pyrogram of poly(vinyl chloride) at 750°C for 15 seconds. Peaks: 1 = HCl, 2 = benzene, 3 = toluene, 4 = naphthalene.

1.2.2 SIDE GROUP SCISSION

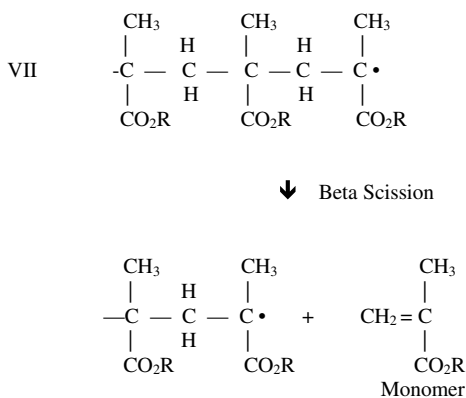
When poly(vinyl chloride) (PVC) is pyrolyzed, no such oligomeric pattern occurs. Instead of undergoing random scission to produce chlorinated hydrocarbons, PVC produces aromatics, especially benzene, toluene, and naphthalene, as shown in Figure 1.2. This is the result of a two-step degradation mechanism that begins with the elimination of HCl from the polymer chain (structure V), leaving the polyunsaturated backbone shown as structure VI.



Upon further heating, this unsaturated backbone produces the characteristic aromatics seen in the pyrogram. This mechanism has been well characterized, and the occurrence of chlorinated aromatics is used as an indication of polymer defect structures, as in the work of Lattimer and Kroenke.⁸

1.2.3 MONOMER REVERSION

A third pyrolysis behavior is evidenced by polymers such as poly(methyl methacrylate). Because of the structure of methacrylate polymers (structure VII), the favored degradation is essentially a reversion to the monomer.



Monomer production is for the most part unaffected by the R group, so that poly(methyl methacrylate) will revert to methyl methacrylate, poly(ethyl methacrylate) will produce ethyl methacrylate, etc. This proceeds in copolymers as well, with the production of both monomers in roughly the original polymerization ratio. Figure 1.3 shows a pyrogram of poly(butyl methacrylate), with the butyl methacrylate monomer peak by far the predominant product. A pyrogram of a copolymer of two or more methacrylate monomers would contain a peak for each of the monomers in the polymer.

1.2.4 RELATIVE BOND STRENGTHS

The question of which degradation mechanism a particular polymer will be subjected to — random scission, side group scission, monomer reversion, or a combination of these — is simplified by considering the nature of thermal degradation as a free radical process. All of the degradation products shown, as well as minor constituents, and deviations to the simplified rules are consistent with the following general statements:

Pyrolysis degradation mechanisms are free radical processes and are initiated by breaking the weakest bonds first.

The composition of the pyrolysate will be based on the stability of the free radicals involved and on the stabilities of the product molecules.

Free radical stability follows the usual order of $3^\circ > 2^\circ > 1^\circ > \text{CH}_3$, and intramolecular rearrangements, which produce more stable free radicals, play an important role, particularly the shift of a hydrogen atom.

Abundance

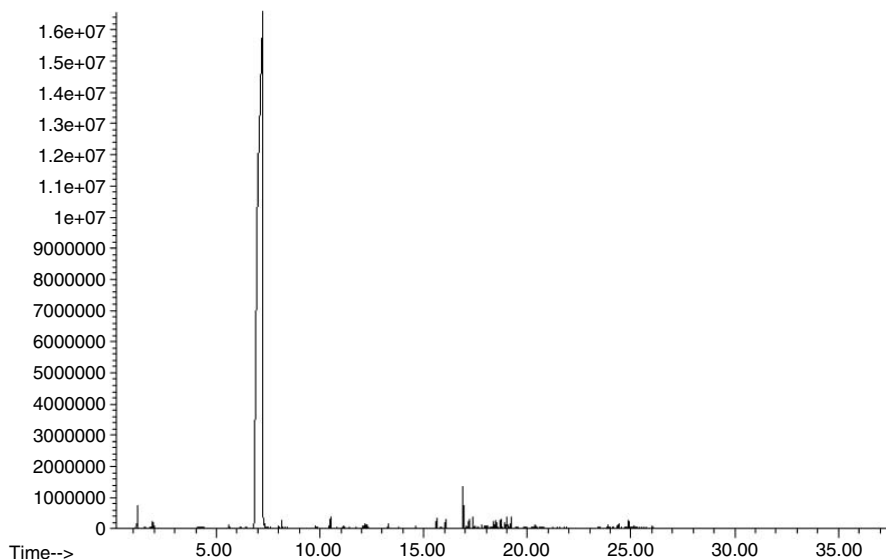
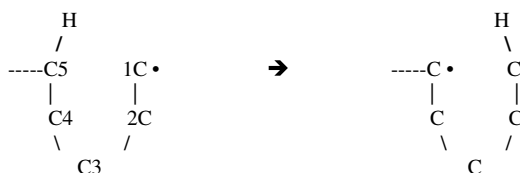


FIGURE 1.3 Pyrogram of poly(butyl methacrylate), showing large monomer peak (750°C for 15 seconds).

A quick review of the previous degradation examples will help show how each of the above categories is in reality just one aspect of the general rule of free radical processes.

1.2.4.1 Polyolefins

Poly(ethylene) and the other polyolefins contain only C—C bonds and C—H bonds. Since an average C—C bond is about 83 kcal/mole and a C—H bond 94 kcal/mole, the initiation step involves breaking the backbone of the molecule, with subsequent stabilization of the free radical. In the case of poly(ethylene), the original free radicals formed are terminal or primary. Hydrogen abstraction from a neighboring molecule creates a C—H bond (stable product) and a new, secondary free radical, which may then undergo beta scission to form an unsaturated end. In addition, transfer of a hydrogen atom from the carbon 5 removed from the free radical (via a six-membered ring) transforms a primary free radical to a secondary, increasing the free radical stability.



This new secondary free radical will undergo either beta scission or another 1–5 H shift. Beta scission produces a molecule of hexene, the trimer of ethylene, while a second 1–5 shift moves the unpaired electron to carbon 9. Beta scission of this new free radical would generate a molecule of decene, the pentamer. This stabilization by 1–5 hydrogen shifting explains the increased abundance of products in the pyrolysate of poly(ethylene) containing 6, 10, and 14 carbons. These products are the result of performing a 1–5 hydrogen shift one, two, and three times, respectively (see Figure 1.1, in which 10 and 14 carbon species are marked).

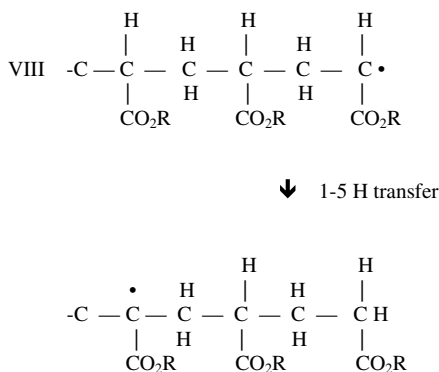
1.2.4.2 Vinyl Polymers

Poly(vinyl chloride) contains C—C, C—H, and C—Cl bonds, with the C—Cl bonds weakest at about 73 kcal/mole. Consequently, the first step is the loss of Cl•, which subsequently combines with hydrogen to form HCl, leaving the unsaturated polymer backbone, with formation of the very stable aromatic products upon further heating.

1.2.4.3 Acrylates and Methacrylates

Carbons in the chain of a methacrylate polymer are bonded to the CO₂R side group, the CH₃ side group, hydrogens, and other chain carbons (structure VII), with C—C bonds being weaker than C—H bonds. Of the C—C bonds, the ones making up the chain are the weakest and produce the most stable free radicals, since breaking C—CH₃ produces CH₃•, the least stable free radical. In addition, the free radicals produced are already tertiary, the most stable, and there is no hydrogen atom on carbon 5 to shift, so no additional pathway. Consequently, beta scission with an unzipping back to the monomer represents the most stable product formed by the most stable free radical.

With poly(acrylates), on the other hand, the methyl groups are absent (structure VIII), so there are hydrogens available to shift. Bond dissociation produces a secondary free radical, which can be stabilized by the 1–5 H shift to a tertiary free radical.



When this new free radical undergoes beta scission, the acrylate trimer is formed, with the three monomeric units connected in the same way that they were in the

polymer. Consequently, the poly(acrylates) pyrolyze to produce monomer, dimer, and most especially trimer, while the poly(methacrylates) produce mostly monomer.

1.3 EXAMPLES AND APPLICATIONS

Analytical pyrolysis is frequently considered to be a technique mainly applied to the analysis of polymers, which may at first seem fairly limited. However, when one considers that proteins, polysaccharides, plastics, adhesives, paints, etc., are included in this general category of polymers, the list of applications becomes much longer. Natural and synthetic polymers, in the forms of textile fibers, wood products, foods, leather, paints, varnishes, plastic bottles and bags, and paper and cardboard, make up the bulk of what we come into contact with every day. In fact, it is difficult to sit in a room and touch something — paint, paneling, carpet, clothing, countertop, telephone, upholstery, books — that is not made of some sort of polymer. Consequently, the study of materials using pyrolysis has become a very broad field, including such diverse topics as soil nutrients, plastic recycling, criminal evidence, bacteria and fungi, fuel sources, oil paintings, and computer circuit boards. The examples in this chapter will review in only a very general way some of the applications of analytical pyrolysis. Subsequent chapters treat some of these areas in greater depth.

1.3.1 FORENSIC MATERIALS

The application of pyrolysis techniques to the study of forensic samples has a long and well-documented history, including a review of pyrolysis-mass spectrometry as a forensic tool in 1977 by Saferstein and Manura,⁹ and a general review by Wheals.¹⁰ A wide variety of sample types have been investigated, including chewing gum, rubber and plastic parts from automobiles, drugs, and blood stains.

Perhaps the best known forensic application of pyrolysis is the analysis of paint flakes from automobiles, a standard practice in many laboratories backed by substantial libraries of pyrograms and sample materials. Munson et al.¹¹ describe their work using pyrolysis-capillary gas chromatography-mass spectrometry (GC/MS) for the analysis of paint samples, and Fukuda¹² has published results on nearly 80 paints used in the Japanese automobile industry. Kochanowski and Morgan¹³ describe a multivariate statistical approach to the discrimination of 100 automotive paints using pyrolysis-GC/MS, and a good evaluation of library searching, using both pyrolysis-GC/MS and FT-IR, was published by Chang et al.¹⁴ Ways in which automotive paint formulations have changed, partly in response to environmental concerns, have also been studied via pyrolysis.¹⁵ The same techniques may be applied to paint samples recovered from nonautomotive sources, including house paints and tool and machine coatings, as well as varnishes from furniture and musical instruments. Armitage et al.¹⁶ have used a laser micropyrolysis system to characterize paint, as well as photocopy toner and fibers.

Most automotive finishes are applied in layers, which may be removed selectively and analyzed individually, or pyrolyzed intact. An advantage provided by pyrolysis is that the inorganic pigment material is left behind and only the organic

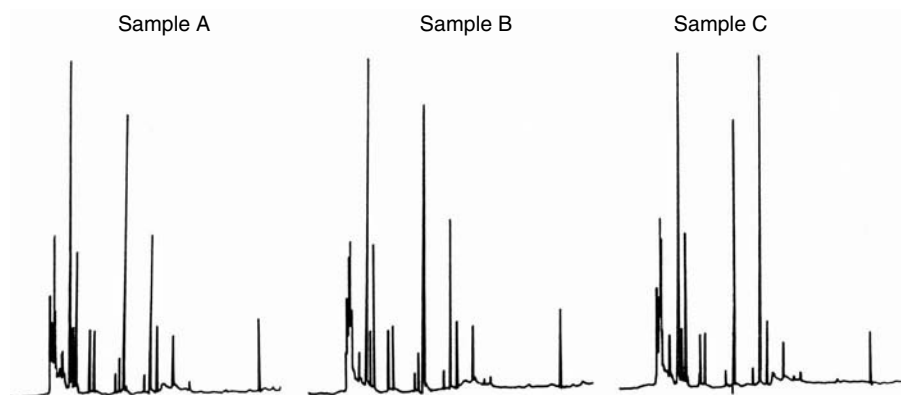


FIGURE 1.4 Comparison of paint pyrolyses, showing paints A and B matching, C being a different formulation.

pyrolysate transferred to the analytical instrument. Because of the great variety of polymeric materials used as paints and coatings, including acrylics, urethanes, styrenes, epoxies, etc., the resulting pyrograms may be quite complex. It is not always necessary to identify all of the constituents involved, however, to make comparisons among related paints. Figure 1.4 shows a comparison of three paint samples of similar monomer composition. Although many of the peaks are very similar for all three formulations, the inversion on the relative peak height in the second and third largest peaks makes it relatively straightforward to see that paints A and B are the same formulation and paint C is not a match.

Frequently, samples like paint flakes present a problem to the analytical lab because they are small, nonvolatile, and opaque with inorganic pigments. Since pyrolysis prepares a volatile organic sample from a polymer or composite, it offers the ability to introduce these organics to an analytical instrument separate from the inorganics, using only a few micrograms of sample. This extends the use of analytical techniques such as mass spectrometry and FT-IR spectroscopy to the investigation of small complex samples. When an opaque paint is pyrolyzed, the organic constituents are volatilized and available for analysis apart from the pigment material. A paint formulation based on methacrylate monomers, for example, will pyrolyze to reveal the methacrylates despite the presence of the pigment, and techniques such as FT-IR, which were previously unable to provide good spectral information, may be applied to the pyrolysate only. Figure 1.5 shows the pyrolysis-FT-IR comparison of poly(methyl methacrylate) and poly(ethyl methacrylate). In each case, a 200- μg sample of the solid polymer was pyrolyzed for 5 seconds in a cell fitted directly into the sample compartment of the FT-IR. The cell was positioned so that the FT-IR beam passed directly over the platinum filament of the pyrolyzer. The samples were pyrolyzed and the pyrolysate scanned for 10 seconds, producing the spectra shown. This system, details of which are published,¹⁷ permits the rapid scanning of polymer-based materials, requiring approximately 1 minute per sample.

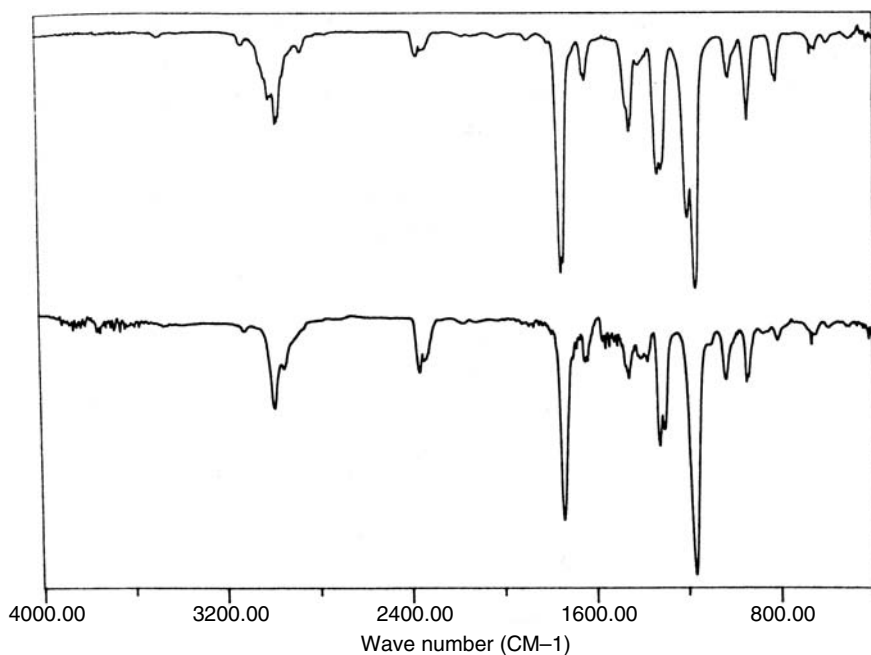


FIGURE 1.5 Comparison of poly(methyl methacrylate) (top) and poly(ethyl methacrylate) (bottom) by pyrolysis-FT-IR.

1.3.2 FIBERS AND TEXTILES

Almost all clothing is made from fibers of natural polymers such as the proteins in silk and wool, cellulose in cotton, synthetic polymers, including the various nylons and polyesters, or blends of both natural and synthetic polymers. Since these polymers are all chemically different, the pyrolysates they generate are all distinctive and provide a ready means of fiber analysis. Significant work has been done in the analysis and comparison of the various nylons by Tsuge et al.,¹⁸ among others, as well as acrylate and methacrylate/acrylonitrile copolymer fibers by Saglam¹⁹ and Almer.²⁰ A good overview of fiber analysis by pyrolysis-MS was published by Hughes et al.²¹

Figure 1.6 shows a pyrogram of silk fibers, which are made of the protein fibroin, which is nearly 50% glycine. Figure 1.7 is a pyrogram of the polyamide nylon 6/12, which is formulated using a diamine containing 6 carbons and a dicarboxylic acid containing 12 carbons. Although both silk and nylon are polyamides, the chemical differences between them make distinctions using pyrolysis gas chromatography relatively simple. The same techniques may be used to differentiate among the various nylon formulations, to distinguish silk from wool, etc.

Polymer blends used in clothing may be analyzed in the same manner. Because the degradation of a specific polymer is largely an intramolecular event, the presence of two different fibers pyrolyzed simultaneously generally produces a pyrogram resembling the superimposition of the pyrograms of the two pure materials. A good

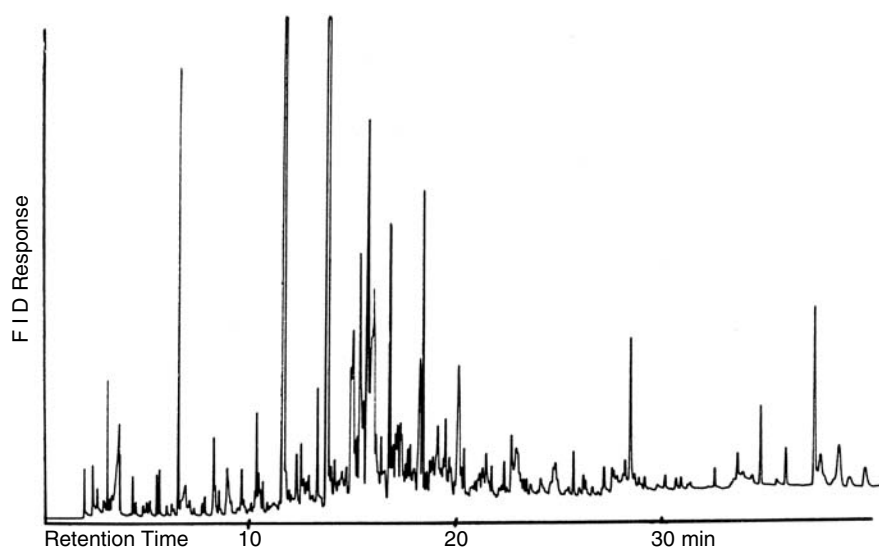


FIGURE 1.6 Pyrolysis of silk thread (675°C for 10 s in a glass-lined system).

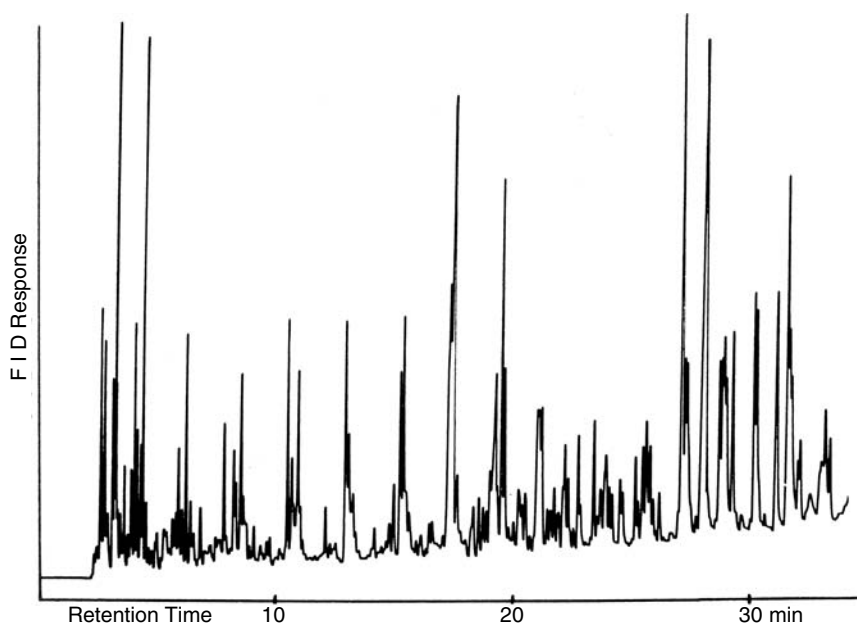


FIGURE 1.7 Pyrogram of nylon 6/12 (800°C for 10 s).

example of this is shown in Figure 1.8, which compares pyrograms of cotton, polyester, and cotton/polyester blend threads. Each sample was a piece of thread 1 cm in length, pyrolyzed at 750°C. The top pyrogram shows just cotton, which produces large amounts of CO₂ and H₂O, as well as some larger molecules, which appear in the chromatogram. The bottom pyrogram is of polyester only, which produces a larger abundance of chromatographic peaks. The center pyrogram is the result of pyrolyzing a 50/50 cotton/polyester blend thread. Even though the cellulose and polyester are copyrolyzed, the patterns of each individually are easily discernible. Specific peaks are marked C for cotton and P for polyester, indicating peaks associated only with the pure material. The effects of adding flame retardants to cotton fabrics have been studied by Zhu et al.,²² and Washall and Wampler²³ have published further examples of pyrograms of complex, multicomponent systems.

1.3.3 PAPER, INK, AND PHOTOCOPIES

Paper (which is primarily cellulose), printing ink, writing ink, and photocopy toners have all been analyzed by pyrolysis, sometimes independently as pure materials and sometimes intact as a fragment of a document. Zimmerman et al.²⁴ used pyrolysis-GC to extend the specificity of toner identification in photocopies. Ballpoint pen ink, various papers, and photocopy toners have been analyzed using a combination of headspace sampling and pyrolysis by Wampler and Levy.²⁵

Photocopy toner materials are generally complex formulations of pigments and polymers unique to a specific manufacturer. The formulations of these toners frequently include poly(styrene), polyesters, acrylic polymers, methacrylic polymers of various side chain lengths, and other additives. The formulations vary from manufacturer to manufacturer and also year to year as improvements are made and new processes introduced. Figure 1.9 shows a comparison of a Kodak and a Xerox photocopy made in 1985. The pyrograms were prepared by pyrolyzing a single letter punched from each photocopy. The punch, both paper and toner letter, was pyrolyzed at 650°C in a small quartz tube and analyzed by capillary gas chromatography. The paper, which is essentially cellulose and produces a pyrogram like the one shown for cotton thread in Figure 1.8, contributes many of the smaller peaks, including the one marked G, which is furfural. The synthetic polymers in the toner materials pyrolyze to generate the larger peaks, including A, methyl methacrylate, and J, which is styrene. A multivariate statistical approach to the analysis of photocopy and printer toners is presented by Egan et al.²⁶

When the same analysis is carried out using a sample of paper that was written upon with ballpoint pen, three sets of peaks are produced. Because the ink was applied as a fluid, there may be traces of the liquid or semiliquid vehicle remaining in the sample. In addition, there are the peaks resulting from actual pyrolysis of nonvolatile ink constituents and from the paper itself. Since less ink is applied than in the case for photocopy toner, the peaks from the paper generally make up a larger part of the chromatogram for ink analysis than for toner analysis.

Figure 1.10 shows the pyrogram resulting from pyrolyzing a 2-mm² piece of paper with ballpoint ink on it. All of the peaks labeled with numbers are cellulose pyrolysates from the paper. Peaks X and Y are from the ink vehicle and will show

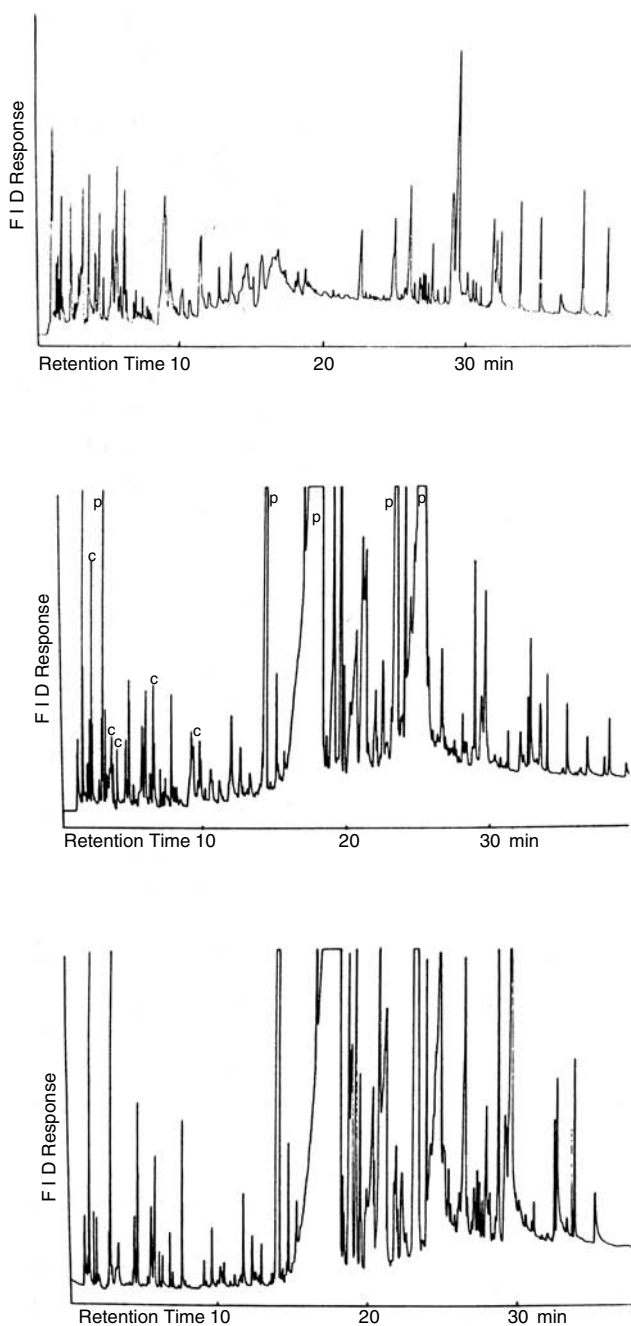


FIGURE 1.8 Comparison of pyrograms obtained from cotton (top), polyester (bottom), and cotton/polyester blend (center).

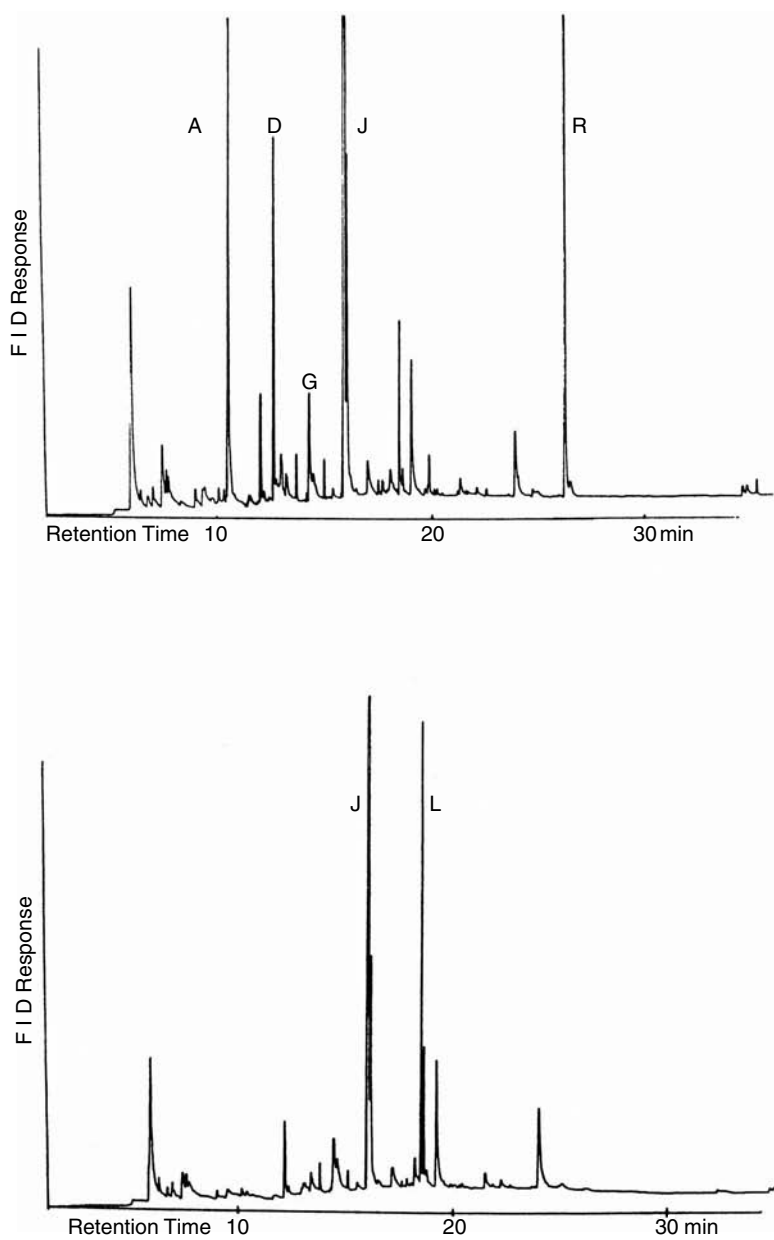


FIGURE 1.9 Comparison of Kodak (top) and Xerox (bottom) photocopy toners on paper.

Frequently, art and archeological samples must be investigated in layers, since protective coatings are generally applied over the original artwork, which itself may have been applied onto a prepared surface. The identification may involve analysis of the binder used in a subsurface, the oil or resin in the artwork, and the natural or synthetic polymer present in the protective coating. An example of this is shown in Figure 1.11. The sample came from an Egyptian sarcophagus that was believed to originate from about the fourth century A.D. The object was constructed of wood,

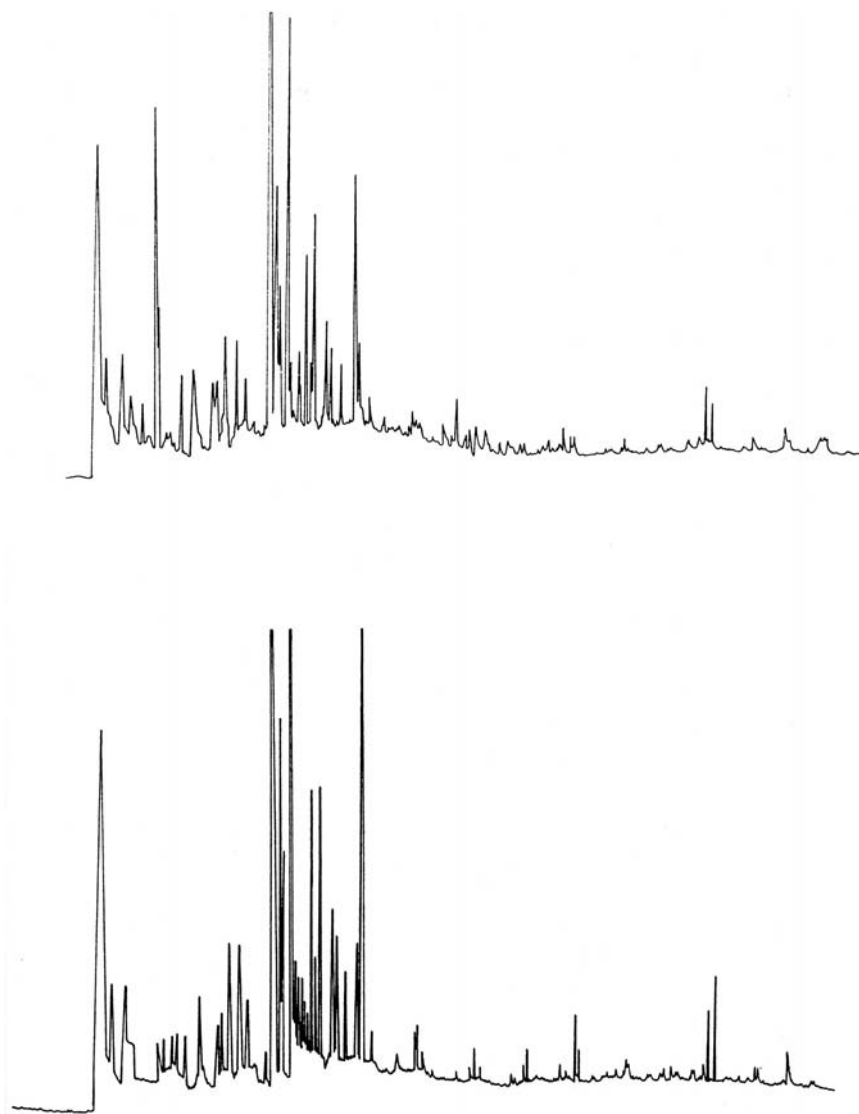


FIGURE 1.11 Pyrolysis (500°C for 20 s) of Egyptian sarcophagus ground material for binder content (bottom), compared to sample of ancient animal glue (top).

which was covered with a white layer (the ground) of essentially inorganic material, used as a base for decorative paintings. It was decided to investigate the organic binder used in preparing the ground as a measure of the authenticity of the sarcophagus. If an ancient material had been used, the authenticity would be supported; if a modern adhesive was detected, the sarcophagus would be fraudulent. Various natural binder materials were proposed and investigated, including egg, wax, animal glue, and copal resin. When a sample of the ground layer was pyrolyzed at 500°C, the pyrogram matched that produced from ancient animal glue, which had been independently authenticated.

An extensive review of pyrolysis applications in the analysis of artwork and antiquities has been published by Shedrinsky et al.,³⁴ with examples including glues and other adhesives, oil paints, varnishes, natural resins, and reference to the famous Van Meegeren case.

1.3.5 SYNTHETIC POLYMERS

Perhaps the widest application of analytical pyrolysis is in the analysis of synthetic polymers, from the standpoints of product analysis and quality control as well as polymer longevity, degradation dynamics, and thermal stability. Several specific polymers have been discussed in Section 1.2, and subsequent chapters treat specific families of polymers in detail.

That individual polymers may be distinguished from one another fairly readily has been demonstrated, for example, telling poly(ethylene) from poly(propylene), as in Figure 1.1, or poly(methyl methacrylate) from poly(butyl methacrylate). Since pyrolysis generates fragments that retain molecular structures intact, however, much finer distinctions may be made. Defect structures, branching, head-to-head or tail-to-tail linking, extraneous substitutions, and efficiency of curing have all been investigated. Copolymers may be studied, revealing the monomers involved and even the relative amounts of each monomer present in the final polymer. Wang,³⁵ for example, has explored the microstructure of thermoplastic copolymers formed using a variety of monomers. Branching, cross-linking,³⁶ and even the stereochemistry of polymers may be investigated, since the positioning of side groups in different stereochemical orientations produces pyrolysates of different composition.

Copolymers of methyl methacrylate and ethyl acrylate (EA), varying from 2 to 32% EA, have been studied by Shen and Woo,³⁷ showing a calibration curve for the determination of monomer ratios in unknowns. Similar work for copolymers of butadiene and acrylonitrile is reported by Weber.³⁸ When a copolymer is pyrolyzed, the resulting pyrogram may be quite complex, as in the case of polyolefins, or rather simple, if the polymer chain unzips to a monomer. If the monomers are all methacrylates, for example, the pyrogram will show major peaks for each of the corresponding monomers involved. Even for more complex materials, however, the pyrograms are characteristic of the original macromolecular system. Information is present indicating whether the sample is a physical blend of homopolymers or the result of copolymerization of monomers. In the latter case, fragments will be present that incorporate molecules of both monomers. These fragments could not result from the pyrolysis of homopolymers but rather indicate the position of monomer units

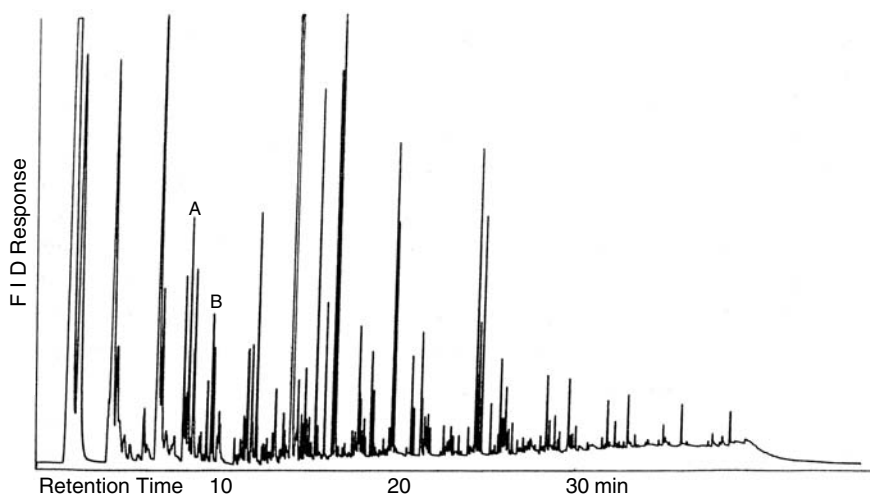


FIGURE 1.12 Pyrogram of a copolymer of poly(propylene) and 1-butene, with peaks marked A and B associated with the propylene monomer and 1-butene, respectively.

relative to each other in the macromolecule. It is possible to identify small fragments resulting from only one or the other of the monomers and thus study the effect of relative monomer concentration on abundance of specific peaks in the pyrogram. Figure 1.12 shows the pyrogram of a copolymer of polypropylene and 1-butene, with peaks marked A and B, associated with the propylene monomer and 1-butene, respectively. Similar work, comparing copolymers and polymer blends of ethylene and propylene, has been published by Tsuge et al.³⁹

In addition to the polymer matrix itself, information may be obtained about additives, such as tackifying resins in rubber,⁴⁰ flame retardants in polystyrenes,⁴¹ plasticizers, antioxidants, etc. The study of polymers using pyrolysis in general has been broadened by techniques permitting hydrolysis and methylation, typically by the addition of tetramethyl ammonium hydroxide to the sample, as described in a review by Challinor.⁴²

1.3.6 NATURAL MATERIALS AND BIOLOGICALS

A rapidly growing area of pyrolytic investigation involves the study of natural materials and biopolymers. Although fuel sources,^{43,44} kerogens,^{45,46} and coals^{47,48} have been analyzed for decades, more recently analysts are employing pyrolysis techniques in analyzing soil materials,⁴⁹ microorganisms,^{50,51} and biomass.⁵² Smith et al.⁵³ describe a chemical marker for the differentiation of group A and group B streptococci, and *Salmonella* strain characterization has been demonstrated by Tas et al.⁵⁴ Environmental samples are being analyzed as well, as in the case of the spruce needle analysis performed by Schulten et al.⁵⁵ in conjunction with a study of forest death in Germany.

Although biological samples may be more complex than pure polymers, the degradation of biopolymers must follow the same kinds of chemical processes,

producing a volatile distribution that, if complex, is also representative of the original material. Biopolymers include polyamides, as proteins, and polysaccharides, such as cellulose. Biological samples are likely to be complex systems based on such biopolymers with the addition of other, sometimes characteristic materials. Wood, for example, includes the basic macromolecules of cellulose and lignin, and different wood species differ from each other in the presence and amounts of additional substances, including terpenes. Microorganisms, including bacteria and fungi, have been studied in the intact state as well as in isolated parts, such as cell walls.

Figure 1.13 shows a comparison of two polymers of glucose — cellulose and starch. Since these materials are both composed of the same monomer, it is understandable that the pyrograms are similar. Cellulose and starch do differ, however, in the orientation of the linkage between the glucose units, and this difference affects the kinds and relative abundances of the pyrolysate products formed. Gelatin, hair, and nail are also similar in that they are all protein-based materials, but easily distinguishable in the pyrograms shown in Figure 1.14.

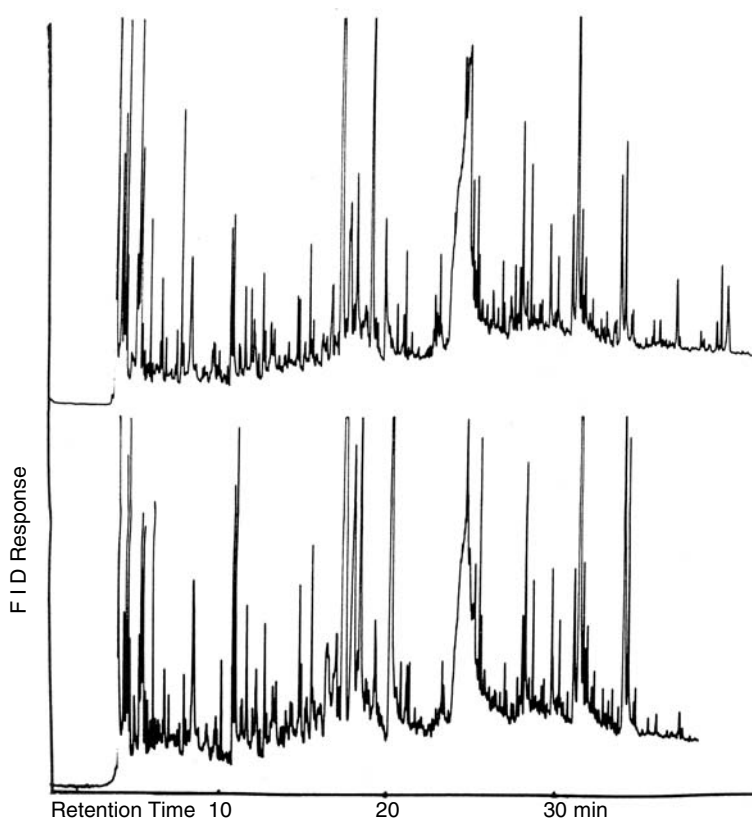


FIGURE 1.13 Comparison of two polymers of glucose pyrolyzed at 750°C for 10 s — cellulose (top) and starch (bottom).

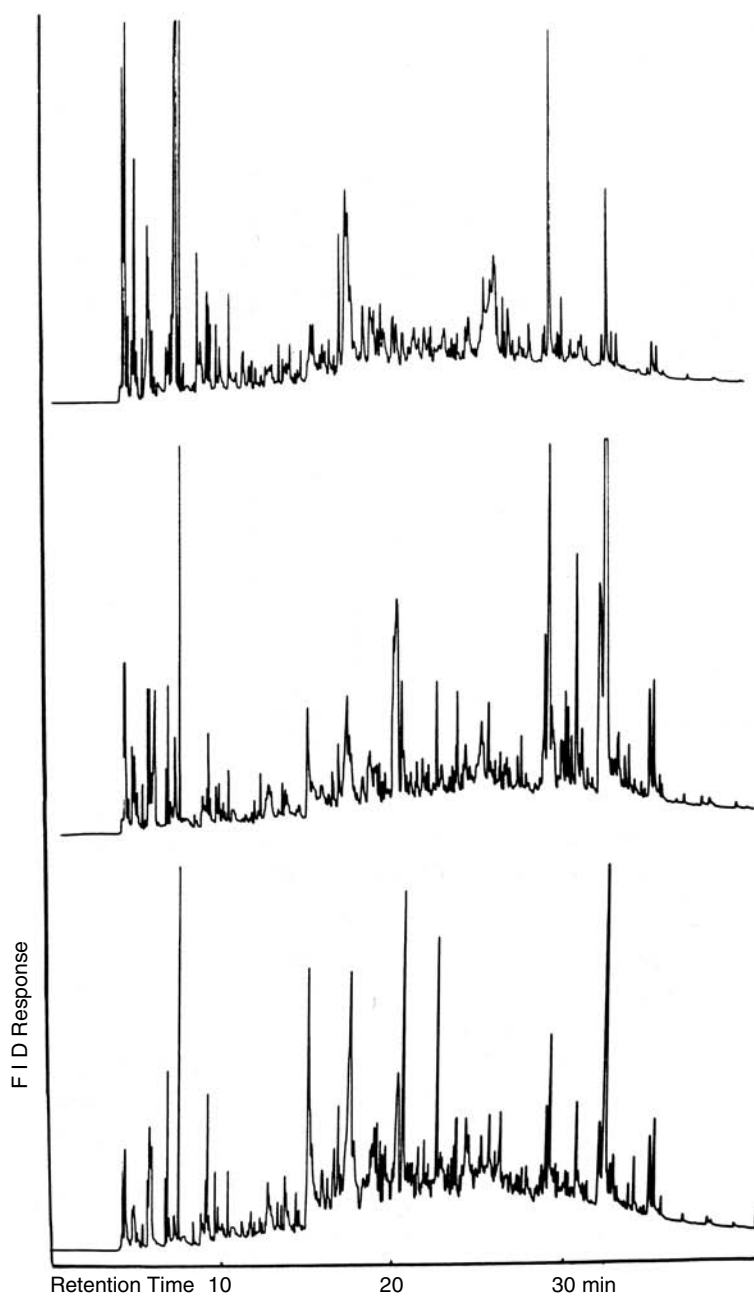


FIGURE 1.14 Comparison of three protein materials pyrolyzed at 750°C for 10 s — gelatin (top), human hair (center), and human fingernail (bottom).

Besides plant materials, environmental applications include assays of soil and sediment contaminants, including biogenic⁵⁶ as well as man-made.⁵⁷ Agricultural applications treat biomass as well as forages and crops.⁵⁸

1.3.7 PAINTS AND COATINGS

In addition to automotive finishes and artistic media discussed above, there are many other polymeric products applied to materials as protective coatings. These include varnishes, using both natural and synthetic materials, shellac,⁵⁹ alkyd and latex architectural paints, decorative paints, spray paint, plastic coatings, laminates, and sealants. Many of these incorporate drying oils, which contain long-chain fatty acids that appear in the pyrogram along with pyrolysis fragments of the polymers used. Polyurethanes are frequently added to the formulations and, upon pyrolysis, regenerate the diisocyanate. Alkyd housepaints are glyceryl phthalate polyesters and produce a major peak for phthalic anhydride. Paints using acrylic polymers and copolymers with styrene, vinyl toluene, and methyl styrene produce at least the monomers and frequently dimers and trimers.

Figure 1.15 shows the pyrogram of a typical latex emulsion interior wall paint. These paints frequently contain substantial amounts of vinyl acetate. Like polyvinyl chloride, polyvinyl acetate loses the side group and forms aromatics, so acetic acid, benzene, toluene, and naphthalene are formed. In Figure 1.15, peak 1 is acetic acid, peak 3 is toluene, and peak 6 is naphthalene. Benzene coelutes with the large acetic acid peak, but may be determined by looking at ion 78. In addition to the polyvinyl acetate, the paint formulation includes methyl methacrylate (peak 2) butyl acrylate (peak 5), and even a small amount of styrene (peak 4). The inorganic pigments used in the paint (frequently a large amount of titanium dioxide) stay behind in the sample tube and do not interfere with the analysis.

1.3.8 TRACE-LEVEL ANALYSES

Pyrolysis techniques may be used to analyze minor constituents in a system in addition to looking at the polymeric matrix itself. Since the macromolecules involved generally degrade without interacting with each other, even a trace level of one polymer contained within another may be expected to produce characteristic pyrolysates, and thus be identified and even quantified. The matrix need not be polymeric, or even organic, and analysts are using pyrolysis to look at coatings on minerals such as clays, pigments, and glass surfaces. Ezrin and Lavigne⁶⁰ have published a technique for the analysis of silicone polymers in the parts per billion range in recycled papers. A method for quantitating various paper additives using internal standards has been shown by Odermatt et al.,⁶¹ while a variety of contamination products have been studied by del Rio et al.⁶² The contamination of soil with polymeric, nonvolatile, or semivolatile compounds, including trinitrotoluene,⁶³ has been addressed, as has the presence of trace levels of polymers in pharmaceuticals.⁶⁴

An example of this last application may be seen in Figure 1.16. When the pharmaceutical material was purified by elution from a bed of polymer beads, some

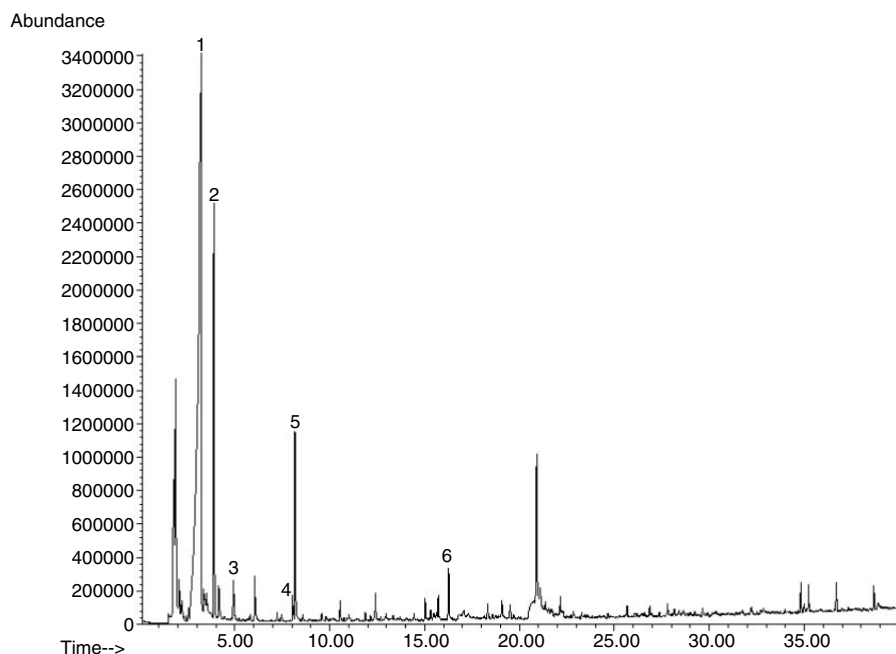


FIGURE 1.15 Interior latex paint pyrolyzed at 750°C. Peaks: 1 = acetic acid, 2 = methyl methacrylate, 3 = toluene, 4 = styrene, 5 = butyl acrylate, 6 = naphthalene.

of the polystyrene dissolved in the solvent used and became part of the dried finished product. To determine the amount of polystyrene present in the pharmaceutical powder, the product was pyrolyzed. Almost all of the peaks seen in the pyrogram (many of which are off-scale to show the styrene) came from pyrolyzing the pharmaceutical, and in this case were of no interest. The polystyrene, even at such trace levels, did provide a monomer peak in the pyrogram, marked with an arrow in Figure 1.16. The pure pharmaceutical was demonstrated not to produce styrene as a pyrolysate peak by itself, so this styrene monomer became a direct indication of the level of polystyrene that ended up in the finished product.

Polymeric materials then, whether natural (such as cellulose, resins, and proteins) or synthetic (such as polyolefins, nylons, and acrylics), behave in reproducible ways when exposed to pyrolysis temperatures. This permits the use of pyrolysis as a sample preparation technique to allow the analysis of complex materials using routine laboratory instruments. Pyrolytic devices may now be interfaced easily to gas chromatographs, mass spectrometers, and FT-IR spectrometers, extending their use to solid, opaque, and multicomponent materials. Laboratories have long made use of pyrolysis for the analysis of paint flakes, textile fibers, and natural and synthetic rubber and adhesives. The list of applications has been expanded to include documents, artwork, biological materials, antiquities, and other complex systems that may be analyzed with or without the separation of various layers and components involved.

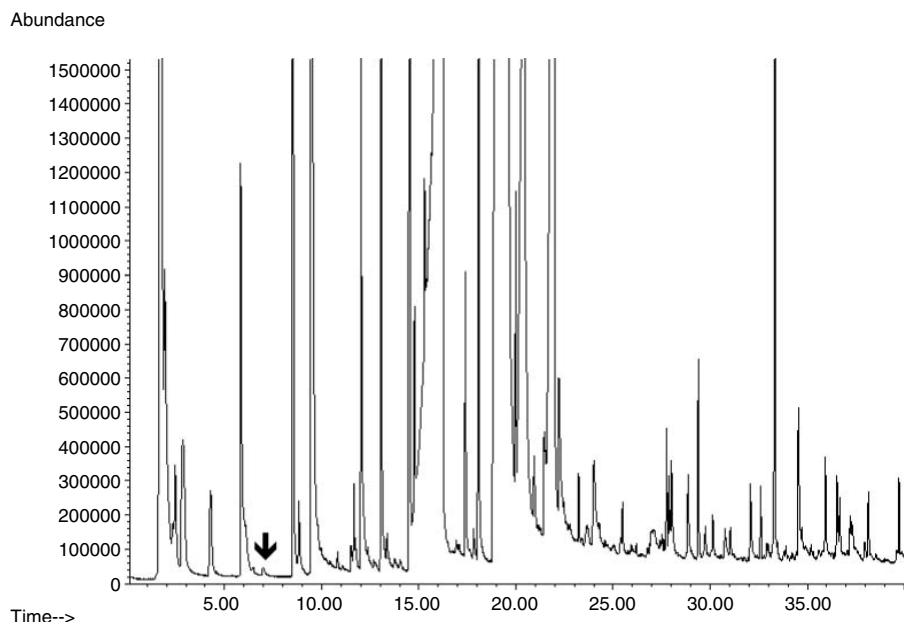


FIGURE 1.16 Pyrolysis of pharmaceutical showing trace amounts of styrene from polystyrene.

REFERENCES

1. W.I. Irwin, *Analytical Pyrolysis: A Comprehensive Guide*, Marcel Dekker, New York (1982).
2. S.A. Liebman and E.J. Levy, *Pyrolysis and GC in Polymer Analysis*, Marcel Dekker, New York (1985).
3. T.P. Wampler, *J. Anal. Appl. Pyrolysis*, 16: 291–322 (1989).
4. M. Blazsó, *J. Anal. Appl. Pyrolysis*, 39: 1–25 (1997).
5. S.L. Morgan, A. Fox, L. Larsson, and G. Odham, *Analytical Microbiology Methods, Chromatography and Mass Spectrometry*, Plenum Press, New York (1990).
6. S. Tsuge, Y. Sugimura, T. Nagaya, T. Murata, and T. Takeda, *Macromolecules*, 13: 928–932 (1980).
7. T.P. Wampler, *J. Anal. Appl. Pyrolysis*, 15: 187–195 (1989).
8. R.P. Lattimer and W.J. Kroenke, *J. Appl. Polym. Sci.*, 25: 101–110 (1980).
9. R. Saferstein and J.J. Manura, *J. Forens. Sci.*, 22: 749–756 (1977).
10. B.B. Wheals, *J. Anal. Appl. Pyrolysis*, 2: 277–292 (1981).
11. T.T. Munson, D.G. McMinn, and T.L. Carlson, *J. Forens. Sci.*, 30: 1064–1073 (1985).
12. K. Fukuda, *Forens. Sci. Int.*, 29: 227–236 (1985).
13. B.K. Kochanowski and S.L. Morgan, *J. Chrom. Sci.*, 38: 100–108 (2000).
14. W. Chang, C. Yu, C. Wang, and Y. Tsai, *Forens. Sci. J.*, 2: 47–58 (2003).
15. T.P. Wampler, G.A. Bishea, and W.J. Simonsick, *J. Anal. Appl. Pyrolysis*, 40/41: 79–89 (1997).
16. S. Armitage, S. Saywell, C. Roux, C. Lennard, and P. Greenwood, *J. Forens. Sci.*, 46: 1043–1052 (2001).

17. J.W. Washall and T.P. Wampler, *Spectroscopy*, 6: 38–42 (1991).
18. S. Tsuge, H. Ohtani, T. Nagaya, and Y. Sugimura, *J. Anal. Appl. Pyrolysis*, 4: 117–131 (1982).
19. M. Saglam, *J. Appl. Polym. Sci.*, 32: 5717–5726 (1986).
20. J. Almer, *Can. Soc. Forens. Sci. J.*, 24: 51–64 (1991).
21. C. Hughes, B.B. Wheals, and M.J. Whitehouse, *J. Anal. Appl. Pyrolysis*, 103: 482–491 (1978).
22. P. Zhu, S. Sui, B. Wang, and G. Sun, *J. Anal. Appl. Pyrolysis*, 71: 645–655 (2004).
23. J.W. Washall and T.P. Wampler, *J. Chrom. Sci.*, 27: 144–148 (1989).
24. J. Zimmerman, D. Mooney, and M.J. Kimmet, *JFSCA*, 31: 489–493 (1986).
25. T.P. Wampler and E.J. Levy, *LC-GC*, 4: 1112–1116 (1987).
26. W.J. Egan, R.C. Galipo, B.K. Kochanowski, S.L. Morgan, E.G. Bartick, M.L. Miller, D.C. Ward, and R.F. Mothershead, *J. Anal. Bioanal. Chem.*, 376: 1286–1297 (2003).
27. L.R. Ember, *C&E News*, 79: 51–59 (2001).
28. A.M. Shedrinsky, T.P. Wampler, and N.S. Baer, *The Identification of Dammar, Mastic, Sandarac and Copals by Pyrolysis Gas Chromatography*, Wiener Berichie uber Naturwissenschaft in der Kuns, VWGO, Wien (1988).
29. D. Scalarone and O. Chiantore, *J. Sep. Sci.*, 27: 263–274 (2004).
30. F. Cappitelli, *J. Anal. Appl. Pyrolysis*, 71: 405–415 (2004).
31. M.M. Wright and B.B. Wheals, *J. Anal. Appl. Pyrolysis*, 11: 195–212 (1987).
32. S.A. Buckley, A.W. Scott, and R.P. Evershed, *Analyst*, 124: 443–452 (1999).
33. B.A. Stankiewicz, J.C. Hutchins, R. Thomson, D.E. Briggs, and R.P. Evershed, *Rapid Commun. Mass Spectrom.*, 11: 1884–1890 (1998).
34. A.M. Shedrinsky, T.P. Wampler, N. Indictor, and N.S. Baer, *J. Anal. Appl. Pyrolysis*, 15: 393–412 (1989).
35. F.C. Wang, *J. Anal. Appl. Pyrolysis*, 71: 83–106 (2004).
36. K. Oba, Y. Ishida, H. Ohtani, and S. Tsuge, *Macromolecules*, 33: 8173–8183 (2000).
37. J.J. Shen and E. Woo, *LC-GC*, 6: 1020–1022 (1988).
38. D. Weber, *Int. Lab.*, 9: 51–54 (1991).
39. S. Tsuge, Y. Sugimura, and T. Nagaya, *J. Anal. Appl. Pyrolysis*, 1: 222–229 (1980).
40. S.W. Kim, *Rapid Commun. Mass Spectrom.*, 13: 2518–2526 (1999).
41. E. Jakab, M.D. Uddin, T. Bhaskar, and Y. Sakata, *J. Anal. Appl. Pyrolysis*, 68/69: 83–99 (2003).
42. J.M. Challinor, *J. Anal. Appl. Pyrolysis*, 61: 3–34 (2001).
43. R.P. Philp, *Org. Geochem.* 6: 489–501 (1984).
44. H. Bar, R. Ikan, and Z. Aizenshtat, *J. Anal. Appl. Pyrolysis*, 10: 153–162 (1986).
45. A.J. Barwise, A.L. Mann, G. Eglinton, A.P. Gowear, A.M. Wardroper, and C.S. Gutteridge, *Org. Geochem.*, 6: 343–349 (1984).
46. A.K. Burnham, R.L. Braun, H.R. Gregg, and A.M. Samoun, *Energy Fuels*, 1: 452–458 (1987).
47. J.J. Delpuch, D. Nicole, D. Cagniat, P. Cleon, M.C. Foucheres, D. Dumay, J.P. Aune, and A. Genard, *Fuel Proc. Technol.*, 12: 205–241 (1986).
48. A.M. Harper, H.L.C. Meuzelaar, and P.H. Given, *Fuel*, 63: 793–802 (1984).
49. J.M. Bracewell and G.W. Robertson, *Geoderma*, 40: 333–344 (1987).
50. H. Engman, H.T. Mayfield, T. Mar, and W. Bertsch, *J. Anal. Appl. Pyrolysis*, 6: 137–156 (1984).
51. C. Gutteridge, *Meth. Microbiol.*, 19: 227–272 (1987).
52. T.A. Mime and M.N. Soltys, *J. Anal. Appl. Pyrolysis*, 5: 111–131 (1983).
53. C.A. Smith, S.L. Morgan, C.D. Parks, A. Fox, and D.G. Pritchard, *Anal. Chem.*, 59: 1410–1413 (1987).

54. A.C. Tas, J. DeWaart, and J. Van der Greef, *J. Anal. Appl. Pyrolysis*, 11: 329–340 (1987).
55. H.-R. Schulten, N. Simmleit, and H.H. Rump, *Int. J. Environ. Anal. Chem.*, 27: 241–260 (1986).
56. D.S. Garland, D.M. White, and C.R. Woolard, *J. Cold Regions Eng.*, 14: 1–12 (2000).
57. D. Fabbri, C. Trombini, and I. Vassura, *J. Chromatogr. Sci.*, 36: 600–604 (1998).
58. A.S. Fontaine, S. Bout, Y. Barriere, and W. Vermerris, *J. Agric. Food Chem.*, 51: 8080–8087 (2003).
59. L. Wang, Y. Ishida, H. Ohtani, and S. Tsuge, *Anal. Chem.*, 71: 1316–1322 (1999).
60. M. Ezrin and G. Lavigne, *ANTEC 2002 Plastics Annu. Technol. Conf.*, 2: 2046–2050 (2002).
61. J. Odermatt, D. Meier, K. Leicht, R. Meyer, and T. Runge, *J. Anal. Appl. Pyrolysis*, 68/69: 269–285 (2003).
62. J. del Rio, M. Hernando, P. Landin, A. Gutierrez, and J. Romero, *J. Anal. Appl. Pyrolysis*, 68/69: 251–268 (2003).
63. J.M. Weiss, A.J. McKay, C. DeRito, C. Watanabe, K.A. Thorn, and E.L. Madsen, *Environ. Sci. Technol.*, 38: 2167–2174 (2004).
64. S. Muguruma, S. Uchino, N. Oguri, and J. Kiji, *LC-GC Int.*, 12: 432–436 (1999).

2 Instrumentation and Analysis

Thomas P. Wampler

CONTENTS

2.1	Introduction	28
2.2	Pyrolysis Instruments	28
2.2.1	General Considerations	28
2.3	Analytical Pyrolysis at Rapid Rates	29
2.3.1	Furnace Pyrolyzers	29
2.3.1.1	Design	30
2.3.1.2	Sample Introduction	30
2.3.1.3	Temperature Control	31
2.3.1.4	Advantages of Furnace Pyrolyzers	31
2.3.1.5	Disadvantages of Isothermal Furnaces	32
2.3.2	Heated Filament Pyrolyzers	32
2.3.3	Inductively Heated Filaments: The Curie-Point Technique	33
2.3.3.1	Design	33
2.3.3.2	Sample Introduction	34
2.3.3.3	Temperature Control	35
2.3.3.4	Advantages of Curie-Point Systems	35
2.3.3.5	Disadvantages of Curie-Point Systems	35
2.3.4	Resistively Heated Filaments	36
2.3.4.1	Design	36
2.3.4.2	Sample Introduction	37
2.3.4.3	Interfacing	38
2.3.4.4	Temperature Control	38
2.3.4.5	Advantages of Resistively Heated Filament Pyrolyzers	39
2.3.4.6	Disadvantages of Resistively Heated Filament Pyrolyzers	39
2.4	Pyrolysis at Slow or Programmed Rates	40
2.4.1	Programmable Furnaces	40
2.4.2	Resistively Heated Filaments at Slow Rates	40
2.5	Off-Line Interfacing	41
2.6	Multistep Analyses	42

2.7	Autosamplers.....	43
2.7.1	Furnace Autosamplers.....	43
2.7.2	Curie-Point Autosamplers.....	43
2.7.3	Resistive Heating Autosamplers	43
2.8	Sample Handling and Reproducibility	44
2.8.1	Sample Size and Shape.....	44
2.8.2	Homogeneity	44
	References.....	46

2.1 INTRODUCTION

To perform an analysis by pyrolytic techniques in the laboratory, it is necessary to assemble a system that is capable of heating small samples to pyrolysis temperatures in a reproducible way, interfaced to an instrument capable of analyzing the pyrolysis fragments produced. This chapter will discuss the various methods available for the convenient pyrolysis of laboratory samples and some general considerations regarding the interface of such units to analytical instruments. In addition, concerns about sample preparation, experimental reproducibility, and sources of error will be discussed.

A typical pyrolytic analysis involves sample preparation, pyrolysis, transfer of the pyrolysate to the analytical instrument, and then analysis. Pyrolysis-gas chromatography (GC) is still the most common technique, but pyrolysis-mass spectrometry (MS) and pyrolysis-Fourier-transform infrared (FT-IR) spectrometry are also common. In any system, the quality of the results will be no better than that permitted by any of its parts, and therefore it is important not only to use a reliable pyrolysis technique, but also to be aware of the effects of sample variations, mechanical and pneumatic connections, and instrument optimization. Although many analysts still design and use their own pyrolysis devices, variations in conditions and design frequently make it difficult to achieve reproducibility. The availability of a variety of pyrolysis instruments commercially has done much to improve the quality of pyrolysis experiments and reduce the frustrations common to early analysts.

Although there is a multitude of ways in which a sample could be heated sufficiently to break bonds, this chapter will treat only those ways that are readily available in the form of laboratory equipment. These instruments may be categorized as furnaces, both isothermal and programmable, inductively heated filaments, and resistively heated filaments. Interesting work has been done using lasers, solar radiation, electric arc, and other nonconventional heating units, but these experiments are frequently one-of-a-kind systems and are beyond the scope of this book.

2.2 PYROLYSIS INSTRUMENTS

2.2.1 GENERAL CONSIDERATIONS

In the typical analysis by pyrolysis, it is essential to heat a small sample to its final temperature as quickly as possible. Samples are generally small because of the

sampling capacity of the analytical instrument. For example, most gas chromatographic columns and detectors cannot handle more than a few micrograms of sample. This works to the advantage of an analyst who is using pyrolysis as a sample introduction technique, since a small sample will heat to its endpoint temperature quickly, with less thermal gradient than a large sample. It is important to heat the entire sample to the endpoint quickly, especially if one is studying the effects of pyrolysis temperature on the composition of the pyrolysate. Samples slowly heated will undergo considerable degradation while the pyrolysis instrument is still heating to the final set point temperature, and a large sample will degrade according to the temperature distribution across the sample as it is heated. Consequently, reproducibility may depend heavily on the ability of the pyrolysis instrument to heat the sample uniformly and to achieve the final temperature before the sample has already begun degradation. Pyrolysis instruments commercially available are capable of heating filaments to temperatures in excess of 800°C in milliseconds, producing rapid degradation of small, thin samples.

There are experiments and conditions, however, under which it is impossible or undesirable to pyrolyze the sample at such a fast rate. Large samples, used because they are nonhomogeneous or low in organic content, may be analyzed by pyrolysis, but the effects of the slower heating rate and thermal gradient through a large sample must be taken into account. In addition, there are experiments and techniques in which slow heating is specifically the point (such as thermogravimetric analysis or time-resolved spectroscopic analyses), and reproducible, slow-heating profiles, larger sample capacity, or both are advantages rather than obstacles.

2.3 ANALYTICAL PYROLYSIS AT RAPID RATES

The three most widespread techniques used to pyrolyze samples rapidly for analysis by GC, MS, or FT-IR are isothermal furnaces; Curie-point (inductively heated) filaments; and resistively heated filaments. There are specific design advantages to each technique, depending on the sample to be analyzed and the physical requirements of the experiment conducted. Each way is capable of providing reproducible pyrolysis for small samples, and many laboratories use more than one type of instrument. The selection of one technique over another depends frequently on personal preference, experimental requirements, budget, or availability. Since each technique heats in its own fashion, it is important to keep the physical differences in mind when comparing pyrolysis results. Having chosen (or inherited) any specific instrument, it is important to understand its heating characteristics to capitalize upon its advantages and minimize the effects of its drawbacks.

2.3.1 FURNACE PYROLYZERS

In order to pyrolyze samples rapidly for introduction to a gas chromatograph, furnace pyrolyzers are generally held isothermally at the desired pyrolysis temperature and the samples introduced into the hot volume. Carrier gas is generally routed through the furnace to remove the pyrolysate quickly from the pyrolysis zone to minimize secondary pyrolysis.

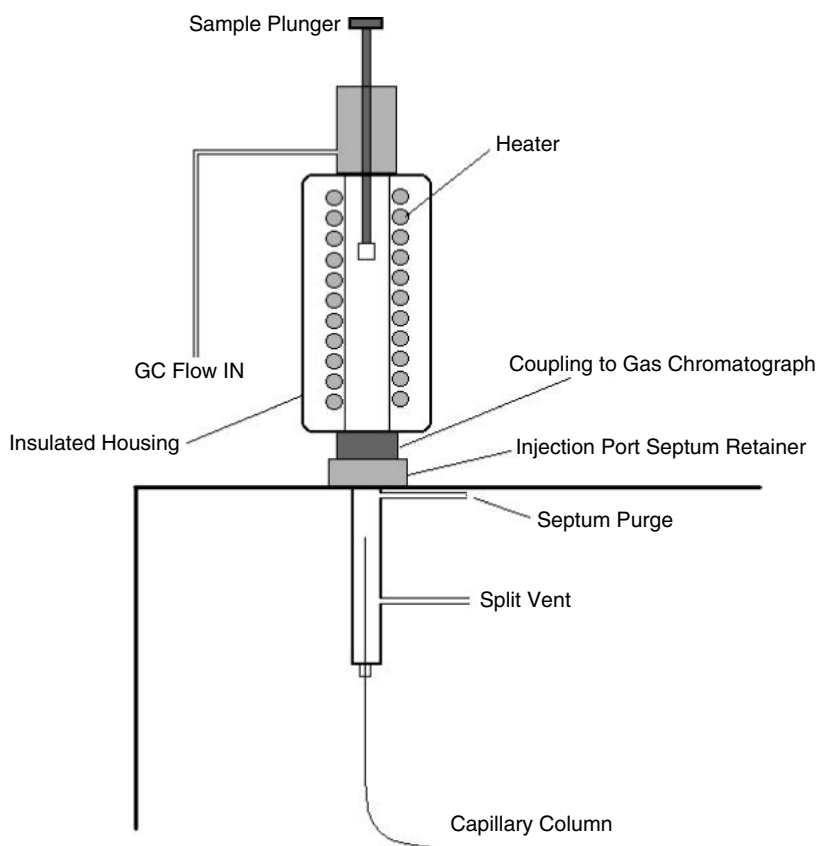


FIGURE 2.1 Microfurnace pyrolyzer installed on gas chromatograph injection port.

2.3.1.1 Design

Isothermal furnace pyrolyzers are generally designed to be small enough to mount directly onto the inlet of a gas chromatograph. They are normally constructed of a metal or quartz tube, which is wrapped with a heating wire, then insulated (Figure 2.1). Carrier flow enters the top or front of the furnace, sweeping past a sample inlet or delivery system, then exits directly into the injection port of the chromatograph. Furnace pyrolyzers must contain enough mass to stabilize the temperature, which is generally held to within $\pm 1^\circ\text{C}$. A temperature sensor (thermocouple or resistance thermometer device) is usually installed between the heater and the furnace tube to indicate the wall temperature.

2.3.1.2 Sample Introduction

Care must be taken to introduce the sample for pyrolysis into the furnace without admitting air, since the pyrolysis zone is already hot and degradation begins immediately. The heating rate of the sample is dependent on the sample material itself

and on the composition of the sample introduction device. In the simplest configuration, a liquid sample is injected into the furnace using a standard syringe; the sample then vaporizes and is followed by pyrolysis.

Solid samples present more of a problem, since they cannot be injected using a standard syringe. Some analysts dissolve soluble materials and inject the solution, pyrolyzing both the sample material and the solvent. Solid-injecting syringes have been designed that work on the principle of a needle inside a needle. The inside needle has a groove or slot into which a solid material may be placed. This needle then slides up into the outer needle for injection through the sample port of the furnace. Once inside the furnace, the inner needle is extended beyond the outer sheath, delivering the sample into the pyrolysis area.

Another approach has been developed by Shin Tsuge at the University of Nagoya in Japan.¹ His furnace pyrolyzer includes a cool chamber where samples are loaded into a small crucible above the hot zone. Once the sample is in place, the cup is rapidly lowered into the furnace for pyrolysis.

2.3.1.3 Temperature Control

The heating of a small, isothermal furnace is almost always achieved using a resistive electrical element wound around the central tube of the furnace. The temperature is monitored by a sensor, which feeds back temperature data to the controller, where adjustments are made for deviations from the set point. It must be stressed that the temperature measured (and displayed) using this sensor is the temperature of the system at that specific location. Depending on the diameter, thickness, and mass of the furnace tube, the temperature experienced by the sample inside the tube may be quite different. It is possible to position a thermocouple inside the furnace to monitor temperature closer to the location of sample introduction. The temperature and rate of heating of the sample will also depend on the sample size and mass and on the residence time inside the furnace. If the carrier gas is traveling too slowly through the furnace, the sample may degrade, then have time for the pyrolysate material to interact with the furnace wall, producing secondary pyrolysis products. In general, reasonable results may be duplicated on the same instrument using the same displayed wall temperature, making the assumption that the internal temperature caused by this wall temperature is also reproduced.

2.3.1.4 Advantages of Furnace Pyrolyzers

Because of their simple construction and operation, furnace pyrolyzers are frequently inexpensive and relatively easy to use. Since they are operated isothermally, there are no controls for heating ramp rate or pyrolysis time. The analyst simply sets the desired temperature and, when the furnace is at equilibrium, inserts the sample. Although this simplicity may lose its attractiveness as soon as the analyst requires control over heating rate or time, there are some experiments and sample types that capitalize on the design of a furnace. Liquid, especially gaseous samples, are pyrolyzed much more easily in a furnace than by a filament-type pyrolyzer. Because filament pyrolyzers depend on applying a cold sample to the filament and then

heating, it is very difficult to use them for any liquid that is readily volatile, or for gases. The furnace, however, since it is already hot, may receive an injection of a gas or liquid as easily as (or more easily than) a solid sample. Moreover, filament-type pyrolyzers are almost always housed or inserted into a heated zone, which prevents condensation of the pyrolysis products, since the actual pyrolysis filament is heated for only a few seconds. Samples that may be solids at room temperature may still melt or vaporize inside the heated chamber, or may denature in the case of proteins. A furnace with a good sample introduction system may permit the pyrolysis of such samples by thrusting them rapidly into the hot zone of the pyrolyzer, before they have a chance to undergo adverse lower-temperature changes.

2.3.1.5 Disadvantages of Isothermal Furnaces

Perhaps the greatest concern when using an isothermal furnace pyrolysis instrument is the size and construction of the pyrolysis chamber itself. To ensure thermal stability, the furnace tube is considerably larger than the sample inserted into it. This produces a relatively large volume through which the sample must pass before entering the analytical device, with a large hot surface area. In some designs, this pyrolysis tube is quartz, in others, metal. Particularly with metal systems, the possibility exists that the initial pyrolysis will produce smaller organic fragments, which may then encounter the hot surface of the furnace tube and undergo secondary reactions. To counter this, furnaces are almost always operated with a high flow rate through the tube (e.g., 100 ml/minute), generally necessitating split capillary analysis. This high flow rate reduces the residence time for the sample inside the hot zone, and the required high split ratio is generally not a problem unless one is sample limited or unless the sample analyzed is low in organic content.

The nature of heating and sample introduction in a furnace precludes one from knowing the temperature rise time of the sample, which will depend on the nature of the sample, its size, and geometry. In addition, the mass, which gives the furnace its thermal stability, also gives it thermal inertia. If one is establishing the effect of pyrolysis temperature on the products, or optimizing the production of fragments of interest, one must allow equilibration time between temperature changes to establish stability at the new temperature.

2.3.2 HEATED FILAMENT PYROLYZERS

Isothermal furnaces achieve a fairly fast sample heating by keeping the pyrolysis instrument hot and injecting samples into it. Heated filament pyrolyzers take the opposite approach in that the sample is placed directly onto the cold heater, which is then rapidly heated to pyrolysis temperature. Commercially, two heating methods are used: resistance heating, in which a controlled current is passed through the heating filament, and inductive heating, in which the current is induced into the heating filament, which is made of a ferromagnetic metal. Each type achieves very fast heating rates by using a small filament, and consequently, the sample size must be limited to an amount compatible with the mass of the filament. This sample size is usually in the low to high microgram range, which is compatible with gas

chromatograph column capacities providing the sample is essentially all organic in nature. For larger samples or materials of low organic content, filaments may not be able to heat the sample efficiently, and a furnace style may be more appropriate

2.3.3 INDUCTIVELY HEATED FILAMENTS:

THE CURIE-POINT TECHNIQUE

It is well known that electrical current may be induced into a wire made of ferromagnetic metal by the use of a magnet, and this is the principle used to heat the filaments of a Curie-point pyrolysis system. If one continues to induce a current, the wire will begin to heat and continue to heat until it reaches a temperature at which it is no longer ferromagnetic. At this point, the metal becomes paramagnetic and no further current may be induced in it. Consequently, the heating of the wire stops — the Curie point of the specific metal alloy used. This Curie-point temperature is different for each ferromagnetic element and also for different alloys of these metals. For example, a wire made entirely of iron will become paramagnetic and stop heating at a temperature of 770°C, while an alloy of 40% nickel and 60% cobalt will reach 900°C.

In a Curie-point pyrolyzer, an oscillating current is induced into the pyrolysis filament by means of a high-frequency coil. It is essential that this induction coil be powerful enough to permit heating the wire to its specific Curie-point temperature quickly. In such systems, the filament temperature is said to be self-limiting, since the final or pyrolysis temperature is selected by the composition of the wire itself, and not by some selection made in the electronics of the instrument. Properly powered, a Curie-point system can heat a filament to pyrolysis temperature in milliseconds. Providing that wires of the same alloy composition are used each time, the final temperature is well characterized and reproducible.

2.3.3.1 Design

Curie-point pyrolysis systems must be designed to permit easy insertion of the wire containing the sample into the high-frequency coil, in a chamber which is swept with carrier gas to the analytical instrument. Two approaches may be taken: (1) the pyrolysis chamber, which is surrounded by the coil, is opened and the sample wire is dropped or placed inside, or (2) the sample wire is attached to a probe that is inserted through a septum into the chamber, which is surrounded by the coil (Figure 2.2). The coil chamber may be attached directly to the injection port of the gas chromatograph, or it may be part of a larger module, which is isolated from the GC by a valve. In the latter design, the sample may be introduced and removed easily without interrupting the carrier gas flow of the gas chromatograph.

Because the Curie-point filament is heated inductively, no connections are made to the wire. This facilitates autosampling and permits loading the wires into glass tubes for sampling and insertion into the coil zone. Unlike the isothermal furnace, which is on continuously, the Curie-point wire is heated only briefly and is cold the rest of the time. This necessitates heating the pyrolysis chamber separately to prevent immediate condensation of the fragments made during pyrolysis. Therefore, Curie-

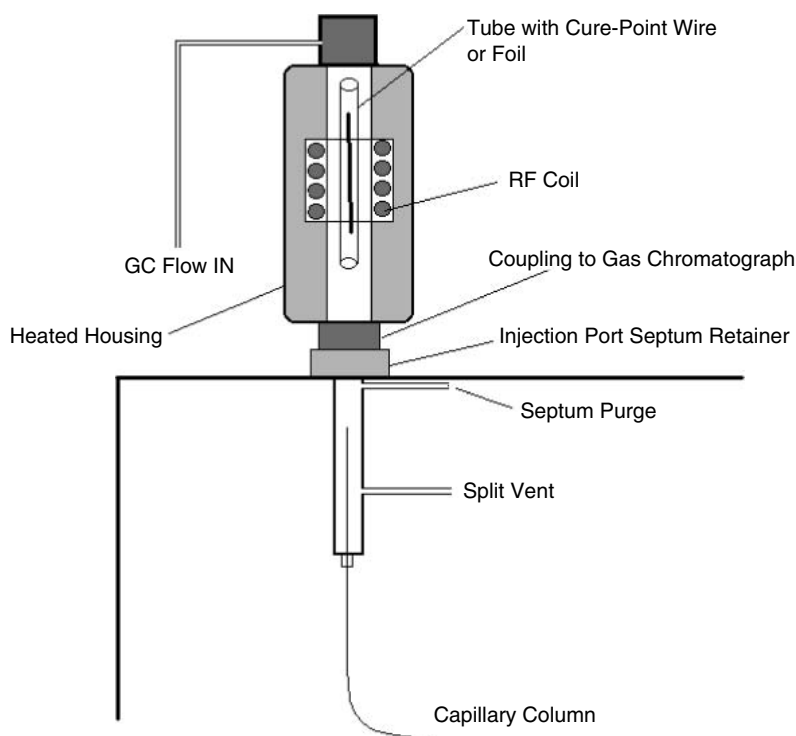


FIGURE 2.2 Curie-point pyrolyzer installed on gas chromatograph injection port.

point pyrolyzers have controls for the parameters of the pyrolysis wire and also temperature selection for the interface chamber housing the wire.

2.3.3.2 Sample Introduction

To capitalize upon the very rapid heating rates possible using the Curie-point technique, the sample and wire should be kept to a low mass. The technique is best suited to the analysis of samples that may be coated onto the filament as a very thin layer. Soluble materials may be dissolved in an appropriate solvent and the wire dipped into the solution. As the solvent dries, it leaves a thin deposit of the sample material, which will then heat rapidly and uniformly to pyrolysis temperature when the wire is heated. Paints, varnishes, and soluble polymers may be analyzed in this way quite easily.

Pyrolysis samples that are not soluble must be applied to the wires in some other fashion.² Finely ground samples may be deposited onto the wire from a suspension, which is then dried to leave a coating of particles on the wire. Another approach is to apply the sample as a melt, which then solidifies onto the wire. To attach materials that will not melt or form a suspension, some analysts flatten the wire or create a trough in it. Some samples are held in place by bending or crimping the wire around the material, although this introduces concerns about the thermal continuity of a

Curie-point material that has been distorted. To encapsulate a sample completely, some systems use a foil³ of ferromagnetic material instead of a wire. The sample is placed in the center of a piece of metal foil, which is then wrapped around it and dropped into the high-frequency coil chamber, just as a standard wire would be.

2.3.3.3 Temperature Control

Control of the pyrolysis temperature in a Curie-point instrument is achieved solely by the alloy of the ferromagnetic material used. Pyrolysis of a material at a variety of temperatures requires a selection of Curie-point wires of different alloy compositions. These wires are generally purchased from the manufacturer of the instrument, and each manufacturer offers a variety of alloys covering a fairly wide temperature range. The analyst therefore has no access to temperature settings. Reproducible and accurate temperature control thus relies on the accuracy of the wire alloy, the power of the coil, and the placement of the wire into the system. One may be reasonably confident that the sample wire achieves the theoretical temperature if the instrument has enough power to induce current sufficient to heat the wire to its limit. Use of wires from one manufacture lot throughout an experiment will increase the likelihood of temperature reproducibility, as will attention to sample loading and placement.

2.3.3.4 Advantages of Curie-Point Systems

The self-limiting temperature of an inductively heated wire and the rapidity with which it heats are major advantages of the Curie-point system. Using wires of the same manufacture and alloy, one may be confident that the sample is heated to a specific and known temperature in a rapid and reproducible manner. Since there is no temperature control setting, there is no temperature calibration to perform.

Curie-point systems have some additional advantages from the standpoint of convenience. The sample wires may be coated with sample, then placed into a glass tube for storage so that one may prepare several samples at once and subsequently load them into the pyrolyzer. In addition, since the heating wire need not be connected to a source of power, insertion into the unit is simple and may be readily automated⁴ by placing wires in glass tubes into a feeding magazine or into a multiposition autosampler. Although the wires may be cleaned and reused, they may also be discarded after one use, eliminating concerns about carryover of sample from one analysis to another.

2.3.3.5 Disadvantages of Curie-Point Systems

Since the temperature of pyrolysis is a function of the Curie-point wire alloy composition, the wire, and consequently the sample, may be heated to that temperature only. If it is desired to evaluate several different pyrolysis temperatures, or to study the behavior of a sample material at different temperatures, it is necessary to use a different Curie-point wire for each run. Therefore, it is not possible with a Curie-point system to optimize the pyrolysis temperature of a sample by placing the material into the instrument and increasing the temperature in a stepwise fashion,

observing the pyrolysis products after each heating. The fact that the sample is in contact with a different metal at each different temperature produces concerns about the catalytic effect of the metal during heating for only very small samples, since in larger samples energy is conducted through the sample material itself and pyrolysis takes place without contacting the metal surface. The analyst is, however, limited to the pyrolysis temperatures provided by the Curie-point wires or foils offered by the manufacturer. Curie-point materials are generally provided for temperatures ranging from 350 to 1000°C, covered by 10 to 20 specific alloys. Investigations at temperatures between the Curie points of the materials offered are not possible.

Although most pulse pyrolysis analyses benefit from the very rapid temperature rise time experienced by a Curie-point filament, there are investigations in which the analyst wishes to control the heating rate during pyrolysis. This has been attempted by modulating the power supplied to the coil, but for commercial instruments, slowing the heating rate is not possible. For experiments requiring the slow, linear heating of a sample material, a programmable furnace or resistively heated filament pyrolyzer is required.

2.3.4 RESISTIVELY HEATED FILAMENTS

Like the Curie-point instruments, resistively heated filament pyrolyzers operate by taking a small sample from ambient to pyrolysis temperature in a very short time. The current supplied is connected directly to the filament, however, and not induced. This means that the filament need not be ferromagnetic, but that it must be physically connected to the temperature controller of the instrument. Filaments are generally made of materials of high electrical resistance and wide operating range and include iron, platinum, and nichrome.⁵

2.3.4.1 Design

As with Curie-point systems, the filament of a resistively heated pyrolyzer must be housed in a heated chamber that is interfaced to the analytical device. This interface chamber is generally connected directly to the injection port of a gas chromatograph, with column carrier gas flowing through it. The sample for pyrolysis is placed onto the pyrolysis filament, which is then inserted into the interface housing and sealed to ensure flow to the column (Figure 2.3). When current is supplied to the filament, it heats rapidly to pyrolysis temperatures and the pyrolysate is quickly swept into the analytical instrument.

The pyrolysis filament may be shaped for convenience of sampling and may be a flat strip, foil, wire, grooved strip, or coil. In the case of the coil, a small sample tube or boat is inserted into the filament so that the sample is not heated directly by the filament, but is in effect inside a very small, rapidly heating furnace. The pyrolysis filament must be connected to a controller capable of supplying enough current to heat the filament rapidly, with some control or limit since the materials used for filaments are not self-limiting. The temperature of the filament may be monitored using the resistance of the material itself or some external measure, such as optical pyrometry⁶ or a thermocouple.⁷

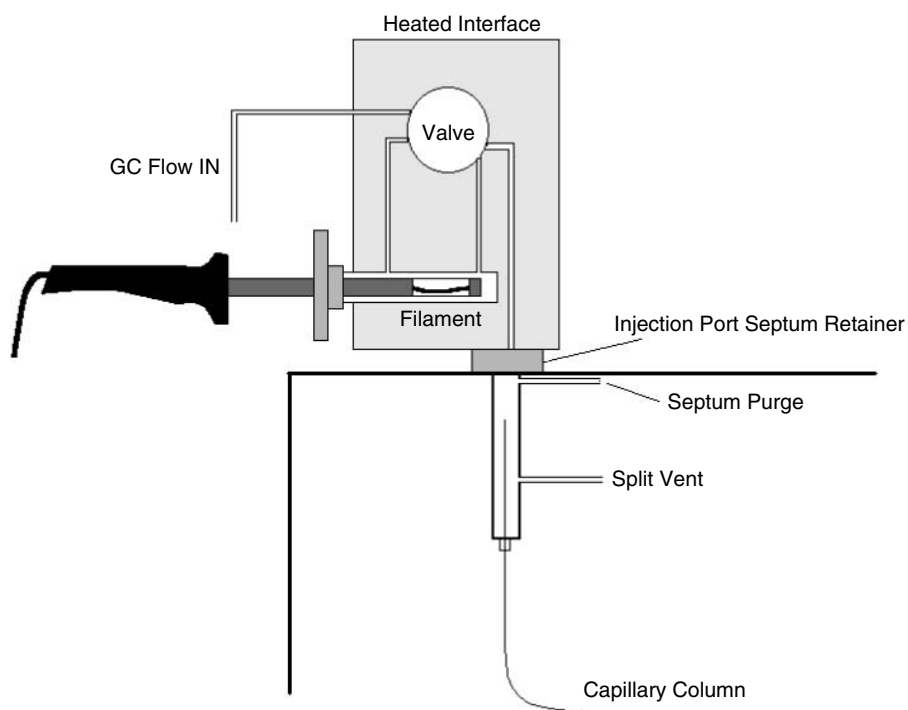


FIGURE 2.3 Resistively heated filament pyrolyzer installed on gas chromatograph injection port.

The filament used may be made to be quite small and is therefore capable of being inserted into instruments other than gas chromatographs, including the sample cell of infrared spectrometers and the ion source of a mass spectrometer.⁸

2.3.4.2 Sample Introduction

Samples may be applied to resistively heated filaments in the same manner used for Curie-point wires. Soluble materials may be deposited from a solvent, which is then dried before pyrolysis. However, the solution is generally applied to the filament from a syringe, instead of dipping, since the filament is attached to a probe or housing. Insoluble materials may be melted in place to secure them before pyrolysis. Since the filament may be a flat ribbon or contain a grooved surface, placement of some solid materials may be simpler than when using a Curie-point wire.

Since the sample must be placed onto the filament before it is inserted into a heated chamber with carrier flow, placement of fibers and fine powders presents a problem. If these materials may not be melted onto the filament, they may fall off or blow off in the carrier gas stream before pyrolysis. Consequently, these sample types are generally analyzed using a small quartz tube, which is inserted into a coiled filament. The sample may be placed into the tube, held in position using plugs of quartz wool, weighed, and then inserted into the coiled element for pyrolysis. It

must be remembered that the sample is now insulated by the wall of the quartz tube, so the temperature rise time and final temperature will not be the same as those for a sample pyrolyzed directly on a filament. Use of a quartz tube, however, does extend the use of a filament pyrolyzer to materials such as soils, ground rock samples, textiles, and small fragments of paint.

Viscous liquids, such as heavy oils, may be applied directly to the surface of a filament or may be pyrolyzed while suspended on the surface of a filler material, such as quartz wool inside a quartz tube. Lighter liquids, especially anything easily vaporized, will probably be evaporated from the filament by the heat of the interface before pyrolysis and are probably better studied using a furnace-type pyrolyzer.

2.3.4.3 Interfacing

Filament pyrolysis instruments may be designed small enough to insert directly into the analytical device, especially the injection port of a gas chromatograph or the ion source of a mass spectrometer. In these cases, one need only ensure that the filament is positioned so that the pyrolysate may enter the analytical portion of the instrument, and that the filament probe is sealed into the unit so that there are no leaks. For most gas chromatographs equipped with capillary inlets, however, considerable attention has been paid to the elimination of dead volume, and there is not sufficient room to accommodate a pyrolyzer. In these cases, some heated interface must be attached upstream of the injection port to house the pyrolyzer and ensure efficient transfer of the pyrolysate onto the column. This interface should have its own heater, independent of the pyrolysis temperature, to prevent condensation of pyrolysate compounds, and be of minimal volume. Flow from the gas chromatograph is brought up into the interface, past the filament, and then back into the injection port. In most cases, this means that the chromatograph is open to air when samples are inserted, so the column oven is cooled before samples are introduced or removed. An alternative is to place a valve between the pyrolyzer and the injection port to isolate the chromatograph flow, permitting removal of the filament during a run.⁹

2.3.4.4 Temperature Control

The temperature of a resistively heated filament is related to the current passing through it. Since resistively heated filaments are not self-limiting in the sense that Curie-point filaments are, exacting control of the filament current is essential for temperature accuracy and reproducibility. Early versions of resistively heated pyrolyzers relied on rather approximate control and, given the difficulty of measuring and calibrating the final temperature, produced some mixed results. It must be remembered that the pyrolysis temperature of the filament depends upon the resistance of the filament, which is affected by both temperature and physical condition. A length of resistive wire could be expected to produce the same temperature each time it is heated using the same current, but relating that temperature to an instrument set point, or calibrating the unit after replacing a broken filament, proved problematical.

Current versions of resistively heated pyrolyzers incorporate small computers to control and monitor the filament temperature. These computers may be used to control the voltage used, adjust for changes in resistance as the filament heats, and compensate for differences when broken filaments are replaced. In addition, instruments have been designed that include photodiodes,⁶ which are used by the computer to measure the actual temperature of the filament during a run. Other instruments include a small thermocouple welded directly to the filament for temperature readout, or use the computer to measure the resistance of the filament itself and make adjustments as needed during a program.

Since the temperature and the rate of heating the filament are completely variable, the instrument may control these parameters independently, as single steps or multiple steps. This gives the analyst the control to select any final pyrolysis temperature and to heat the sample to this temperature at any desired rate. Instruments are commercially available that heat as slowly as $0.01^{\circ}\text{C}/\text{minute}$ and as rapidly as $30,000^{\circ}\text{C}/\text{second}$.

2.3.4.5 Advantages of Resistively Heated Filament Pyrolyzers

The central advantage of a resistively heated pyrolyzer is that the filament may be heated to any temperature over its usable range, at a variety of rates. This permits the examination of a sample material over a range of temperatures without the need to change filaments for each temperature. A sample may be placed onto the filament, heated to a set point temperature and the products examined, then heated to higher temperatures in a stepwise fashion without removing the sample or filament from the analytical device. This ability also allows pyrolysis at temperatures between the discrete values permitted by Curie-point filaments, and frequently at temperatures higher than those permitted by furnaces.

The ability to control the rate at which the filament, and thus the sample, is heated extends the use of filament pyrolyzers in two ways. First, it permits the examination of materials and how they are affected by slow heating, duplicating processes such as thermogravimetric analysis (TGA). Second, it permits the interface of spectroscopic techniques with constant scanning for three-dimensional, time-resolved thermal processing. A sample may be inserted directly into the ion source of a mass spectrometer or placed in the light path of an FT-IR, and the products monitored in real time throughout the heating process.¹⁰

2.3.4.6 Disadvantages of Resistively Heated Filament Pyrolyzers

The main disadvantage of a resistively heated pyrolyzer results from the fact that the filament must be physically connected to the controller. The temperature control of a resistively heated filament is based on the resistance of the entire filament loop, including the filament and its connecting wires. Anything that damages or alters the resistance of any part of the loop will have an effect on the actual temperature produced by the controller.

An additional disadvantage may be produced by the fact that the filament must be housed in a heated zone. Introduction of some samples into a heated chamber before pyrolyzing them may produce volatilization or denaturation, altering the nature of the sample before it is actually degraded.

2.4 PYROLYSIS AT SLOW OR PROGRAMMED RATES

Although for most analytical pyrolysis techniques it is advisable to heat the sample to its final temperature as rapidly as possible, there are times when just the opposite is required. To simulate thermal processes, such as TGA on a small scale, or to analyze the degradation products produced from a sample as they are generated, slower, controlled heating is required. These slow-rate experiments demonstrate, for example, that poly(vinyl chloride) degrades in a two-step process, producing HCl at a relatively low temperature and aromatics at elevated temperatures.

While a sample material is slowly heated to its degradation temperature, the volatile products may be swept by a carrier gas into an analytical instrument or collected onto a trap for analysis as a composite. Alternatively, the sample may be pyrolyzed directly in the analytical instrument, while scans are collected continuously. This produces a time-resolved picture of the production of specific products, as measured by the abundance of specific masses or absorbance at specific wavelengths.

Slow pyrolysis is generally produced using either a programmable furnace or resistively heated filament pyrolyzer.

2.4.1 PROGRAMMABLE FURNACES

The design and interfacing of furnace pyrolyzers has been discussed. The same mass and thermal stability that make typical furnaces useful for isothermal applications may be used to provide reproducible heating profiles at slow rates for large samples. Several programmable furnace pyrolysis instruments are available commercially, with the most common application being the examination of fuel source samples.¹¹ These materials are generally ground rock from oil well core drillings or shale deposits, and the majority of the sample is inorganic and nonvolatile. Consequently, a rather large sample must be heated to extract the organics, generally performed at a rate of 50 to 100°C/minute.

Programmable furnaces may be interfaced to a gas chromatograph, generally with some sort of intermediate trapping, but are rarely interfaced directly to spectroscopic techniques. Thermogravimetric analysis coupled with Fourier-transform infrared spectroscopy (TGA-FT-IR) is an important exception, since many thermal units are capable of heating samples to pyrolysis temperatures, with the resulting pyrolysate swept directly into the cell of the FT-IR.¹²

2.4.2 RESISTIVELY HEATED FILAMENTS AT SLOW RATES

Since the temperature and rate of heating of a resistive filament pyrolyzer are functions of the current, these instruments are frequently used to provide slow

programs in addition to pulse-heating pyrolyses. The advantage of the resistive filament is that the sample may be placed directly onto the filament during heating, so that there is no thermal gradient as experienced with a furnace design. In practice, however, the sample is more likely placed into a quartz tube and heated using a coiled filament, creating a small quartz furnace inside of the resistive element.

As with the slowly heated furnace, a collection step is generally required when producing a sample for gas chromatography, since the pyrolysate may be produced over the course of several minutes. For some applications, collection may be done directly onto the gas chromatograph column, at either ambient or subambient temperatures. For direct mass spectrometry or FT-IR spectrometry in a time-resolved fashion, the pyrolyzer is either inserted into an expansion chamber, which is flushed or leaked into the spectrometer, or inserted directly into the instrument. Specially designed probes permit operation at pyrolysis temperatures directly in the ion source of a mass spectrometer if it was originally equipped with a solids probe. For FT-IR, a heated pyrolysis chamber may be flushed with carrier gas into a light pipe, or a cell used that positions the filament of the pyrolyzer directly below the light path for real-time pyrolytic analysis.

2.5 OFF-LINE INTERFACING

For many experiments, including the slow rate pyrolyses discussed above, it may be advantageous or necessary to install the pyrolysis device away from the analytical instrument, with a collection or trapping system between. This may be accomplished in a variety of ways, both manually and automatically.

For manual isolation, the pyrolysis device may be flushed with a stream of carrier gas that is routed through a trap, either sorbent or thermal, using dry ice or liquid nitrogen. The pyrolysate is swept from the pyrolyzer and through the trap, where the carrier gas is vented but the organics are frozen or adsorbed. The trap is then disconnected from the pyrolyzer and taken to the analytical instrument where the pyrolysate is either thermally revaporized or extracted with a solvent and injected. An early method of performing pyrolysis-IR was to allow the pyrolysate to condense onto a window, which was then inserted into the IR and scanned. These techniques also permitted the use of pyrolysis devices to heat samples in atmospheres incompatible with the analytical instrument or at pressures or flows not permissible in the analyzer. For example, a sample may be heated in oxygen for combustion studies, with the reaction products collected, then transferred to a gas chromatograph.¹³ Normal installation of a pyrolyzer would require the use of oxygen as the GC carrier, which is incompatible with column phases.

An analyst performing many off-line pyrolyses or reactant gas studies will probably select an automatic means of isolating the pyrolysis end of the experiment from the analytical. This is typically done by employing a valve in a heated oven to place the collection device alternately on-line with the pyrolyzer or with the analytical device. Commercial systems are available that incorporate this valve in a programmable controller to automate the process, as well as in manually operated modes. The pyrolysis chamber carrier gas is directed through the valve to the trap,

or alternately to vent. During an experiment, the pyrolysis gas, inert or reactant, is routed through a sorbent or cold trap, where the pyrolysate is collected. During this time, the analytical device, generally a gas chromatograph, is swept with inert carrier as usual. When the valve is rotated, only the trap is inserted into the GC analytical flow, and the collected analytes are heated and transferred to the column for analysis. The pyrolyzer itself and its flow never touch the analytical instrument. This design permits heating the sample material slowly or for as long as desired, with transfer of the composite-collected pyrolysate for a single GC analysis. Systems have also been designed with multiple traps for the stepwise collection of multiple fractions from the sample as it is heated, with subsequent GC analysis of the material from each trap.

2.6 MULTISTEP ANALYSES

Frequently the samples analyzed in a laboratory by pyrolysis are complex materials that include a polymer matrix plus other volatile or semivolatile organic compounds. Pyrolysis permits the analysis of the polymer, but in heating the sample, the other components are also either pyrolyzed, desorbed, or volatilized. These include plasticizers, antioxidants, dyes, fillers, and other intentional ingredients, as well as residual monomers, solvents and processing agents, or contaminants. It is frequently possible to liberate the volatile and semivolatile compounds from the polymer thermally, at temperatures too low to produce pyrolysis, so the matrix remains intact. This has led to the use of pyrolysis instruments to perform thermal extractions at lower temperatures, in addition to pyrolysis. The same sample may be heated sequentially to increasingly higher temperatures to deliver selected ranges of compounds for analysis. Sometimes two steps, a low temperature followed by pyrolysis, are sufficient, but increasingly, multiple-step programs are being employed to provide greater specificity. These techniques are attractive for several reasons, including the elimination of solvent extractions and the ability to have the steps automated, starting the GC each time. They are especially useful in discriminating between monomer that is produced during pyrolysis and residual monomer in the product, and in distinguishing products that may come from an additive instead of the matrix.

To be practical in these analyses, the pyrolyzer must have the ability to heat the sample material over a wide range of temperatures and to operate at lower temperatures without preheating the sample or introducing cold spots. Isothermal interfaces are usually a problem in that if they are hot enough to transfer all the pyrolysis products to the GC, they are probably too hot for the desorption steps, and volatiles will be lost while the sample is inserted into the unit. What is generally needed is a programmable interface or a separate heating zone for the desorption and pyrolysis steps.

Curie-point pyrolyzers are generally not used in this stepwise fashion, since they are limited to one temperature per sample because of the way heating is controlled. Microfurnaces, however, have been designed with a separate desorption zone,¹⁴ so that a sample may be manually lowered into a low-temperature zone for a first run, retrieved, and then lowered into the pyrolysis zone for a second run. Filament pyrolyzers are now available with a low-mass, programmable interface zone along

with computer-controlled filament temperature. Samples may be placed into the cold interface, which is then programmed to heat rapidly for desorption, and then cooled between runs. Since the filament temperature is controlled by the computer, any number of subsequent runs at higher temperatures may be made automatically, heating the interface to an appropriate temperature before the filament is heated.

2.7 AUTOSAMPLERS

In the interest of efficiency, autosamplers have become increasingly important in analytical laboratories. Autosampling systems are now available for all three types of pyrolysis equipment: furnaces, Curie point, and resistively heated filament.

2.7.1 FURNACE AUTOSAMPLERS

Most of the autosampling pyrolysis systems available use a sample magazine or carousel to introduce prepared samples into a common heater. In the furnace type,¹⁵ samples are placed into deactivated steel cups that are dropped sequentially into the furnace for pyrolysis, then ejected pneumatically after the analysis. Temperatures up to 800°C are achievable, and the carousel has space for up to 48 sample cups.

2.7.2 CURIE-POINT AUTOSAMPLERS

One of the first approaches to pyrolysis autosampling involved the interfacing of multiple Curie-point coil interfaces to a common injection port.¹⁶ This provided up to 12 analyses, each one with its own Curie-point wire, so the different samples could be pyrolyzed at different temperatures. This design has been replaced with the approach of dropping the individual samples into a common high-frequency coil, which has increased the number of samples possible. In one design, the sample wires are held in glass tubes that are loaded from a carousel into the coil.¹⁷ In another, the samples are folded into a foil of ferromagnetic metal and delivered magnetically from a stack of sample foils.¹⁸ In either case, each sample is limited to one temperature, although different metals (and therefore different temperatures) may be used for each sample. The stacked magazine style of sample introduction permits the analysis of up to 20 samples, while the tube carousel design provides for 24.

2.7.3 RESISTIVE HEATING AUTOSAMPLERS

Two approaches to autosampling with resistively heated filaments are available, one in which multiple filaments are used and one in which a common filament is used. The former uses up to 14 different filament interfaces,¹⁹ each of which is connected sequentially to the gas chromatograph for pyrolysis. The computer permits individual control of each filament, so each sample may be analyzed using a different program. Like the Curie-point systems, the samples may be placed directly onto the heating filament.

In the other version,²⁰ a common coil filament is used, into which samples placed into quartz tubes are dropped. The quartz tubes are delivered from a carousel, which can hold up to 35 samples. Different pyrolysis conditions may be programmed for

each sample, and multiple runs may be performed on each tube. Between runs, the sample is taken off-line from the GC and purged to vent, then placed back on-line for the next analysis.

2.8 SAMPLE HANDLING AND REPRODUCIBILITY

It is not enough to have a pyrolyzer for which the endpoint temperature and heating rate are well characterized to guarantee reproducible results. Sampling, sample handling, introduction, and transfer from the pyrolyzer into the analytical device must be performed with attention to all the inaccuracies that may be introduced. The effects of instrument design and interfacing have been discussed. The most common sources of error in sample manipulation will now be briefly described. The most important areas of concern are sample preparation, including size and shape, homogeneity, and contamination.

Using microsyringes, it is relatively easy to introduce a 1- μ l or smaller sample into a gas chromatograph injection port. Preparing and inserting a solid sample that is only a few micrograms, on the other hand, presents some difficulties. This is particularly the case if the sample is an insoluble material of an inconsistent makeup throughout, such as plant material or layers of paint. Even analysts confident in their ability to prepare small slices of a sample are concerned about whether that piece is representative of the whole.

2.8.1 SAMPLE SIZE AND SHAPE

If a sample material is soluble, microliter-sized portions of the solution may be deposited onto the surface of the pyrolysis instrument using a syringe, which not only regulates the amount of sample material, but also causes the sample to be spread as a thin film, which heats and pyrolyzes readily. One of the advantages of pyrolysis as an analytical technique, however, is its benefits in the analysis of difficult solids, which have limited solubility, such as polymers. In these cases, it is necessary to make samples of the same size and shape consistently for reproducible results. Since analytical pyrolyzers are designed to heat small samples rapidly, it is easy to overload the pyrolyzer with too much sample. This not only affects the rate at which the sample heats, related to the thermal gradient through the thickness of the material, but may also overload the analytical device, causing contamination and carryover into the next analysis. Generally, 10 to 50 μ g of sample is desirable for direct pyrolysis-GC, and about twice that for direct pyrolysis-FT-IR. A thin slice placed on its side is preferable to a cube or sphere, and melting the sample into a film is sometimes helpful if the sample will cooperate. In any event, it is important to use nearly the same size and shape sample each time to be sure that at a minimum the sample material goes through the same heating process each time.

2.8.2 HOMOGENEITY

Ensuring that a sample of solid material only a few micrograms large is homogeneous, and therefore representative of the material from which it was taken, presents

a constant problem to analysts. The inability to obtain several samples of identical composition frequently casts suspicion on the technique of analytical pyrolysis, since the results obtained show poor reproducibility. This lack of reproducibility may be interpreted as the result of unexplained or unreliable reactions occurring in the sample during pyrolysis, when in fact it is actually an indication that the samples are different from each other.

Some samples have such large, obvious differences in composition from end to end that nonhomogeneity is self-evident. Materials such as plant leaves, soils and rocks, scrapings, textiles, and laminated products will clearly provide different materials from different physical areas sampled. Since few analysts have the luxury of analyzing pure homogeneous materials, these concerns must be addressed and the effects of nonhomogeneous samples on the pyrolysis results established for each analysis.

Analysts sampling materials for which homogeneity is a concern have devised several methods to deal with the problem. If possible, the sample material may be ground to a fine powder from which small portions are taken for analysis. There is sometimes a concern that the grinding process or the heat produced during it may alter the sample so that the results are no longer representative. Many materials, however, have been ground successfully under cryogenic conditions, resulting in a powdered sample that has not been heated sufficiently to volatilize any of its constituents. Other analysts have chopped samples finely using a scalpel and then analyzed several of the small fragments together. Again, if the material or materials comprising the sample are soluble, dissolving them and working from a solvent provides an easy way to ensure homogeneity and sample size reproducibility.

Some analysts have elected to pyrolyze large samples when concerned that a small sample cannot be made to be representative. A sample of about 1 mg, if pyrolyzed using an instrument powerful enough to heat it effectively, may produce better reproducibility than a smaller sample, which is less representative. In such cases, it is also essential to limit the amount of the pyrolysate entering the analytical instrument, generally by use of a splitter with a large split ratio or by passing the pyrolysate in a carrier gas through a small sample loop attached to a valve that is interfaced to the analytical unit. It is also important to be mindful of the increased amounts of residue and char produced, requiring cleaning to prevent contamination from run to run.

Another way to deal with nonhomogeneous samples is to analyze the individual constituents independently. Since analytical instruments are sensitive enough to respond to very small samples, it is sometimes possible to remove specific portions of an overall sample and investigate them separately. For example, specs of contamination in a polymer melt, discolorations, particles in papers or pulp, different strata in mineral samples, layers of paint, etc., may be studied independently as well as part of the whole sample material. It is important to remember that the individual constituents in a mixture will each pyrolyze in a way consistent with its molecular makeup, and that the entire sample will amount to the sum of its individual parts.

REFERENCES

1. S. Tsuge and H. Matsubara, *J. Anal. Appl. Pyrolysis*, 8: 49–64 (1985).
2. A. Venema and J. Veurlink, *J. Anal. Appl. Pyrolysis*, 7: 207–214 (1985).
3. N. Oguri and P. Kim, *Int. Lab.*, 19: 59–62 (1989).
4. H.-R. Schulten, W. Fischer, and H.J. Walistab, *J. High Res. Chromatogr. Chromatogr. Commun.*, 10: 467–469 (1987).
5. E.M. Anderson and I. Ericsson, *J. Anal. Appl. Pyrolysis*, 3: 13–34 (1981).
6. I. Ericsson, *Chromatographia*, 6: 353–358 (1973).
7. R.S. Lehrle, J.C. Robb, and J.E. Suggate, *Eur. Polym. J.*, 8: 443–461 (1982).
8. J.B. Pausch, R.P. Lattimer, and H.L.C. Meuzelaar, *Rubber Chem. Technol.*, 56: 1031–1044 (1983).
9. T.P. Wampler and E.J. Levy, *Am. Biotechnol. Lab.*, 5: 56–60 (1987).
10. J.W. Washall and T.P. Wampler, *Spectroscopy*, 6: 38–42 (1990).
11. B. Horsfield, *Geochim. Cosmochim. Acta*, 53: 891–901 (1989).
12. P.R. Solomon, M.A. Serb, R.M. Carangelo, R. Bassilakis, D. Gravel, M. Baillargeon, F. Baudais, and G. Vail, *Energy Fuels*, 4: 319–333 (1990).
13. T.P. Wampler and E.J. Levy, *J. Anal. Appl. Pyrolysis*, 8: 153–161 (1985).
14. S. Tsuge, H. Ohtani, C. Watanabe, and Y. Kawahara, *Am. Lab.*, 35: 32–37 (2003).
15. Frontier Laboratories Ltd., Fukushima, Japan.
16. Fischer Labor-und Verfahrenstechnik, Meckenheim, Germany.
17. GSG Mess-und Analysengeräte, Bruchsal, Germany.
18. Japan Analytical Industry Co., Tokyo.
19. Pyrol AB, Lund, Sweden.
20. CDS Analytical, Inc., Oxford, PA.

3 Pyrolysis Mass Spectrometry: Instrumentation, Techniques, and Applications

C.J. Maddock and T.W. Ottley

CONTENTS

3.1	Introduction	48
3.1.1	History	48
3.1.2	Instrument Design	48
3.1.2.1	Direct Insertion Probes	48
3.1.2.2	Modified GC/MS for Pyrolysis-MS	49
3.1.2.3	Py-MS Instruments	52
3.2	Data Analysis	55
3.2.1	Multivariate Statistics	55
3.2.2	Artificial Neural Networks	57
3.3	Applications	59
3.3.1	Microbial Characterization	59
3.3.2	Organic Geochemistry	59
3.3.3	High-Value Products	59
3.3.4	Forensics	59
3.3.5	Polymers	59
3.4	Sample Preparation	60
3.4.1	Curie-Point Foils and Filament Ribbons	60
3.4.1.1	Soluble Solids	60
3.4.1.2	Insoluble Solids	60
3.4.1.3	Bacteria and Yeasts	61
3.4.1.4	Blood or Blood Cultures	61
3.4.1.5	Liquids	61
3.4.2	Curie-Point Ribbons	62
3.4.3	Curie-Point Wires	62
	References	63

3.1 INTRODUCTION

3.1.1 HISTORY

Pyrolysis-mass spectrometry (Py-MS) has found many applications in microbiology, geochemistry, and soil and polymer sciences. However, its development has been historically hindered by the lack of competitively priced instrumentation, which has restricted the number of laboratories able to use the technique. Furthermore, because of the nature and complexity of the data produced, a heavy reliance upon statistical techniques has been required for data analysis. This specific problem has benefited greatly from the development of powerful personal computers and the increased availability of suitable software, as well as the reduction in price of mass spectrometers and the production of specific libraries for pyrolysis work.

Probably the first pyrolysis-mass spectrometer was described by Meuzelaar and Kistemaker.¹ This instrument was based on a Riber quadrupole mass spectrometer and used the Curie-point pyrolysis method first described by Giacobbo and Simon.² This development eventually produced two commercial instruments — the Extranuclear 5000 (Extranuclear Laboratories, Pittsburgh, PA), effectively a copy of the FOM machine, and the Pyromass 8-80 (VG Gas Analysis, Middlewich, England), based on the same principles but using a small magnetic mass spectrometer.

Both systems were based on existing instrumentation used for conventional mass spectrometry. This made them prohibitively expensive and only a few were sold. A significant reduction in the cost of a pyrolysis-mass spectrometer could be achieved only through the development of a dedicated instrument. Subsequently, a truly dedicated and automated pyrolysis mass spectrometer, the PYMS-200X (Horizon Instruments, Sussex, England), was developed and found its principal use in microbiology. This instrument has been fully described elsewhere,³ together with typical applications.⁴⁻⁶ Applications were limited because of the mass range offered by this instrument, 12 to 200 daltons. Further development of the technique led to the production of the RApYD-400 system, with a mass range of 12 to 400 daltons, allowing more applications to be addressed.

Schulten⁷ has coupled pyrolysis with field ionization mass spectrometry (Finnigan MAT 731), providing a soft ionization technique, with the production of molecular ions after pyrolysis. This approach has been used to study complex natural materials such as coal and soil organic matter. Alternative techniques, adapting existing equipment, have also been employed, including replacing the solids probe of the mass spectrometer with a pyrolysis probe and modifying a gas chromatography-mass spectrometry (GC/MS) system to use the mass detector for pyrolysis-MS work.

3.1.2 INSTRUMENT DESIGN

3.1.2.1 Direct Insertion Probes

Many mass spectrometers, especially larger, research-oriented units (as opposed to GC detectors), are equipped with a solids probe inlet port. This is a vacuum locking inlet that permits the insertion of a solid sample on a heatable probe directly into



FIGURE 3.1 Direct insertion probes for mass spectrometers.

the ion source of the mass spectrometer. These probes are capable of heating a small sample of material to volatilize or desorb compounds, which are then ionized and produce a mass spectrum. Pyrolysis probes have been designed as direct replacements for these probes, but with a filament capable of reaching over 1000°C, so that the sample may be pyrolyzed directly into the ion source. A picture of such a pyrolysis direct insertion probe is shown in Figure 3.1. The pyrolysis probes generally utilize a sample tube inserted into a resistively heated coil, so the heating rate may be fast or slow. With fast or pulse rates, a composite mass spectrum is produced, which may be quite complex, since it contains information about all of the compounds created during pyrolysis. When the sample is heated at slower rates, a thermal separation is provided, which can help isolate compounds and give evidence of which compounds are generated at a specific temperature. This sort of experiment may be done at rates generally used for thermogravimetry, providing direct MS information regarding which compounds are evolved through a heating regime. Programmed heating also helps shed light on degradation mechanisms and in kinetic work, especially when the material degrades in several steps.

3.1.2.2 Modified GC/MS for Pyrolysis-MS

The use of a direct insertion probe for pyrolysis-MS requires that the mass spectrometer be equipped with an inlet for a solids probe. Most mass spectrometers used in analytical labs are configured as detectors for gas chromatographs and are relatively simple and inexpensive, but are rarely equipped with a probe inlet. The only way for a sample compound to enter a mass spectrometric detector is via the capillary column inlet, configured to accept a piece of fused silica. Nevertheless, if the capillary column is removed and replaced with a piece of fused silica sufficiently restrictive to limit the flow into the mass spectrometer, pyrolysis-MS data may be

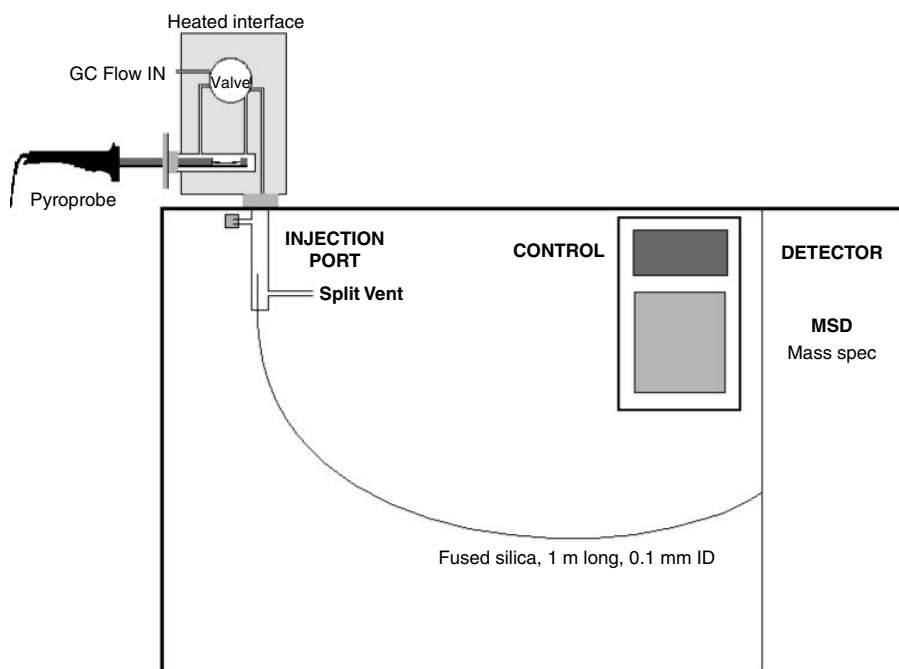


FIGURE 3.2 Modified GC for pyrolysis/MSD.

obtained. Sample loading is still controlled using the injection port splitter, so the sample is introduced into the mass spectrometer in a stream of helium at the same concentration that would be seen from a GC experiment. A 1-m length of 0.1-mm fused silica is generally sufficient to transfer sample into the mass spectrometer at a flow rate capable of being handled by the vacuum pump. A diagram of such an arrangement is shown in Figure 3.2.

The major drawback in trying to perform Py-MS using a modified GC system lies in the fact that the analytes must travel through the fused silica before they are ionized, so there is a short delay between the production of the compounds via pyrolysis and their ionization. Direct insertion systems, on the other hand, produce the pyrolysate right in the ion source. The consequence of this is that only stable molecules are seen, and early, reactive products may be missed. The same is the case for doing Py-GC/MS as well, so much useful information may still be obtained. Figure 3.3 shows a typical result obtained by pyrolyzing a piece of polystyrene directly to the mass selective detector (MSD) of an Agilent GC/MS. The run takes less than 0.5 minutes, and the inset shows the mass spectrum taken at the apex of the peak. If the heating rate is slowed, a time- (or temperature-) resolved analysis is produced. In Figure 3.4, a piece of polyurethane has been heated at 100°C/minute. A two-step evolution is evident, with the first peak consisting mostly of toluene diisocyanate, while the second peak represents oxygenated compounds resulting from the degradation of the polyol portion of the polyurethane.

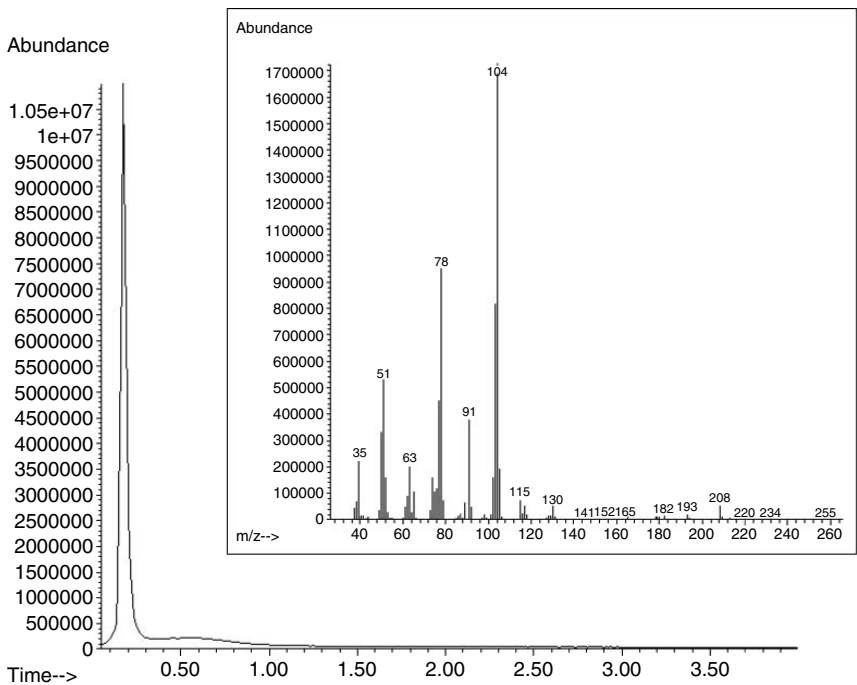


FIGURE 3.3 Pyrolysis of polystyrene at GC injector through fused silica to mass detector.

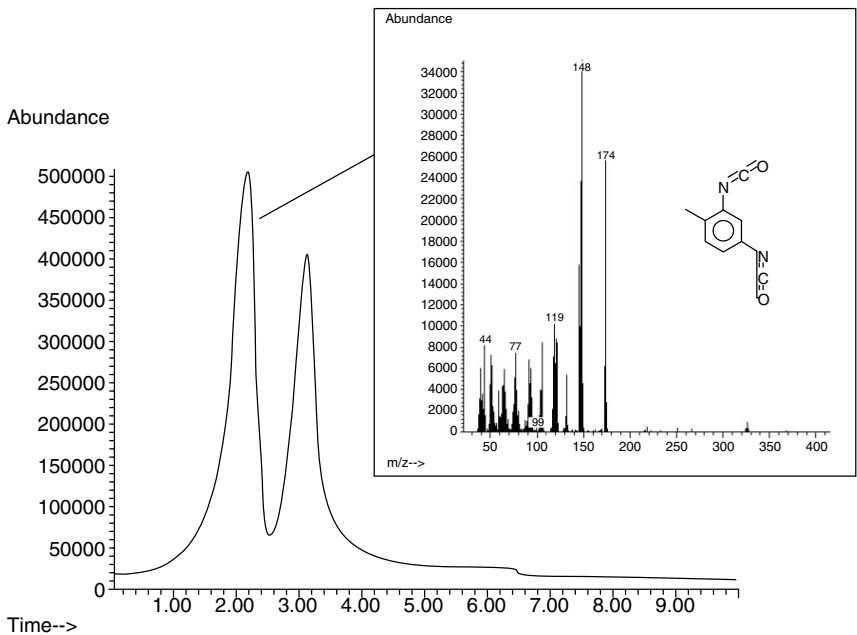


FIGURE 3.4 Polyurethane heated at 100°C/minute.

3.1.2.3 Py-MS Instruments

Pyrolysis-mass spectrometer systems produced so far have contained the common features of loading system, pyrolysis region, expansion chamber, and molecular beam before reaching the mass spectrometer ion source. The FOM Autopysms, the Pyromass 8-80, the Extranuclear 5000, and the PYMS-200X have all been detailed elsewhere.^{1,3,8} A description of the RAPyD-400 will serve to show how such dedicated instruments are configured.

The RAPyD-400 is a bench-top, quadrupole-based mass spectrometer utilizing the method of Curie-point heating for sample introduction. The system is capable of being loaded with up to 150 samples, which can then be processed unattended.

The three basic elements of the RAPyD-400 — the vacuum system, the inlet system, and the quadrupole analyzer — can be seen in Figure 3.5. The quadrupole analyzer, which itself consists of two separate parts, lies inside the main vacuum chamber. The high vacuum is attained using a turbomolecular pump, which is backed by a dual-stage rotary pump mounted externally to the main system. The sample inlet system is connected to the ion source of the mass spectrometer via a heated molecular beam tube. Around the underside of the ion source is a copper cold finger, which is cooled by liquid nitrogen and used as a sample dump to prevent carryover from one sample to another.

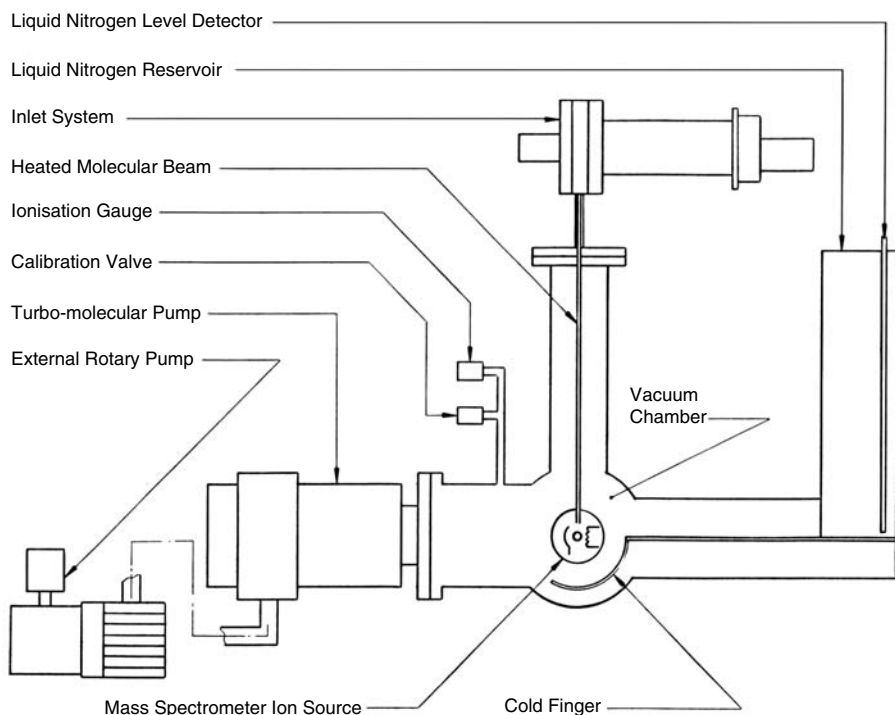


FIGURE 3.5 Vacuum system schematic for the Horizon Instruments RAPyD-400.

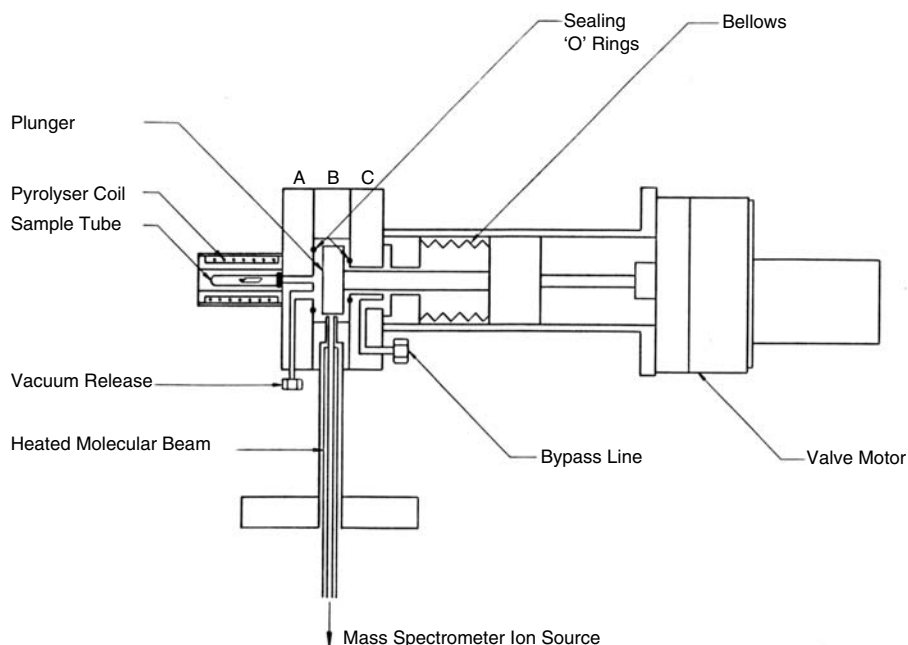


FIGURE 3.6 Inlet system for the Horizon Instruments RApD-400.

Once loaded onto the automation system, each sample tube is taken in turn and presented to the inlet system, which is detailed in Figure 3.6. The o-ring on the open end of the tube is used to form a seal on the outer face of the inlet system. Once this seal has been made, the inlet system valve plunger can move from position A to position B, where it closes off the molecular beam to the ion source and allows the air inside the glass sample tube to be evacuated via the bypass pumping line. Once this has been achieved, the plunger moves from position B to position C, closing the bypass line and opening the molecular beam tube. An expansion chamber has now been created. Once pyrolysis takes place and the resultant gas has evolved, the pyrolyzate expands into the vacant space and is then taken to the ion source via the heated molecular beam.

On arrival at the ion source, the pyrolyzate gas is subjected to bombardment by electrons with a nominal energy of 25 eV in classic EI mass spectrometry. The resultant charged molecules produced are transmitted by the quadrupole, and a mass spectrum of the pyrolysate is recorded by an electron multiplier operating in pulse-counting mode.

The pyrolysis-field ionization mass spectrometry system used by Schulten⁹ produces pyrolysis directly in the ion source. A high electric field strength between the emitter and the cathode, typically 14 kV, produces soft ionization and creates the molecular ions with little secondary fragmentation. Heating rates of about 1°C/sec permit the generation of thermograms through the heating range, in the same way that the collection of mass spectra from a detector produce a total ion chromatogram in GC/MS.

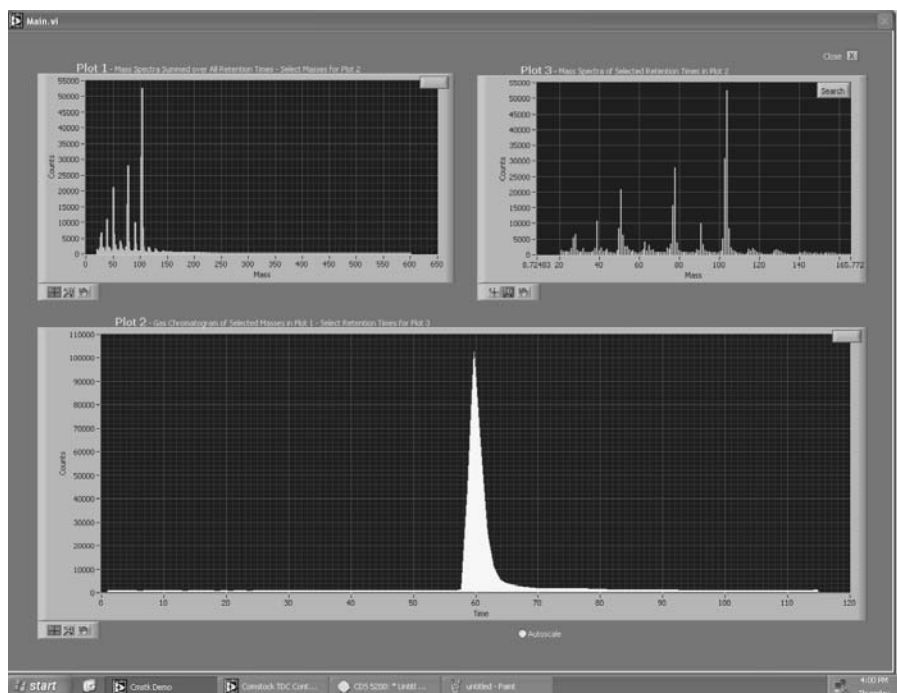


FIGURE 3.7 PyTOF analysis of styrene/butadiene copolymer at 750°C.

As in the example using the oven of the gas chromatograph as a heated transfer zone from the pyrolyzer to the mass spectrometer, any mass spectrometer that is compatible with a heated inlet could be used to make a direct pyrolysis-mass spec system. Havey et al.¹⁰ have taken this approach in creating a microfabricated pyrolyzer interfaced to a quadrupole ion trap mass spectrometer. Time-of-flight mass spectrometers (TOF MSs), for example, are also easily adapted to such a direct pyrolysis MS interfacing. Figure 3.7 shows the screen of a TOF analysis (Comstock MiniTOF, Oak Ridge, TN) of a sample of a styrene/butadiene copolymer. The inlet to the mass spectrometer was a piece of 0.1-mm fused silica, which was connected to a filament pyrolyzer with a heated interface. The lower window shows the composite peak produced when the copolymer was heated to 750°C for a few seconds. The upper windows show the averaged spectra for the whole experiment on the left and a selected spectrum on the right. The copolymer was 85% styrene, and the mass spectrum contains a large peak at mass 104 for styrene (as well as the other masses produced from styrene) and a peak at 39, a prominent mass in the spectrum of butadiene. Figure 3.8 shows a comparison of the spectra from two different styrene/butadiene copolymers, 28% styrene on the top and 85% styrene on the bottom, produced with this system. The ability to produce clearly different spectra even from copolymers using the same monomers permits the creation of spectral libraries for the pyrolysates of various polymers. These libraries may be edited and searched using the same software used for searching the spectra of individual peaks in a

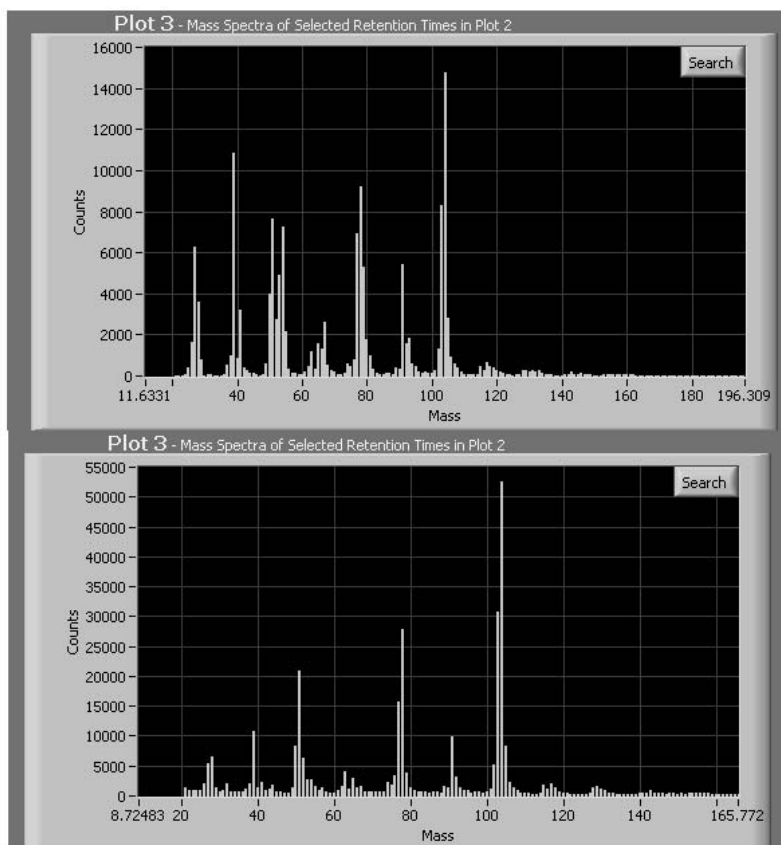


FIGURE 3.8 PyTOF spectra of two styrene/butadiene copolymers. Top, 28% styrene; bottom, 85% styrene.

chromatogram. The differences between the spectra generated from similar sample materials are the basis for many of the Py-MS applications, some of which may necessitate more sophisticated computer analysis to derive the distinctions and associations required.

3.2 DATA ANALYSIS

3.2.1 MULTIVARIATE STATISTICS

Chemometrics is the application of numerical techniques to the identification of, or discrimination between, chemical substances. Expressed more simply, it is the attempt to make relatively simple quantitative measurements and then to use the

data obtained in various ways to give the maximum amount of information regarding the differences between samples.

In truth, most analytical methods make use of the concept of chemometrics, at least to some extent, but some techniques are much more suitable than others. Obviously, all forms of spectroscopy can yield a large amount of numerical data, but mass spectroscopy is ideally suited for two reasons.

In a mass spectrum, ions are recorded over a certain mass range, but within that range (at low to medium resolution) only integer mass values are possible, the separation between peaks corresponding approximately to the mass of a neutron.

Second, it is possible to make use of single ion counting methods to record an actual numerical result (the number of ions) directly at each mass position. Thus, a two-dimensional data matrix is the immediate result.

Multivariate statistical methods as part of the general chemometrics discipline are particularly well suited for the analysis of complex mass spectra. An excellent introduction to these techniques has been written by Manly.¹¹

One of the main reasons for using multivariate statistics is to reduce a large amount of very complex data down to a form where it can be readily understood. This usually means that any graphical output needs to be in two or three dimensions only. In effect, this means using principal components, canonical variates, and clustering analyses.

Principal components analysis is a well-established multivariate statistical technique that can be used to identify correlations within large data sets and to reduce the number of dimensions required to display the variation within the data. A new set of axes, principal components (PCs), are constructed, each of which accounts for the maximum variation not accounted for by previous principal components. Thus, a plot of the first two PCs displays the best two-dimensional representation of the total variance within the data. With pyrolysis mass spectra, principal components analysis is used essentially as a data reduction technique prior to performing canonical variates analysis, although information obtained from principal components plots can be used to identify atypical samples or outliers within the data and as a test for reproducibility.

Canonical variates (CVs) analysis is the multivariate statistical technique that takes into account sample replication or any other *a priori* structure within the data and attempts to discriminate between the sample groups. CVs are derived in a manner similar to that of PCs except that their axes are constructed to maximize the ratio of between-group to within-group variance. Thus, a plot of the first two CVs displays the best two-dimensional representation of the sample group discrimination. Examination of the associated mass loadings/weightings allows chemical interpretation. Large mass loadings reflect masses significant to the discrimination in a particular direction. The application of graphical rotation facilitates the construction of factor spectra showing the contribution of masses to the discrimination of a specific sample group. Factor spectra are often representative of pure compounds or classes of components aiding chemical interpretation of the observed discrimination.

The use of hierarchical cluster analysis leading to the construction of dendrograms and minimum spanning trees for data sets where the samples analyzed have

a high degree of relatedness is often the most useful way to display the total discrimination within the data because all the variance is displayed in two dimensions.

Although there are other multivariate techniques that can be applied to mass spectral data, the ones discussed here tend to be the most widely applied. In reality, there are more checks on validity that are made at different stages. This is to avoid any lack of confidence in the results obtained.

3.2.2 ARTIFICIAL NEURAL NETWORKS

A related approach to multivariate statistics is the use of artificial neural networks (ANNs), which are by now a well-known means of uncovering complex, nonlinear relationships in multivariate data. ANNs can be considered collections of very simple computational units, which can take a numerical input and transform it (usually via a weighted summation) into an output.¹²⁻¹⁴ The relevant principle of supervised learning in ANNs is that they take numerical inputs (the training data) and transform them into desired (known, predetermined) outputs. The input and output nodes may be connected to the external world and to other nodes within the network. The way in which each node transforms its input depends on the so-called connection weights (or connection strengths), which are modifiable. The output of each node to another node or to the external world then depends on both its weight strength and the weighted sum of all its inputs, which are then transformed by a (normally nonlinear) weighting function referred to as its activation function. For the present purposes, the great power of neural networks stems from the fact that it is possible to train them. Training is effected by continually presenting the networks with the known inputs and outputs and modifying the connection weights between the individual nodes, typically according to a back-propagation algorithm, until the output nodes of the network match the desired outputs to a stated degree of accuracy. The network, the effectiveness of whose training is usually determined in terms of the root mean square (RMS) error between the actual and the desired outputs averaged over the training set, may then be exposed to unknown inputs and will immediately output the best fit to the outputs. If the outputs from the previously unknown inputs are accurate, the trained ANN is said to have generalized.

The reason this method is so attractive to pyrolysis-mass spectroscopy (Py-MS) data is that it has been shown mathematically¹⁵ that a neural network consisting of only one hidden layer, with an arbitrary large number of nodes, can learn any arbitrary (and hence nonlinear) mapping to an arbitrary degree of accuracy. ANNs are also considered to be robust to noisy data, such as that which may be generated by Py-MS.

A neural network usually consists of three layers, representing inputs, output, and a hidden layer, which is used to make the connections (Figure 3.9). By training a neural network with known data, it is possible to obtain outputs that can accurately predict such things as polymer concentration mix.

ANNs can be trained using pyrolysis-mass spectra as the inputs and the known concentrations of target analytes as the outputs. For each input (one mass spectrum), there should normally be one output. The trained network can then be tested with

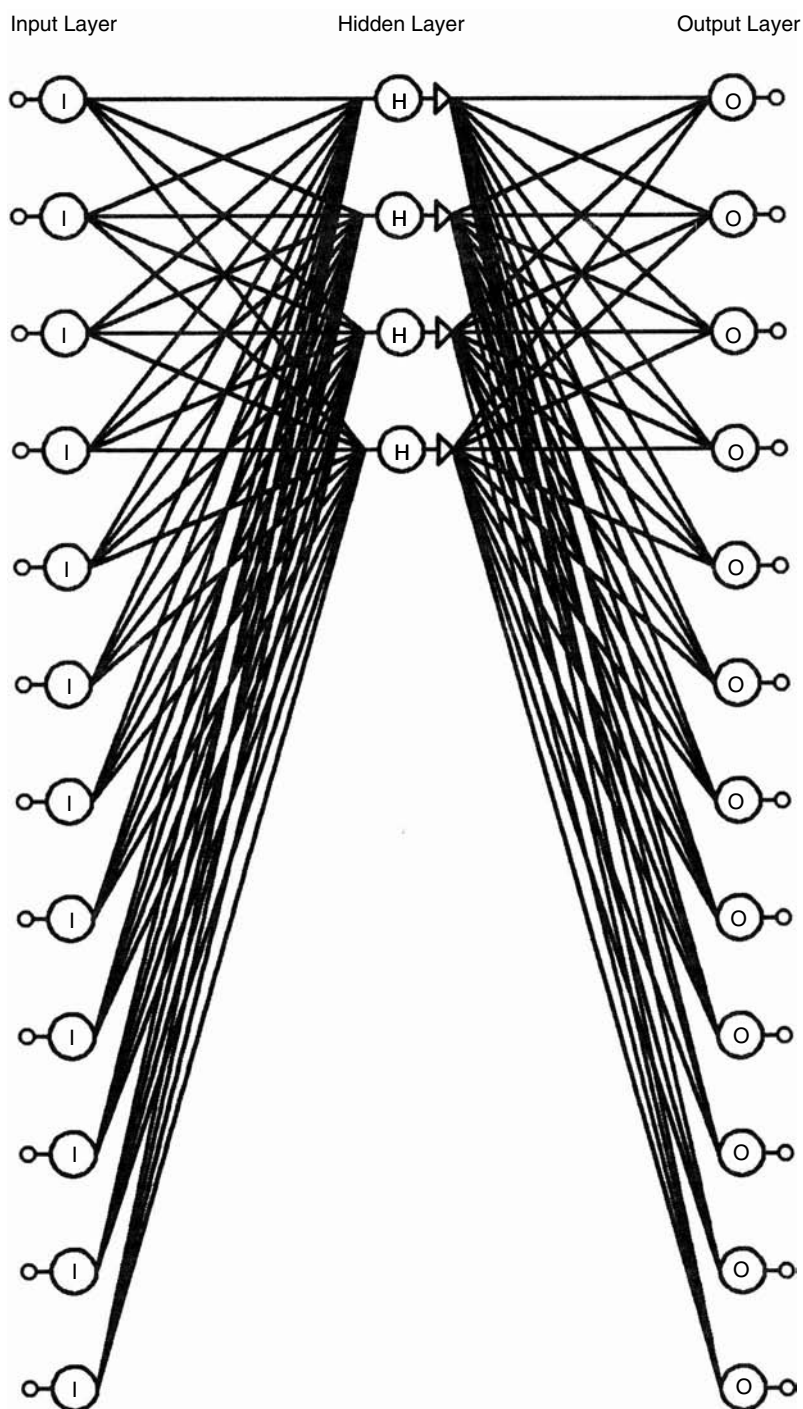


FIGURE 3.9 Typical artificial neural network structure.

the pyrolysis-mass spectra of unknowns to accurately predict the concentration or authenticity of the unknowns.

3.3 APPLICATIONS

3.3.1 MICROBIAL CHARACTERIZATION

The rapid accurate discrimination and characterization of microorganisms is the goal of many diagnosticians. Py-MS has proven to be a rapid and inexpensive epidemiological typing technique, applicable to a wide range of bacterial pathogens, and it can be used to identify the source of an infectious outbreak as well as giving an assessment of the relatedness of bacterial isolates.^{5,16,17} Work has been done on whole cells¹⁸ and in the detection of *Bacillus* spores.¹⁰

3.3.2 ORGANIC GEOCHEMISTRY

The characterization of sedimentary organic matter in terms of type and maturity is a prerequisite in the determination of the petroleum-generating potential of sediments. The nonextractable material, the kerogen, consisting of complex high-molecular-weight fragments, when subjected to Py-MS and multivariate analysis, gives excellent discrimination into the three universally recognized types.¹⁹ Coals^{20,21} have been studied extensively from the standpoint of product formation and structure. The organic material in soils has also been investigated by pyrolysis-MS, including contributions from plants to soil carbon,²² humic acids,⁹ and fatty acids.²³

3.3.3 HIGH-VALUE PRODUCTS

Authentication and the detection of adulteration are serious problems within the citrus juice industry. Traditional multicomponent analysis methods are limited by the time required to perform the individual analyses and to construct the database required. Py-MS rapidly provides fingerprints of the original juice, which facilitates the use of multivariate pattern recognition procedures to detect potentially adulterated samples and to confirm authentication, as well as helping in quality control. More recently, the combination of Py-MS and ANNs has been applied to problems of adulteration within the olive oil industry,²⁴ shellfish,²⁵ and milk.²⁶

3.3.4 FORENSICS

In applications for the characterization of car, house, and fine art paints, Py-MS is valuable in obtaining quick and reproducible fingerprints that can subsequently be matched for identification purposes, whether it be by the forensic scientist or the polymer chemist.²⁷

3.3.5 POLYMERS

Identification involving the comparison of pyrograms by library matching²⁸ or multivariate analysis allows an unknown sample to be compared with standard materials

in both basic research and quality control. Underlying information concerning backbone structures based on monomer, dimer, and trimer ratios, etc., can be elucidated from the pyrograms.^{29,30}

3.4 SAMPLE PREPARATION

The techniques of pyrolysis-mass spectrometry and gas chromatography both rely upon a good physical contact between the sample to be analyzed and the supporting material. Over the years, various shapes of materials have been developed to hold samples prior to pyrolysis. Many of these methods have been described elsewhere.^{8,31,32}

In all aspects of sample preparation, cleanliness is of vital importance. The aim in preparing a sample is to obtain a thin coating of material over the inside surfaces of a foil (which is formed into a V), around the surface of a wire, crimped in a ribbon or placed onto a filament, with between 5 and about 25 μg dry weight. The method for doing this depends on the type of sample.

3.4.1 CURIE-POINT FOILS AND FILAMENT RIBBONS

3.4.1.1 Soluble Solids

Many substances may be dissolved in either water or an organic solvent. The technique is to dissolve sufficient material so that a conveniently small volume of solution will contain the right amount of solid. This concentration is normally a few milligrams per milliliter. Using a 10- μl syringe, extract about 3 μl of solution and place along the inside fold of the sample foil, if using a Curie-point pyrolyzer, or directly onto the foil or ribbon of a resistively heated filament pyrolyzer. Ensure that the liquid does not run over the edges of the foil or ribbon. Even with 5 μl this is not too difficult, but the addition may be made stepwise if desired. Solvent may be dried by gently heating the Curie-point foil or using the dry function of the filament unit. Once dry, push the sample Curie-point foil into the tube using a depth gauge. The same depth gauge should be used for all samples. By ensuring that all the samples lie in the same position within the induction coil, another potential variable is removed. When using resistively heated filaments, the sample should be applied to the center of the ribbon each time for the same reason.

3.4.1.2 Insoluble Solids

The method here is similar to that preceding, except that the material must first be ground down to a fine powder, using, for example, a pestle and mortar, and then kept in suspension while being pipetted onto the foil or ribbon. A suitable suspension medium is either water or acetone, and ultrasonic agitation will keep the fine particles in suspension. This method is particularly attractive for samples such as glycogen.

In applications where profiling (fingerprinting) is more important than any form of quantification, powdered materials can be mixed into a paste with water or a suitable solvent. The paste can then be smeared onto the foil or ribbon, and the water/solvent evaporated in a drying oven for Curie-point foils, or by using the dry function for filaments.

Alternatively, for materials such as rubber and other polymers, a small piece of the material may be crimped with a heavy pair of forceps to hold the sample in the Curie-point foil. Once released, foils can be inserted into glass sample tubes with the same pair of forceps and positioned using a depth gauge. For resistively heated filaments, the sample may be placed onto the ribbon, which is then heated quickly to melt or fix the sample to the surface of the filament.

For samples such as paint chips, fibers, minerals, and so on, which are difficult to grind or suspend and are not soluble, an alternative is to place the sample into a quartz tube that is surrounded by either a coil of ferromagnetic material for Curie-point units or resistive wire for filaments.

3.4.1.3 Bacteria and Yeasts

In the case of actively growing colonies on plates, all that is necessary is to pick up a small portion with a disposable loop or flamed wire and smear on both inside faces of the Curie-point foil or on top of the filament ribbon. Avoid picking up any of the substrate with the culture. With a little practice, it is possible to obtain the correct amount of material (20 μg) without difficulty. For some bacteria, particularly those in the Actinomycetes family, it is preferential to grow them on a filter placed on top of the medium. This will also prevent the media from being sampled with the colony.

In the preparation of the glass tubes, quartz tubes, and foils prior to sample loading, it is important that none are touched by hand. The method described by Sanglier et al.⁵ has proven to work well for foils used inside glass tubes. In this method, pyrolysis foils and tubes are washed in acetone, then dried overnight at 27°C. A single foil is inserted, with flamed forceps, into each pyrolysis tube so as to protrude about 6 mm from the mouth. The tubes may then be stored at 80°C in a clean, dry oven or vacuum dessicator until needed. For each strain, small amounts of biomass (25 μg) are scraped from three different areas of the inoculated plate and smeared onto the protruding foil. The assembled foils are placed in an 80°C oven for 15 minutes to dry the biomass.

Liquid cultures can be handled in a way similar to that of suspended solids in that they can be pipetted onto foils or ribbons. Cultures presented on slopes can be treated as if they had been plated out.

3.4.1.4 Blood or Blood Cultures

These may be treated in the same way as soluble compounds, but the volume of liquid applied to the foil should be much less (1 to 2 μl). Also, the samples should not be dried in warm air; instead, they should be left in a vacuum dessicator for a short time.

3.4.1.5 Liquids

Many liquids requiring analysis will in fact be solutions but often too dilute to use directly. In the case of whiskey, for example, the concentration must first be increased by a factor of 10 before a sample can be taken. This can be done by blowing a jet of dry nitrogen over the surface of about 10 ml of liquid contained in a beaker and

evaporating down to 1 ml. This takes about 30 minutes. Three microliters of the concentrate may then be applied to the foil or ribbon and allowed to dry. Alternatively, the whole 10-ml aliquot can be evaporated to dryness and then reconstituted with 1 ml of the original sample. Either of these two methods should be used in preference to dispensing 10 individual 3- μ l aliquots on top of each other once the previous aliquot has dried.

In liquid samples, such as fruit juice, olive oil, and milk, the concentration of dissolved solids is sufficient that no preconcentration is required.

3.4.2 CURIE-POINT RIBBONS

For some solid samples it may be more convenient to use a Curie-point ribbon sample carrier. These ribbons take the place of wires in instruments specifically designed to take them.

Taking a ribbon with the folding lines facing upwards and a flat-ended pair of pliers, fold up the two sides until they are vertical. At this stage it may be advisable to clean the ribbons before further use.

Place a sample of material in the ribbon and then fold down both sides to cover the sample, making a tent. Now fold the long end of the ribbon completely over the top of the tent and squeeze gently.

Most of these ribbons are made from pure iron, so they need to be protected from water vapor. As supplied, they are normally packed under argon, which should prevent oxidation. After initial folding and cleaning, it may be preferable to store them in a pure solvent — hexane is recommended for this purpose.

3.4.3 CURIE-POINT WIRES

For solutions, suspensions, and sticky materials (bacteria, resins, etc.), it is quite acceptable to use a straight ferromagnetic wire as the sample holder. For solid samples, a wire has to be prepared in such a way as to be able to firmly hold the sample in place.

Coating of a wire evenly with a solution or suspension is most desirable to enhance reproducibility. To this end, the use of wire coating units is of great help.¹ This can be achieved by rotating the wires slowly about their axes while applying the liquid medium. As the solvent evaporates, a uniform coating is deposited, which aids reproducibility. Up to six wires can be prepared at a time. Wires are held by the end 10 mm with tweezers or pliers and inserted into one of the holes in the guide plate at the front of the wire coater. The wire then pushes into a small socket, which will hold it firmly. This part of the wire can be cut off before analysis, so slight contamination is not important at this stage. With the rotation speed set to a mid-value, solutions of approximately 3 μ l are applied using a small syringe or pipette, one drop at a time, to the same position on each wire. After a short time the coating will form uniformly as the solvent evaporates. If necessary, rotation speed can be varied to improve the uniformity of coating.

REFERENCES

1. H.L.C. Meuzelaar and P.G. Kistemaker, Techniques for fast and reproducible fingerprinting by pyrolysis mass spectrometry, *Anal. Chem.*, 45: 587 (1973).
2. H. Giacobbo and W. Simon, Technique for pyrolysis and subsequent gas chromatographic analysis of samples smaller than a microgram, *Pharm. Acta Helvetica*, 39: 162 (1964).
3. R.E. Aries, C.S. Gutteridge, and T.W. Ottley, Evaluation of a low cost, automated pyrolysis-mass spectrometer, *J. Anal. Appl. Pyrolysis*, 9: 81–98 (1986).
4. K. Orr, F.K. Gould, P.R. Sisson, N.F. Lightfoot, R. Freeman, and D. Burdess, Rapid interstrain comparison by pyrolysis mass spectrometry in nosocomial infection with *Xanthomonas malthophilia*, *J. Hosp. Infect.*, 17: 187–195 (1991).
5. J.J. Sanglier, D. Whitehead, G.S. Saddler, E.V. Ferguson, and M. Goodfellow, Pyrolysis mass spectrometry as a method for the classification and selection of actinomycetes, *Gene*, 115: 235–242 (1992).
6. R. Goodacre, D.B. Kell, and G. Bianchi, Olive oil quality control by using pyrolysis mass spectrometry and artificial neural networks, *Oliva*, 47 (1993).
7. H.-R. Schulten, Biochemical, medical and environmental applications of field ionization and field desorption mass spectrometry, *Int. J. Mass Spectrom. Ion Phys.*, 32: 97 (1979).
8. W.J. Irwin, *Analytical Pyrolysis: A Comprehensive Guide*, Marcel Dekker, New York (1982).
9. H.-R. Schulten, in *Humic and Fulvic Acids: Isolation, Structure and Environmental Role*, ACS Symposium Series 651, Washington, D.C., J. Gaffney, N. Marley, and S. Clark, Eds., ACS, 42–56, 1996.
10. C.D. Havey, F. Basile, C. Mowry, and K.J. Voorhees, Evaluation of a micro-fabricated pyrolyzer for the detection of *Bacillus anthracis* spores, *J. Anal. Appl. Pyrolysis*, 72: 55–62 (2004).
11. B.J.F. Manly, *Multi-variate Statistical Methods*, Chapman & Hall, London (1986).
12. P.D. Waiserman, *Neural Computing: Theory and Practice*, Von Nostrand-Reinhold, New York (1989).
13. D.E. Rumelhart, J.L. McClelland, and the PDP Research Group (Eds.), *Parallel Distribution Processing: Experiments in the Microstructure of Cognition*, Vol. 2. Cambridge, MA: MIT Press (1986).
14. J. Hertz, A. Krogh, and R.G. Palmer, *Introduction to the Theory of Neural Computation*, Addison-Wesley, CA (1991).
15. K. Hosnik, M. Stinchcombe, and M. White, Universal approximation of an unknown mapping and its derivatives using multilayer feed-forward networks, *Neural Net.*, 3: 551–560 (1990).
16. L.A. Shute, C.S. Gutteridge, J.R. Norris, and R.C.W. Berkeley, Curie-point pyrolysis mass spectrometry applied to characterization and identification of selected *Bacillus* species, *J. Med. Microbiol.*, 130: 343–355 (1984).
17. R. Freeman, F.K. Gould, R. Wilkinson, A.C. Ward, N.F. Lightfoot, and P.R. Sisson, Rapid inter-strain comparison by pyrolysis mass spectrometry of coagulase: negative staphylococci from persistent CAPD peritonitis, *Epidemiol. Infect.*, 106: 239–246 (1991).
18. P. Mketova, C. Abbas-Hawks, K.J. Voorhees, and T.L. Hadfield, Microorganism Gram-type differentiation of whole cells based on pyrolysis-high resolution mass spectrometry data, *J. Anal. Appl. Pyrolysis*, 67: 109 (2003).

19. T.I. Eglinton, S.R. Larter, and J.J. Boon, Characterization of kerogens, coals and asphaltenes by quantitative pyrolysis mass spectrometry, *J. Anal. Appl. Pyrolysis*, 20: 25–45 (1991).
20. N.E. Vanderborgh, J.M. Williams, and H.-R. Schulten, Volatilization processes during heating of coals and model polymers, *J. Anal. Appl. Pyrolysis*, 8: 271–290 (1985).
21. N. Simmleit, Y. Yun, H.L.C. Meuzelaar, and H.-R. Schulten, in *Advances in Coal Spectroscopy*, H.L.C. Meuzelaar, Ed., Plenum Publishing, New York (1992).
22. Y. Kuzyankov, P. Leinweber, D. Sapronov, and K. Eckhardt, *J. Plant Nutr. Soil Sci.*, 166: 719–723 (2003).
23. G. Jandi, P. Leinweber, H.-R. Schulten, and K. Eusterhues, The concentrations of fatty acids in organo-mineral particle-size fractions of a Chernozem, *Eur. J. Soil. Sci.*, 55: 459 (2004).
24. R. Goodacre, D.B. Kell, and G. Bianchi, Olive oil quality control by using pyrolysis mass spectrometry and artificial neural networks, *Olivae*, 47: 36–39 (1993).
25. M. Cardinal, C. Viallon, C. Thonat, and J.-L. Berdague, Pyrolysis-mass spectrometry for rapid classification of oysters according to rearing area, *Analusis*, 28: 825–829 (2000).
26. R. Goodacre, Use of pyrolysis mass spectrometry with supervised learning for the assessment of the adulteration of milk of different species, *Appl. Spectrosc.*, 51: 1144–1153 (1997).
27. D.A. Hickman and I. Jane, Reproducibility of PyMS using three different pyrolysis systems, *Anahyst*, 104: 334–347 (1979).
28. K. Qian, W. Killinger, and M. Casey, Rapid polymer identification by in-source direct pyrolysis mass spectrometry and library searching techniques, *Anal. Chem.*, 68: 1019–1027 (1996).
29. C.J. Curry, Pyrolysis mass spectrometry studies of adhesives, *J. Anal. Appl. Pyrolysis*, 11: 213–225 (1987).
30. W.A. Westail, Temperature programmed pyrolysis mass spectrometry, *J. Anal. Appl. Pyrolysis*, 11: 3–14 (1987).
31. RAPyD-400 Pyrolysis Mass Spectrometer Instruction Manual, Horizon Instruments Ltd.
32. Curie-Point Pyrolyser Instruction Manual, Horizon Instruments Ltd.

4 Microstructure of Polyolefins

Shin Tsuge and Hajime Ohtani

CONTENTS

4.1	Introduction	65
4.2	Instrumentation for Pyrolysis Hydrogenation-Gas Chromatography	65
4.3	Analysis of Polyolefins	66
4.3.1	Short-Chain Branching in LDPE	66
4.3.2	Microstructures of Polypropylenes	71
4.3.3	Sequence Distribution in Ethylene-Propylene Copolymers	77
	References	80

4.1 INTRODUCTION

Among the most commonly utilized synthetic polymers are polyolefins, such as polyethylenes (PEs), polypropylenes (PPs), and ethylene-propylene copolymers (P(E-co-P)s). Despite their simple elemental compositions, consisting of only carbon and hydrogen, it is well known that their physical properties are quite dependent on the microstructural features, such as short- and long-chain branchings, stereoregularities, chemical inversions of monomer enchainment, sequence distributions, etc.¹

The structural characterization of polyolefins has been carried out most extensively by means of molecular spectroscopy, such as Fourier-transform infrared (FT-IR), ¹H-nuclear magnetic resonance (NMR), and ¹³C-NMR.¹ On the other hand, high-resolution pyrolysis-gas chromatography (Py-GC), which incorporates the pyrolysis-hydrogenation technique and high-resolution capillary column separation, provides a simple but powerful technique to study the microstructures of polyolefins.²⁻⁴ In this chapter, the instrumental aspects of high-resolution Py-hydrogenation GC (Py-GC) are first discussed briefly, and then its applications to the rapid estimation of short-chain branchings in low-density PEs, stereoregularity differences and chemical inversions of the monomer units in PPs, and the study of sequence distributions in P(E-co-P)s are demonstrated.

4.2 INSTRUMENTATION FOR PYROLYSIS HYDROGENATION-GAS CHROMATOGRAPHY

When saturated polyolefins such as PE and PP are exposed to high temperatures under an inert atmosphere, they yield various hydrocarbon fragments that reflect

the microstructures of the original polymers. These consist mainly of a series of α,ω -diolefins, α -olefins, and n-alkanes. If some short-chain branches exist in the polymer chain, the resulting degradation products are further complicated by additional diastereomeric, geometrical, and positional isomers. Thus, the number of possible isomers becomes large in those fragments as a function of the containing carbon atoms, with the result that complete chromatographic separation is not an easy task, even when a high-resolution capillary column is extremely useful.

Figure 4.1 illustrates a flow diagram for a typical pyrolysis-hydrogenation capillary column gas chromatographic system, which was developed in the authors' laboratory.⁴⁻⁶ In the inlet liner between the furnace-type pyrolyzer and the splitter, a hydrogenation catalyst, Diasolid H (80-0 mesh), coated with 5 wt% of Pt was packed. If necessary, a precut region containing the same packing material but coated with an ordinary polydimethylsiloxane liquid phase was put in the upper region of the inlet. This precut would protect the activity of the catalyst and the high efficiency of the capillary column from tarry or nonvolatile degradation products that decrease resolution. Both the precut and the catalyst in the inlet were maintained at 200°C. About 0.1 to 0.5 mg of the polymer sample was pyrolyzed, typically at 650°C under a flow of hydrogen carrier gas (50 ml/min), which was also used as the hydrogenation gas. A fused-silica or a deactivated stainless steel capillary column was used in a temperature programming mode over a range typically extending from 40 to 300°C at a rate of 5°C/min. A flame ionization detector (FID) was used for the peak detection in the pyrograms, and the peak assignment was mostly carried out by a directly coupled gas chromatography-mass spectrometry (GC/MS) system.

Employing this technique, not only do the resulting pyrograms of polyolefins become extremely simple, but they are also highly resolved, since those peaks of both α -olefins and α,ω -diolefin with the same carbon number are combined into the associated alkane peak and geometrical isomers are extinguished. This situation is illustrated in Figure 4.2 as the change in the pyrogram of a low-density PE (LDPE) and in Figure 4.3 for the typical C_{13} products of PP before and after hydrogenation.

4.3 ANALYSIS OF POLYOLEFINS

4.3.1 SHORT-CHAIN BRANCHING IN LDPE

The probable model branching structures for practically utilized PEs are illustrated in Figure 4.4. Among them, LDPEs, which are synthesized in the high-pressure method, are known to have both short-chain branching (SCB) and long-chain branching (LCB). According to the polymerization mechanisms, the former SCB consists mostly of ethyl (C_2), butyl (C_4), and amyl (C_5); methyl (C_1), propyl (C_3), and larger than hexyl ($>C_6$), if any, are minor components. The type and concentration of SCB in LDPEs, which vary according to the polymerization conditions, affect many properties of these polymers. Therefore, the characterization of SCB plays a very important role in clarifying the structure-property relations for LDPEs.

Although quantitative analyses of SCB have been extensively studied by ^{13}C -NMR spectroscopy, such analyses require fairly long measuring times (from hours to days)

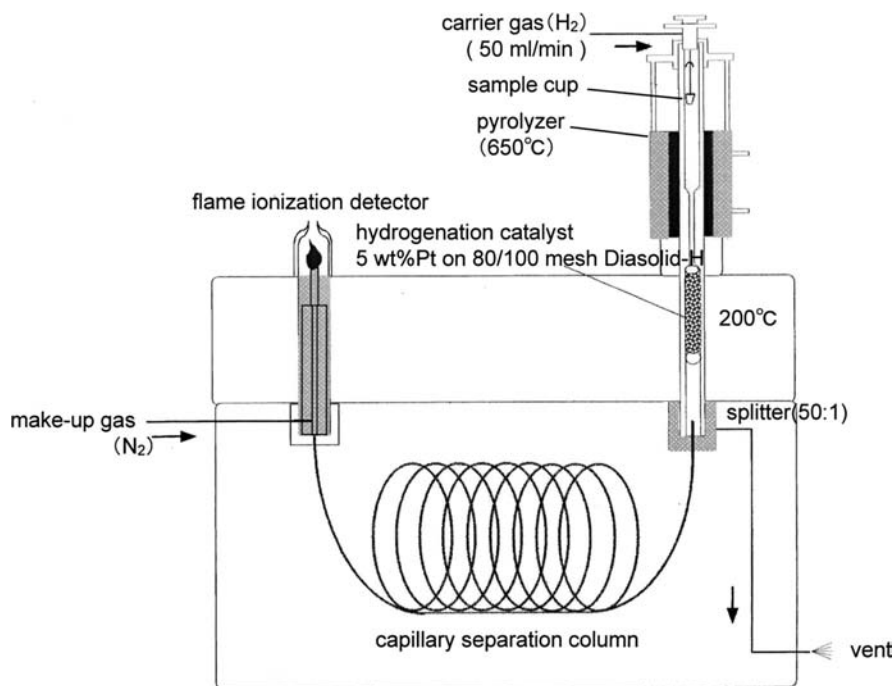
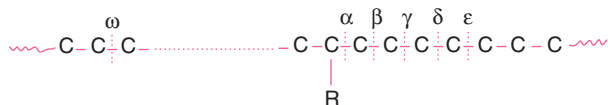


FIGURE 4.1 Schematic flow diagram for high-resolution pyrolysis-hydrogenation gas chromatographic system.

and relatively large sample sizes (10–100 mg).^{7,8} In contrast, Py-GC requires a minimum sample size (about 0.1 mg) during a simple and rapid (about 1 h) operation.

As shown in Figure 4.2, the pyrogram of LDPE without hydrogenation (A) consists mainly of serial triplets corresponding to α,ω -diolefins, α -olefins, and n -alkanes with additional weak but heavily complexed isoalkane, isoalkene, and isoalkadiene peaks between the strong serial peaks. After hydrogenation (B), these triplets are simplified into singlets of the corresponding n -alkanes and various isoalkanes that are characteristic of the SCB in the LDPE.^{5,9–11}

Figure 4.5 shows a typical high-resolution pyrogram of an LDPE measured by use of the in-line hydrogenation technique.¹² As shown in the expanded pyrogram in Figure 4.5 for the C₁₁ components, the isoalkane peaks, which reflect the SCB, are clearly separated between the serial n -alkane peaks, which are mostly attributed to the longer methylene sequences in the LDPE. Such isoalkanes are formed through combination of two thermal scissions along the polymer chain containing the SCB:



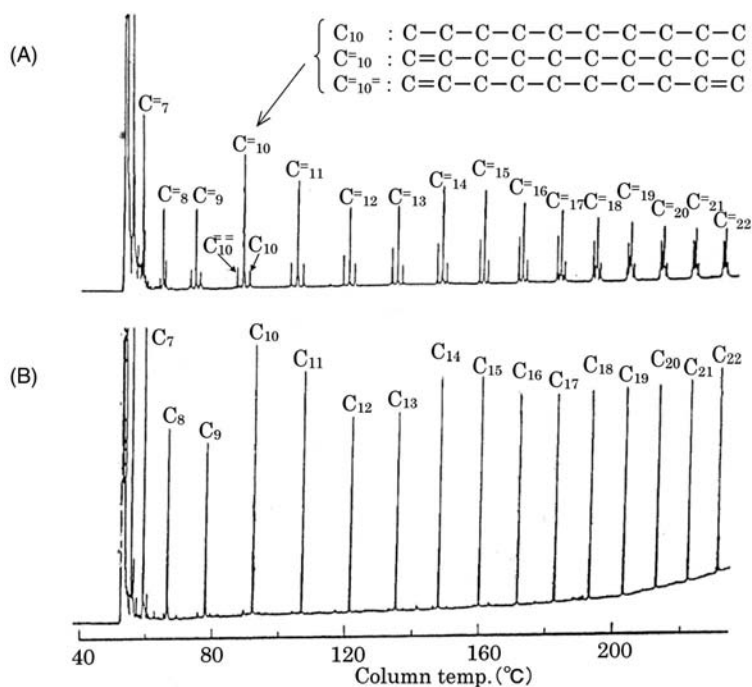


FIGURE 4.2 Typical high-resolution pyrograms of low-density PE before (A) and after (B) hydrogenation.⁵

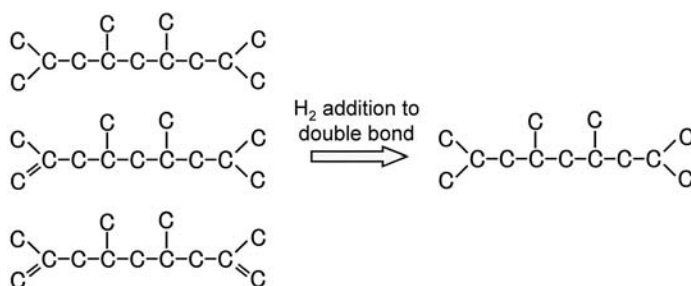


FIGURE 4.3 Hydrogenation of C_{13} pyrolysis products of PP.

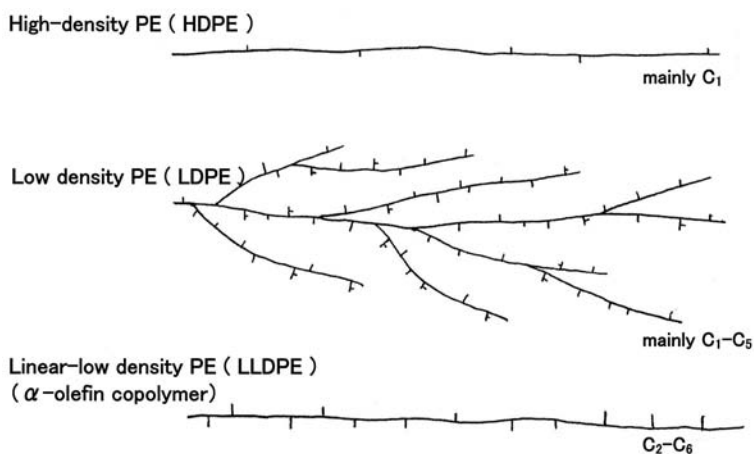


FIGURE 4.4 Probable branching structures for various PEs.

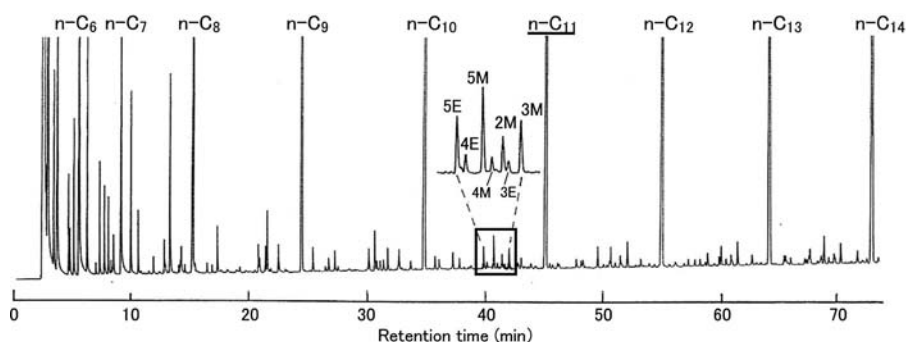


FIGURE 4.5 Typical high-resolution hydrogenated pyrogram of LDPE at 650°C. 2M, 2-methyldecane; 3M, 3-methyldecane; 4M, 4-methyldecane; 5M, 5-methyldecane; 3E, 3-ethylnonane; 4E, 4-ethylnonane; 5E, 5-ethylnonane [12]. (From H. Ohtani et al., *Macromolecules* 17: 2558–2559 (1984). With permission.)

In the case of a methyl branch ($R=CH_3$), for instance, α and ω , β and ω , γ and ω , δ and ω , and ϵ and ω scissions followed by hydrogenation would yield n-alkane, 2-methyl-, 3-methyl-, 4-methyl-, and 5-methyl-isoalkanes, respectively. Similarly, from the moiety of possible SCBs (C_1 to C_6), the corresponding isoalkanes are expected to occur.

Figure 4.6 shows the typical portions of the expanded pyrograms around C_{11} fragments for a LDPE and those of five model copolymers for methyl, ethyl, butyl, amyl, and hexyl branches.¹² Once relative peak intensities characteristic of the SCBs are determined using well-defined model polymers with known amounts of possible SCBs, the relative abundance of the SCBs in the LDPE can easily be estimated by the peak simulation of the observed isoalkane peaks in the pyrogram of the LDPE.^{12–15}

Table 4.1 summarizes the SCB contents obtained by this method for the four LDPEs, along with those found by ^{13}C -NMR spectroscopy.¹² As a whole, the estimated individual short branch contents and the total values are in fairly good agreement with

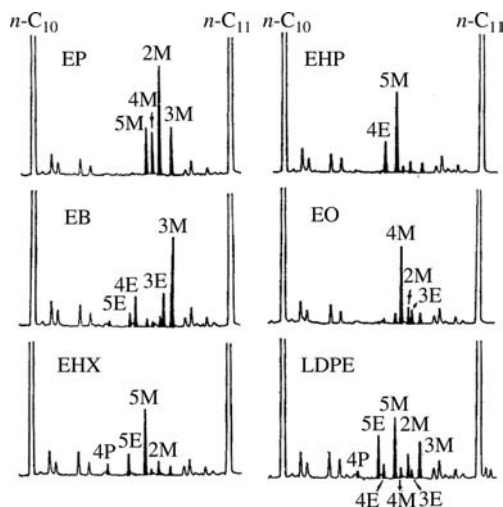


FIGURE 4.6 Expanded hydrogenated pyrograms of ethylene-propylene (EP), ethylene-1-butene (EB), ethylene-1-hexene (EHX), ethylene-1-heptene (EHP), and ethylene-1-octene (EO) reference copolymers and LDPE in the C_{11} region. 2M, 3M, 4M, 5M, 3E, 4E, and 5E are the same as those in Figure 4.5, and 4P is 4-propyloctane [12]. (From H. Ohtani et al., *Macromolecules* 17: 2558–2559 (1984). With permission.)

TABLE 4.1

Estimated SCB Contents in Low-Density Polyethylenes [12]

Sample	Short Chain Branches/1000 C ^a						Total ^c
	Methyl	Ethyl	Butyl	Amyl	Hexyl	Longer ^b	
LDPE-A	1.3 (0.4)	4.9 (6.4)	8.3 (7.4)	2.3 (2.6)	0.2	(2.8)	17.0 (19.9)
LDPE-B	1.5 (0.5)	7.2 (7.2)	11.2 (8.5)	2.2 (2.7)	0.3	(3.5)	22.4 (24.9)
LDPE-C	1.3 (0.5)	4.8 (5.4)	8.6 (6.4)	1.9 (2.2)	0.4	(2.4)	17.0 (17.3)
LDPE-D	1.0 (0.1)	2.1 (2.3)	4.5 (2.4)	0.6 (0.7)	0.3	(0.1)	8.5 (6.7)

^a Data in parentheses are obtained by ^{13}C -NMR.

^b Longer branches than C_7 are not considered in the case of Py-HGC.

^c Values by ^{13}C -NMR involve the propyl branch content between 0.2 and 0.5.

Source: H. Ohtani et al., *Macromolecules* 17: 2558–2559 (1984). With permission.)

those obtained by ^{13}C -NMR spectroscopy. Thus, the high-resolution Py-GC combined with in-line hydrogenation is an effective tool for the determination of the SCB with short analysis time and minimal amounts of sample, and can detect SCB even at concentrations as low as a few per 10,000 carbons.¹⁴ In addition, the existence of pair or branched branches in the LDPEs is also suggested.^{12,16} This technique was also successfully applied to study the SCB distributions as a function of molecular weight for a given LDPE sample¹⁷ and to determine the SCB content in polyvinyl chloride after the hydrogen substitution of the chlorine atoms in the polymer chain.^{6,14}

TABLE 4.2
Possible Pyrolysis Fragments of PP

Fragments	Chemical Structure(s) [C*: Asymmetric C]	Enantiomers	Diastereoisomers
Monomer	$\begin{array}{c} \text{C}=\text{C} \\ \\ \text{C} \end{array}$	X	X
Dimer	$\begin{array}{c} \text{C}=\text{C}-\text{C}-\text{C} \\ \quad \\ \text{C} \quad \text{C} \end{array}$	X	X
Trimer	$\begin{array}{c} \text{C}=\text{C}-\text{C}-\text{C}^*-\text{C}-\text{C} \\ \quad \quad \\ \text{C} \quad \text{C} \quad \text{C} \end{array}$	○	X
Tetramer	Meso (m): $\begin{array}{c} \text{C}=\text{C}-\text{C}-\text{C}^*-\text{C}-\text{C}^*-\text{C}-\text{C} \\ \quad \quad \quad \\ \text{C} \quad \text{C} \quad \text{C} \quad \text{C} \end{array}$	○	⊙
	Racemo (r): $\begin{array}{c} \text{C} \\ \\ \text{C}=\text{C}-\text{C}-\text{C}^*-\text{C}-\text{C}^*-\text{C}-\text{C} \\ \quad \quad \\ \text{C} \quad \text{C} \quad \text{C} \end{array}$		

4.3.2 MICROSTRUCTURES OF POLYPROPYLENES

Many physical solid and solution properties of PPs are keenly affected not only by the average molecular weight and the molecular weight distribution, but also by the configurational characteristics, such as the average stereoregularity, stereospecific sequence length, and degree of chemical inversions of the monomer units along the polymer chains. The in-line hydrogenation technique combined with highly efficient separation by a capillary column was also successfully applied to the conformational characterization of various PPs with different stereospecificity.^{18–22}

Before going into further discussion, Table 4.2 summarizes the relation between the possible pyrolysis products of PP and the information of the original stereoregularity. If the polymer sample decomposes into monomers and dimers, information about the stereoregularity is completely lost. As for trimers, the stereospecific information in the polymer chain is also missing, although there are enantiomers. In the case of tetramers, which provide diastereoisomers, meso and racemo, the information about the original stereoregularities is to be preserved in the fragments. Hence, to study the stereoregularity of PP, the tetramer or larger products in the observed pyrograms should be examined.

Here the possible pentamer components (C_{14} to C_{16}) are illustrated in Figure 4.7 to explain the complicated diastereoisomers formed from the thermal degradation of PPs followed by hydrogenation. As was predicted by this figure, the observed C_{14} , C_{15} , and C_{16} triads on the pyrogram in Figure 4.8 are actually composed of a triplet (mm, mr, rr), a quartet (mm, mr, rm, rr), and a triplet (mm, mr, rr), respectively, where m and r are meso and racemo conformations, respectively.¹⁹

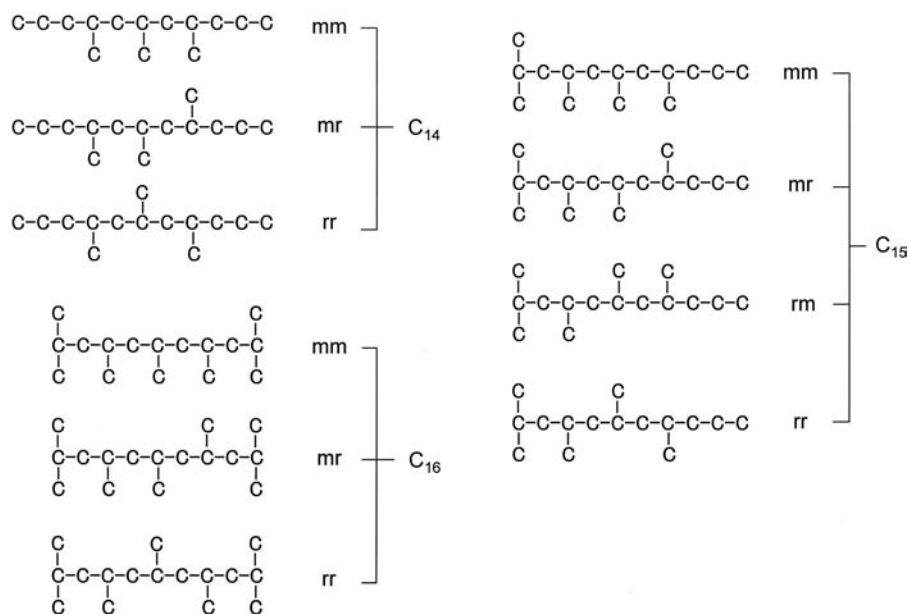


FIGURE 4.7 Possible diastereomeric isomers for the pentamer clusters of C_{14} , C_{15} , and C_{16} . m and r are meso and racemo configurations, respectively [19].

For example, the authors studied PP samples with a variety of stereoregularity synthesized in the presence of different types of Zeigler–Natta (ZN) or metallocene (ML) catalysts, that is, five kinds of isotactic-PP (ZN- $I_{1,2}$ and ML- I_{1-3}), two types of atactic-PP (ZN-A and ML-A), and five kinds of syndiotactic-PP (ZN-S and ML- S_{1-4}). Figure 4.8 illustrates hydrogenation pyrograms of isotactic-PP (ZN- I_2), atactic-PP (ML-A), and syndiotactic-PP (ML- S_1) at 650°C separated by a fused-silica capillary column (0.25 mm i.d. \times 100 m) coated with polydimethylsiloxane.^{20–22} On the pyrogram of isotactic-PP, a series of triplet peaks with long isotactic sequences are observed up to the decads (C_{35} to C_{37}), while the intensities of the peaks associated with syndiotactic and atactic sequences become negligibly small at the higher carbon number regions. These data suggest that the isotactic-PP (ZN- I_2) has fairly long isotactic sequences. Similarly, on the pyrogram of syndiotactic-PP (ML- S_1), fairly intense characteristic triplet series associated with long syndiotactic sequences can be seen up to the nonads (C_{32} to C_{34}). On the other hand, on the pyrogram of atactic-PP (ML-A), complex atactic multiplets are observed up to the decads (C_{35} to C_{37}).

From the relative peak intensities among the tetramers and the pentamers, %m and %r ($r + m = 100\%$), and %mm, %mr + %rm, and %rr ($mm + mr + rm + rr = 100\%$) can be estimated. Then, the average tactic sequence lengths in propylene units can be calculated from the following equation:

$$N_s = 2 \frac{\%r}{\%mr}, N_i = 2 \frac{\%m}{\%mr}$$

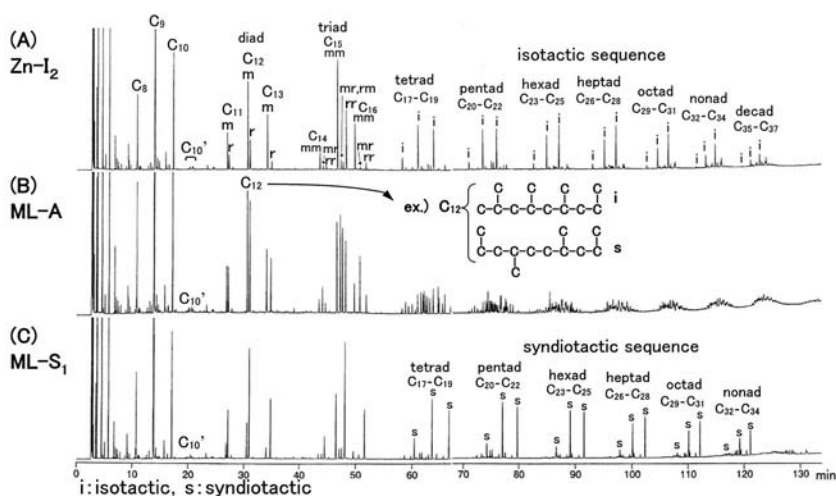


FIGURE 4.8 Typical high-resolution hydrogenated pyrograms of (A) isotactic PP (ZN-I₂), (B) atactic-PP (ML-A), and syndiotactic-PP (ML-S₁). i, s, and h represent isotactic, syndiotactic, and heterotactic products, respectively [22].

where N_s and N_i are the average syndiotactic and isotactic sequence lengths, respectively.²³

Figure 4.9 shows two partial pyrograms for atactic-PP, ZN-A, and ML-A, which are almost comparable (50%) in %m and %r.²² Expectedly, the meso and racemo pair peaks of the tetramer region show almost the same intensities for both PP samples. However, it is interesting to note that the relative intensities of heterotactic peaks (mr and rm) against those of mm and rr in pentamer region are still comparable for ML-A, while the heterotactic peak intensities for ZN-A are significantly weaker than those of ML-A. These data suggest that ML-A is a typical atactic PP whose N_s and N_i are relatively smaller, while ZN-A has longer tactic sequences. This result is also supported by the data in Table 4.3, in which the observed values of N_s and N_i by Py-HGC using the data of C₁₃ tetramers and C₁₆ pentamers are in fairly good agreement with those obtained by ¹³C-NMR.^{20–22}

In practical use of PP materials, a small difference in the stereoregularity in highly isotactic PP is often critical. Nowadays, pentad tacticity of PP is generally evaluated by ¹³C-NMR. On the other hand, the pentad tacticity in PP was also estimated more sensitively and rapidly by Py-HGC.²² Figure 4.10 shows the expanded pyrogram of atactic PP (ML-A) and 10 possible kinds of diastereoisomeric structures for C₂₂ products reflecting the pentad tacticity. Thus, the original pentad tacticity in the PP sample should be estimated from the relative peak intensities in the heptamer (C₂₀ to C₂₂) region. Unfortunately, it is difficult to isolate all the peaks in this region of the pyrogram observed by a flame ionization detector and in the total ion chromatogram mode of MS, mainly because the products with different carbon numbers should partially overlap each other, as shown in Figure 4.10.

The C₂₂ products, therefore, were selectively observed by Py-HGC-MS in mass chromatograms at $m/z = 310$, corresponding to the molecular ion of C₂₂ products.

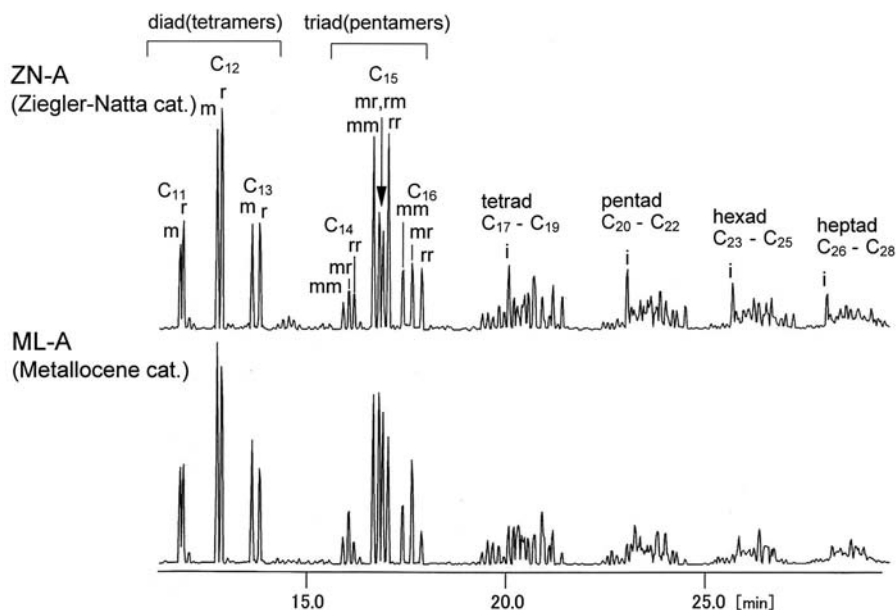


FIGURE 4.9 Detailed pyrograms of two atactic-PP samples, ZN-A and ML-A for tetramer (C_{11} - C_{13}) and pentamer (C_{14} - C_{16}) regions [22].

TABLE 4.3
Estimated Average Syndiotactic
Sequence Length (N_s) and Isotactic
Sequence Length (N_i) by Py-HGC
and ^{13}C -NMR [21,22]

PP Sample	Py-HGC		^{13}C -NMR	
	N_s	N_i	N_s	N_i
ML-I ₁	1.7	5.0		
ML-I ₃	5.2	31.9	2	65
ML-A	1.6	2.2	2	2
ML-S ₁	25.2	4.6	65	1
ML-S ₄	19.2	4.6	48	3
ZN-I ₂	5.7	39.8	2	198
ZN-A	2.8	2.9		
ZN-S	10.5	4.7	8	3

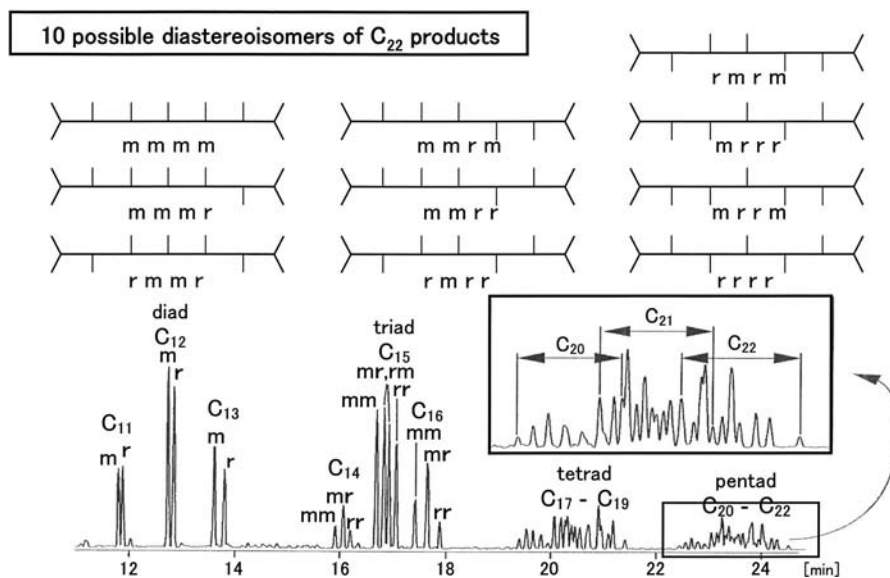


FIGURE 4.10 Expanded pyrogram of atactic PP (ML-A) and possible diastereoisomeric structures of C_{22} products reflecting pentad tacticity.

Figure 4.11 shows the typical pyrograms of several PP samples in the mass chromatogram mode at $m/z = 310$. For the sample ML-A, 10 peaks are clearly separated in the mass chromatogram that correspond to the number of possible C_{22} products. The pentad tacticity of these 10 peaks can be assigned as shown in Figure 4.11 based on the general tendency for elution (the products with the meso-structure elute faster) and the observed peak intensities for the PP samples with various stereospecificities.

Figure 4.12 illustrates a relationship between the relative peak intensities of isotactic pentad (mmmm fractions) obtained by Py-HGC and ^{13}C -NMR. Although the values by Py-HGC were slightly smaller, probably due to the stereoisomerization during pyrolysis,²¹ quite good linear relation was observed in the whole range of stereoregularity. In particular, a slight difference in the isotactic pentad for the highly isotactic region (mmmm fraction is more than 90%) was also able to be evaluated by Py-HGC using a trace amount of sample and relatively short measuring period. This feature is suitable for the characterization of the PP materials in practical use.

So far in the discussion of the stereoregularity in PPs, only the repeated head-to-tail (H-T) structures were assumed. However, it has been pointed out that the regioirregular (head-to-head (H-H) and tail-to-tail (T-T)) structures (chemical inversions) should exist together with a 1,3-addition structure along the polymer chain to some extent depending on the polymerization conditions.¹ Among the degradation products from PPs, those larger than pentamers ($>C_{11}$) should pertain not only to the positional, but also to the diastereomeric isomers. Therefore, C_{10} components, which exclusively reflect the differences in the positions of methyl groups, were carefully separated to determine the chemical inversions of the monomer units.¹⁹⁻²¹

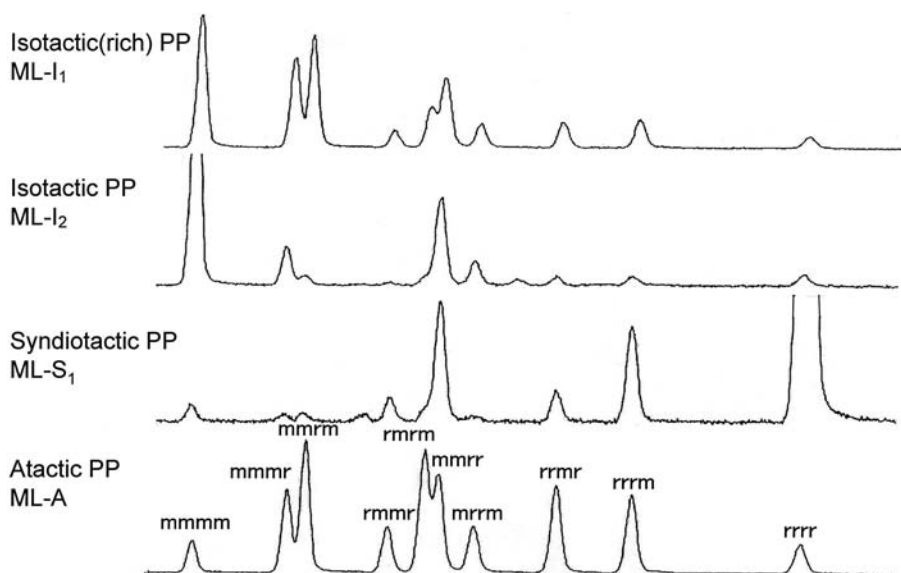


FIGURE 4.11 Expanded mass chromatograms of pyrolysis products from PP samples with different stereoregularity at m/z 310 corresponding to C_{22} products.

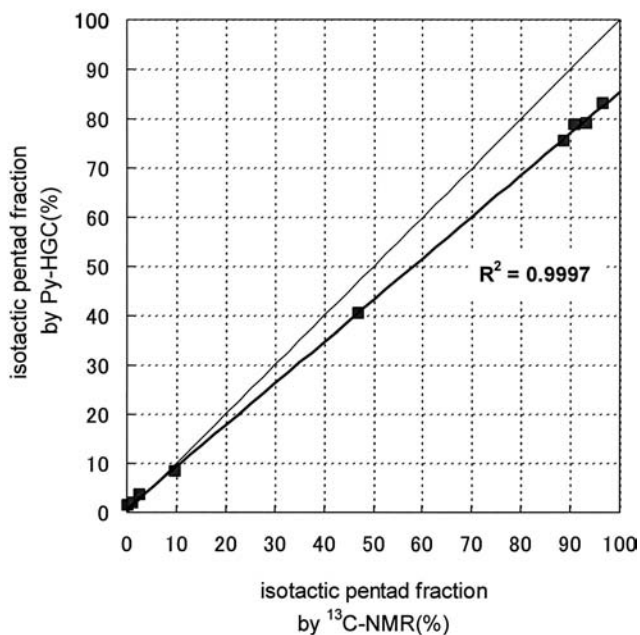


FIGURE 4.12 Relationship between the isotactic pentad fractions estimated by Py-HGC and ^{13}C -NMR. Diagonal lines represent an ideal relation.

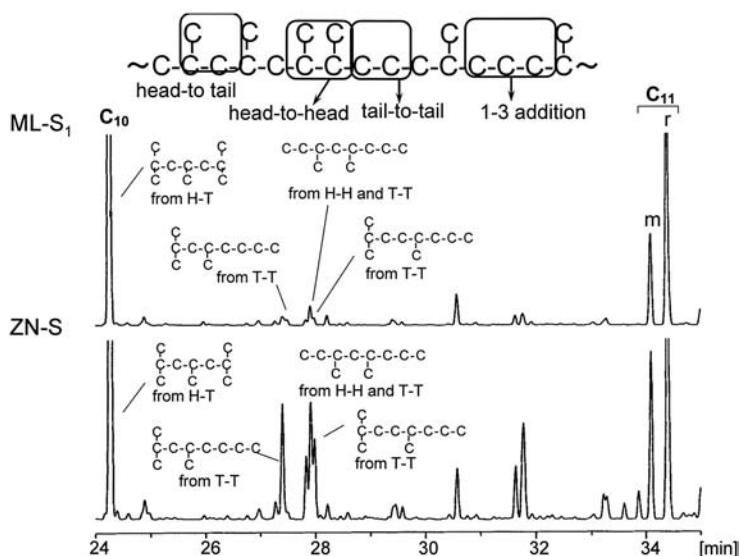


FIGURE 4.13 Expanded pyrograms for the C₁₀ region for the highly syndiotactic PPs prepared with metallocene (ML) and Ziegler-Natta (ZN) type catalyst.

Figure 4.13 shows the expanded pyrogram for the C region for highly syndiotactic PPs prepared using a Ziegler-Natta and a metallocene catalyst (ML-S₁ and ZN-S). Among the observed peaks in this region, the main fragment representing the successive H-T structure is 2,4,6-trimethylheptane (peak C), while the other minor products are mostly associated with either H-H or T-T structures, possibly along with a 1,3-addition structure to some extent. From the relative peak intensities between these clearly separated C peaks, the amounts of the chemical inversions (regioirregularity) in PPs can be estimated.

Figure 4.14 shows the relationships between the observed %T-T for the various PPs and the %r in the C₁₃ tetramers, which is a measure of their syndiotactic nature.^{20,21} From these data, it is apparent that the syndiotactic PPs prepared with the vanadium-based Ziegler-Natta (ZN) catalyst system (ZN-S) have many more chemical inversions than those prepared with the titanium-based ZN catalyst system (ZN-Is and ZN-A). It is very interesting to note that the amounts of chemical inversions increase as the syndiotacticity for PP prepared with ZN catalyst rises. This fact suggests that the majority of chemical inversions exist in the syndiotactic portions formed during polymerization using ZN-type catalyst, while the catalytic control with isotactic-specific propagation yield mostly H-T linkages. On the other hand, as for the metallocene catalyst system, the degree of chemical inversion is almost unchanged regardless of the tacticity.

4.3.3 SEQUENCE DISTRIBUTION IN ETHYLENE-PROPYLENE COPOLYMERS

As shown in Figure 4.15, the pyrogram of P(E-co-P)s generally consists of the peaks associated with those from PE, PP, and hybrid products of ethylene and propylene

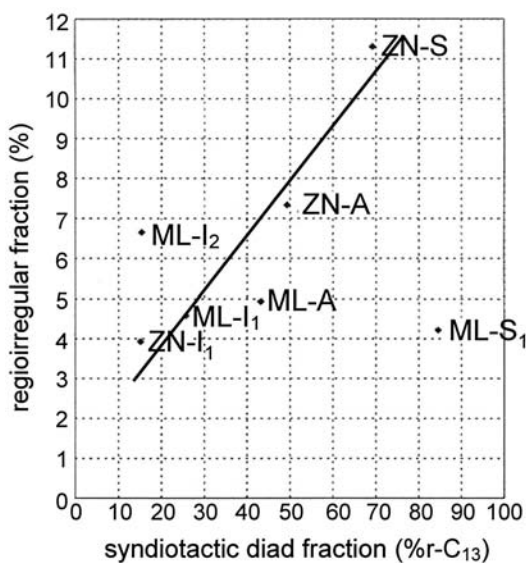


FIGURE 4.14 Relationships between observed tail-to-tail % and syndiotacticity for various PPs.

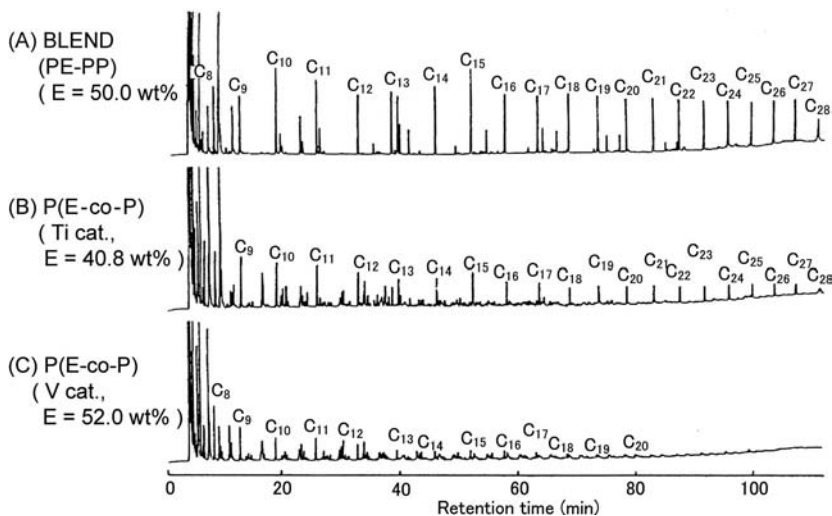


FIGURE 4.15 High-resolution hydrogenated pyrograms of (A) blend (PE-PP), (B) P(E-co-P) obtained by Ti catalyst, and (C) P(E-co-P) obtained by V catalyst [24]. (From Y. Tsuge et al., *J. Anal. Appl. Pyrol.* 1: 226-228 (1980). With permission.)

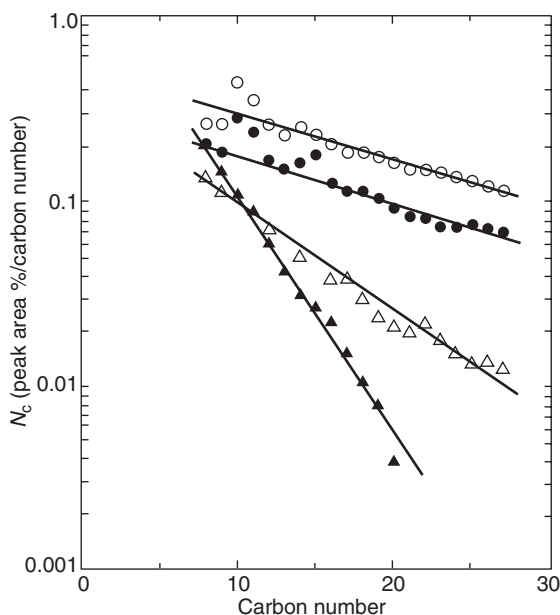


FIGURE 4.16 Relationships between carbon number and molar yield (N_c) for the series of n -alkane peaks on the pyrograms of P(E-co-P)s and the related polymers at 650°C. ○, PE; ●, blend (PE/PP=50/50 wt %); △, P(E-co-P)(Ti catalyst, E = 40.8 wt %); ▲, P(E-co-P)(V catalyst, E = 52.0 wt %) [24]. (From Y. Tsuge et al., *J. Anal. Appl. Pyrol.* 1: 226-228 (1980). With permission.)

units.²⁴ Here it is interesting to note that the P(E-co-P) sample synthesized with the use of a Ti catalyst shows much stronger serial n -alkane peaks than the sample synthesized in the presence of a V catalyst, despite the fact that the latter has higher ethylene content than the former. This is closely associated with the sequence distribution of ethylene units in the polymer chain.

In order to illustrate the difference in the ethylene sequences in the P(E-co-P)s, the relationships between carbon number and the relative molar yields (N_c) for the serial n -alkane peaks on the pyrogram of the copolymers are shown in Figure 4.16, together with that for PE and a blend of PE and PP. The intensities of n -alkane peaks on the pyrogram of PE are known to decrease as a semilogarithmic function against the carbon number of the n -alkanes, since random scission is predominating the thermal degradation of PE.²⁵⁻²⁸ Naturally, the physical blend of PE and PP shows a gentle slope almost equivalent to PE itself. On the other hand, the steeper the slope, the shorter the average sequence length of ethylene units in the P(E-co-P)s. Hence, this method should be effective for comparing the average sequences in the copolymer system containing ethylene units.

REFERENCES

1. S. van der Ven, *Polypropylene and Other Polyolefins: Polymerization and Characterization*, Studies in Polymer Science 7, Elsevier, Amsterdam, (1990).
2. J. van Scotten and J.K. Evenhuis, *Polymer*, 6: 343 (1965).
3. L. Michajlov, P. Zugenmaier, and H.-J. Cantow, *Polymer*, 12: 70 (1971).
4. S. Tsuge, *Trends Anal. Chem.*, 1: 87 (1981).
5. Y. Sugiura and S. Tsuge, *Macromolecules*, 12: 512 (1979).
6. S. Mao, H. Ohtani, S. Tsuge, H. Niwa, and M. Nagata, *Polym. J.*, 31: 79 (1999).
7. T. Usami and S. Takayama, *Macromolecules*, 17: 1756 (1984).
8. J.C. Randall, *J. Macromol. Sci. Rev. Macromol. Chem. Phys.*, C29: 201 (1989).
9. M. Seeger and E.M. Barrall II, *J. Polym. Sci. Polym. Chem. Ed.*, 13: 1515 (1975).
10. D.H. Ahlstrom and S.A. Liebman, *J. Polym. Sci. Polym. Chem. Ed.*, 14: 2478 (1976).
11. O. Mlejnek, *J. Chromatogr.*, 191: 181 (1980).
12. H. Ohtani, S. Tsuge, and T. Usami, *Macromolecules*, 17: 2557 (1984).
13. Y. Sugimura, T. Usami, T. Nagaya, and S. Tsuge, *Macromolecules*, 14: 1787 (1981).
14. S.A. Liebman, D.H. Ahlstrom, W.H. Starnes, Jr., and F.C. Schilling, *J. Macromol. Sci.-Chem.*, A17: 935 (1982).
15. J. Tulisalo, J. Seppala, and K. Hastbacka, *Macromolecules*, 18: 1144 (1985).
16. M.A. Haney, D.W. Johnston, and B.H. Clampitt, *Macromolecules*, 16: 1775 (1983).
17. T. Usami, Y. Gotoh, S. Takayama, H. Ohtani, and S. Tsuge, *Macromolecules*, 20: 1557 (1987).
18. M. Seeger and H.-J. Cantow, *Makromol. Chem.*, 176: 2059 (1975).
19. Y. Sugimura, T. Nagaya, S. Tsuge, T. Murata, and T. Takeda, *Macromolecules*, 13: 928 (1980).
20. S. Tsuge and H. Ohtani, *Analytical Pyrolysis, Technique and Applications*, K.J. Voorhees, Ed., Butterworth, London, p. 407 (1984).
21. H. Ohtani, S. Tsuge, T. Ogawa, and H.-G. Elias, *Macromolecules*, 17: 465 (1984).
22. H. Ohtani, K. Kamimoto, and S. Tsuge, to be published.
23. B.D. Coleman and T.G. Fox, *J. Polym. Sci. A*, 1: 3183 (1963).
24. S. Tsuge, Y. Sugimura, and T. Nagaya, *J. Anal. Appl. Pyrol.*, 1: 221 (1980).
25. M. Seeger, H.-J. Cantow, and S. Marti, *Z. Anal. Chem.*, 276: 267 (1975).
26. M. Seeger and H.-J. Cantow, *Makromol. Chem.*, 176: 1411 (1975).
27. M. Seeger and R.J. Gritter, *J. Polym. Sci. Polym. Chem. Ed.*, 15: 1393 (1977).
28. M. Seeger and H.-J. Cantow, *Polym. Bull.* 1: 347 (1979).

5 Degradation Mechanisms of Condensation Polymers: Polyesters and Polyamides

Hajime Ohtani and Shin Tsuge

CONTENTS

5.1	Introduction	81
5.2	Polyesters	81
5.3	Polyamides	89
	References	101

5.1 INTRODUCTION

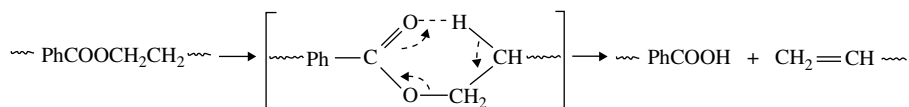
Polymer characterization by analytical pyrolysis often necessitates a detailed understanding of how polymer degradation proceeds by heating *in vacuo* or in an inert atmosphere. Yet it is not an easy task to elucidate the degradation pathway of condensation polymers with heteroatoms in their backbone chains, because thermal degradation yields a number of complex polar compounds.¹ However, recent developments have provided highly specific pyrolysis devices, advanced gas chromatographs (GCs), and mass spectrometers (MSs) and specific identification of pyrolysis products by GC/MS systems. Consequently, it has become feasible, to a large extent, to deduce the complex thermal degradation behavior of condensation polymers using analytical pyrolysis methods such as pyrolysis-GC (Py-GC) and pyrolysis-MS (Py-MS). In this chapter, the thermal degradation of two types of typical condensation polymers — polyesters and polyamides — is discussed, focusing on the mechanisms of pyrolysate formation mainly under flash pyrolysis conditions, in which the polymer sample is rapidly exposed to elevated temperatures of 500°C or more.

5.2 POLYESTERS

Poly(alkylene terephthalate)s such as poly(ethylene terephthalate) (PET) and poly(butylene terephthalate) (PBT) are widely used in the fields of fibers and thermoplastics. Homologous series of poly(alkylene terephthalate)s — PET, poly(tri-

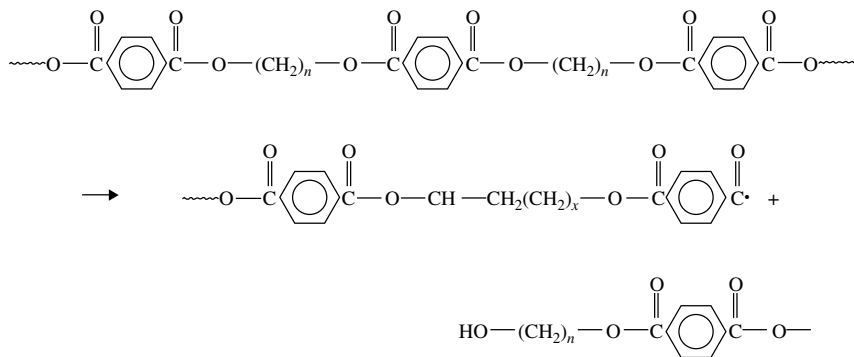
methylene terephthalate) (PTT), PBT, poly(pentamethylene terephthalate) (PPT), and poly(hexamethylene terephthalate) (PHT) — have been studied by Py-GC.^{2,3} Figure 5.1a to e illustrates the high-resolution pyrograms of PET, PTT, PBT, PPT, and PHT, respectively.³ The assignments of the characteristic peaks and their relative yields are listed in Table 5.1. The pyrograms show analogous patterns. The fragments containing two terephthalic acid units (g and h), with high molecular weight (up to 494), provide information about relatively long sequences in the polymer chain. These were observed on the pyrograms by using a thermally stable and chemically inert fused-silica capillary separation column (FSCC).

It has been proposed that the degradation of these polyesters is initiated by random scission of the ester linkages, through a six-membered cyclic transition state, to give an alkenyl and a carboxyl end group:⁴⁻⁶



Furthermore, at elevated temperatures used for flash pyrolysis, the acid-form terminals are often somewhat reduced to the more stable phenyl terminals by elimination of carbon dioxide. Thus, the main pyrolysis products are composed of compounds with alkenyl, phenyl, or carboxyl end groups reflecting the polymer structure. However, the dibasic acids, such as terephthalic acid, which are also expected to form, were not detected. This is due to their high polarity — even when using FSCC — while the fragments with an acid end group were observed as clearly separated peaks (i and j). On the other hand, α - and ω -dienes are most likely formed among the low boiling point products from PBT, PPT, and PHT through the cyclic transition state at two neighboring ester linkages.⁷ On the basis of the results described above, the common degradation pathways of poly(alkylene terephthalate) are summarized in Figure 5.2.³

The same basic degradation pathways were reported for PET and PBT by other Py-GC^{8,9} and Py-MS¹⁰⁻¹⁶ studies. In addition, tetrahydrofuran was observed as one of the major products from PBT.^{9,13} Furthermore, another pathway involving the transfer of a hydrogen atom with CO-O bond scission to yield a hydroxyl end group was also indicated by Py-electron impact ionization (EI)-MS as follows:^{11,12,14}



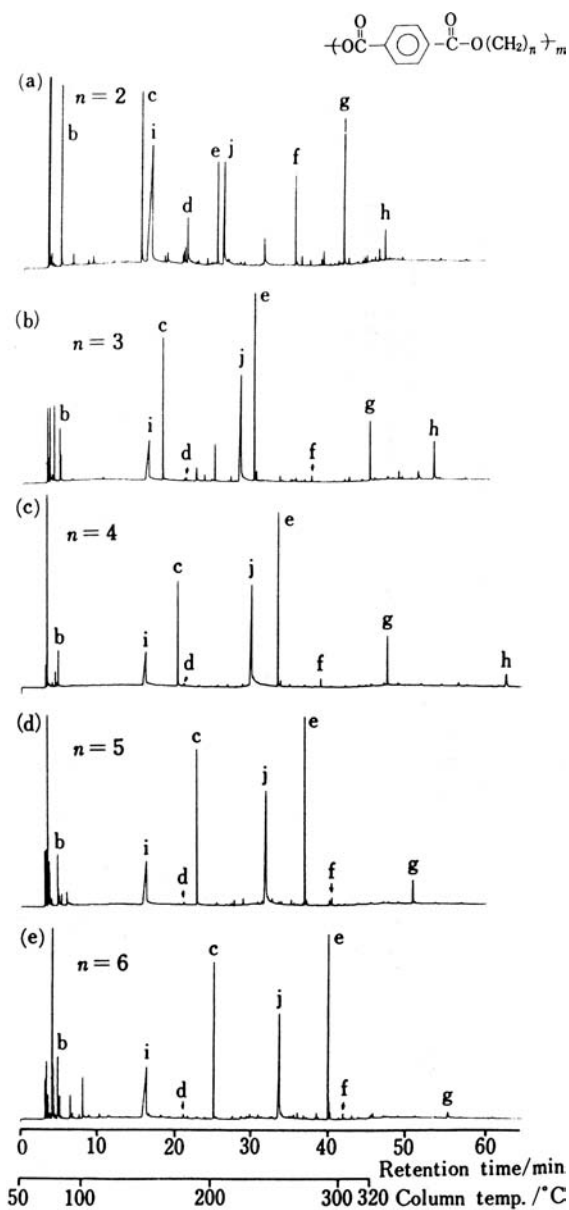

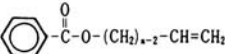
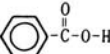

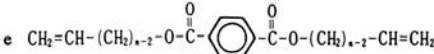
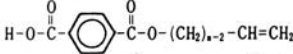
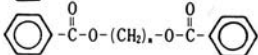
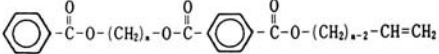
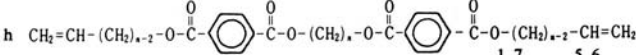


FIGURE 5.1 Pyrograms of (a) PET, (b) PTT, (c) PBT, (d) PPT, and (e) PHT at 590°C [3]. Peak notations correspond to those in Table 5.1. (H. Ohtani et al., *Anal. Sci.*, 2: 180–182 (1986). With permission.)

TABLE 5.1

Assignment and Relative Intensities of the Characteristic Peaks on the Pyrograms of Terephthalate Polyesters (Peak Notations as in Figure 5.1)

Peak notations	Structure ^a	PET	Relative PTT	peak intensity, PBT	^b % PPT	PHT
Small products ^c		19.0	9.6	37.6	34.8	38.6
b		5.1	2.3	1.5	1.7	2.7
c		5.9	8.5	6.7	7.5	7.0
i		32.0	14.2	10.4	13.3	15.1
d		1.8	>0.3	>0.3	>0.3	>0.3
e		3.7	21.7	13.2	17.6	11.3
j		9.2	26.0	21.7	21.0	14.2
f		3.4	0.6	0.7	0.6	>0.5
g		5.7	4.5	4.1	2.2	0.9
h		1.7	5.6	3.1	—	—

a. $n=2$ (PET), 3 (PTT), 4 (PBT), 5 (PPT) and 6 (PHT).

b. Relative peak area (%) among all peaks appearing on the pyrograms.

c. Total intensities of the peaks with shorter retention times than that of benzene.

Source: H. Ohtani et al., *Anal. Sci.*, 2: 180–182 (1986). With permission.

A series of poly(alkylene phthalate)s¹⁷ and some unsaturated polyesters^{18,19} were also investigated by Py-GC. The major pyrolysis products for these polyesters were the associated diols and anhydrides, such as phthalic anhydride and maleic anhydride, as well as the products formed through the six-membered cyclic transition state. Moreover, various kinds of cyclic ethers and cyclic esters were also observed in considerable quantities. The general scheme of the degradation of poly(alkylene phthalate)s is shown in Figure 5.3.¹⁷

Thermal degradation of aliphatic polyesters has been investigated mainly by Py-MS.^{20–27} Dominant degradation products were cyclic monomer (lactone); cyclic oligomers; or liner oligomers with ketene, hydroxyl, carboxyl, or alkenyl end groups. The relative yields of the characteristic products strongly depended on the chain length and the branching structure between the neighboring ester groups in the polymer chain, as well as on the degradation condition. For example, Py-chemical ionization-MS analysis of several polylactones with various chain lengths indicated that only poly(β -propiolactone) degraded mainly via the six-membered ring transition state to form liner products with a carboxyl and a vinyl end group, whereas the

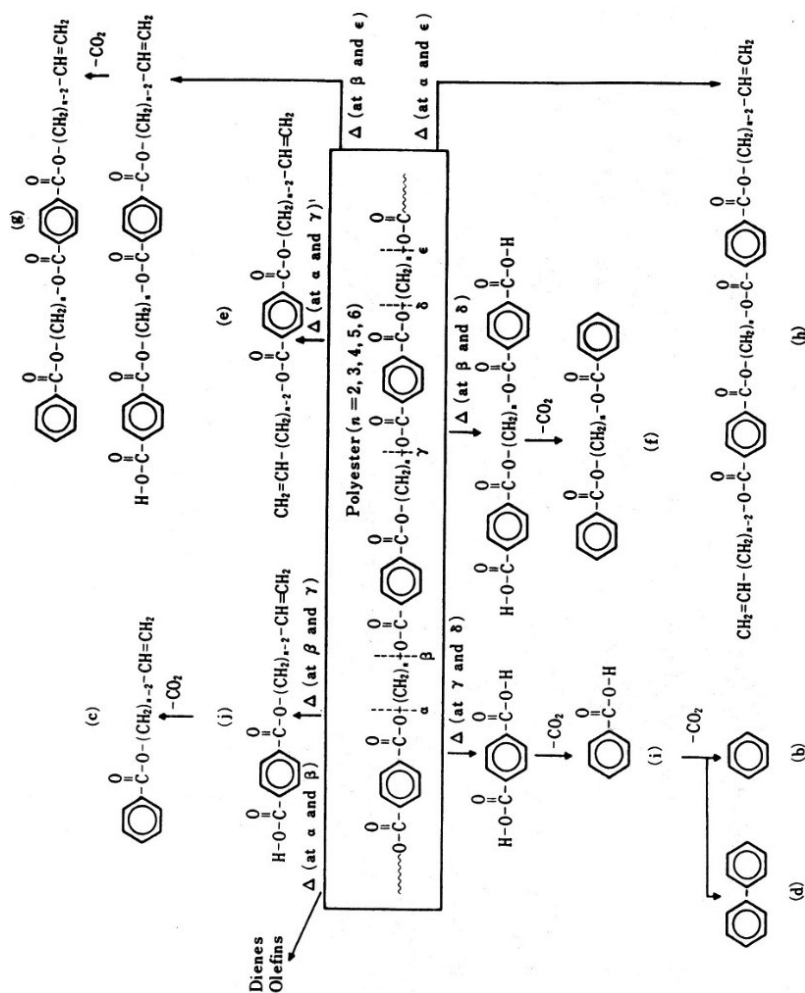


FIGURE 5.2 Thermal degradation mechanisms of the terephthalate polyesters on the basis of the pyrograms at 590°C [3]: Δ : thermal cleavage; b-j correspond to the peaks in Figure 5.1. (H. Ohtani et al., *Anal. Sci.*, 2: 180–182 (1986). With permission.)

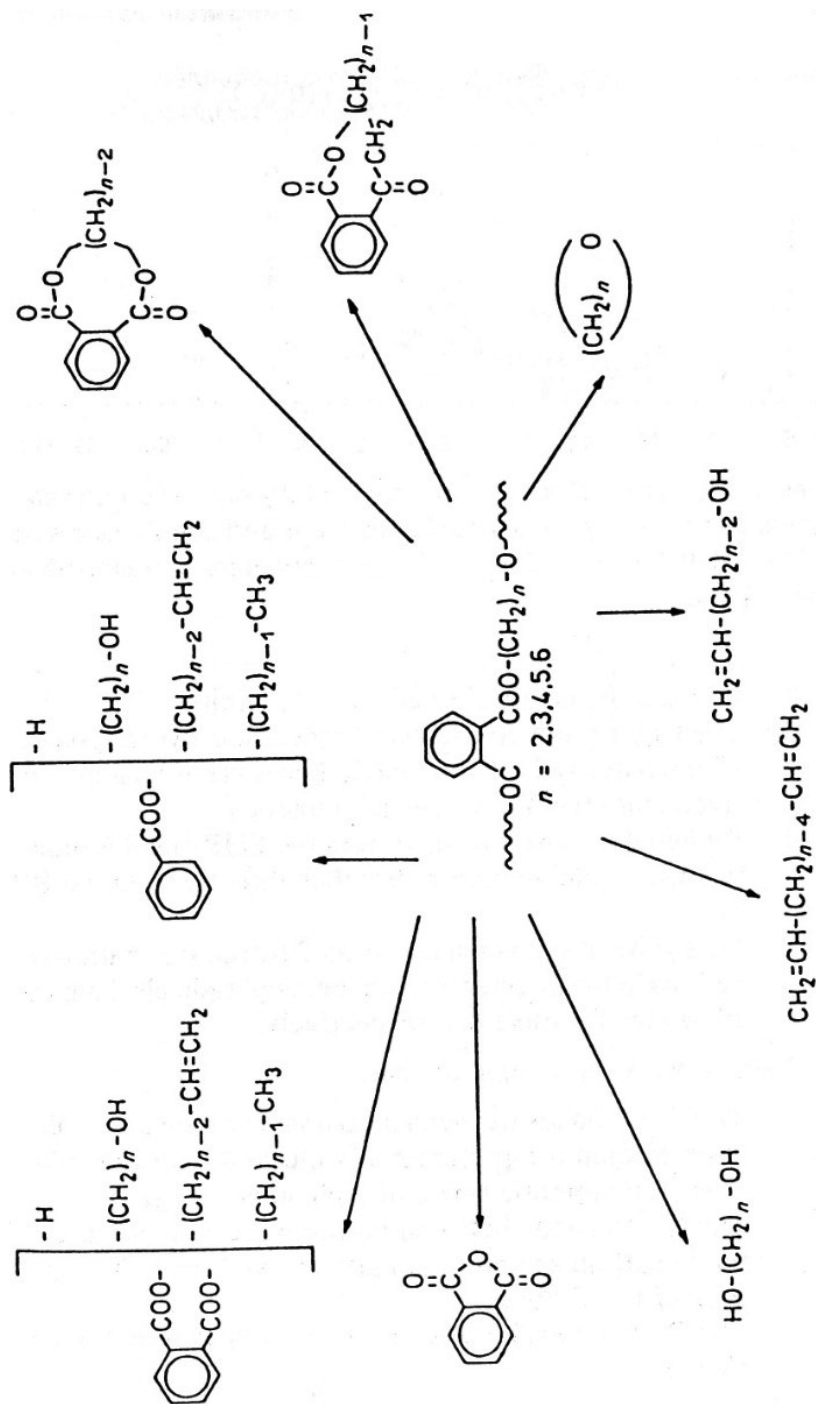


FIGURE 5.3 General scheme of thermal degradation of poly(alkylene phthalates) [17]. (C.T. Vijayakumar et al., *Eur. Polym. J.*, 23: 863 (1987). With permission.)

other polylactones predominantly decomposed by intramolecular transesterification reactions to form cyclic oligomers.²⁵

Recently, thermal degradation of poly(butylenes succinate-*co*-butylene adipate) was studied by Py-GC by focusing on its biodegradability.²⁸ The pyrolysates observed in the pyrogram at 500°C included linear ester products with carboxylic, olefinic, or alkyl end groups, and various cyclic monomers and oligomers, together with cyclopentanone from an adipic acid unit and tetrahydrofuran from a butane diol unit. Figure 5.4 shows the formation pathways for the linear and cyclic ester products. It was interesting to note that the relative yields of the alkyl ester products could be a good measure for the degree of biodegradation.²⁸

In the case of poly(ϵ -caprolactone) (PCL), the major pyrolysis product observed by Py-GC was ϵ -caprolactone monomer, along with minor amounts of cyclic and linear oligomers.^{29,30} The distribution of these products was considerably changed depending on their microstructure, such as end groups. In addition, the thermal degradation of poly(lactic acid) (PLA) has been also widely studied by Py-GC and Py-MS.^{29,31–39} The main pyrolysis products were D-, L- and meso-lactides, and a large number of oligomeric products were also yielded in small amounts. The pyrolysates from PCL and PLA should be formed in a manner similar to that in Figure 5.4.

As for poly(3-hydroxybutyrate), which is one of the representative bacterial polyesters, monomeric (butenoic) and oligomeric (mainly dimeric and trimeric) acids were reported to be observed in the pyrograms, which should be mostly formed through the six-membered transition state.^{29,32,40–45} Due to the presence of a methyl side chain, three types of isomeric structures can be produced for each oligomer, as shown in Figure 5.5. Among these, the trans type of inner olefinic products was usually dominant.

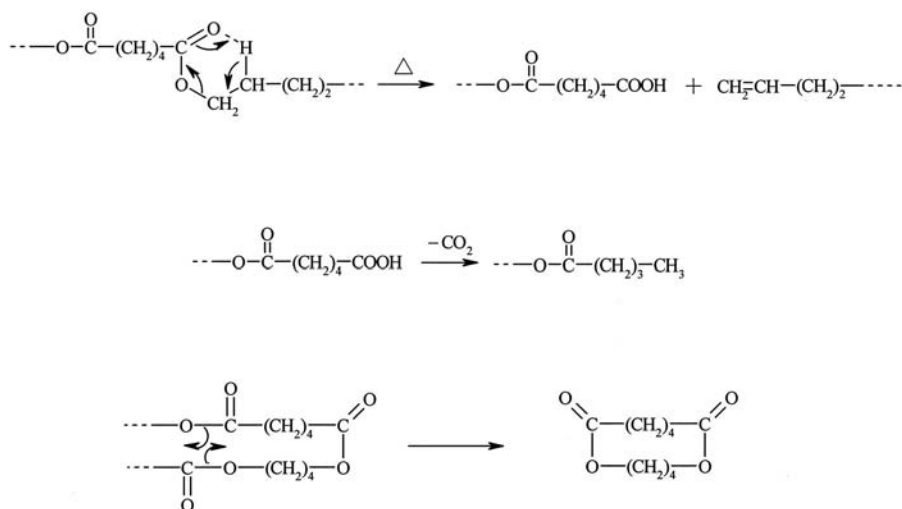


FIGURE 5.4 Major degradation pathways for poly(butylene succinate-*co*-butylene adipate) [28]. (H. Sato et al., *Polym. Degrad. Stab.*, 73: 327 (2001). With permission.)

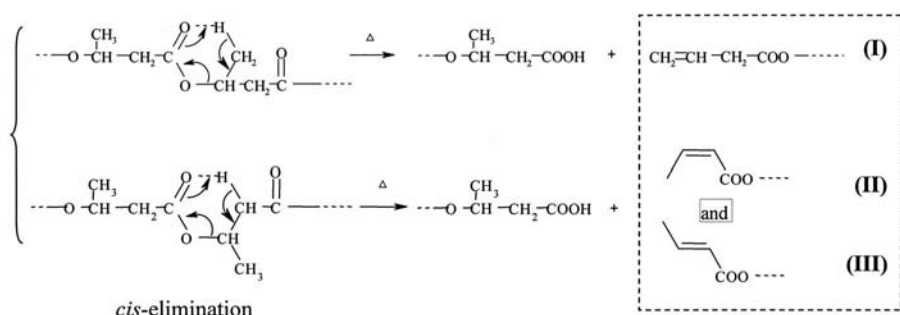


FIGURE 5.5 Degradation pathways for poly(3-hydroxybutylate) to form three types of isomeric structures. (H. Sato et al., *Polym. Degrad. Stab.*, 74: 198 (2005). With permission.)

On the other hand, fully aromatic polyesters based on *p*-hydroxybenzoic acid (PHB) have been recently recognized as some of the most promising high-performance liquid crystalline polymers (LCPs), especially in fields where ever-increasing thermal stability is required. The thermal degradation mechanisms of typical LCPs prepared from PHB, biphenol (BP), and terephthalic acid (TA) were studied by Py-GC/MS.^{46,47} Figure 5.6 shows a typical pyrogram of an LCP sample (PHB/BP/TA = 2/1/1) at 650°C, with peak identification summarized in Table 5.2.⁴⁷ The general origin of the characteristic products shown in Figure 5.7 (estimated by examining the LCPs with different comonomer ratios) and that containing deuterated terephthalate units⁴⁷ show:

1. Phenol is almost exclusively formed from the PHB moiety.
2. Benzene is mostly formed from TA units.
3. The larger products, such as biphenol, *p*-hydroxyphenylbenzoate, and 4,4'-biphenyldibenzoate, are mainly derived from the TA or BP moieties.

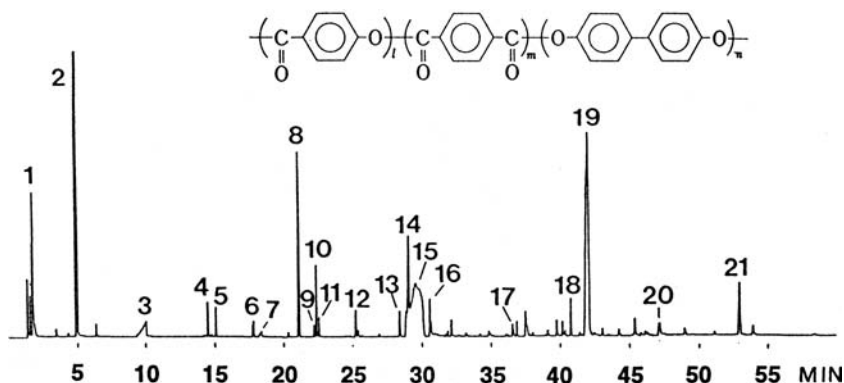


FIGURE 5.6 Pyrogram of a liquid crystalline fully aromatic polyester consisting of *p*-hydroxybenzoic acid, biphenol, and terephthalic acid at 650°C (PHB/BP/TA = 2/1/1) [47]. Peak numbers correspond to those in Table 5.2.

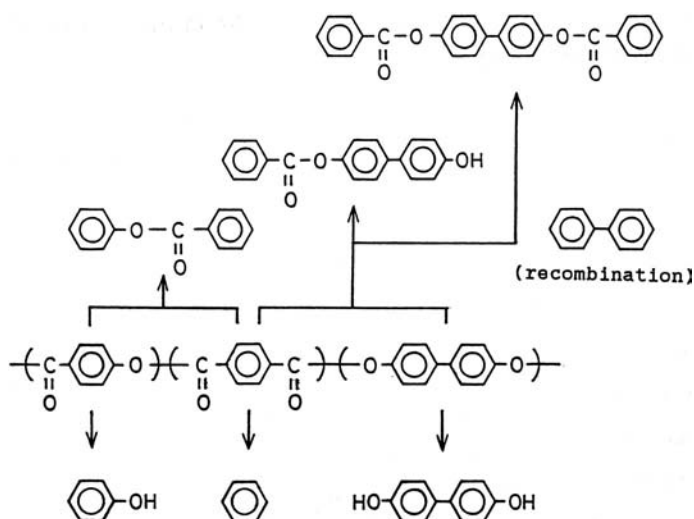


FIGURE 5.7 Thermal degradation mechanisms of an aromatic polyester [47]. (K. Sueoka et al., *J. Polym. Sci. A*, 29: 1907–1908 (1991). With permission.)

4. Biphenyl is mostly formed from the PHB and TA moieties via recombination rather than directly from the BP moiety.
5. Phenyl benzoate is mainly formed by recombination reactions between phenoxy and benzoyl radicals from the PHB and TA moieties, respectively.

These observations suggest that:


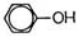
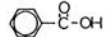
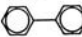
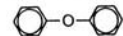
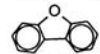

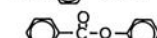
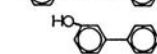
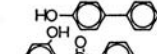
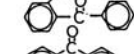
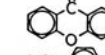
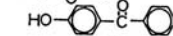

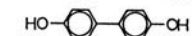
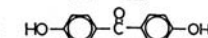
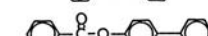
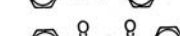
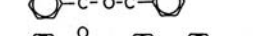
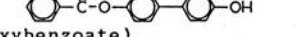

1. The C–O bonds between a carbonyl carbon and a phenolic oxygen are preferentially cleaved over those between an aromatic ring and a phenolic oxygen.
2. The C–C bonds between an aromatic ring and a carbonyl carbon are preferentially cleaved over the other type of C–C bonds.
3. The C–C bonds between aromatic rings are not easily cleaved.

Moreover, inter- and intramolecular ester exchange reactions causing rearranged polyester sequences at the pyrolysis stage were also demonstrated to take place for aliphatics²⁶ and aliphatic-aromatic polyesters⁴⁸ using Py-MS.

5.3 POLYAMIDES

Synthetic polyamides, or nylons, are widely exploited as fibers, moldings, and films. The thermal degradation of a series of aliphatic polyamides was investigated by high-resolution Py-GC.⁴⁹ Both lactam and diamine-dicarboxylic acid types of nylon samples were pyrolyzed at 550°C in a furnace pyrolyzer under a flow of nitrogen carrier gas, and the resulting degradation products were continuously separated by a capillary separation column. Table 5.3 summarizes the various classes of common

TABLE 5.2
Assignment of the Characteristic Peaks in the Pyrogram of a Fully Aromatic Polyester [47]

peak no.	products	structure
1	benzene	
2	phenol	
3	benzoic acid	
4	biphenyl	
5	diphenyl ether	
6	benzofuran	
7	p-hydroxybenzoic acid	
8	phenylbenzoate	
9	m-phenylphenol	
10	p-phenylphenol	
11	o-hydroxybenzofuran	
12	xanthone	
13	p-hydroxybenzophenone	
14	phenyl(p-hydroxybenzoate)	
15	biphenol	
16	4,4'-dihydroxybenzophenone	
17	biphenylbenzoate	
18	acetylbenzoate	
19	p-hydroxybiphenylbenzoate	
20	p-hydroxybiphenyl(p'-hydroxybenzoate)	
21	4,4'-biphenyldibenzoate	

Source: K. Sueoka et al., *J. Polym. Sci. A*, 29: 1903 (1991). With permission.

TABLE 5.3
Characteristic Degradation Products from Aliphatic Polyamides [49, 50]

Class of compounds	Abbreviation	Structure
Hydrocarbons	HC	$\begin{cases} \text{CH}_3-(\text{CH}_2)_m-\text{CH}_3 \\ \text{CH}_2=\text{CH}-(\text{CH}_2)_{m-1}-\text{CH}_3 \\ \text{CH}_2=\text{CH}-(\text{CH}_2)_{m-2}-\text{CH}=\text{CH}_2 \end{cases}$
Mononitriles	MN	$\begin{cases} \text{CH}_3-(\text{CH}_2)_m-\text{C}\equiv\text{N} \\ \text{CH}_2=\text{CH}-(\text{CH}_2)_{m-1}-\text{C}\equiv\text{N} \end{cases}$
Amines	AM	$\begin{cases} \text{CH}_3-(\text{CH}_2)_m-\text{NH}_2 \\ \text{CH}_2=\text{CH}-(\text{CH}_2)_{m-1}-\text{NH}_2 \end{cases}$
Lactams	L	$\text{O}=\text{C}-\overset{(\text{CH}_2)_m}{\text{---}}\text{NH}$
Dinitriles	DN	$\text{N}\equiv\text{C}-(\text{CH}_2)_m-\text{C}\equiv\text{N}$
Cyclopentanone	CP	$\begin{array}{c} \text{CH}_2-\text{CH}_2 \\ \quad \diagup \\ \text{CH}_2-\text{CH}_2 \quad \text{C}=\text{O} \end{array}$
Hydrocarbons containing one amide group	HC(A)	$\begin{cases} \text{CH}_3-(\text{CH}_2)_m-\overset{\text{O}}{\underset{\text{H}}{\text{C}}}-\text{N}-(\text{CH}_2)_n-\text{CH}_3 \\ \text{CH}_2=\text{CH}-(\text{CH}_2)_{m-1}-\overset{\text{O}}{\underset{\text{H}}{\text{C}}}-\text{N}-(\text{CH}_2)_n-\text{CH}_3 \\ \text{CH}_2=\text{CH}-(\text{CH}_2)_{m-1}-\overset{\text{O}}{\underset{\text{H}}{\text{C}}}-\text{N}-(\text{CH}_2)_{n-1}-\text{CH}=\text{CH}_2 \end{cases}$
Mononitriles containing one amide group	MN(A)*	$\begin{cases} \text{CH}_3-(\text{CH}_2)_m-\overset{\text{O}}{\underset{\text{H}}{\text{C}}}-\text{N}-(\text{CH}_2)_n-\text{C}\equiv\text{N} \\ \text{CH}_2=\text{CH}-(\text{CH}_2)_{m-1}-\overset{\text{O}}{\underset{\text{H}}{\text{C}}}-\text{N}-(\text{CH}_2)_n-\text{C}\equiv\text{N} \end{cases}$
Mononitriles containing one amide group	MN(A)**	$\begin{cases} \text{CH}_3-(\text{CH}_2)_m-\overset{\text{H}}{\underset{\text{O}}{\text{N}}}-\overset{\text{O}}{\text{C}}-(\text{CH}_2)_n-\text{C}\equiv\text{N} \\ \text{CH}_2=\text{CH}-(\text{CH}_2)_{m-1}-\overset{\text{H}}{\underset{\text{O}}{\text{N}}}-\overset{\text{O}}{\text{C}}-(\text{CH}_2)_n-\text{C}\equiv\text{N} \end{cases}$

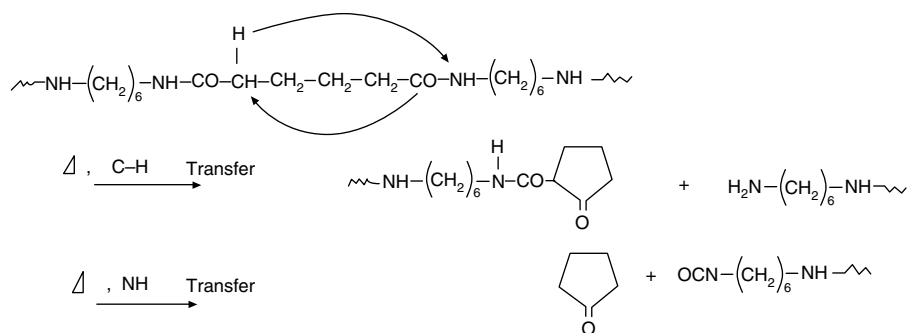
* Formed from ω -aminocarboxylic acid-type nylons.

** Formed from diamine-dicarboxylic acid-type nylons.

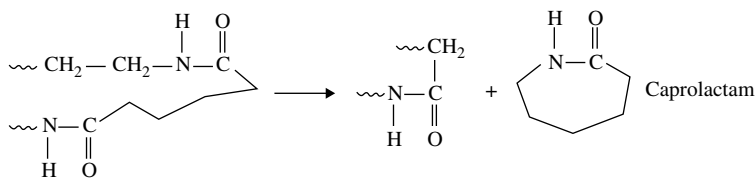
characteristic products observed in the resulting pyrograms.^{49,50} The degradation products were found to be strongly dependent on the number of methylene groups in the polymer chain units.

Figure 5.8 shows the pyrogram of (a) nylon 6 and (b) nylon 6/6 observed by using a glass capillary separation column. The main pyrolysis products in (a) are ϵ -caprolactam^{4,10,49,51,52} and small amounts of nitriles (MN and MN(A)). Polylactams consisting of relatively short methylene chains, such as nylon 4 and 6, tend to regenerate the associated monomeric lactame upon heating.

As shown in Figure 5.6b, the most abundant compound resulting from the thermal degradation of nylon 6/6 is cyclopentanone (CP),^{4,49,50,53-57} which is characteristic of adipic acid-based polyamides. It has been demonstrated by using Py-EI and CI-tandem MS that the formation of CP from nylon 6/6 occurs via a C-H hydrogen transfer reaction to nitrogen to give the primary products bearing amine and ketoamide end groups as follows:⁵⁷



In addition, some nitriles (DN and MN(A)') and ϵ -caprolactam (L) are observed as minor products. The following mechanism was proposed to account for the formation of L from nylon 6/6.⁵⁶



Furthermore, peaks of the associated amines arising from the cleavage of the amide bond are clearly observed on the pyrogram of nylon 6/6 by using a fused-silica capillary separation column,^{50,58} although they are missing in Figure 5.8b.

Figure 5.9 shows the pyrograms of (a) nylon 11, (b) nylon 6/10, and (c) nylon 12/6 observed by using a fused-silica capillary column.^{50,58} Fairly strong peaks of mononitriles (MNs) are observed in (a), while that of the associated lactam (L) becomes very small. This suggests that the thermal degradation of nylon 11 is mainly associated with homolytic cleavage of the CH_2-NH bond to form a double bond

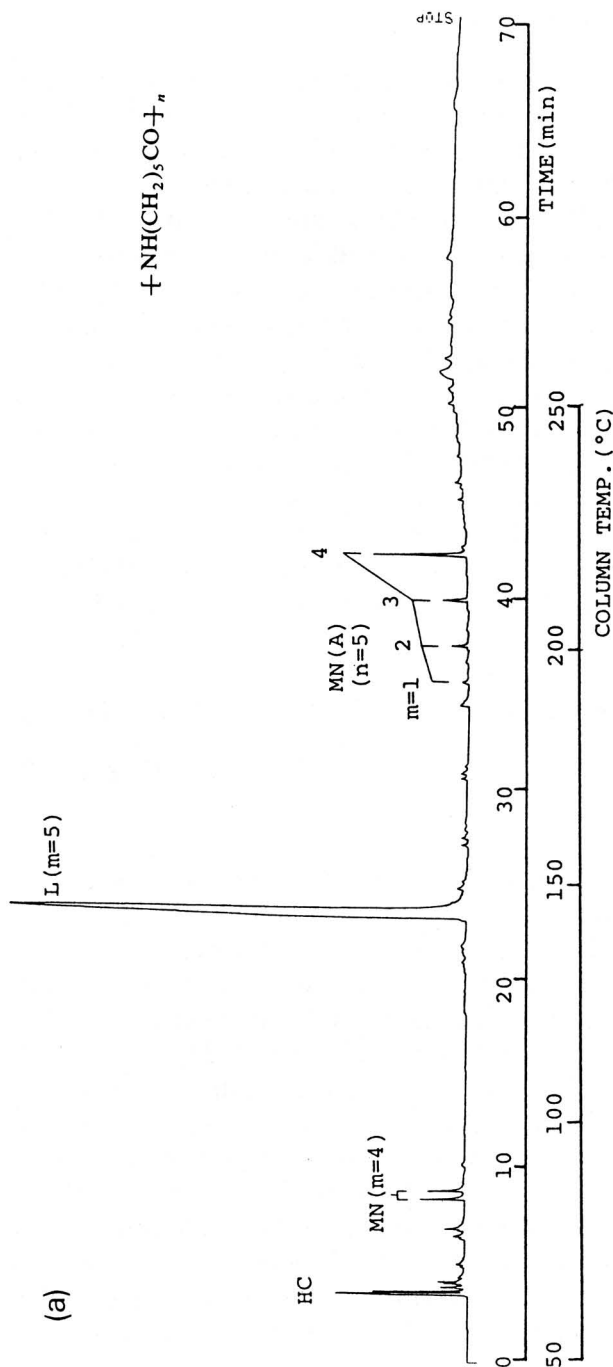


FIGURE 5.8 Pyrograms of nylons at 550°C observed by a glass capillary column; (a) nylon 6, (b) nylon 6/6 [49]. (H. Ohtani et al., *J. Anal. Appl. Pyrol.*, 4: 122-126 (1982). With permission.)

Continued.

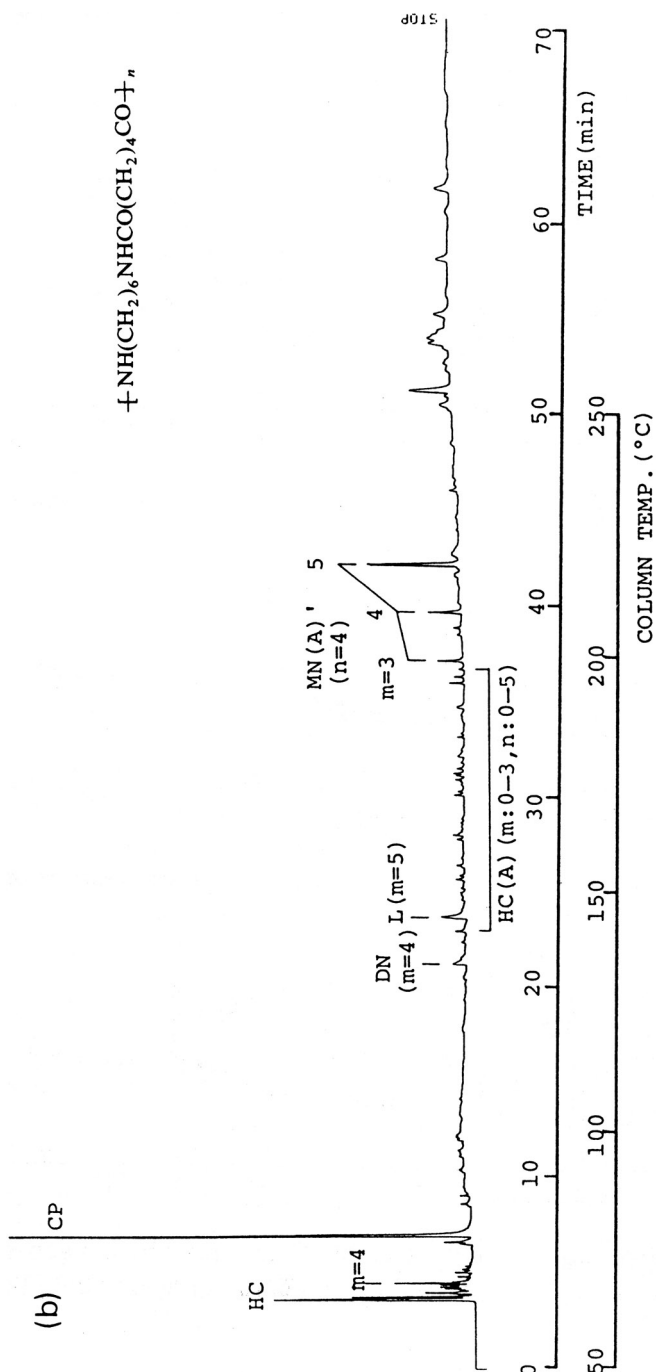
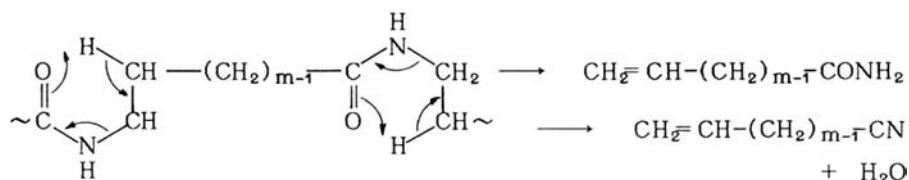


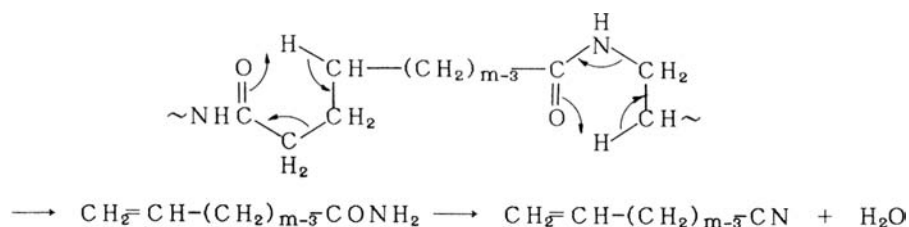
FIGURE 5.8 Continued.

and an amide or a nitrile group through the six-membered cyclic transition state (*cis* elimination).^{4,49,59} The most intense olefinic MNs, where carbon number corresponds to that of the successive methylene groups in the polymer chain plus 1, are formed through the following *cis* eliminations followed by the dehydration reaction:⁴⁹



The minor peaks of saturated MNs are always accompanied by those of the olefinic MNs. In addition, the smaller MNs and the associated hydrocarbons (HCs) are formed through the further C–C bond cleavages. The main degradation pathway is basically the same for the poly lactams, including relatively longer methylene chains such as nylon 8, 11, and 12.⁴⁹

One of the most characteristic products in Figure 5.9b is cebaonitrile (DN(*m* = 8)). Large quantities of dinitriles are formed via the *cis* elimination reactions at the neighboring amide groups across a dicarboxylic acid unit in the diamine-dicarboxylic acid type of polyamide chain except for the adipic acid-based polyamides.⁴⁹ Moreover, a series of mononitriles are also observed in the pyrograms. Among these, the most intense peak is that of the second longest unsaturated mononitrile. This fact suggests that the *cis* elimination reaction might take place at the opposite side of the amide bond as follows:⁶⁰



Similar to nylon 6/6, the most characteristic peak for nylon 12/6 is CP formed from the adipic acid moiety. In addition, a series of HC triplets and those of amine (AM) doublets^{50,58} up to C₁₂ are formed in considerable amounts through the C–C and amide bond cleavages.

Thermal degradation of various aliphatic polyamides was also studied by Py-EIMS,^{10,59,61} Py-field ionization (FI), and field desorption (FD)-MS.^{52,60,62,63} The Py-EIMS studies demonstrated that the polylactams mainly decomposed to cyclic oligomers, whereas the favored decomposition pathways of diamine-dicarboxylic acid-type polyamides were the *cis* elimination reaction and the cleavage of the amide bond, which also occurred in the polylactams with a large number of methylene groups, such as nylon 12. On the other hand, Py-FIMS of various diamine-dicar-

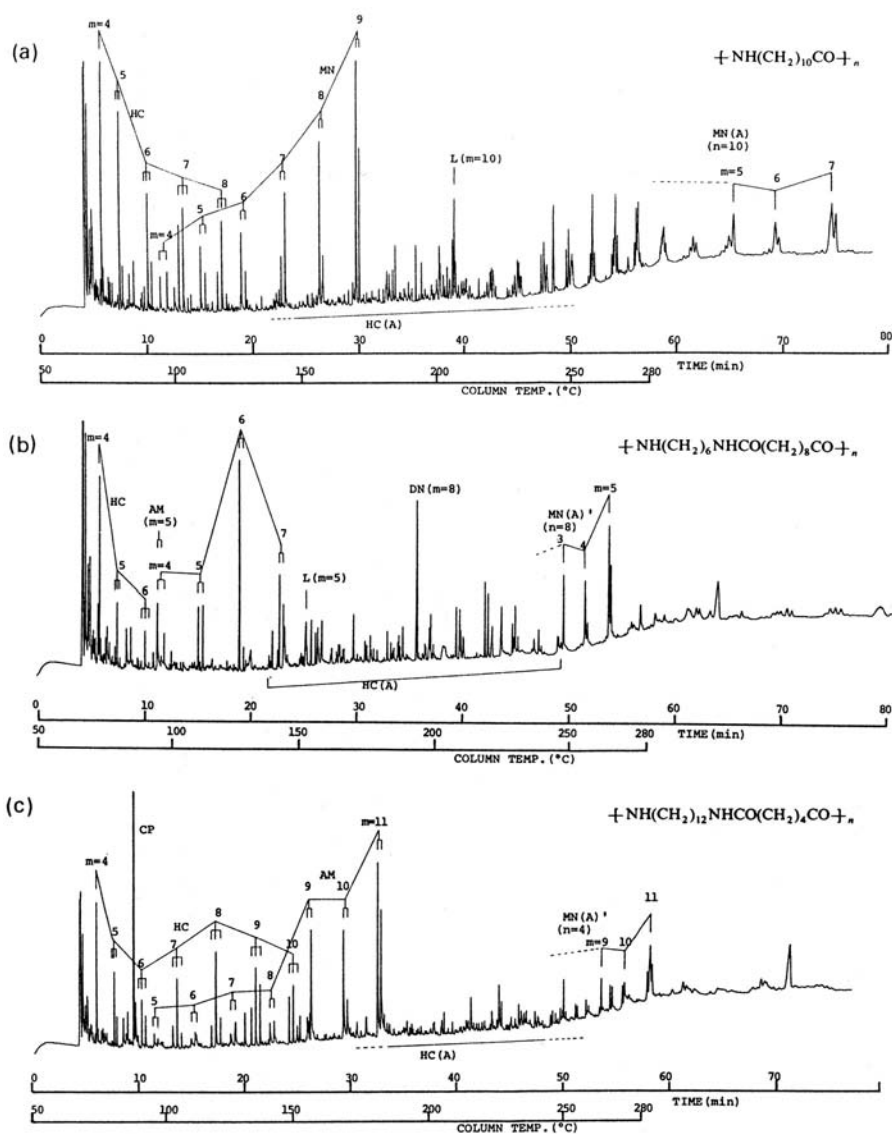
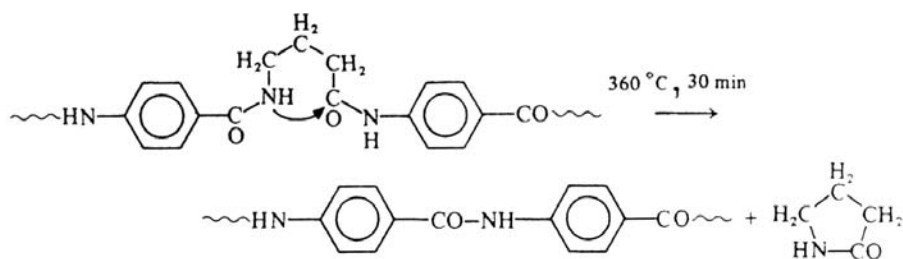


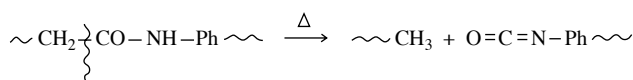
FIGURE 5.9 Pyrograms of nylons at 550°C observed by a fused-silica capillary column; (a) nylon 11, (b) nylon 6/10, (c) nylon 12/6 [50, 58].

boxylic acid-type polyamides illustrated that the main pyrolysis products detected were protonated dinitriles and various protonated nitriles, as well as oligomers up to 1000 daltons, except for the polyamides containing adipic acid subunits, for which protonated amines and diamine were observed in large amounts.⁶⁰ Recently, a comprehensive review for thermal degradation of aliphatic polyamide (nylons) has been published.⁶⁴

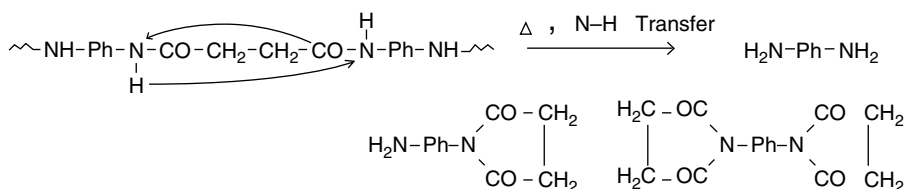
Thermal decomposition of aliphatic-aromatic polyamides was mainly investigated by Py-MS. It was found in an early study that the thermal degradation of copolyamides formed from aliphatic and aromatic amino acids occurred almost exclusively through the bond scission in the aliphatic moieties.⁶⁵ It was shown by Py-EIMS that thermal degradation of copolyamides of *p*-aminobenzoic acid and some aliphatic amino acids yielded poly-*p*-aminobenzoic acid via the elimination of lactams:



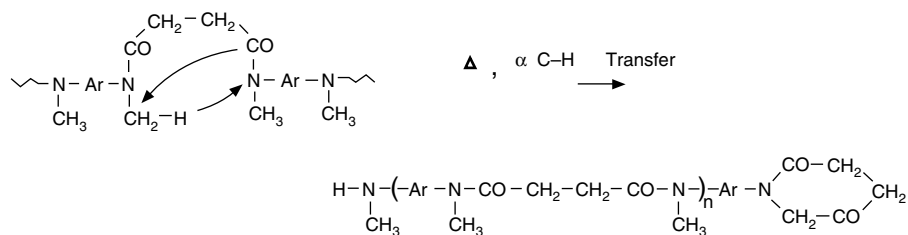
The other favored reactions are the cleavage of the CO–NH bond to form *o*-aminophenyl end groups, the *cis* elimination to form amide and vinyl end groups, and the cleavage of the CH₂–CO bond to form isocyanate end groups:⁶⁶



Recently, the thermal decomposition processes of various aliphatic-aromatic polyamides were investigated by Py-GC/MS and Py-MS using both CI and EI modes.^{67–69} The thermal decomposition of the polyamides of aromatic-diamine and aliphatic-dicarboxylic acid was strongly influenced by the structure of the aliphatic subunits.⁶⁷ The formation of compounds with succinimide and amine end groups was observed in the pyrolysis of the polyamides containing succinic subunits via an intramolecular exchange and a concomitant N–H hydrogen transfer,

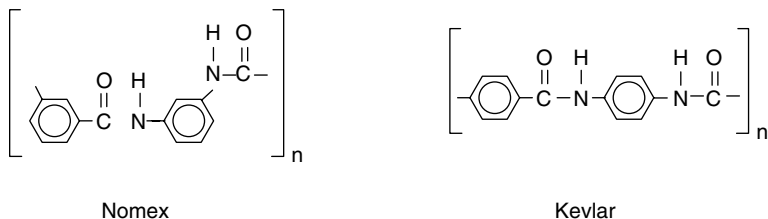


while the primary products were compounds with amine and keto amide end groups in the pyrolysis of the polyamides containing adipic subunits. In addition, the *N*-methyl-substituted polyamide decomposed via a hydrogen transfer process from the methyl group to the nitrogen atom with formation of compounds with amine or 2,5-piperidione end groups:⁶⁸



On the other hand, the primary thermal decomposition of polyamides of aliphatic-diamine and aromatic-dicarboxylic acid proceeded via the *cis* elimination process with formation of the products containing amide and olefin end groups.⁶⁹ Nitrile end groups also proved to be formed by dehydration of the amide groups formed in the primary process.

Various investigations of the thermal degradation of wholly aromatic polyamides (aramids), such as poly(1,3-phenylene isophthalamide) (Nomex) and poly(1,4-phenylene terephthalamide) (Kevlar), have also been reported.^{52,70-74}



In an early Py-FIMS study,⁵² benzonitrile and other pyrolysates with amine or nitrile end groups were recorded as the main pyrolysis products of Kevlar at 600°C. In another paper on the pyrolysis of Nomex at 550°C, the primary low-boiling volatiles identified by GC/MS were CO, CO₂, H₂O, and benzonitrile.⁷⁰ Considerable amounts of benzene, methane, toluene, 1,3-tolunitrile, etc., were also observed. The presence of at least 17 additional degradation products was detected by high-performance liquid chromatography (HPLC) in the condensable products, among which the two major components were 1,3-dicyanobenzene and 3-cyanobenzoic acid. These observations supported a mechanism that involved the cleavage of an aromatic-NH bond followed by the loss of H₂O to form aromatic nitriles. Cleavage of the CO-NH bond, hydrolysis, and decarboxylation explained the other major products.

On the other hand, the pyrolysis products of a Nomex-type aramid and its chloro-derivative at 450 and 550°C were identified by GC-Fourier-transform infrared (FTIR) and GC/MS.⁷¹ The end groups of the volatile degradation products reported were amine, nitrile, carboxylic acid, and phenyl for both one-ring and two-ring compounds. The formation of the two-ring compounds occurred preferably at 450°C, whereas pyrolysis at 550°C yielded predominantly the one-ring compounds. Moreover, Nomex and Kevlar were pyrolyzed at several temperatures between 300 and 700°C.⁷² At lower temperatures, water was almost exclusively formed as a volatile

degradation product, accompanied by traces of carbon dioxide. Hydrolysis products were formed with increasing temperature, followed by the formation of nitriles and products containing a phenyl end group. Derivatives of toluene and biphenyl, HCN and hydrocarbons were observed at high temperatures. The results reported in these two papers^{71,72} suggested that the homolytic cleavages involving all the nonaromatic ring bonds as well as hydrolytic reactions took place during the degradation of these aramids. At lower temperatures the hydrolytic mechanism was dominant, whereas at higher temperatures homolytic reactions became increasingly important. Furthermore, it has been reported that for Nomex the cleavage of the N–H bond is both thermodynamically and kinetically favored at the beginning of the thermal degradation over the scission of the other bond in the polymer main chain.⁷³

Recently, thermal degradation of Nomex and Kevlar was studied by Py-FIMS and Py-GC.⁷⁴ In Py-FIMS, the polymer samples were pyrolyzed in the ion source by heating from 50 to 750°C at the rate of 1.2°C/sec. The relative abundances of the thermal degradation products are listed in Table 5.4. Possible intermediate products used to form the observed compounds through the hydrolytic and homolytic decomposition processes are summarized in Table 5.5. Kevlar and Nomex mostly gave the same kinds of signals, but several showed strong differences in their relative abundances. Higher abundances of the degradation products containing carboxylic acid groups were generally observed for Nomex, whereas Kevlar yields higher abundances of fragments resulting from cleavage of the carbonyl/phenyl bond. In general, nitriles were formed at higher temperatures over carboxylic acids. As the subsequent decarboxylation reactions from carboxylic acids are favored at higher temperatures, the amounts of carboxylic acids from Nomex decrease with increasing pyrolysis temperature, and those from Kevlar are smaller than those from Nomex because of the higher thermal stability of the former.

On the other hand, the pyrograms observed in flash Py-GC at 720°C almost entirely consisted of the fragments formed via homolytic degradations, although many were identical with those observed by Py-FIMS. In addition, the difference between Nomex and Kevlar with Py-GC was much less than those observed in Py-FIMS. Moreover, the formation of secondary products, such as biphenyl derivatives in Py-GC, was much less than that in Py-FIMS. The differences between the results by Py-GC and by Py-FIMS could be attributed to the difference in the final pyrolysis temperature and the heating rate.

TABLE 5.4
Pyrolysis Field Ionization Mass Spectrometry, Tentatively Assigned
Pyrolyzates of Aromatic Polyamides [74]

m/z	Thermal degradation products	Relative abundance	
		Kevlar	Nomex
78	C ₆ H ₆	0.5	5
93	H ₂ N—C ₆ H ₅	7	10
103	C ₆ H ₅ —CN	15	35
108	H ₂ N—C ₆ H ₄ —NH ₂	29	55
117	NC—C ₆ H ₄ —CH ₃	0.7	3
118	NC—C ₆ H ₄ —NH ₂	12	3
122	C ₆ H ₅ —COOH	1	13
128	NC—C ₆ H ₄ —CN	1	5
134	H ₂ N—C ₆ H ₄ —N = C = O	7	2
147	NC—C ₆ H ₄ —COOH	0.5	5
154	C ₆ H ₅ —C ₆ H ₅	0.3	1
166	HOOC—C ₆ H ₄ —COOH	1	12
169	C ₆ H ₅ —C ₆ H ₄ —NH ₂	1	1.5
179	C ₆ H ₅ —C ₆ H ₄ —CN	1	4
194	H ₂ N—C ₆ H ₄ —C ₆ H ₄ —CN	6	6
197	C ₆ H ₅ —NH—CO—C ₆ H ₅	11	2
212	H ₂ N—C ₆ H ₄ —NH—CO—C ₆ H ₅	100	70
222	C ₆ H ₅ —NH—CO—C ₆ H ₄ —CN	10	1
237	H ₂ N—C ₆ H ₄ —NH—CO—C ₆ H ₄ —CN	74	31
238	O = C = N—C ₆ H ₄ —NH—CO—C ₆ H ₅	23	10
241	C ₆ H ₅ —NH—CO—C ₆ H ₄ —COOH	1	5
256	H ₂ N—C ₆ H ₄ —NH—CO—C ₆ H ₄ —COOH	4	100
282	O = C = N—C ₆ H ₄ —NH—CO—C ₆ H ₄ —COOH	2	5
316	C ₆ H ₅ —CO—NH—C ₆ H ₄ —NH—CO—C ₆ H ₅	55	14
	C ₆ H ₅ —NH—CO—C ₆ H ₅ —CO—NH—C ₆ H ₅		
331	H ₂ N—C ₆ H ₄ —NH—CO—C ₆ H ₄ —CO—NH—C ₆ H ₅	21	25
341	C ₆ H ₅ —CO—NH—C ₆ H ₄ —NH—CO—C ₆ H ₄ —CN	37	12
346	H ₂ N—C ₆ H ₄ —NH—CO—C ₆ H ₄ —CO—NH—C ₆ H ₄ —NH ₂	18	66
360	C ₆ H ₅ —CO—NH—C ₆ H ₄ —NH—CO—C ₆ H ₄ —COOH	2	19
385	monomer + 147	1	3
435	monomer + 197	2	0
450	monomer + 212	11	7
475	monomer + 237	1.5	1.5
476	monomer + 238	4	0.5

Source: H.-R. Schulten et al., *Angew. Makromol. Chem.*, 155: 7–17 (1987). With permission.

TABLE 5.5
Possible Intermediate Products from Aromatic Polyamides through
Hydrolytic and Homolytic Decomposition [74]

Type of decomposition	Possible intermediate products
(A) Hydrolytic decomposition	
(B) Homolytic decomposition	

Source: H.-R. Schulten et al., *Angew. Makromol. Chem.*, 155: 7–17 (1987). With permission.

REFERENCES

1. G. Montaudo and C. Puglisi, *Thermal Degradation of Condensation Polymers*, S.L. Aggarwal and S. Russo, Eds., Pergamon Press, Oxford, pp. 227–251 (1992).
2. Y. Sugimura and S. Tsuge, *J. Chromatogr. Sci.*, 17: 269 (1979).
3. H. Ohtani, T. Kimura, and S. Tsuge, *Anal. Sci.*, 2: 179 (1986).
4. S.A. Liebman and E.J. Levy, Eds., *Pyrolysis and GC in Polymer Analysis*, Vol. 29, Marcel Dekker, New York (1985); J.H. Flynn and R.E. Florin, Degradation and pyrolysis mechanism, pp. 179–186; D.H. Ahlstrom, Microstructure of synthetic polymers, pp. 256–269; R. Saferstein, Forensic aspect pyrolysis, pp. 350–353.
5. N. Grassie and G. Scott, *Polymer Degradation and Stabilization*, Cambridge University Press, Cambridge, U.K., pp. 33–41 (1985).
6. I.C. McNeil, *Thermal Degradation*, Vol. 6, *Polymer Reactions*, G.C. Eastmond, A. Ledwith, S. Russo, and P. Sigwald, Eds., Pergamon Press, Oxford, pp. 490–495 (1989).
7. V. Passalacqua, F. Pilati, V. Zamboni, B. Fortunato, and P. Manaresi, *Polymer*, 17: 1044 (1976).

8. M.E. Bednas, M. Day, K. Ho, R. Sander, and D.M. Wiles, *J. Appl. Polym. Sci.*, 26: 277 (1981).
9. C.T. Vijayakumar and J.K. Fink, *Thermochim. Acta*, 59: 51 (1982).
10. A. Zeman, *Angew. Makromol. Chem.*, 31: 1 (1973).
11. I. Luederwald and H. Urrutia, *Makromol. Chem.*, 177: 2079 (1976).
12. I. Luederwald and H. Urrutia, Direct pyrolysis of aromatic and aliphatic polyesters in the mass spectrometer, in *Analytical Pyrolysis*, C.E.B. Jones and C.A. Cramers, Eds., Elsevier, Amsterdam, pp. 139–148 (1977).
13. R.M. Rum, *J. Polym. Sci. Polym. Chem. Ed.*, 17: 203 (1979).
14. R.E. Adams, *J. Polym. Sci. Polym. Chem. Ed.*, 20: 119 (1982).
15. D.C. Conway and R. Marak, *J. Polym. Sci. Polym. Chem. Ed.*, 20: 1765 (1982).
16. I. Luederwald, *Pure Appl. Chem.*, 54: 255 (1982).
17. C.T. Vijayakumar, J.K. Fink, and K. Lederer, *Eur. Polym. J.*, 23: 861 (1987).
18. G.H. Irzl, C.T. Vijayakumar, J.K. Fink, and K. Lederer, *Polym. Degrad. Stab.*, 16: 53 (1986).
19. C.T. Vijayakumar and K. Lederer, *Makromol. Chem.*, 189: 2559 (1988).
20. I. Luederwald and H. Urrutia, *Makromol. Chem.*, 177: 2093 (1976).
21. I. Luederwald, *Makromol. Chem.*, 178: 2603 (1977).
22. H.R. Kricheldorf and I. Luederwald, *Makromol. Chem.*, 179: 421 (1978).
23. E. Jacobi, I. Luederwald, and R.C. Schultz, *Makromol. Chem.*, 179: 429 (1978).
24. M. Doerr, I. Luederwald, and H.-R. Schulten, *Fresenius Z. Anal. Chem.*, 318: 339 (1984).
25. D. Garazzo, M. Gluffrida, and G. Montaudo, *Macromolecules*, 19: 1643 (1986).
26. B. Plage and H.-R. Schulten, *J. Anal. Appl. Pyrol.*, 15: 197 (1989).
27. B. Plage and H.-R. Schulten, *Macromolecules*, 23: 2649 (1990).
28. H. Sato, M. Furuhashi, D. Yang, H. Ohtani, S. Tsuge, M. Okada, K. Tsunoda, and K. Aoi, *Polym. Degrad. Stab.*, 73: 327 (2001).
29. Y. Aoyagi, K. Yamashita, and Y. Doi, *Polym. Degrad. Stab.*, 76: 53 (2002).
30. H. Abe, N. Takahashi, K.J. Kim, M. Mochizuki, and Y. Doi, *Biomacromolecules*, 5: 1480 (2004).
31. F.-D. Kopinke, M. Remmler, K. Mackenzie, M. Moeder, and O. Wachen, *Polym. Degrad. Stab.*, 53: 329 (1996).
32. F.-D. Kopinke and K. Mackenzie, *J. Anal. Appl. Pyrol.*, 40/41: 43 (1997).
33. F. Khabbaz, S. Karksson, and A.-C. Albertsson, *J. Appl. Polym. Sci.*, 78: 2369 (2000).
34. Y. Fan, H. Nishida, S. Hoshihara, Y. Shirai, Y. Tokiwa, and T. Endo, *Polym. Degrad. Stab.*, 79: 547 (2003).
35. Y. Fan, H. Nishida, Y. Shirai, and T. Endo, *Polym. Degrad. Stab.*, 80: 503 (2003).
36. H. Nishida, T. Mori, S. Hoshihara, Y. Fan, Y. Shirai, Y. Tokiwa, and T. Endo, *Polym. Degrad. Stab.*, 81: 515 (2003).
37. Y. Fan, H. Nishida, Y. Shirai, Y. Tokiwa, and T. Endo, *Polym. Degrad. Stab.*, 86: 197 (2004).
38. H. Abe, N. Takahashi, K.J. Kim, M. Mochizuki, and Y. Doi, *Biomacromolecules*, 5: 1606 (2004).
39. Y. Fan, H. Nishida, T. Mori, Y. Shirai, and Y. Doi, *Polymer*, 45: 1197 (2004).
40. B.E. Watt, S.L. Morgan, and A. Fox, *J. Anal. Appl. Pyrol.*, 19: 237 (1991).
41. R.S. Lehrle and R.J. Williams, *Macromolecules*, 27: 3782 (1994).
42. R.S. Lehrle, R.J. Williams, C. French, and T. Hammond, *Macromolecules*, 27: 3782 (1994).
43. F.-D. Kopinke, M. Remmler, and K. Mackenzie, *Polym. Degrad. Stab.*, 52: 25 (1996).
44. S.-D. Li, J.-D. He, P.H. Yu, and M.K. Cheung, *J. Anal. Appl. Pyrol.*, 19: 237 (1991).

45. A. Gonzalez, L. Irusta, M.J. Fernandez-Berridi, M. Iriarte, and J.J. Iruin, *Polym. Degrad. Stab.*, 87: 347 (2005).
46. B. Crossland, G.J. Knight, and W.W. Wright, *Br. Polym. J.*, 18: 371 (1986).
47. K. Sueoka, M. Nagata, H. Ohtani, N. Nagai, and S. Tsuge, *J. Polym. Sci. A*, 29: 1903 (1991).
48. M. Giuffrida, P. Marvigna, G. Montaudo, and E. Chiellini, *J. Polym. Sci. A*, 24: 1643 (1986).
49. H. Ohtani, T. Nagaya, Y. Sugimura, and S. Tsuge, *J. Anal. Appl. Pyrol.*, 4: 117 (1982).
50. S. Tsuge, *Chromatogr. Forum*, 1: 44 (1986).
51. H. Senoo, S. Tsuge, and T. Takeuchi, *J. Polym. Sci.*, 9: 315 (1971).
52. H.-J. Duessel, H. Rosen, and O. Hummel, *Makromol. Chem.*, 177: 2434 (1976).
53. L.J. Peebles, Jr., and M.W. Huffma, *J. Polym. Sci. A*, 9: 1807 (1971).
54. F. Wiloth, *Makromol. Chem.*, 144: 263 (1971).
55. C. David, Thermal degradation of polymers, in *Comprehensive Chemical Kinetics*, Vol. 14, *Degradation of Polymers*, C.H. Bamford and C.F.H. Tipper, Eds., Elsevier, Amsterdam, pp. 104–121, 130–153 (1975).
56. D.M. MacKerron and R.P. Gordon, *Polym. Degrad. Stab.*, 12: 277 (1985).
57. A. Ballisteri, D. Garozzo, M. Giuffrida, and G. Montaudo, *Macromolecules*, 20: 2991 (1987).
58. S. Tsuge, H. Ohtani, H. Matsubara, and M. Ohsawa, *J. Anal. Appl. Pyrol.*, 17: 181 (1987).
59. I. Luederwald and F. Merz, *Angew. Makromol. Chem.*, 74: 165 (1978).
60. H.-R. Schulten and B. Plage, *J. Polym. Sci. A*, 26: 2381 (1988).
61. I. Luederwald, F. Merz, and M. Rothe, *Angew. Makromol. Chem.*, 67: 193 (1978).
62. U. Bahr, I. Luederwald, R. Mueller, and H.-R. Schulten, *Angew. Makromol. Chem.*, 120: 163 (1984).
63. B. Plage and H.-R. Schulten, *J. Appl. Polym. Sci.*, 38: 123 (1989).
64. S.V. Levchik, E.D. Well, and M. Lewin, *Polym. Int.*, 48, 532 (1999).
65. H.R. Kricheldorf and E. Leppert, *Makromol. Chem.*, 175: 1731 (1974).
66. I. Luederwald and H.R. Kricheldorf, *Angew. Makromol. Chem.*, 56: 173 (1976).
67. A. Ballisteri, D. Garozzo, M. Giuffrida, P. Maravigna, and G. Montaudo, *Macromolecules*, 19: 2963 (1983).
68. A. Ballisteri, D. Garozzo, G. Montaudo, and M. Giuffrida, *J. Polym. Sci. A*, 25: 2531 (1987).
69. A. Ballisteri, D. Garozzo, P. Maravigna, G. Montaudo, and M. Giuffrida, *J. Polym. Sci. A*, 25: 1049 (1987).
70. D.A. Chatfield, I.N. Einhorn, R.W. Michelson, and J.H. Futrell, *J. Polym. Sci. Polym. Chem. Ed.*, 17: 1367 (1979).
71. Y.P. Khanna, E.M. Pearce, J.S. Smith, D.T. Burkitt, H. Njuguna, D.M. Hindenlang, and B.D. Forman, *J. Polym. Sci. Polym. Chem. Ed.*, 19: 2817 (1981).
72. J.R. Brown and A.J. Power, *Polym. Degrad. Stab.*, 4: 179 (1989).
73. A.L. Bhuiyan, *Eur. Polym. J.*, 19: 195 (1983).
74. H.-R. Schulten, B. Plage, H. Ohtani, and S. Tsuge, *Angew. Makromol. Chem.*, 155: 1 (1987).

6 The Application of Analytical Pyrolysis to the Study of Cultural Materials

Alexander Shedrinsky and Norbert S. Baer

CONTENTS

6.1	Introduction	105
6.2	Instrumental Considerations	107
6.3	Analysis of Materials	109
6.3.1	Waxes	109
6.3.2	Natural Resins	114
6.3.3	Amber	115
6.3.4	Oils and Fats	119
6.3.5	Synthetic Polymers	121
6.3.6	Siloxanes	124
6.3.7	Proteins	125
	References	126

6.1 INTRODUCTION

The application of analytical pyrolysis in any of its several variations — pyrolysis-gas chromatography (Py-GC), pyrolysis-mass spectrometry (Py-MS), pyrolysis-gas chromatography-mass spectrometry (Py-GC/MS), pyrolysis-gas chromatography-Fourier-transform infrared (Py-GC/FTIR) — has proven to be one of the most useful approaches to analyzing materials of art and archaeology. Since our previous review¹ was published in 1989, four major conservation laboratories (Metropolitan Museum of Art, Getty Conservation Institute, Musée du Louvre, and the National Gallery of Art [U.S.]) have become involved in the application of this analytical technique²⁻⁷ to the analysis of organic media such as gums, waxes, natural resins, and synthetic polymers.

In the Netherlands the multidisciplinary project “Molecular Aspects of Aging of Painted Art” (MOLART) was created by the Dutch Organization for Scientific

Research (NWO). The focus of this project was the determination of the present chemical and physical condition of works of art produced from the 15th to the 20th centuries. Considering the fact that a substantial part of this research was done at the FOM Institute for Atomic and Molecular Physics under the coordination and supervision of Dr. Jaap Boon, pyrolysis techniques played a very prominent role during the 8 years of the MOLART project.

It is totally outside the scope of this chapter to provide our readers with a full list of references resulting from this undertaking, but all of the information can be found in the final report, edited by M. Clarke and J. Boon.⁸

As a sign of our times, the first review article in Chinese on the subject of this chapter was published in 2003.⁹ This paper mainly presents the use of Py-GC/MS in the identification of binding media, pigments, or dyes in paintings.

There are many reasons for the increasing popularity of this method in museum laboratories. Primary is the circumstance that many art materials such as amber, ivory, paper, and wood are both nonvolatile and insoluble. Other materials (e.g., drying oils, lacquers, and some synthetic polymers) become insoluble and nonvolatile upon aging. This alone makes them unsuitable for conventional analysis requiring solubility (e.g., high-performance liquid chromatography [HPLC]) or high volatility (e.g., GC). Another attractive feature of analytical pyrolysis is the very small sample size required (10 to 100 μg), which makes analytical pyrolysis a virtually nondestructive technique. Another attractive reason is the absence in most applications of any required preliminary chemical treatment of the sample prior to the analysis, coupled with the simplicity of the procedure and relatively low cost of equipment in the case of Py-GC-flame ionization detector (FID). Of course, a high degree of sophistication for the MS in Py-MS or Py-GC/MS can bring the instrumentation costs into the high-cost range. The absence of chemical treatment is especially important because very often such pretreatment can cause rearrangements in labile molecules of analyzed materials.

Since this chapter was first published 10 years ago, a very noticeable tendency in pyrolysis research can be observed: fewer investigators are using Py-GC/FID as a fingerprinting technique, and more and more use Py-GC/MS as a method of choice for both fingerprinting and decoding the structure of analyzed compounds. This tendency could be explained by substantial improvements in MS detectors, enrichment of available MS libraries of compounds, and appearance of reasonably priced GC/MS instrumentation. To be fair, it should be mentioned that the price range of pyrolysis equipment for the last 10 years has risen quite substantially, in line with quality and sophistication.

At the same time, there are certain limitations and difficulties in the interpretation of the resulting pyrograms for cultural materials that deserve serious consideration. In spite of the growing interest in the pyrolysis technique, one should not overstate its apparent superficial simplicity.

One may note that some researchers have simply purchased a set of reference materials from reputable chemical producers, pyrolyzed them, and published the results, claiming that the problem of distinguishing among them has been solved. Unfortunately, this is not the case. A thorough investigation of pyrolysis patterns of fresh and aged materials must be conducted. The aged materials of definite prove-

nance can often be obtained from museum collections or as a result of intensive artificial aging procedures, though one must again exercise caution since the end products of natural and artificial aging may differ.

Comparison of the results of analysis of fresh and aged materials can lead to very different conclusions. For example, in the case of dammar and mastic, it is very easy to distinguish between the fresh samples of these resins, but after extensive artificial aging, dammar will retain its characteristic profile while mastic can give a completely unrecognizable one.¹⁰

One must emphasize that analytical pyrolysis is a very valuable tool in analysis of artistic and archaeological materials only as a result of very thorough and systematic research programs, rather than sporadic efforts.

There are two areas of complication related to analytical pyrolysis in the above-mentioned field. One has to do with sampling and the other with instrumentation. The first is very specific for this particular area of research, while the second will affect any application of analytical pyrolysis. From the point of view of sampling, it is quite obvious that, as with every comparative technique, analytical pyrolysis requires an extensive reference library of pyrograms. This condition can be easily met in case of modern materials, but becomes almost insurmountable when someone is looking for samples of material ranging from a few hundred to a few thousand years in age or, in the case of amber and copal, millions of years.

Another potential complication is based on the fact that artists seldom used absolutely pure materials, but rather preferred to use complicated mixtures. Considering old varnish recipes¹¹⁻¹³ or oil media,^{14,15} one can immediately recognize the complexity and the resulting uncertainty in the composition of these mixtures: it is easy to overlook minor peaks that are overshadowed by the signals of the major components.

Another trap is the fact that very often the art object has been restored using materials superficially similar to, but quite different from, the original (e.g., beeswax substituted by paraffin). Identification of this later addition could lead one to misleading conclusions. A further stumbling block is the understandable reluctance of curators to provide samples of adequate size. In practical terms, it means that it is very difficult to undertake controlled or replicate experiments to confirm or reject ambiguous results. Similarly, the extremely small size of the sample leads one to ask how representative it is. This is especially the case when artists use mixed media (or vary composition throughout the artifact).

In addition to the difficulties arising from the samples of art and archaeological materials, there are those posed by pyrolysis equipment.

6.2 INSTRUMENTAL CONSIDERATIONS

Though the detailed pros and cons of different types of pyrolysis apparatus are discussed elsewhere,¹⁶ we feel obliged to share our own experience, working for 6 years with the CDS Pyroprobe 120. This system is well known and in wide use. It produces a highly predictable temperature time profile for the filament and provides a means of varying the heating rate linearly over the initial temperature rise period (ramp control).

Among the definite advantages of the Pyroprobe over Curie-point pyrolyzers are the absence of solvent and grinding for sample introduction, ease in weighing the sample, and freedom of temperature choice. It is also hard to overestimate the possibilities provided by CDS Pyroprobe to carry out so-called sequential pyrolyses¹⁷; i.e., the pyrolysis temperature and time are chosen in a way that each pyrolysis affords only fractional decomposition of the sample. This additional capability of the CDS instrumentation was successfully used to identify the provenance of amber artifact from Hasanlu.¹⁸

At the same time, the very fact that CDS Pyroprobe is combined with a GC instrument through an interface can cause certain problems. Due to the relatively large surface area of the interface between the GC instrument and the pyrolyzer, a memory effect is often obtained where high molecular weight compounds from previous analyses still produce GC traces in subsequent runs. Especially notorious in this regard are paraffins, waxes, and various oils. For example, it is very difficult to get rid of traces of palmitic acid. Even heating the interface to 300°C between runs does not always permit elimination of these shadow traces. We strongly recommend a blank run (sometimes two) between the actual analyses because these shadow traces can interfere with current pyrograms.

Similar complications were observed for Curie-point pyrolyzers. In a recent review,¹⁹ the author complained that:

a well-known trapping effect in Curie point pyrolysis devices is condensation of tar on the glass liners which are generally used to hold the ferromagnetic probes. This condensation can be reduced by heating of the glass liners and a very close interfacing of GC column and pyrolysis chamber,²⁰ but drop out of higher molecular weight fractions is unavoidable.

Another danger associated with the instrument is the possibility that during the actual run the needle that introduces the gaseous product into the GC column can become clogged. It is unavoidable that after a hundred analyses some of the less volatile components will be deposited inside the needle. Sooner or later they will clog it, but unfortunately it is very difficult to predict this precisely because the clogging depends not only on the number of runs, but also on the nature of the materials analyzed. For example, it is rare to have problems with “unzipping” synthetic materials, which under pyrolysis conditions produce mainly monomers, dimers, and trimers. However, significant problems can occur when analyzing old, heavily oxidized, drying oil samples, ambers, and similar materials.

A serious consideration when comparing results from different laboratories is the temperature of pyrolysis. What must be stated clearly is the fact that the temperature of pyrolysis differs dramatically depending on what kind of filament has been used, i.e., coil filament with a quartz tube or a platinum ribbon. The CDS Pyroprobe uses the resistive filament simultaneously as the heating element and the temperature sensor. The ribbon filament needs only 8 msec to reach 600°C,¹⁵ but a sample in the coil filament is inside a quartz tube. This means that when the temperature of the coil is 650°C, the temperature inside the quartz tube will be substantially lower. Comparing published results on acrylic polymers²¹ and our own

observations, we can say that this difference can be ca. 150°C; i.e., to obtain the same pyrogram with Paraloid B-72 that was obtained at 500°C on the Pt ribbon, we had to heat our sample in the quartz tube to 650°C.

Also a word of caution could be offered about any attempted comparative study where researchers have used both types of filaments. Perhaps as a result of Pt catalytic effects or because of differences in temperature rise profiles, it is quite difficult to obtain identical pyrograms on different filaments even when the difference in temperature is taken into consideration.

Finally, we note another limitation. The CDS Pyroprobe coil filaments are initially all evenly spaced, but after intensive use these individual loops very often can touch each other. This has a far-reaching and quite important consequence; the resistance of the coil will increase, and as a result the real temperature will be much higher than the nominal reading.

In this chapter we will critically review mainly those publications that deal directly with the application of analytical pyrolysis to the examination of art or archaeological objects. It should be indicated nevertheless that a substantial literature devoted to analysis of such materials as wood, polysaccharides, textiles, proteins, and numerous synthetic polymers can be found in other chapters of this book.

In this text we will only briefly note work done using homemade equipment or with old-type packed columns, even if the reported results were quite significant but now are mainly of historical interest. For a more extended discussion of these studies, consult our previous review.¹

6.3 ANALYSIS OF MATERIALS

For the convenience of specialists working in this field, we will discuss all the data according to the class of materials.

6.3.1 WAXES

Analytical pyrolysis proved itself a most suitable technique for the analysis of waxes because they are not readily soluble in organic solvents and, considering the molecular size of their major components (from 30 to 60 carbon atoms), are not very volatile.

One of the first publications dealing with a great variety of waxes²² used Py-MS for its analysis. There is some confusion about results of this investigation. On the one hand, the author claims that "Py-MS was found to provide a rapid and unambiguous method of characterizing the waxes in the reference collection but discrimination within the class was rather poor," while the same publication contains a table (no. 4) that represents "major ions in the zone and their relative abundance," where all the samples but three show the same very uncharacteristic ion mass numbers 43, 57, and 111, and some (no. 18 — spermaceti wax) fragments that are very difficult to imagine (for example, mass 229). Also, it is difficult to accept the explanation that "Fig. 1 is typical of 15 of the reference waxes," which includes such chemically different materials as beeswax, carnauba wax, spermaceti, shellac wax, rice wax, earth wax, and paraffin wax. It appears the high ionization energy (70 eV)

caused such an excessive fragmentation that, as a result, very uncharacteristic ions were obtained. At the same time, the relatively low temperature of the MS jet separator (200°C) prevented heavy fragments from reaching the mass spectrometer. Also surprising is the choice of the mass range on the above-mentioned Fig. 1. It covers the area between 1 to 250 mass units, in spite of the fact that the most characteristic and informative ions should be found in much higher mass numbers. For example, Py-MS analysis of the notorious Flora bust in the Berlin museum²³ revealed the presence of spermaceti wax mixed with beeswax through the presence of the undeniably strong ions with mass of 480 (cetyl palmitate ester, the major component (95.4%) of spermaceti max, MW = 480) and also few very strong signals at 224, which represent alkene resulting from dehydration of cetyl alcohol, and 257, which could be accounted for as a protonated molecule of palmitic acid (MW = 256). This analysis was performed using a very gentle ionization energy (12 eV) and choosing a very wide range of mass from 1 to 1000.

Interesting results were also published by Puchinger and Stachelberger²⁴ applying Py-GC and Py-GC/MS to the study of two synthetic waxes and beeswax, finding very clear differences in their fingerprints. A few technical details raise some questions: very short time (2 sec), which makes it difficult to pyrolyze material inside the quartz tube; very high temperature (800°C), which can cause extensive fragmentation; and high carrier gas rate (25 ml/min), which can cause substantial cooling and decrease the degree of product separation in a GC column.

As an illustration of the practical application of their method, the same authors using Py-GC analyzed a few samples from the surface of the Renaissance sculpture *Jungling von Magdalensberg* and found that all of them contain beeswax.²⁵ In spite of the fact that analytical results of this investigation are quite convincing, it is hard not to raise an objection from an art historical point of view. There is no evidence that this beeswax represents the original material from the time of manufacture. It is well known that beeswax can be used as a protective coating for bronzes and could have been applied quite recently, for example, in the 18th, 19th, or even in the current century. As it was demonstrated later,²⁶ the fingerprints of beeswax are practically unaffected even by very substantial intervals of time.

Our own results²⁶ using Py-GC for more than 40 analyzed wax samples produced quite distinctive fingerprints even within the same class (for example, plant waxes). Also, as was demonstrated by the comparison of beeswax from fresh samples to some approximately 4000 years old, the fingerprints for this material are very stable and could be easily recognized in spite of minor differences in the middle portion of the pyrogram (see Figure 6.1). Only in beeswax, in the last portion of pyrogram, which represents undecomposed hydrocarbons, can one easily spot differences in the amount of even- and odd-carbon substances (in beeswax odd carbon number hydrocarbons will always dominate).

As a practical application of these results, we note that the “oldest wax sculpture in the world”²⁷ in the collections of the Metropolitan Museum of Art was found to be made of modern paraffin²⁸ (see Figure 6.2). This finding definitely casts doubt about the authenticity of this object because paraffin is a product of the 19th century. For comparison, Figure 6.3 to Figure 6.6 show pyrograms of spermaceti, stearine, candelilla, and carnauba waxes, respectively.

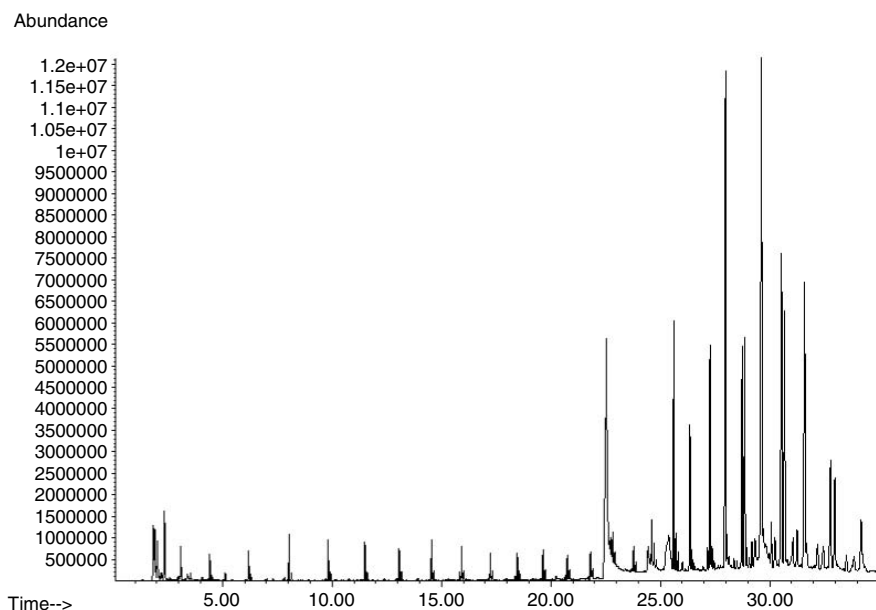


FIGURE 6.1 Pyrogram of natural, unbleached beeswax. The peak at 23 min is hexadecanoic acid.

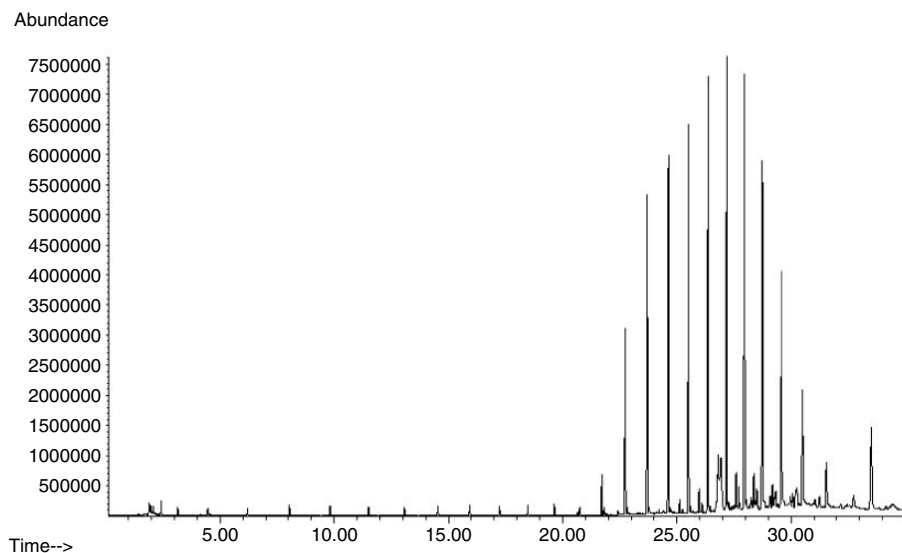


FIGURE 6.2 Pyrogram of paraffin wax.

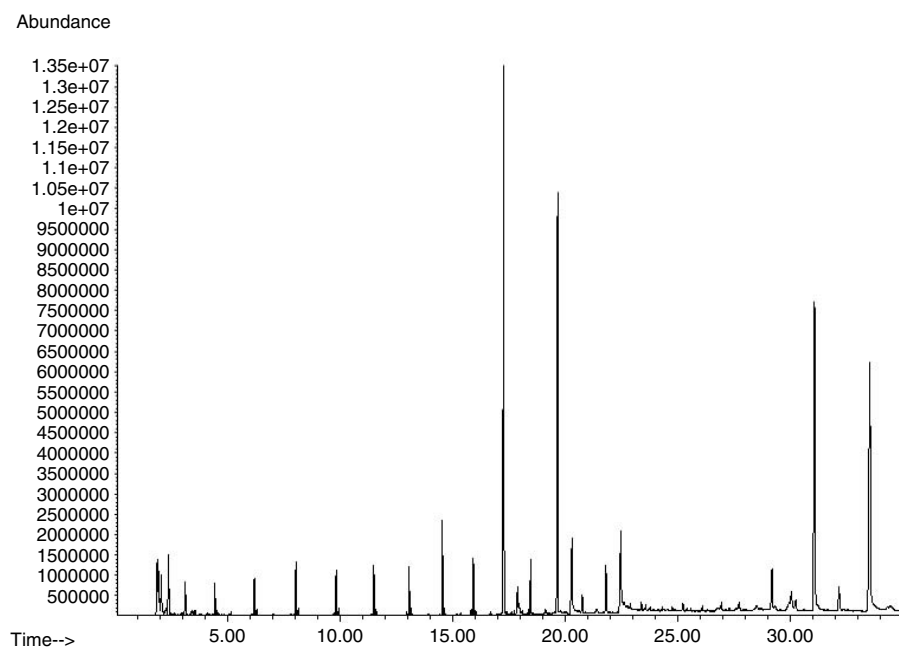


FIGURE 6.3 Pyrogram of spermaceti wax (U.S.P.).

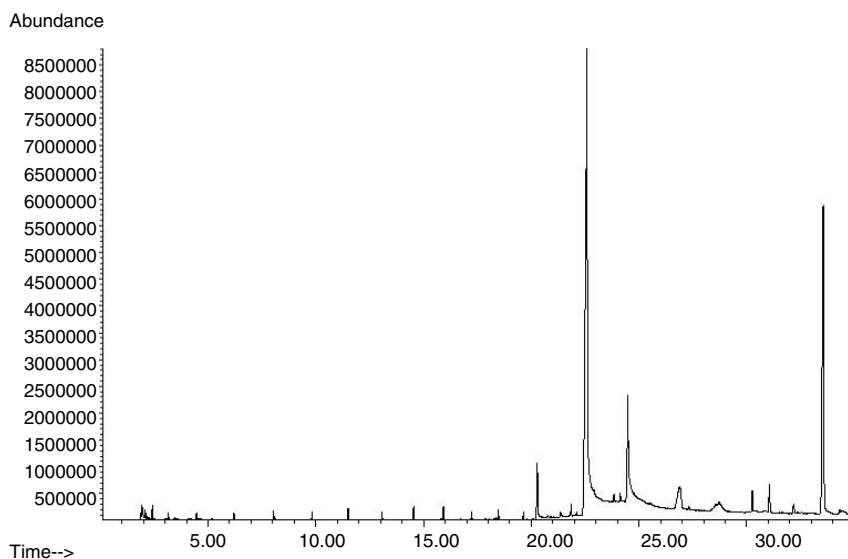


FIGURE 6.4 Pyrogram of stearine wax.

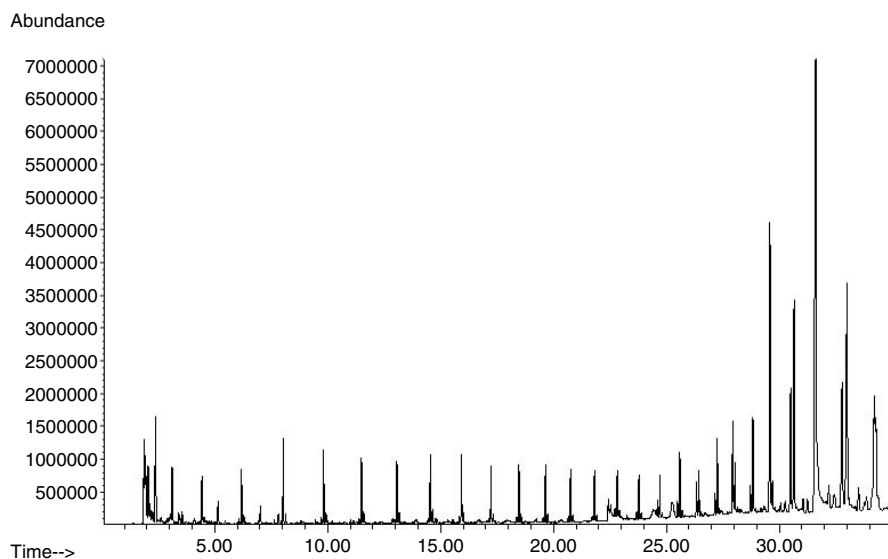


FIGURE 6.5 Pyrogram of crude candelilla wax.

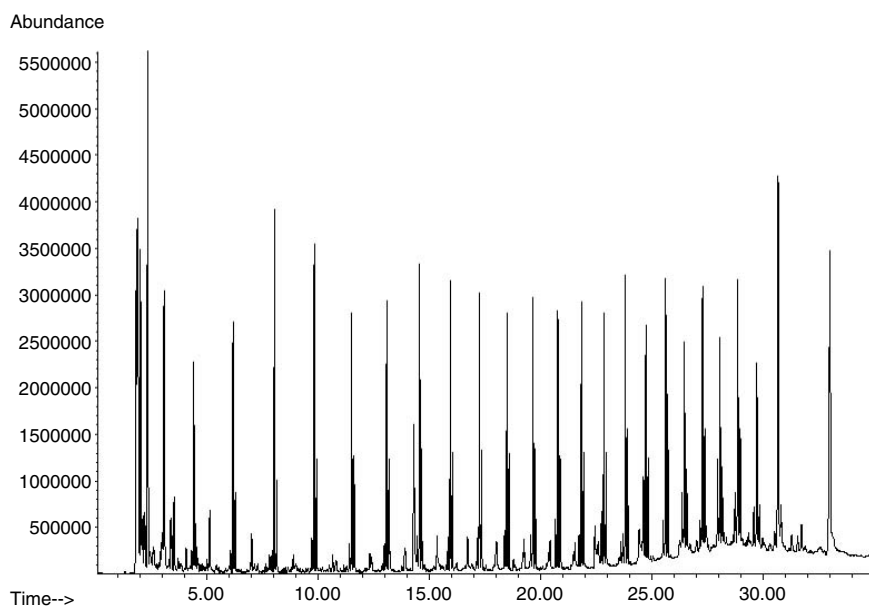


FIGURE 6.6 Pyrogram of yellow carnauba wax 1.

Another interesting approach to wax analysis, simultaneous pyrolysis-alkylation-gas chromatography, was also reported by Challinor,²⁹ who used tetramethyl ammonium hydroxide (TMAH) to alkylate acids of different waxes, making them more volatile. He concluded that the different waxes may be readily distinguished by the distribution of fatty acid methyl esters and fatty alcohols.

6.3.2 NATURAL RESINS

One of the most interesting classes of compounds, from the point of view of their importance in the field of art and archaeology, is natural resins. The past 15 years have brought some remarkable successes in this area of analysis and at the same time revealed some very fundamental difficulties that are not so easily overcome.

From initial, sometimes quite naïve, attempts to characterize natural resins on the basis of low molecular weight uncharacteristic products,³⁰ research in this particular area moved in very sophisticated directions: Py-GC, Py-GC/MS, in-source Py-MS, and simultaneous pyrolysis methylation (SPM).^{31–40}

As a result of dramatic improvements in GC equipment (e.g., introduction of fused-silica capillary columns) and a choice of correct GC conditions, even a regular Py-GC was able to solve some problems that other analytical methods were unable to solve. For example, IR analyses were unable to differentiate between dammar and mastic: two major natural resins used for varnishes.⁴¹ This problem was settled by using Py-GC,^{10,31} and as was proved by this investigation, dammar has an extremely characteristic fingerprint (see Figure 6.7 and Figure 6.8 for pyrograms) that is practically independent of age or source of this resin. The same paper deals also with sandarac and copals, but the very uncertainty of the term *copal* creates difficulties in distinguishing among them. The same authors examined a wide range of different copals in their other work,⁴² but this result will be discussed together with amber analysis.

A most impressive study in natural resins analysis was done by van Aarssen et al.⁴³ and was devoted to the characteristics of a biopolymer isolated from fossil and

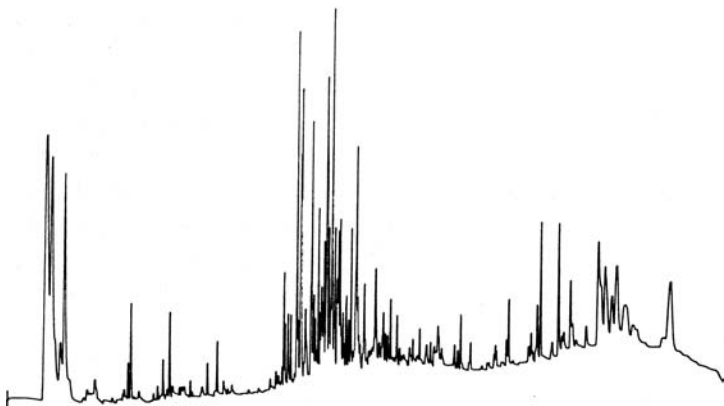


FIGURE 6.7 Representative pyrogram of typical dammar sample.

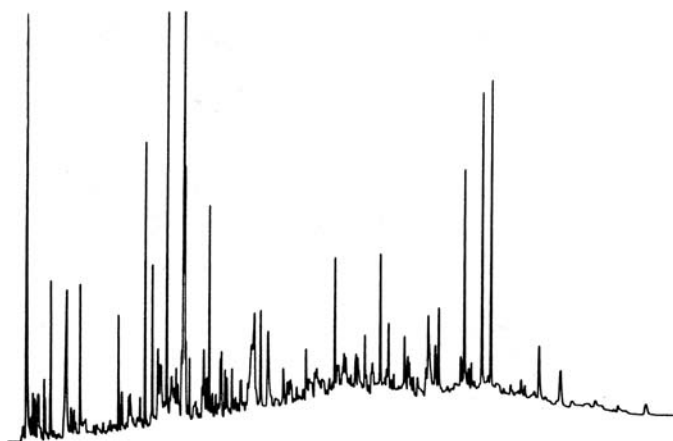


FIGURE 6.8 Pyrogram of typical mastic sample.

extended dammar resin (this fraction is known to conservators or conservation scientists as β -resin fraction in dammar). The most interesting result of this study from our point of view is not the finding that this fraction consists of a linear polymeric cadinene (the presence of the cadinane carbon skeleton in dammar was suggested much earlier⁴⁴) but the whole approach, that is, the use of three different pyrolysis methods: flash pyrolysis, open-system isothermal furnace pyrolysis, and closed-system isothermal pyrolysis. These three different pyrolysis methods gave complementary results and yielded information about the structure of β -dammar. It was concluded from flash pyrolysis data that this polymer is

a linear polysesquiterpene in which the monomers are linked by one carbon bond. From the open system isothermal furnace pyrolysis it became clear that the basic structural unit is a cadin-5,6-ene. The closed system isothermal pyrolysis revealed that bicadinanes can be formed from the polymer, implying the presence of a bond between monomers at position C_1 – C_{13} .

The practical importance of this finding is the fact that even after extensive aging by UV irradiation and heat, dammar still possesses these very characteristic peaks in the middle of the program, caused by the stereoisomers of C_{15} compounds with a cadinane carbon skeleton.¹⁰

6.3.3 AMBER

In light of the recently developed high interest in ambers, we decided to discuss these fossilized natural resins as a separate topic. For this reason, even information about fake ambers (mostly synthetic polymers) will be included in this discussion. Ambers have long proved difficult to examine. IR and FTIR spectroscopy provided useful tools in the determination of amber origins, but in a comprehensive review of the subject, Beck⁴⁵ stated:

I regret to say that we have not yet found the way to distinguish with any degree of confidence between the various kinds of non-Baltic amber. All we can do with a rather high level of certainty, is to say whether a given artifact is of Baltic amber or not.

When ambers were analyzed by Py-GC,⁴² Py-MS,³³ and Py-GC/MS,³⁴⁻⁴⁰ this situation changed dramatically.

The very first attempt in 1985 to analyze amber by Py-MS provided “a general picture of the chemical structure of amber and plant resins which after close comparison by multivariate (statistical) analysis, can be used for differentiation classification and identification purposes.”³³ At the same time, the authors admitted that it is difficult to give a detailed interpretation of the mass peaks, and it is almost impossible to trace back the various fragments to the original molecular entities. Another limitation of this study was the modest set of samples available. Further, several were of unclear origin. In this study, the authors used a Curie-point pyrolyzer (Fe/N alloy) at 510°C. The volatile pyrolysis products passed through a heated expansion chamber (150°C) into an open cross-beam-type ionizer operating at 14 eV. Processing of spectral data was carried out on a CDC Cyber 7600 system.

The next interesting study was done by Boon's group at the FOM Institute for Atomic and Molecular Physics (Amsterdam). They reported on data obtained by Py-GC and Py-GC/MS of recent and fossil copals and ambers from six continents. Although this study was not published, after its first original presentation at the 8th International Symposium, “Pyrolysis 88,” it became a part of the “Amber Profiling Project at FOM.”

As the authors of this project stated:

It is our intention to make a mass spectrometric atlas of geological and archaeological ambers and other resins. This atlas will contain a high resolution pyrolysis gas chromatogram, the EI and CI pyrolysis mass spectra and relevant Py-GC/MS data on the specimens.

This ambitious and very useful undertaking will require the collective efforts of scientists all over the world to overcome the main problem that plagues many researchers in this area: the unreliability of samples.

In the meantime, Grimaldi et al.'s group published the results of an investigation entitled “Occurrence, Chemical Characterization and Paleontology of the Fossil Resins from New Jersey.”⁴⁶ Using FTIR and Py-GC to examine fossil resins containing insect inclusions, the authors found that Cretaceous fossil resin is a true amber (it has terpenoid origin), but the unique tertiary fossil resin is composed mostly of polystyrene (a product of the genus *Liquidamber* from the Hamamelidaceae family).

In our own early work,⁴⁷ we analyzed a modest group of ambers and copals to demonstrate the ability of Py-GC to differentiate among specimens of different origins.

In 1989 to 1991, as a confirmation of our long-standing interest in natural resins in general and in ambers in particular, we used Py-GC to analyze a wide variety of different ambers and copals from the collection of the American Museum of Natural

History and other sources. In the course of this investigation, which included more than 40 samples from areas around the world, we were able for the first time to analyze by Py-GC samples of Japanese amber from the Fuji area. In an interesting finding we established that one fossil resin sample from Montana was almost pure natural polystyrene.⁴² On the basis of data obtained, attributions of some doubtful samples were done in a blind experiment and a number of fake amber imitation materials were uncovered. As a main result of this work, we reached the conclusion that Py-GC can be a valuable addition to the analytical methods routinely used in the study of amber, giving, in many cases, much more convincing fingerprints than other methods, e.g., FTIR.

Much richer information about ambers can be obtained by using the combined approach of Py-MS and Py-GC/MS. The most interesting work to date was presented at the conference "Amber in Archaeology" and published in its proceedings.³²

This paper is a preliminary report on the potential of Py-MS and Py-GC/MS to characterize ambers, copals, and other resins in microgram scale. A wide range of analyzed samples make this publication especially attractive. Py-MS methods employed by these authors compared with the earlier work done by Poinar and Haverkamp³³ permitted them to discriminate thermally desorbable compounds from fragments of the macromolecular skeleton resulting from pyrolytic dissociation. Using Py-GC/MS, the researchers overcame an important disadvantage of the Py-MS approach — the lack of isomer information, which is a particular drawback in the case of terpenoids.

The combined efforts of an international group of scientists⁴⁸ also permitted the full characterization of fossil polystyrene, which was found initially in Germany (1883) and later in the U.S. (Montana, New Jersey). Curiously enough, this material is atactic, as was proved by Py-GC and confirmed by H-nuclear magnetic resonance (NMR) spectra.

A systematic study "The Nature and Fate of Natural Resins in the Geosphere" was recently published by K. Anderson et al.³⁶⁻³⁹ It includes major amber and copals and such very rare materials as Tymir amber, which had not been systematically studied from the chemical point of view. The authors used Py-GC/MS and alternated direct pyrolysis with pyrolytic methylation, which was achieved by co-pyrolysis with tetramethyl ammonium hydroxide. The authors suggested a very broad classification scheme for resinates. They propose that most resinates may be classified on the basis of structural characteristics into one of four classes.³⁷ In a later publication, they added a fifth category.³⁸ One can question the validity of this classification or some of the particular conclusions regarding chemical structure of some of the described resins, but in general it is a valuable study that will provide much useful material for fruitful discussions.

A detailed study⁴⁹ was devoted to amber forgeries. It was shown by the authors that analytical pyrolysis (Py-GC, PYGC/MS) can provide undeniable proof that materials under investigation are amber forgeries and also quite precisely characterize the nature of these substitutes. Early Bakelites, modern phenolic resins, polystyrene, epoxy resins, and a wide range of unsaturated polyesters were identified as the most often used materials.

With the wide commercial availability of the last class of compound and sophisticated “artwork,” convincing imitations of large transparent amber pieces with a wide variety of “inclusions” (ants, bees, lizards, mosquitos, etc.) have been prepared.⁵⁰ Py-GC provides a simple test for unmasking of such fakes, and Py-GC/MS can identify quite precisely the structures of the materials used for these purposes.

In the 10 years since the first edition of this book, a significant amount of work has been done on the analysis of ambers and amber look-alike materials using analytical pyrolysis.

The major tendency in all of these works is a switch from Py-GC to Py-GC/MS as a more reliable and convenient technique to differentiate between varieties of ambers and their imitations.

The last two papers dealing with Py-GC analysis of ambers were published by the authors of this chapter in 1995 and 1999.^{51,52} The first of them⁵¹ was devoted to the examination of amber artifacts from different museum collections, including the Metropolitan Museum of Art (New York), the University of Pennsylvania Museum (Philadelphia), the Dahlem Museum (Berlin), the Boston Museum of Fine Art, and the J.P. Getty Museum (Los Angeles). The second one⁵² was devoted to the examination of amber objects from the ethnographic collection of the Israel Museum (Jerusalem). In spite of the successful differentiation among 47 samples taken from this collection, a conclusion was reached that in the case of natural Baltic amber and pressed Baltic amber (a product of 19th and 20th centuries), analytical pyrolysis alone could not determine the difference. Chemically, they are identical, and as a result they produced the same fingerprints in Py-GC. The only way to distinguish between them was to measure their hardness. (In the Mohs’ scale, the hardness of natural Baltic amber is around 2.3 and the hardness of the pressed one is around 3.)

Since 1999 our major efforts in amber analysis concentrated on using the Py-GC/MS method. To illustrate the results of this work, we refer to two papers dealing with amber analysis for the American Museum of Natural History.^{53,54} In both of them we were able to identify the major components of these resins and also evaluate the differences and similarities between certain formations in the Hanna Basin in Wyoming.⁵⁴

As a case in point, we discuss the most recent result of our collaboration with the State Hermitage Museum (St. Petersburg, Russia).^{55,56} In both cases, the subjects of our investigation were archaeological samples, but in the first case the problem was to pinpoint the nature of amber used for making the beads found in the Arzhan-2 burial memorial site located not far from the border between Russia and Mongolia. Considering the proximity of Burma, it was reasonable to suggest that the beads could be made from either Burmese or Baltic ambers. The problem in solving this puzzle was that the fingerprints of the two ambers look confusingly similar. The only substantial difference is the fact that Baltic amber contains succinic acid, which is absent in Burmese amber. Some local or Chinese fossilized resins could also be under consideration as potential materials. We also could not exclude Lebanese amber because in the same burial site some glass beads of Middle Eastern origin were found.

From a simple comparison between Py-GC/MS traces of Burmese, Lebanese, and Baltic ambers and the State Hermitage samples, it was clear that all six samples

from the museum collection were made of Baltic amber (Figure 6.9). This finding was emphasized by the presence of a very strong peak of succinic anhydride with a mass of 56.

The subject of another investigation in the nature of archaeological amber samples (pendants found in the upper reaches of the Western Dvina River) was the fact that a chunk of resinous material found by local residents in the same location was a candidate for the raw material used to make these pendants. Py-GC/MS analysis revealed that all the pendants were made of Baltic amber, and the raw material represented a totally different class of organic compounds — natural gums. Figure 6.10 shows two pyrograms (A for the Baltic amber with a strong peak of succinic anhydride and B for the natural gum with a very characteristic peak of furfural).

Our collaboration with the State Hermitage Museum is continuing. We are now working on an article describing the analysis of some very spectacular objects from the Archaeological Department of this museum, dating to the early Scythian period.

6.3.4 OILS AND FATS

The identification of oil and fats is crucial for both fields of art and archaeology. In art, after the first third of the 15th century, drying oils became the most often used paint media but may have been used even earlier. Archaeological findings of oil-containing jars are common and can range from 400 to a few thousand years in age.^{57–62}

In our previous review¹ we discussed all earlier attempts to analyze these materials using pyrolysis techniques.^{46,62–67} What has become quite clear is that fingerprinting alone with Py-GC is not enough to obtain a sufficient amount of information about the nature of the oil under examination.

Many previous studies dealt with fresh oil samples (or relatively young samples just a few years old), but extensive oxidation processes take place under different conditions. For example, the direct intensive sunlight in many cathedrals, the constant candle heat in front of altar pieces, numerous restorations using unknown and sometimes very strong solvents — all these factors can dramatically affect the condition of the oil layer under examination. Even more, assume that as a result of our analysis we obtained a very accurate description of the modern condition of the old paint layer or archaeological oil sample. It does not mean that we can easily reconstruct the formula of the original material. All fats and oils (with rare exceptions) have more similarities than differences, and the later ones most often are represented by unsaturated acids that suffer the most in the oxidation process. If one would add the deep hydrolysis of oils that is always the case in archaeological samples, the problem of tracing the origin of this fatty material becomes almost insurmountable.

As a rare illustration of the successful application of analytical pyrolysis for oil analysis, J. Boon⁶⁸ demonstrated that high-temperature in-source Py/MS can deal simultaneously with the analysis of oily compounds of an artist's paint and the analysis of inorganic components derived from the pigments. This work deals with Yellow Ochre oil paint (Talens van Gogh series), but even in the case of fresh material the author refrained from jumping to any conclusion about the nature of oil media (linseed, walnut oil, poppy seed, etc.).

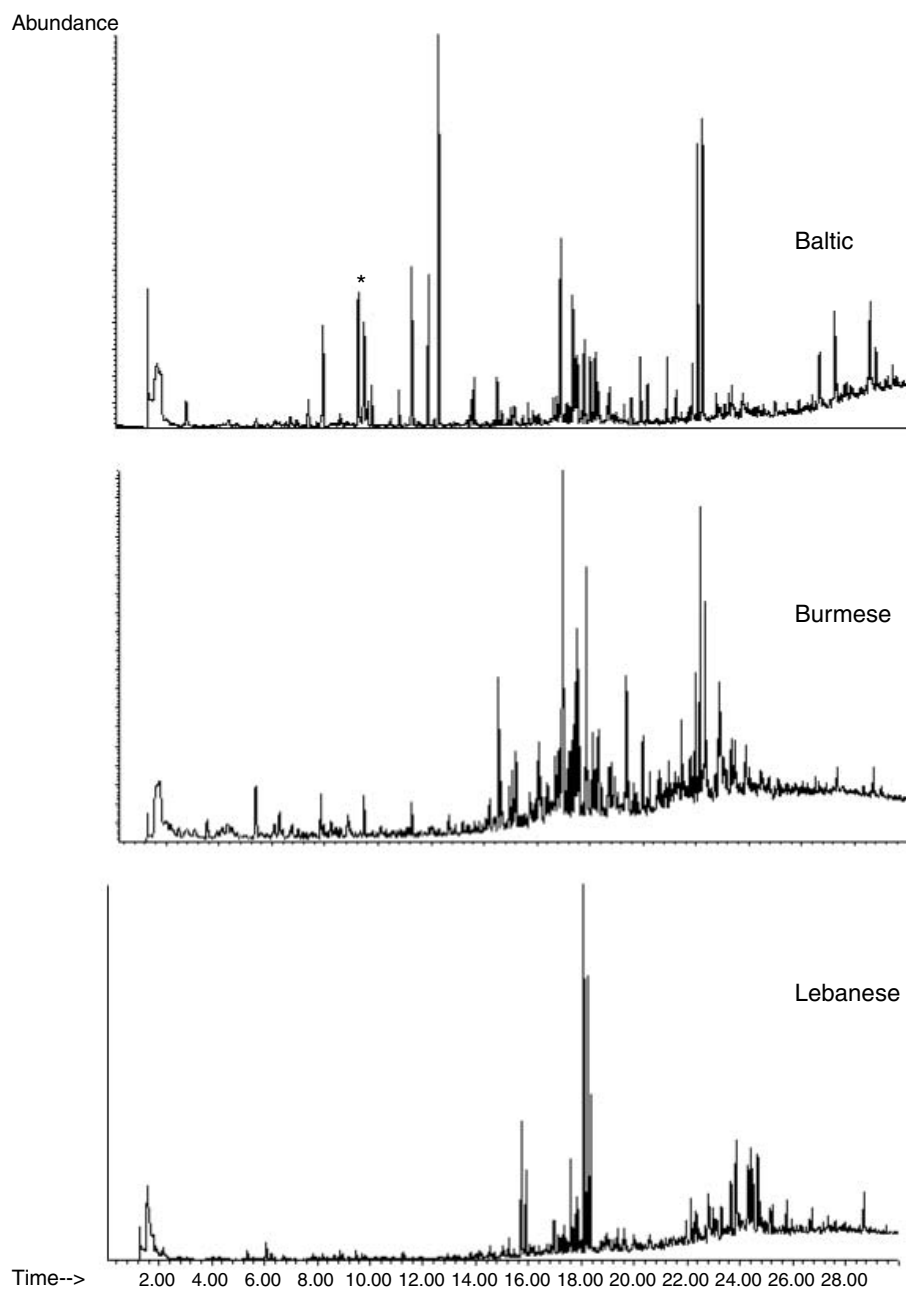


FIGURE 6.9 A comparison of Baltic, Burmese, and Lebanese ambers. * Marks succinic anhydride, characteristic of Baltic amber.

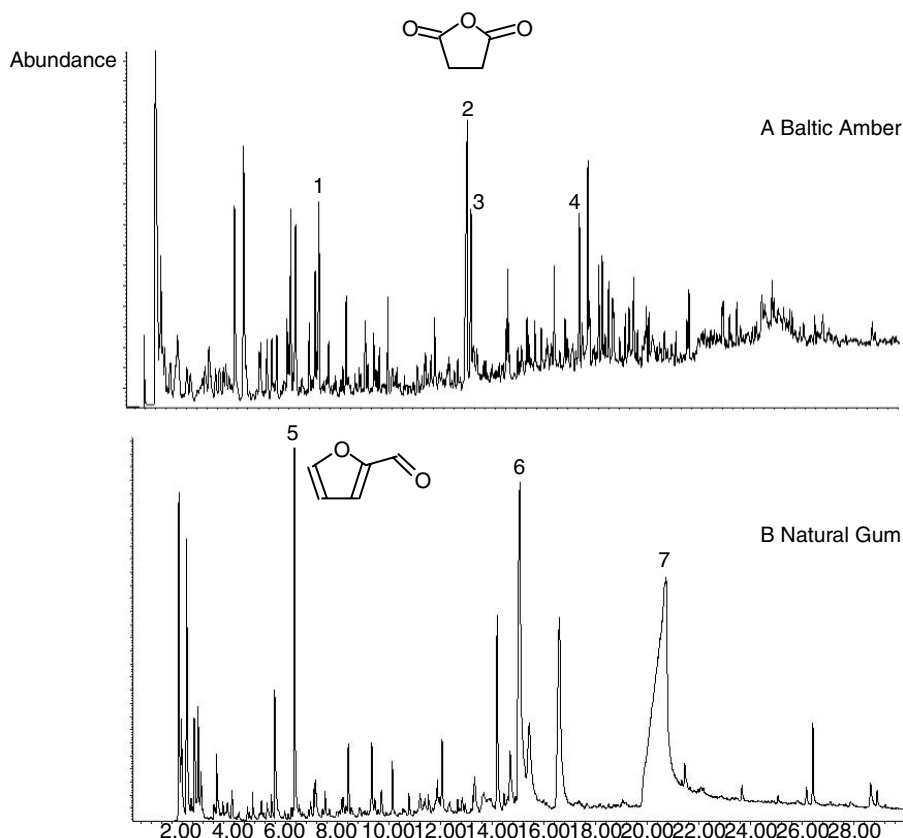


FIGURE 6.10 1 = Camphene, 2 = Succinic anhydride, 3 = Camphor, 4 = Borneol, 5 = Furancarboxaldehyde (Furfural), 6 = Hydroxymethyl furancarboxaldehyde, 7 = Levoglucosan.

In light of this statement, it is easy to appreciate the restraint of the authors of their publication dealing with molecular archaeology.⁶⁹ They determined, using Py-MS and PY-GC/MS, remains of lipids in prehistorical pottery and residues but stated that “the identification of original foodstuffs based on the relative distribution of free fatty acids in an archaeological sample is a difficult process.” Also, they admitted that mono-, di-, or triacylglycerides could not have been detected with the pyrolysis technique utilized.

For the most recent and comprehensive results in pyrolysis analysis of different oils used in painting, we recommend Reference 8, which provides more than a dozen articles, reports, and comments on this subject.

6.3.5 SYNTHETIC POLYMERS

The application of synthetic materials in art and conservation increased dramatically over the past 50 years. Among the reasons for this phenomenon are the loss of availability for some traditional materials and the improved longevity, strength,

resistance to yellowing, etc., offered by synthetic substitutes. A further consideration was cost.

Synthetic adhesives and acrylic paints are but two examples of synthetic polymers widely used in art and conservation. However, these products generally were not specifically developed for conservation purposes, and most manufacturers, citing "trade secrets," refuse to reveal the precise contents of their products. This is especially true of such additives as antioxidants, flocculants, antifoamers, emulsifiers, etc. Often companies have changed the contents of products, keeping the same name while not informing the customers about these changes. A well-known example is that of ketone resin varnishes.⁷⁰ An extensive review of the thermal analysis of polymers is given in Chapters 4 and 5 of this book. Here we note a few of the applications of pyrolysis in the area of art and conservation.

In an early study, now primarily of historical interest, W. Noble et al.⁷¹ dealt with the characterization of adhesives by pyrolysis gas chromatography and IR spectroscopy. The scope of this study, in which 179 commercial products were analyzed and two complementary analytical methods were employed, provides a useful model, though the applicability of the results is limited by the obsolescence of the instrumentation used.

In 1987, in a much more comprehensive study⁷² from the same laboratory, the authors studied 94 adhesives available in the U.K. Some of them are of considerable importance in art and conservation: poly(vinyl acetate) (PVA), PVA copolymers, acrylics, silicones, carbohydrates, and epoxy-based adhesives. It was demonstrated that Py-MS is capable not only of determining the main products of pyrolysis and producing reliable fingerprints, but also of detecting some of the additives present in small tiny amounts, e.g., tackifiers, antioxidants, and plasticizers. This is very important in the light of growing concern among the conservation scientists over the long-term effects of additives on conservation and art materials. Besides the widely known and well-described work of E. DeWitte et al.,⁷³ and DeWitte and Terfve,⁷⁴ who used analytical pyrolysis to identify a number of synthetic resins of importance in a very systematic study, there is the work published by the Louvre conservation laboratories.^{4,5} Sonoda and coworkers investigated ketone resins by using Py-GC/MS and made a quite thorough study on identification of synthetic materials in modern paintings, including polymeric varnishes and binders, synthetic organic pigments, and media, using Py-GC and x-ray diffraction (in the case of pigments). Among many interesting conclusions, the authors observed that analytical pyrolysis is a very convenient tool for analysis of new synthetic materials and could be "indispensable to determine or to confirm the painting technique or the study its alteration."

Furthermore, they note that:

the dates of the first synthesis or of the first industrial and commercial production being generally known, the identification of these materials gives a time reference which may permit one to study the authenticity of the painting or to specify the nature and the age of the repainting.⁴

In the second part of their investigation,⁵ the authors provided extensive historical data on the nature and methods generally used for the analysis of organic synthetic

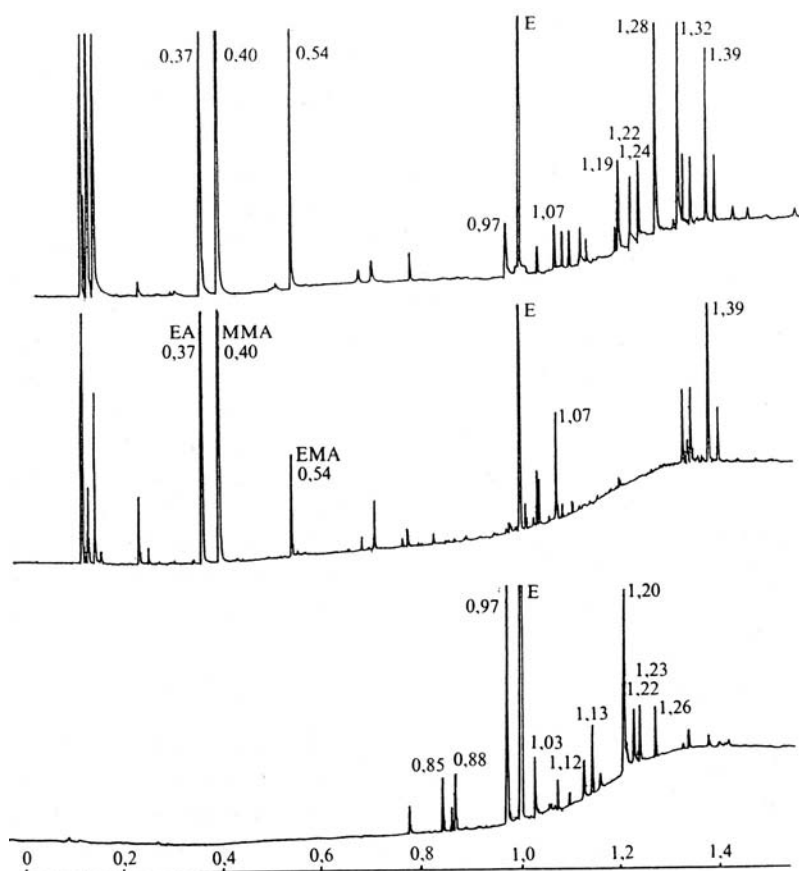


FIGURE 6.11 Pyrogram of Hooker Liquitex Green (top), Liquitex Medium (center), and the green pigment. Retention times are relative to the internal standard dodecane (marked E). EA = ethyl acrylate, MMA = methyl methacrylate, EMA = ethyl methacrylate. (Adapted from Ref. 5.)

pigments and also demonstrated that two techniques, Py-GC and x-ray diffraction, could be complementary and very useful in the identification of these pigments. Moreover, Py-GC was also able to identify and differentiate the synthetic binding medium used in some paintings without any further analysis. Figure 6.11 shows an example of an acrylic painting medium with its pigment, along with the medium and the pigment material pyrolyzed separately. What is also of practical importance is that several examples were given showing the relevance of these methods to the investigation of modern paintings: identification of the technique and diagnosis of alterations, not to mention a characterization of retouchings or restoration materials.

In her latest article published in *Studies in Conservation* (1999), N. Sonoda⁷⁵ deals with the characterization of organic azo pigments by Py-GC. Considering the fact that this type of pigment accounts for the largest amount of synthetic pigments used in artists' materials, it is easy to appreciate the results of this study.

The most recent and most comprehensive study of synthetic paints using Py-GC/MS was undertaken by T. Learner⁷⁶ from the Tate Gallery (London). This article on the analysis of synthetic resins found in 20th-century paint media was published in 1995.⁷⁷ There he described the use of two methods, Py-GC/MS and FTIR, for the characterization of 20th-century synthetic resins. In his latest paper, Learner substantially broadens the set of resins, using not just artistic synthetic paints, but also paints intended for other, more commercial or industrial markets, since many modern and contemporary artists used this type of material for their oeuvre (for example, Willem de Kooning, Francis Picabia, Pablo Picasso, Jackson Pollock, and Frank Stella to name just a few).

Also, unlike in References 4 to 6, Learner was able to use the much more sophisticated method of Py-GC/MS (instead of Py-GC) and more modern equipment. In conclusion, the author stated, "Py-GC/MS was shown to be an extremely effective analytical method for detecting all the principal classes of synthetic polymers that have been used as binding media in paint formulations" (Learner,⁷⁶ p. 238). But he also reached another logical conclusion:

Although not discussed here, the technique [Py-GC/MS] was just as suited to characterizing synthetic grounds and primers, which are formulated with the same types of polymeric binder. It was also capable of detecting the main classes of resin used in the synthetic varnishes as well as azo-organic pigments.

A year later, a very similar article was published in *Plastics in Art (History, Technology, Preservation)*.⁷⁸ The scope of this study was much smaller than the previous one (only alkyds, acrylates, silicone resins, and polyvinyl acetate were investigated) but the method was the same (Py-GC/MS using a Curie-point pyrolyzer), as were the conclusions.

Three more papers, presented at the 13th Triennial Meeting of the ICOM Committee for Conservation (Rio de Janeiro, September 22–27, 2002), should be mentioned.^{79–81} They all deal with synthetic materials but on a variety of topics, from detection of potential residue on objects previously cleaned with aqueous gel⁷⁹ to analysis of plastic and rubber items in the collection of the National Cinema Museum in Toronto.⁸⁰ The last case is a very unusual one because many objects in these collections (9000 according to the authors) were created just for making a movie and never were designed to last. But now they have become museum items and need to be cleaned, restored, stored, and exhibited. Py-GC/MS analysis was instrumental in coping with some of these problems. It is worth mentioning that one should be careful in comparing the results of all these studies, because the fragmentation of the analyzed materials could be affected by the differences in pyrolyzing devices. In Reference 8, the FOM-4LX Curie-point pyrolyzer was used, but in Reference 80 the investigators used a CDS Pyroprobe 1000 heated filament system.

6.3.6 SILOXANES

The thermal decomposition of linear and branched polydimethyl-siloxanes and their derivatives^{82–89} has been studied extensively. All of these papers were published

outside the conservation literature but are relevant because in the last 15 years, great interest in the use of these polymers as stone consolidants has developed. Some of these publications, in spite of the sometimes antiquated equipment used, could be very useful tools in analysis of this material.

6.3.7 PROTEINS

This field should be as important to art and conservation as natural resins and waxes. It includes such diverse materials as gelatin, egg white, egg yolk, casein, and vegetable proteins. In practical terms, this field covers quite a range of very different substances, including adhesives, binding media, horn, ivory, tortoise shell, wool, silk, etc.

However, as J. Mills and R. White⁹⁰ state,

As the proteins of museum objects are concerned there are no unique amino acids for particular proteins whose presence serves to identify them, but an identification is often possible by means of a quantitative assay of the amino acids.

One can argue that, for example, hydroxyproline is quite noticeable in collagen (12.8%) and completely absent in keratin (wool) or fibrin (silk) or could be found in gelatin (7.4%) but has a zero content in egg white, egg yolk, and casein — materials very often used as adhesives and binding media.

Another example is cystine, found in some structural proteins. It could be as high as 12.8% (wool) or 8.2% (feather) but completely absent in collagen and fibroin (silk).

In theory, analytical pyrolysis with its absence of sample pretreatment should be very useful in the light of the known fact that:

some epimerization of the amino acids at the common asymmetric center can take place when they are liberated by base hydrolysis of proteins. Also loss of amino acids during hydrolysis occurs through formation of humins. These are dark brown substances formed by condensation of amino groups and the indole nucleus of tryptophan with aldehydes formed *in situ*.⁹⁰

The other complication was mentioned in the thorough research done by Halpine,⁹¹ who used HPLC for protein identification, observing that tryptophan was not detectable because it was completely destroyed during derivatization.

In an effort to avoid all these problems of derivatization, Chiavari and Calletti⁹² and Chiavari et al.⁹³ published articles dealing with the subject of amino acids and proteins analyzed by Py-GC/MS and its application to identification of ancient painting media.

According to their results, in contrast to HPLC, the presence of tryptophan is “neatly revealed through the generation of a series of indoles by Py-GC/MS.” At the same time, they found that “hydroxyproline gave a dehydration product similar to that of proline.” Glycine, alanine, and threonine yielded pyrograms of little diagnostic significance. For unknown reasons, histidine also did not produce any meaningful pyrolysis products. But 15 of 19 analyzed amino acids did provide some very interesting mass spectra.

As usual, some questions arose when the authors moved to the analysis of real paint media. They stated that “the main pyrolysis fragment of rabbit glue was pyrrole which was absent or of very low intensity in all the other media.” Also, they detected the presence of pyrocoll ($C_{10}H_{22}O_3N_3$, MW = 232) and 3,6-(2-methylpropyl)-2,5-diketopiperazine ($C_{12}H_{22}O_2N_2$, MW = 226). After presenting these data, the authors state that “these compounds can be ascribed to the thermal decomposition of hydroxyproline ..., which has been shown to generate such fragments” (in their previous investigation of amino acids).⁹⁴ There is some problem with this statement, since pyrrole was generated also by glutamic acid, which is plentiful not just in animal glue (10%), but also in egg yolk (15%), egg white (14%), and casein (20%). As for the other two compounds, they are absent in the fragmentation products of hydroxyproline according to Table I of their previous publication.⁹⁰

At the same time, there is a very interesting observation about indole and methylindole revealed by Py-GC/MS as products of thermal decomposition of tryptophan in egg white, because this amino acid is absent in animal glue and is usually lost in the acid hydrolysis workup common to conventional GC and HPLC. Also, there is a very detailed comparison between conventional techniques (like GC and HPLC) and analytical pyrolysis methods in the end of the article.

What is quite obvious is that much more work should be done in this particular area to arrive at reliable qualitative and quantitative results. It is hard to argue with a pessimistic assessment given in one of the most interesting articles devoted to this subject:⁹⁴

The composition of pyrolysates of proteins is still obscure despite the effort of several researchers. This is partly due to the different structures of the amino acids, the different stabilities of the various peptide bonds and the overall heterogeneity of the peptide. On the other hand there has been very little uniformity in the methods used for pyrolysis and hence different parts of the pyrolysates are always studied.

Finally, for the sake of completeness, three other papers dealing with proteinous materials^{29,95} or identification of substances applied during chemical processing of wool⁹⁶ should be mentioned. Otherwise, this field is not very well explored.

REFERENCES

1. Shedrinsky, A.M., T.P. Wampler, N. Indictor, and N.S. Baer, Application of analytical pyrolysis to problems in art and archaeology: a review, *J. Anal. Appl. Pyrol.*, 15: 393–412 (1989).
2. Shedrinsky, A.M., R.E. Stone, and N.S. Baer, Pyrolysis gas chromatographic studies on Egyptian archaeological specimens: organic patinas on the “three princesses gold vessels,” *J. Anal. Appl. Pyrol.*, 20: 229–238 (1991).
3. Derrick, M.R. and D.C. Stulik, Identification of natural gums in works of art using pyrolysis-gas chromatography, in *Proceedings of the ICOM Conference for Conservation*, Dresden, 1990, Vol. 1, pp. 9–13.
4. Sonoda, N. and J.P. Rioux, Identification des Matériaux Synthétiques dans les Peintures Modernes. I. Vernis et Liants Polymères, *Stud. Conserv.*, 35: 189–204 (1991).

5. Sonoda, N., J.P. Rioux, and A.R. Duval, Identification des Matériaux Synthétiques dans les Peintures Modernes. II. Pigments Organiques et Matière Picturale, *Stud. Conserv.*, 38: 99–127 (1993).
6. Mestdagh, H., C. Rolando, M. Sablier, and J.P. Rioux, Characterization of ketone resins by pyrolysis/gas chromatography/mass spectrometry, *Anal. Chem.*, 64: 2221–2226 (1992).
7. National Gallery of Art, 1992 Annual Report, Washington, DC, pp. 43–44.
8. MOLART, A multidisciplinary NWO PRIORITEIT project on Molecular Aspects of Aging in Painted Works of Art, Final report and highlights 1995–2002, M. Clarke and J. Boon, Eds., FOM Institute AMOLF, Amsterdam (2003) (also MOLART home page: www.amolf.nl/research/biomacromolecular_mass_spectrometry/molart/molart.html).
9. He, L. and G. Liang, Application of pyrolysis gas chromatography-mass spectrometry in the conservation and investigation of art objects, *Sci. Conserv. Archeol.*, 1: 306–316 (2003).
10. Shedrinsky, A.M. and N.S. Baer, Py-GC Analysis of Aged Damar and Mastic, unpublished results.
11. Hurst, H.G., *A Manual of Painters, Colours, Oils and Varnishes*, 5th ed., revised by N. Heaton, London (1913).
12. Theophilus, *An Essay upon Various Arts*, trans. with notes by R. Hendrie, London (1847).
13. Mills, J.S. and R. White, *The Organic Chemistry of Museum Objects*, Butterworth, London (1987), p. 99.
14. White, R., A review with illustrations of resin/oil varnish mixtures, methods applicable to the analysis of resin/oil varnish mixtures, report 2/16/81, in *ICOM Committee for Conservation, 6th Triennial Meeting*, Ottawa, 1981.
15. Havel, M., Un élément nouveau dans la couche picturale de la peinture moderne: le vernis de retoucher. Un exemple: le vernis de retoucher Vibert, report 19/72/10, in *ICOM Committee for Conservation, Triennial Meeting*, Madrid, 1972.
16. Irwin, W.J., *Analytical Pyrolysis*, Marcel Dekker, New York (1982).
17. Ericson, I., *J. Chromatogr. Sci.*, 16: 340 (1978).
18. Shedrinsky, A., C. Beck, and N.S. Baer, Analysis of Amber Artifacts from Hasanlu, unpublished results.
19. Boon, J.J., Analytical pyrolysis mass spectrometry: new vistas opened by temperature-resolved in-source PYMS, *Int. J. Mass Spectrom. Ion Proc.*, 118/119: 755–787 (1992).
20. Boon, J.J., A.D. Pouwels, and G.B. Eijkel, *Biochem. Soc. Trans.*, 125: 170–174 (1987).
21. DeWitte, E. and A. Terfve, The use of Py-GC/MS technique for the analysis of synthetic resins, in *Science and Technology*, N.S. Brommelle and G. Thomson, Eds., International Institute for Conservation, London (1982), pp. 16–18.
22. Wright, M.M. and B.B. Wheals, Pyrolysis-mass spectrometry of natural gums, resins and waxes and its use for detecting such materials in ancient Egyptian mummy cases (Cartonajes), *J. Anal. Appl. Pyrol.*, 11: 195–211 (1987).
23. Boon, J., private communication.
24. Puchinger, L. and H. Stachelberger, Pyrolyse-gaschromatographische Prüfung organischer Rohstoffe am Beispiel der Wachse, *Fat. Sci. Technol.*, 92/96: 243–248, 1990.
25. Puchinger, L., H. Stachelberger, and G. Banik, *Identifizierung Organischer Materialien an Objekten der bildenden Kunst, Wiener Berichte fiber Naturwissenschaft in der Kunst*, Band 6/7/8 (1989/90/91).
26. Shedrinsky, A.M., T.P. Wampler, and N.S. Baer, Pyrolysis gas chromatography (PyGC) applied to the study of natural waxes in art and archaeology, in *Science, Technology and European Cultural Heritage*, N.S. Baer, C. Sabbioni, and A.L. Sors, Eds., Butterworth-Heinemann, Oxford (1991), pp. 553–558.

27. Von Bull, P.R., *Vom Wachs, Hoechst Beitrage zur Kenntnis der Wachse*, Band I, Beitrag 1, Farbwerke Hoechst A.G., Frankfurt (M), Hoechst (1963), p. 36.
28. Shedrinsky, A.M., J. Boon, R.E. Stone, and N.S. Baer, unpublished results.
29. Challinor, J.M., The scope of pyrolysis methylation reactions, *J. Anal. Appl. Pyrol.*, 20: 15–24 (1991).
30. Takiura, K., A. Yamaji, and H. Yuki, Analysis of natural resins by pyrolysis gas chromatography. I. Classification of natural resins by pyrograms (Y. Zasshi), *J. Pharm. Soc. Jpn.*, 93: 769–775 (1973).
31. Shedrinsky, A.M., T.P. Wampler, and N.S. Baer, The identification of dammar, mastic, dandarac and copals by pyrolysis gas chromatography, *Wiener Berichte fiber Naturwissenschaft in der Kunst, Doppelband*, 4/5 (1987/88), pp. 12–25.
32. Boon, J.J., A. Tom, and J. Pureveen, Microgram scale pyrolysis mass spectrometric and pyrolysis gas chromatographic characterisation of geological and archaeological amber and resin samples, in *Amber in Archaeology: Proceedings of the Second International Conference on Amber in Archaeology*, Liblice, Tsjechoslovakia, October 30–November 2, 1990, Curt W. Beck and Jan Bouzek, Eds., in collaboration with Dagmar Dresleova, pp. 9–27.
33. Poinar, G.O. and J. Haverkamp, Pyrolysis mass spectrometry in the identification of amber samples, *J. Baltic Stud.*, 16: 210–220 (1985).
34. Anderson, K.B., R.E. Botto, G.R. Dyrkacz, R. Hayatsu, and R.E. Winans, Analysis and comparison of two Victorian brown coal resinites, *ACS Div. Fuel Chem. Preprints*, 34: 752–758 (1989).
35. Anderson, K.B. and R.E. Winans, Structure and structural diversity in resinites as determined by pyrolysis-gas chromatography-mass spectrometry, *ACS Div. Fuel Chem. Preprints*, 36: 765–773 (1991).
36. Anderson, K.B. and R.E. Winans, The nature and fate of natural resins in the geosphere. I. Evaluation of pyrolysis-gas chromatography-mass spectrometry for the analysis of natural resins and resinites, *Anal. Chem.*, 63: 2901–2908 (1991).
37. Anderson, K.B., R.E. Winans, and R.E. Botto, The nature and fate of natural resins in the geosphere. II. Identification, classification and nomenclature of resinites, *Org. Geochem.*, 18: 829–841 (1992).
38. Anderson, K.B. and R.E. Botto, The nature and fate of natural resins in the geosphere. III. Re-evaluation of the structure and composition of highgate copalite and glessite organic geochemistry, *Org. Geochem.*, 20: 1027–1038 (1993).
39. Anderson, K.B., The nature and fate of natural resins in the geosphere. IV. Middle and upper Cretaceous amber from the Taimyr Peninsula, Siberia: evidence for a new structural subclass of resinite, *Org. Geochem.*, 21: 209–212 (1994).
40. Anderson, K.B., New evidence concerning the structure, composition and maturation of class I (polylabdanoid) resinites, in *Amber, Resinite and Fossil Resins*, ACS Symposium Series, K. Anderson and J. Crelling, Eds., ACS, Washington, DC (1996), pp. 105–129. Anderson, K. and B. LePage, Analysis of fossil resins from Axel Heiberg Island, Canadian Arctic, in *ibid.*, pp. 170–192.
41. Feller, K.L., Dammar and mastic infrared analysis, *Science*, 120: 1069–1070 (1954).
42. Shedrinsky, A.M., D. Grimaldi, T.P. Wampler, and N.S. Baer, Amber and copal: pyrolysis gas chromatographic (PyGC) studies of provenance, *Wiener Berichte fiber Naturwissenschaft in der Kunst*, 6/7/8 (1989/90/91), pp. 37–62.
43. van Aarssen, B.G.K., J.W. de Leeuw, and B. Horsfield, A comparative study of three different pyrolysis methods used to characterize a biopolymer isolated from fossil and extant dammar resins, *J. Anal. Appl. Pyrol.*, 20: 125–139 (1991).

44. Shigemoto, T., Y. Ohtani, A. Okagawa, and M. Summoto, NMR study of beta-resene, *Cell. Chem. Technol.*, 21: 249 (1987).
45. Beck, C.W., *Journal of Baltic Studies*, Special issue: Studies in Baltic Amber, Vol. XVI, No. 3 (1985).
46. Grimaldi, D., C. Beck, and J. Boon, Occurrence, chemical characterization and paleontology of the fossil resins from New Jersey, *Novitates*, AMNH, No. 2948 (1989), pp. 1–27.
47. Shedrinsky, A., T. Wampler, N. Indictor, and N.S. Baer, The use of pyrolysis gas chromatography in the identification of oils and resins found in art and archaeology, *Conserv. Cult. Prop. India*, 21: 35–41 (1988).
48. Pastorova, I., T. Weeding, and J.J. Boon, 3-Phenylpropanylcinnamate, a copolymer unit in Sieburgite fossil resin: a proposed marker for the Hammamelidaceae, *Organic Geochem.*, 29 (5–7): 1381–1393 (1998).
49. Shedrinsky, A.M., D.A. Grimaldi, J.J. Boon, and N.S. Baer, Application of Py-GC and Py-GC/MS for unmasking of faked ambers, *J. Anal. Appl. Pyrol.*, 25: 77–95 (1993).
50. Grimaldi, D., A. Shedrinsky, A. Ross, and N.S. Baer, *Forgeries in Amber: History, Identification, and Case Studies*, Curator, AMNH (1994).
51. Shedrinsky, A. and N. Baer, The Application of Analytical Pyrolysis to the Examination and Conservation of Amber Artifacts from Museum Collections, paper presented at Proceedings of the Symposium on the Conservation of Cultural Artifacts, Taipei, 1995.
52. Shedrinsky, A., E. Muchawsky-Schnapper, Z. Aizenshtat, and N. Baer, Application of analytical pyrolysis to the examination of amber objects from the ethnographic collection of the Israel Museum, in *Investigations into Amber: Proceedings of the International Interdisciplinary Symposium: Baltic Amber and Other Fossil Resins*, September 2–6, 1999, B. Gdansk Kosmowska-Ceranowicz and H. Paner, Eds., pp. 207–214.
53. Grimaldi, D., A. Shedrinsky, and T. Wampler, A remarkable deposit of fossiliferous amber from the Upper Cretaceous (Turonian) of New Jersey, in *Studies on Fossils in Amber; with Particular Reference to Cretaceous of New Jersey*, D. Grimaldi, Ed., Backhuys Publishers, Leiden (2000), pp. 1–76.
54. Grimaldi, D., J. Lillegraven, T. Wampler, D. Bookwalter, and A. Shedrinsky, Amber from Upper Cretaceous through Paleocene strata of the Hanna Basin, Wyoming, with evidence for source and taphonomy of fossil resins, *Rocky Mountain Geol.*, 35: 163–204 (2000).
55. Shedrinsky, A., T. Wampler, and K. Chugunov, The examination of amber beads from the collection of the state hermitage museum found in Arzhan-2 burial memorial site, *J. Anal. Appl. Pyrol.*, 71: 69–82 (2004).
56. Shedrinsky, A., T. Wampler, and A. Mazurkevich, *Amber and Amber-Like Resins in the Culture of Pile Dwellers in the Upper Reaches of the Western Dvina River*, Reports of the State Hermitage Museum, LXII, pp. 74–80 (2004).
57. Basch, A., Analysis of oil from two Roman glass bottles, *Israel Explor. J.*, 22: 27–32 (1972).
58. Jaky, M., J. Peredi, and L. Palosl, Untersuchungen eines aus romischen Zeiten stammenden Fettproduktes, *Fette, Seifen, Anstrichmitte*, 66: 1012–1017 (1964).
59. Condamin, J., F. Formenti, M.O. Metais, M. Michel, and P. Blond, The application of gas chromatography to the tracing of oil in ancient amphorae, *Archaeometry*, 18: 195–201 (1976).

60. Condamin, J. and F. Formenti, Detection du contenu d'amplores Antiques (Huile, Vin). Etude methodologique, *Rev. d'Archeometrie*, 2: 43–58 (1978).
61. Seher, A., H. Schiller, M. Krohn, and G. Werner, Untersuchungen von Olproben aus archaologischen Funden, Fette, Seifen, *Anstrichmitte*, 82: 395–399 (1980).
62. Jain, N.C., C.R. Fontan, and P.L. Kirk, Identification of paints by pyrolysis-gas chromatography, *J. Forens. Sci. Soc.*, 5: 102–109 (1965).
63. Stolow, R.L. and G. deW. Rogers, Further studies by gas chromatography and pyrolysis techniques to establish ageing characteristics of works of art, in *Application of Science in Examination of Works of Art*, W.G. Young, Ed., Museum of Fine Arts, Boston (1973), pp. 213–228.
64. Rogers, G. deW., An improved pyrolytic technique for the quantitative characterization of the media of works of art, in *Conservation and Restoration of Pictorial Art*, N. Brommelle and P. Smith, Eds., Butterworth, London (1976), pp. 93–100.
65. Breek, R. and W. Froentjes, Application of pyrolysis gas chromatography on some of Van Meegeren's faked Vermeers and Pieter de Hooghs, *Stud. Conserv.*, 20: 183–189 (1975).
66. Liebman, S.A., E.J. Levy, and T.P. Wampler, Developments in pyrolysis-capillary GC, *J. High Resolut. Chromatogr.*, 7: 172–184 (1984).
67. Nazer, J., C. Young, and R. Giesbrecht, Pyrolysis-GC analysis as an identification method of fats and oils, *J. Food Sci.*, 50: 1095–1100 (1985).
68. Boon, J.J., Analytical pyrolysis mass spectrometry: new vistas opened by temperature-resolved in-source PYMS, *Int. J. Mass Spectrom. Ion Proc.*, 118/119: 758–762 (1992).
69. Oudemans, T. and J. Boon, Molecular archaeology: analysis of charred (food) remains from prehistoric pottery by pyrolysis-gas chromatography/mass spectrometry, *J. Anal. Appl. Pyrol.*, 20: 197–227 (1991).
70. de la Rie, E.R. and A.M. Shedrinsky, The chemistry of ketone resins and the synthesis of a derivative with increased stability and flexibility, *Stud. Conserv.*, 34: 9–19 (1989).
71. Noble, W., B. Wheals, and M.J. Whitehouse, The characterization of adhesives by pyrolysis gas chromatography and infrared spectroscopy, *Forens. Sci.*, 3: 163–174 (1974).
72. Curry, C.J., Pyrolysis-mass spectrometry studies of adhesives, *J. Anal. Appl. Pyrol.*, 11: 213–225 (1987).
73. De Witte, E., M. Goessens-Landrie, E. Goethals, and R. Simonds, The structure of "old" and "ne Paraloid B-72, report 78/16/4," in *ICOM Committee for Conservation, 5th Triennial Meeting*, Zagreb, 1978.
74. de Witte, E. and A. Terfve, The use of a Py-GC/MS technique for the analysis of synthetic resins, in *Science and Technology*, N.S. Brommelle and G. Thomson, Eds., International Institute for Conservation, London (1982), pp. 16–18.
75. Sonoda, N., Characterization of organic azo-pigments by pyrolysis-gas chromatography, *Stud. Conserv.*, 44: 195–208 (1999).
76. Learner, T., The analysis of synthetic paints by pyrolysis-gas chromatography/mass spectrometry (PYGCMS), *Stud. Conserv.*, 46: 225–241 (2001).
77. Learner, T., The analysis of synthetic resins found in twentieth century paint media, in *Resins, Ancient and Modern*, SSCR Conference, Aberdeen (1995), pp. 76–84.
78. Scalarone, D. and O. Chiantore, The use of pyrolysis-GC/MS for the identification of polymeric constituents in artworks, museum and collectible design objects, in *Plastics in Art (History, Technology, Preservation)*, T. van Oosten, Y. Shashoua, and F. Waentig, Eds., Siegl, Munich (2000), pp. 90–104.

79. Khandekar, N., V. Dorge, H. Khanjian, D. Stulik, and A. de Tagle, Detection of residues on the surfaces of objects previously treated with aqueous solvent gels, in *ICOM Committee for Conservation, 13th Triennial Meeting*, Rio de Janeiro, September 22–27, 2002, pp. 352–359.
80. Chiantore, O., D. Sclarone, A. Rava, M. Filippi, A. Pellegrino, and A. Pesenti-Compagnoni, Analysis of materials, restoration practice, design and control of display conditions at the National Cinema Museum in Toronto, in *ICOM Committee for Conservation, 13th Triennial Meeting*, Rio de Janeiro, September 22–27, 2002, pp. 903–910.
81. Cappitelli, F., T. Learner, and A. Cummings, Thermally assisted hydrolysis and methylation-gas chromatography/mass spectrometry for the chemical characterization of traditional and synthetic binders, in *ICOM Committee for Conservation, 13th Triennial Meeting*, Rio de Janeiro, September 22–27, 2002, pp. 231–237.
82. Thomas, T.H. and T.C. Kendrick, Thermal analysis of polydimethylsiloxanes. I. Thermal degradation in controlled atmospheres, *J. Polym. Sci. A*, 27: 537 (1969).
83. Blazsó, M., G. Garzo, and T. Szekely, Pyrolysis gas chromatographic studies on polydimethylsiloxanes and poly(dimethyl silalkylene siloxanes), *Chromatographia*, 5: 485 (1972).
84. Grassie, N. and K.F. Francey, Thermal degradation of polysiloxanes. Part 3. Poly(dimethyl/methylphenyl siloxanes), *Polym. Degr. Stab.*, 2: 53 (1980).
85. Kleinert, J.C. and C.J. Weschler, Pyrolysis gas chromatographic-mass spectrometric identification of poly (dimethylsiloxanes), *Anal. Chem.*, 52: 1245 (1980).
86. Blazsó, M., G. Garzo, and T. Szekely, Py-GC studies on Poly(dimethyl siloxanes) and Poly(dimethyl alkylene siloxanes), *Chromatographia*, 5: 485–492 (1972).
87. Blazsó, M., G. Garzo, K. Andrianov, N. Makarova, A. Chernavski, and L. Petrov, Thermal decomposition of cyclo-linear methylsiloxane polymers, *J. Organometal. Chem.*, 165: 273 (1979).
88. Blazsó, M., E. Gal, and N. Makarova, Thermal decomposition and rearrangement of branched methylsiloxane oligomers, *Polyhedron*, 2: 455 (1983).
89. Blazsó, M., T. Szekely, and N. Makarova, Thermal decomposition of cycloliner and cyclic methylsiloxane polymer, *J. Polym. Sci.*, 23: 2589–2599 (1985).
90. Mills, J.S. and R. White, *The Organic Chemistry of Museum Objects*, Butterworth, London (1987).
91. Halpine, S., Amino acid analysis of proteinaceous media from Cosimo Tura's "The Annunciation with Saint Francis and Saint Louis of Toulouse," *Stud. Conserv.*, 37: 22–38 (1992).
92. Chiavari, G. and G. Galletti, Pyrolysis-gas chromatography/mass spectrometry of amino acids, *J. Anal. Appl. Pyrol.*, 24: 123–137 (1992).
93. Chiavari, G., G. Galletti, G. Lanterna, and R. Mazzeo, The potential of pyrolysis-gas chromatography/mass spectrometry in the recognition of ancient painting media, *J. Anal. Appl. Pyrol.*, 24: 227–242 (1993).
94. Boon, J.J. and J.W. De Leeuw, Amino acid sequence information in proteins and complex proteinaceous material revealed by pyrolysis-capillary gas chromatography: low and high resolution mass spectrometry, *J. Anal. Appl. Pyrol.*, 11: 313–327 (1987).
95. Mariner, W.N. and P. Magidman, Analysis of wool proteins by pyrolysis-gas chromatography, in *Preprints of 198th ACS National Meeting*, Miami, Florida, September 1989.
96. Cutter, E., P. Magidman, and W. Maarmar, Pyrolysis-gas chromatography of Hercosett 125 finish on wool, *Text. Chem. Colorist*, 25: 27–29, 1993.

7 Environmental Applications of Pyrolysis

T.O. Munson

CONTENTS

7.1	Introduction	134
7.2	Applications Related to Air	134
7.2.1	Examination of Air Particulates/Aerosols	135
7.2.1.1	Smoke Aerosols	135
7.2.1.2	Airborne Particulates	136
7.2.1.3	Organics in Urban Airborne Particles	141
7.2.1.4	Bioaerosols.....	141
7.2.1.5	Chloroorganic Compounds in Precipitation.....	141
7.2.2	Examination of Air Pollutants from Thermal Decomposition	142
7.2.2.1	Pyrolysis of Plastic Wrapping Film	142
7.2.2.2	Waste Plastic Processing	143
7.2.2.3	Pyrolysis of Sewage Sludge	146
7.3	Applications Related to Water	147
7.3.1	Wastewater	147
7.3.1.1	Measuring the Organic Carbon in Wastewater	147
7.3.1.2	Analysis of Pulp Mill Effluents Entering the Rhine River.....	147
7.3.2	Surfacewater: Analysis of Natural Organic Matter	150
7.3.3	Analysis of Groundwater Contamination	154
7.4	Analysis of Soil and Sediment	156
7.4.1	Thermal Distillation-Pyrolysis-GC.....	156
7.4.2	Flash Pyrolysis-GC and GC/MS	157
7.4.3	TD-Py-FID Applied to Marine Sediments	161
7.4.4	Rock Eval Pyrolysis.....	163
7.4.5	TMAH-Pyrolysis-GC/MS	164
7.5	Other Environmental Applications	164
7.5.1	Ancient Limestone: Examination by Py-GC and Py-GC/MS	164
7.5.2	Outdoor Bronze Monuments: Examination of Corrosion Patinas by Py-GC/MS.....	166
7.5.3	Digested and Undigested Pollens: Discrimination by Py-MS	169
7.5.4	Spruce Needles: Examination by Py-FIMS	170

7.5.5 Forest Soils: Examination by Py-MBMS.....	170
7.5.6 Analysis of Intractable Environmental Contamination	171
References.....	171

7.1 INTRODUCTION

The stated purpose for this *Applied Pyrolysis Handbook* includes “to be a practical guide to the application of pyrolysis techniques to various samples and sample types.” The subset of this overall scope to be dealt with in this chapter consists of environmental applications of analytical pyrolysis.

A narrow view of this mission would include only the use of analytical pyrolysis techniques (e.g., pyrolysis-mass spectrometry (Py-MS) and pyrolysis-gas chromatography-mass spectrometry (Py-GC/MS)) to identify and measure “contaminants” in samples of outdoor air, soils, sediments, water, and biota. In order to include interesting and useful applications of analytical pyrolysis techniques that otherwise might not be mentioned in the other chapters of this handbook, a broader view of environmental applications will be used to include such topics as the use of analytical pyrolysis to gain an understanding of natural environmental processes, such as the conversion of plant materials into soil, coal, and petroleum hydrocarbons. This subject was included in a recent review paper describing the use of analytical pyrolysis for environmental research.¹ Several other review papers contain references pertinent to environmental analysis.²⁻⁷

No extensive effort has been made to uncover all published reports of pyrolysis use that might be classified as environmental. Instead, time has been devoted to identifying and including good examples of as many different types of environmental applications as possible. Because the intent of this handbook is to be useful, another sensible criterion was to choose published reports that would be readily accessible to an interested reader.

The most useful format in which to display the gathered information did not readily present itself. An obvious choice was to arrange the applications according to the pyrolytic technique described in the report (e.g., Py-GC/MS, Py-MS, and so forth). This approach was not selected for two reasons: specific pyrolysis techniques are discussed in other chapters of this handbook, and it seems appropriate for this chapter to emphasize the applications rather than the techniques. Following this sort of logic, it was decided to sort the applications generally by the type of environmental media to which they apply (i.e., air, water, soil/sediment, and biota).

7.2 APPLICATIONS RELATED TO AIR

Since the term *pyrolysis* as used in the context of this handbook refers to the conversion of large, nonvolatile organic molecules such as organic polymers to smaller volatile organic molecules, it should not be surprising that the reports discussed in this section fall into two general categories: release of organic materials into air by the pyrolytic decomposition of nonvolatile material and the use of

pyrolysis techniques for the examination of particulate/aerosol material recovered from air samples.

7.2.1 EXAMINATION OF AIR PARTICULATES/AEROSOLS

7.2.1.1 Smoke Aerosols

Tsao and Voorhees used Py-MS together with pattern recognition for the analysis of smoke aerosols from nonflaming² and flaming³ combustion of such materials as Douglas fir, plywood, red oak, cotton wool, polyurethanes, polystyrene, polyvinyl chloride, nylon carpet, and polyester carpet. The driving force for these studies was to determine whether this technique could provide a means for assessing the fuels involved in building fires from the analysis of the smoke aerosols formed. Apparently this type of information can be useful in legal actions associated with catastrophic fires, such as the one at the MGM Hotel in Las Vegas.

During flaming combustion, smoke aerosols form, in addition to various other materials, an amorphous polymeric substance that the authors speculated should contain, unchanged, a great deal of the original polymer structure. Because Py-MS had been shown useful for differentiating, classifying, and sometimes characterizing nonvolatile macromolecules, they speculated that Py-MS combined with pattern recognition procedures might be useful in classifying aerosol materials from combustion.

The sample preparation procedures were similar for both of these studies. Smoke aerosols of the materials of interest were produced in the laboratory under either nonflaming² or flaming³ combustion conditions, and the material produced collected on glass fiber filters. The volatile organic fraction was removed from the collected material by gentle heating (50 to 55°C) under vacuum for 24 to 48 h. A portion of the nonvolatile material was then subjected to analysis by Py-MS using a Curie-point pyrolyzer (510°C) interfaced to a quadrupole mass spectrometer via an expansion chamber.

Upon pyrolysis, under both combustion conditions, the material collected from the smoke aerosols produced a unique Py-MS spectrum for each substance. In many cases, visual inspection of the spectra from simple mixtures could lead to the identification of the fuel materials. For more complex mixtures, however, extensive "crunching" of the data was necessary using pattern recognition techniques before judgments could be made as to what fuel mixture might have produced the smoke aerosol analyzed. The authors did demonstrate considerable success in identifying some or all of the fuel components of complex mixtures and speculated that with further experiments and refinement in the applications of chemometric techniques, this approach could become a useful tool in fire investigations.

Those interested in these studies might also be interested in a study of the products of nonflaming combustion of poly(vinyl chloride) in which 2-g samples of the granular polymer were decomposed in a tubular flow reactor under various temperature conditions and gas mixtures.⁴ The evolved products were trapped in cold hexane or styrene and identified using GC and GC/MS. An earlier study along these same lines, using phenol-formaldehyde resin foam, was reported by the same investigator.⁸

There is a rich literature associated with studies of the breakdown or formation of specific chemical compounds and classes of chemical compounds during burning processes. A study of the thermal decomposition of pentachlorobenzene, hexachlorobenzene, and octachlorostyrene in air contained many such citations.⁹ In this study, nearly pure 10- to 20-mg samples of the cited chemicals were decomposed in a vertical combustion furnace and the decomposition product trapped on cooled XAD-4 resin followed by charcoal tubes. The adsorbed components were desorbed with toluene and analyzed using capillary GC and GC/MS. The decomposition products formed depended upon the applied temperature, the oxygen concentration, and the residence time in the hot zone of the combustion chamber.

7.2.1.2 Airborne Particulates

Voorhees et al.¹⁰ reported a study of the insoluble carbonaceous material in airborne particulates from vehicular traffic using Py-MS and Py-GC/MS (in addition to TGA, elemental analysis, and radiocarbon analysis). The solvent-soluble organic compounds separated from atmospheric particulate matter (which encompasses a broad spectrum of solid and liquid particles generally ranging in size from several hundred angstroms to several hundred micrometers) had been extensively studied by numerous investigators. Due to its complexity, the insoluble carbonaceous material (ICM) in urban and rural particulate material had not been studied in depth.

Apparently this complexity had caused earlier attempts to associate ICM with possible formation sources to be highly speculative. In this study, the authors proposed to characterize ICM collected under conditions that would ensure a known source — vehicular traffic.

Air particulate samples were collected on glass microfiber filters in the Eisenhower tunnel on Interstate 70 under conditions designed to minimize particulates other than those formed by the vehicular traffic passing through the tunnel. Water and volatile organics were removed from the samples by drying the filters at 45°C under vacuum for 18 h. The soluble organics were removed from the particulates by successive 18-h Soxhlet extractions with methanol, acetone, methylene chloride, and cyclohexane.

Py-GC/MS of the ICM was accomplished using a Pyroprobe (725°C set temperature, 550°C actual temperature, for 20 sec with the pyrolyzate trapped with liquid nitrogen at the head of a 15-m-long by 0.32-mm-I.D. bonded-phase capillary GC column). The Py-MS was accomplished as described above for the study of smoke aerosols.

The capillary column pyrogram shown in Figure 7.1 and the peak identification list shown in Table 7.1, from the analysis of ICM that had not been sorted by particle size, demonstrate the immense power of this analytical technique. A 0.5-mg sample of ICM containing only a fraction of that amount of organic material (perhaps about 25 µg) was separated into 134 GC peaks, about 90 of which were presumptively identified (that is, by comparison of the unknown spectra to computer library spectra of known compounds). Py-GC/MS analysis of ICM that was size-sorted into four size fractions (<0.6, 0.6 to 2.7, 2.7 to 10.4, and >10.4 µm) showed pyrograms of composition similar to that of the unsorted material.

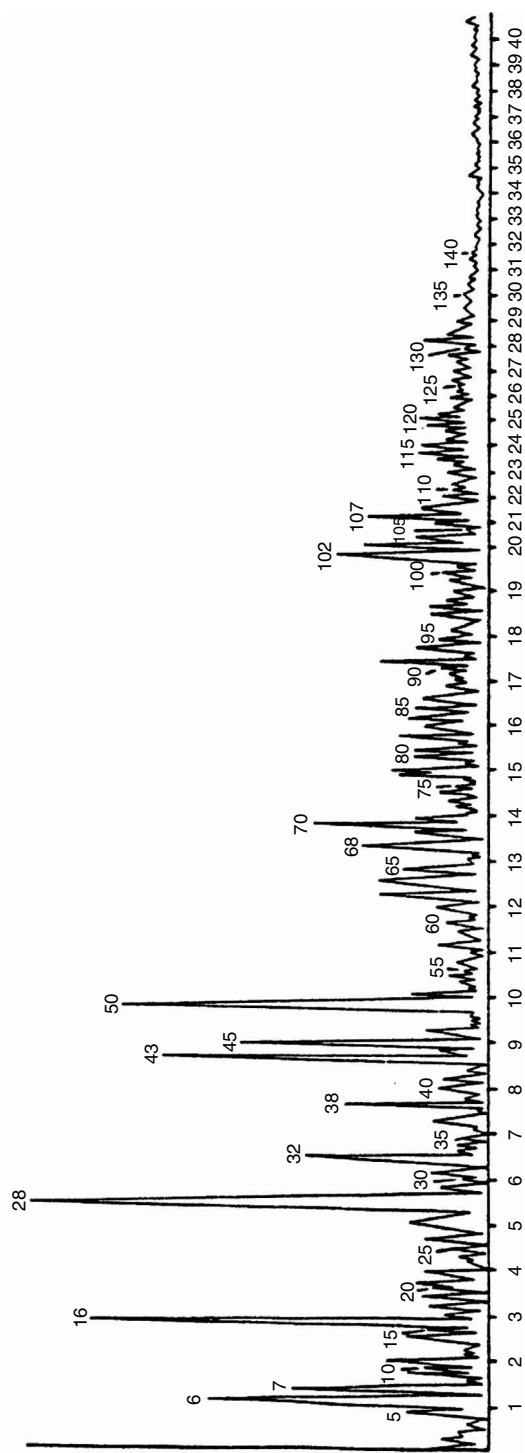


FIGURE 7.1 A 550°C pyrogram of insoluble carbonaceous material from vehicular traffic. (From Voorhees, K.J. et al., *J. Anal. Appl. Pyrol.*, 14: 83 (1988). With permission.)

TABLE 7.1
Peak Identification: Tunnel 2

Peak No.	Compound	Peak No.	Compound
1	1,3-Butadiene	68	1-Ethyl-3-methylbenzene
2	1,3-Butadiene	69	1-Decene
3	Pentane	70	1,2,3-Trimethylbenzene
4	2-Pentene	71	Decane
5	Pentane	72	4- or 5-Decene
6	Acetone	73	Unidentified
7	4-Methyl-2-pentene	74	Unidentified
8	2,3-Dimethyl-2-butene	75	Unidentified
9	Methylpentene	76	C ₄ -Alkylbenzene
10	Hexane	77	1-Methyl-4-(1-methylethyl)benzene
11	2-Methylfuran	78	Unidentified
12	Hexene	79	Unidentified
13	2,3-Dimethylbutadiene	80	2-Propenylbenzene
14	1,3,5-Hexatriene	81	Unidentified
15	2-Hexene	82	Propynylbenzene
16	Benzene	83	Methylpropylbenzene
17	Hexadiene	84	C ₄ -Alkylbenzene
18	Methylcyclopentene	85	Trimethyloctane
19	1-Heptene	86	1-Methyl-2-propylbenzene (or 1,3)
20	Methylhexadiene	87	1-Methyl-2-(propenyl)benzene
21	2-Methylhexadiene	88	Unidentified
22	2,5-Dimethylfuran	89	Unidentified
23	Unidentified	90	C ₄ -Alkenylbenzene
24	Unidentified	91	Undecene
25	Trimethylcyclohexane	92	Undecene
26	1,3,5-Heptatriene	93	Undecene
27	2,4-Heptadiene	94	Ethylidimethylbenzene
28	Toluene	95	C ₄ -Alkenylbenzene
29	2-Methylthiophene	96	Tetramethylbenzene
30	Heptadiene	97	C ₄ -Alkenylbenzene
31	1-Octene	98	C ₄ -Alkenylbenzene
32	Trimethylbutene	99	1-Methyl-2-(1-methylethyl)benzene
33	Unidentified	100	Dimethylstyrene
34	Unidentified	101	Unidentified
35	Octene	102	1- or 3-Methyl-1H-indene
36	Octadiene	103	1,4-Divinylbenzene
37	Unidentified	104	1,3-Divinylbenzene
38	C ₈ H ₁₂	105	Unidentified
39	C ₈ H ₁₂	106	Unidentified
40	C ₈ H ₁₂	107	Naphthalene
41	1-Ethylcyclohexene	108	3-Methyl-1,2-dihydronaphthalene
42	Unidentified	109	Unidentified
43	Ethylbenzene	110	Tridecene
44	Unidentified	111	Unidentified

TABLE 7.1 (Continued)
Peak Identification: Tunnel 2

Peak No.	Compound	Peak No.	Compound
45	1,2- or 1,4-Xylene	112	C ₅ -Alkenylbenzene
46	2,4-Dimethylthiophene	113	Unidentified
47	Unidentified	114	Unidentified
48	Unidentified	115	C ₆ -Alkylbenzene
49	Unidentified	116	C ₆ -Alkylbenzene
50	Styrene	117	C ₅ -Alkenylbenzene
51	Unidentified	118	C ₆ -Alkenylbenzene
52	Unidentified	119	C ₁₃ -Alkene
53	Unidentified	120	Alkylbenzene
54	1,2,3-Trimethylcyclohexane	121	Unidentified
55	Unidentified	122	C ₁₄ -Alkene
56	Unidentified	123	Unidentified
57	Unidentified	124	Unidentified
58	1-Methylethylbenzene	125	Unidentified
59	Unidentified	126	Unidentified
60	Dimethyloctane	127	Unidentified
61	2,4- or 3,4-Dimethylpyridine	128	Alkylbenzene
62	2-Methylstyrene	129	Alkylbenzene
63	Propylbenzene	130	Alkylbenzene
64	Methylethylbenzene	131	Branched C ₁₄ -alkene
65	1,3,5-Trimethylbenzene	132	Branched C ₁₄ -alkene
66	Unidentified	133	Branched C ₁₅ -alkene
67	Unidentified	134	Alkylbenzene

Source: Voorhees, K.J. et al., *J. Anal. Appl. Pyrol.*, 14: 83 (1988). Adapted from Table 3. With permission.

Py-GC/MS of samples (prepared as were the ICM samples) of the four materials thought to be the major sources of the tunnel air particulates — tire rubber, road salt, diesel exhaust, and gasoline exhaust — showed that road salt gave no pyrolysis products and the other three materials gave pyrograms of complexity similar to those of the ICM samples. The overlap of compound types and the absence of unique marker compounds made an assessment of the relative contribution of each of the three sources to the total impractical using the Py-GC/MS profiles.

Figure 7.2 shows the comparison of the Py-MS spectra obtained from the ICM (referred to as tunnel particles in the figure) and the three most likely contributor materials. While there are many ions in common, the patterns of ions in the spectra of the three contributor materials are distinctly different from each other. Using a statistical method for the comparison of the Py-MS spectra of the three contributor materials to the spectrum for the ICM, the authors estimated that diesel exhaust particulates, gasoline exhaust particulates, and tire wear particulates accounted for 64, 26, and 10%, respectively, of the tunnel insoluble carbonaceous material.

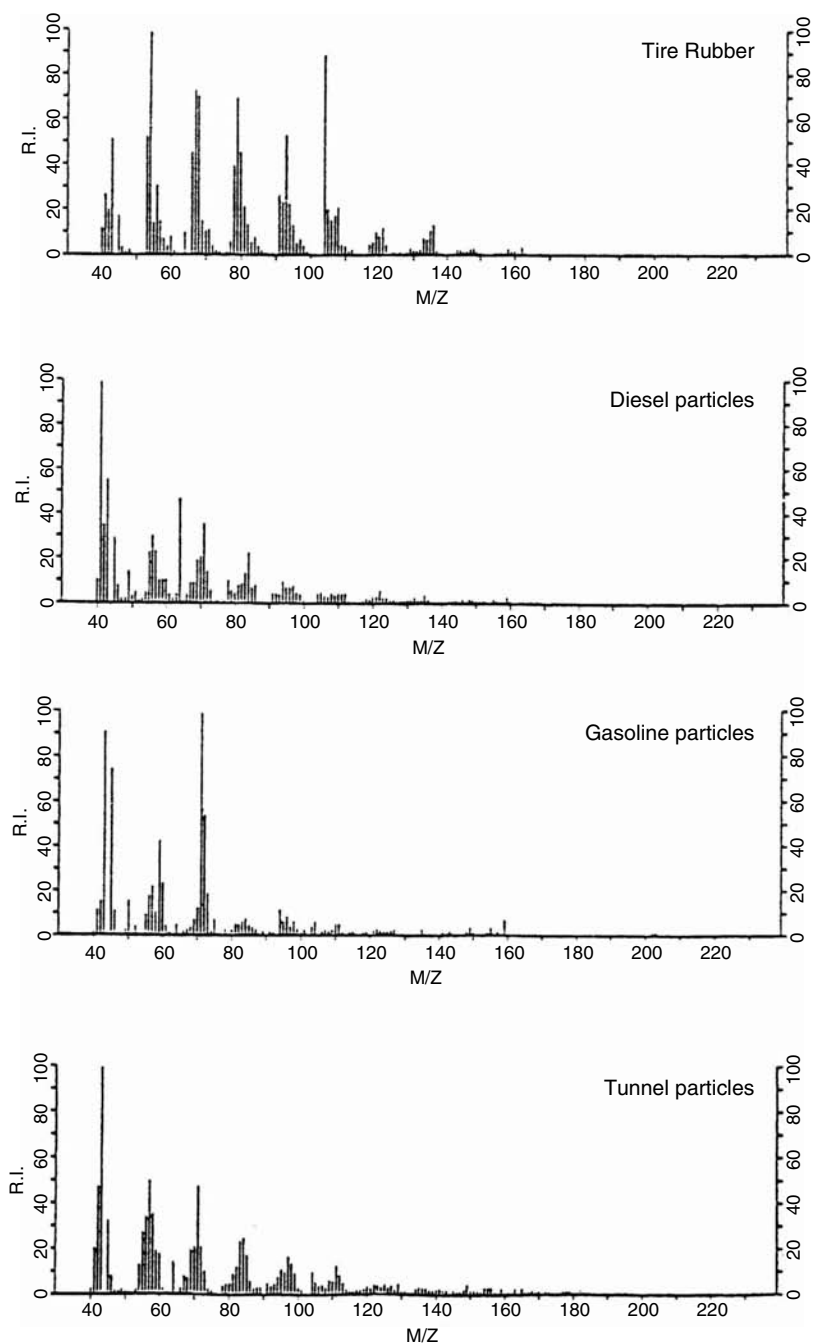


FIGURE 7.2 Py-MS spectra of the tunnel particles and various contributors to that sample. (From Voorhees, K.J. et al., *J. Anal. Appl. Pyrol.*, 14: 83 (1988). With permission.)

7.2.1.3 Organics in Urban Airborne Particles

Curie-point Py-GC/MS was used to examine the organic compounds in urban aerosols.¹¹ Summer and winter samples (1999) were taken from a series of sampling sites in Leipzig, Germany. Size-segregated aerosol samples were collected using a five-stage low-pressure cascade impactor set up in such a way that particulate samples were deposited directly on small pieces of Curie-point foil (590°C). The authors stated that the organic compounds that were measured by the GC/MS were not pyrolysis products, but rather evaporated directly from the particulate matter on the foils during the rapid heating at the Curie point. Various alkanes, polynuclear aromatic hydrocarbons (PAHs), and oxygenated PAHs were observed.

7.2.1.4 Bioaerosols

An analytical problem of considerable interest to the military concerns the detection of bioaerosols — specifically the need for early warning of a foreign biological presence at perimeters of military posts, stations, airfields, and battlefields. Especially desirable would be an analytical device compact enough to be resident upon military vehicles such as tanks and personnel carriers but yet sophisticated enough to provide useful information about the nature of the biological material detected. A study testing the ability of a pyrolysis-gas chromatography-ion mobility spectrometry (Py-GC-IMS) biodetector system to respond to aerosolized biological substances in a Canadian prairie environment showed promising results for this technique.¹² In a series of 42 trials this Py-GC-IMS biodetector was shown not only able to distinguish between biological and nonbiological aerosols, but also able to discriminate between aerosols of a Gram-positive spore, a Gram-negative bacterium, and a protein. The reproducible limits of detection were less than one bacterial analyte-containing particle per 2 l of air.

In order for the biodetector to be able to provide discriminatory data at this level of detection, large (2000-l) air samples were required. A 916 l/min XM-2 aerosol collector/concentrator (25 × 17 × 13 in., 66 lb) interfaced to the Py-GC-IMS biodetector (12 × 16 × 5 in., 15 lb, including the computer) almost continuously collected air particulates, providing a cumulative sample to the biodetector at about 3.5-min intervals. No particulate collection took place during the 0.7 min required for the transfer of the collected particulates from the fourth stage of the XM-2 to the quartz microfiber filter in the pyrolysis tube. At the end of the sample transfer time, the XM-2 resumed sampling and the biodetector processed the transferred sample (drying followed by pyrolysis at 350°C, GC separation of the components of the pyrolyzate, and characterization of the components by IMS). The report provides a wealth of information about the data collected during these field trials.

7.2.1.5 Chloroorganic Compounds in Precipitation

Studies of organic compounds in rain and snow that showed that only a small portion (about 0.1%) of the chlorinated organic material was volatile enough for examination directly by GC techniques prompted a study of the nonvolatile organic compounds in such samples by Py-GC/MS and Py-GC/AED.¹³ The use of atomic emission

detection (AED) was particularly interesting because this detector system allowed specific monitoring for halogenated analytes.

The samples that were presented to the pyrolyzer were some (less than 1 mg) of the solid residue remaining after evaporation to dryness (using a rotary evaporator at 40°C) of 3 to 5 l of rainwater, or a similar amount of the solid residue obtained when 3 to 5 l of rainwater or melted snow was passed through a polyacrylate resin (XAD-8) column, the column eluted with acetonitrile, and the eluate evaporated to dryness. Although the pyrograms showed an abundance of chlorinated organic compounds, interpretation of the results was complicated by the observation (using ³⁵Cl-enriched sodium chloride) that, in the presence of inorganic chloride, many of the observed chlorinated compounds were formed to some extent during pyrolysis of the samples. However, while varying the pyrolysis conditions, it was discovered that, when heated to 150°C prior to pyrolysis, three of the five samples examined (snow from Gdansk, Poland, and rainwater from Sobieszewo, Poland, and Linköping, Sweden) evolved the chlorinated flame retardant, tris(2-chloroethyl) phosphate, clearly not a pyrolysis artifact. In addition, the Py-GC/MS data suggested that carbohydrates and nitrogen-containing biopolymers were abundant in the samples.

7.2.2 EXAMINATION OF AIR POLLUTANTS FROM THERMAL DECOMPOSITION

7.2.2.1 Pyrolysis of Plastic Wrapping Film

Pyrolysis has been used to examine the types of air pollutants that might be generated from various types of waste plastic materials during incineration or thermal decomposition in landfills. One such study¹⁴ used GC and GC/MS to examine the products that were formed when two kinds of widely used plastic wrapping film (made of poly(vinylidene chloride)) were pyrolyzed.

Samples of the wrapping material were pyrolyzed at 500°C in an airflow of 300 ml/min and the products evolved trapped in ice-cold hexane. The concentrated extracts were then analyzed by capillary column GC and GC/MS. Figure 7.3 shows a typical capillary gas chromatogram of the pyrolysis products from one of the wrapping materials. The numbers on the peaks correspond to the numbers of the compounds identified and shown in Table 7.2. The identifications were carried out by comparison of the mass spectra and retention indexes of the sample peaks with mass spectra and retention indexes of authentic compounds. The original form of this table includes the retention indices (calculated using alkanes as references) and average amounts formed calculated from eight runs.

Pyrolyzing the material of interest separately from the analysis allows a greater latitude in the selection of the pyrolysis conditions. For instance, in this case, the gas flow, which contained about 25% oxygen, would have been incompatible with the capillary GC column. On the other hand, direct coupling of the pyrolysis step to the analytical step (Py-GC and Py-GC/MS) would have allowed examination of the most volatile products formed, which could not be done here due to losses during the concentration of the hexane and due to the huge hexane solvent peak in the early portion of the chromatogram. A modern pyrolysis concentrator unit allows the best

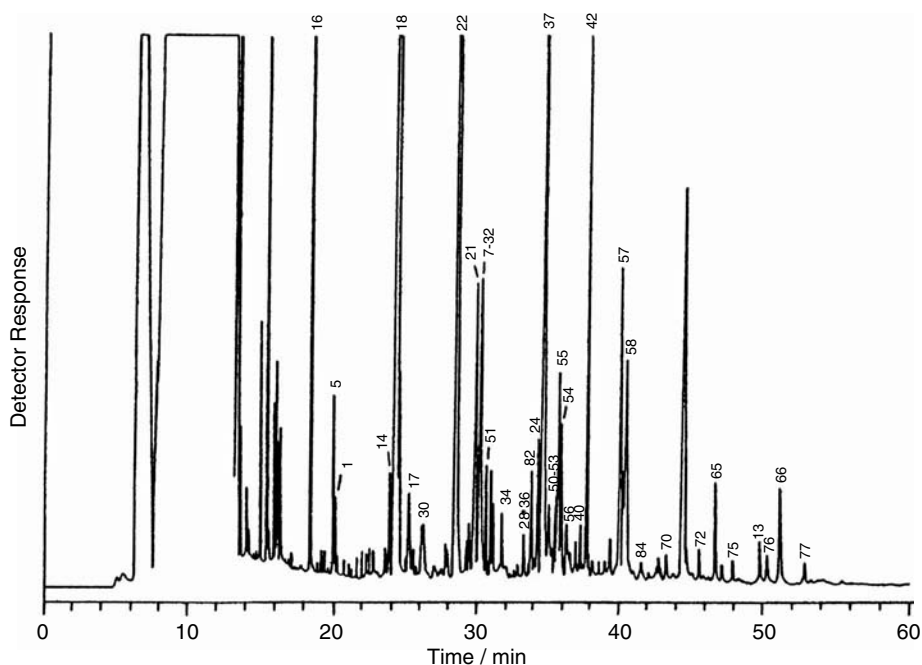


FIGURE 7.3 Typical gas chromatogram of pyrolysis products from a plastic wrapping film. (From Yasuhara, A. and Morita, M., *Environ. Sci. Technol.*, 22: 646 (1988). With permission.)

of both arrangements by providing a gas stream other than the GC carrier gas during pyrolysis (while trapping the pyrolyzate) and then passing the pyrolyzate to the GC column under optimum conditions.

7.2.2.2 Waste Plastic Processing

An ideal way to recycle waste plastics is to remelt them and form new products directly, but this process is usually possible only in the case of rather homogeneous waste streams. With heterogeneous plastic-containing waste streams, however, because other processing steps would be required, landfilling and incineration are the most favored disposal methods from an economic point of view. These disposal processes can lead to environmental problems, especially in the case of halogen-containing plastics such as poly(vinyl chloride) (PVC).

Because PVC is widely used in combination with aluminum, and because ABS (a blend of acrylonitrile, butadiene, and styrene) and PET (polyethyleneterephthalate) may also be in the future, a study was undertaken to examine the use of pyrolysis to process combinations of these plastics and aluminum.¹⁵

The thermal stability of the plastics (separately and in combination with aluminum and under various gas atmospheres) was investigated using thermogravimetry. With this pyrolysis technique, the decomposition of a material is measured as a function of applied temperature by monitoring the weight of the sample as the temperature is increased at a programmed rate. For these experiments, the

TABLE 7.2
Compounds Identified from Pyrolysis of Plastic Wrap

Peak No.	Compound	Peak No.	Compound
1	Trichlorobutadiene	43	Tetrachlorostyrene
2	Trichlorobutadiene	44	Tetrachlorostyrene
3	Pentachlorobutadiene	45	Tetrachlorostyrene
4	2,2,3-Trimethyloxetan	46	Tetrachlorostyrene
5	Styrene	47	2-Chlorophenol
6	Phenylacetylene	48	2,5-Dichlorophenol
7	Naphthalene	49	2,6-Dichlorophenol
8	Biphenyl	50	3,5-Dichlorophenol
9	Methylphenylacetylene	51	Dichlorophenylacetylene
10	Phenanthrene	52	Dichlorophenylacetylene
11	Phenol	53	Trichlorophenylacetylene
12	Benzaldehyde	54	1-Chloronaphthalene
13	Dibutylphthalate	55	2-Chloronaphthalene
14	Benzofuran	56	Chlorotetrahydronaphthalene
15	Dibenzofuran	57	Dichloronaphthalene
16	Chlorobenzene	58	Dichloronaphthalene
17	1,2-Dichlorobenzene	59	Dichloronaphthalene
18	1,3-Dichlorobenzene	60	Dichloronaphthalene
19	1,4-Dichlorobenzene	61	Trichloronaphthalene
20	1,2,3-Trichlorobenzene	62	Trichloronaphthalene
21	1,2,4-Trichlorobenzene	63	Trichloronaphthalene
22	1,3,5-Trichlorobenzene	64	Trichloronaphthalene
23	1,2,3,4-Tetrachlorobenzene	65	Trichloronaphthalene
24	1,2,3,5- or 1,2,4,5-Tetrachlorobenzene	66	Tetrachloronaphthalene
25	4-Chlorotoluene	67	Tetrachloronaphthalene
26	Dichlorotoluene	68	2-Chlorobiphenyl
27	Dichlorotoluene	69	2,4- or 2,5-Dichlorobiphenyl
28	Trichlorotoluene	70	2,3'-Dichlorobiphenyl
29	Tetrachlorotoluene	71	3,5-Dichlorobiphenyl
30	Chlorostyrene	72	3,4- or 3,4'-Dichlorobiphenyl
31	Chlorostyrene	73	2,3,6- or 2,3',6-Trichlorobiphenyl
32	Dichlorostyrene	74	2,3,5- or 2',3,5-Trichlorobiphenyl
33	Dichlorostyrene	75	2,3',4- or 2,3',5-Trichlorobiphenyl
34	Dichlorostyrene	76	3,4',5-Trichlorobiphenyl
35	Dichlorostyrene	77	2,3',5,5'-Tetrachlorobiphenyl
36	Dichlorostyrene	78	2,3',4,5'-Tetrachlorobiphenyl
37	Trichlorostyrene	79	2,2',3,5',6-Pentachlorobiphenyl
38	Trichlorostyrene	80	Chlorobenzofuran
39	Trichlorostyrene	81	Chlorobenzofuran
40	Trichlorostyrene	82	Dichlorobenzofuran
41	Trichlorostyrene	83	Dichlorobenzofuran
42	Tetrachlorostyrene	84	Tetrachlorobenzofuran

Source: Adapted from Table II of Yasuhara, A. and Morita, M., *Environ. Sci. Technol.*, 22: 646 (1988). With permission.

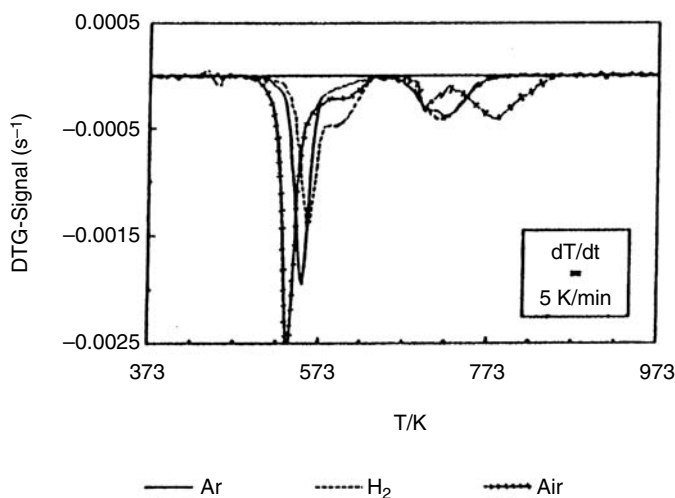


FIGURE 7.4 DTG curves of virgin PVC in different atmospheres. (From Oudhuis, A.B.J. et al., *J. Anal. Appl. Pyrol.*, 20: 321 (1991). With permission.)

temperature was programmed from 300 to 1000 K at 0.083 K/sec. If the data from such a test are plotted as the normalized mass change per unit time (based on the initial sample mass) as a function of temperature, the resulting differential thermogravimetric (DTG) curve provides a profile of the decomposition of the material as a function of temperature. The DTG curves for virgin PVC in different atmospheres (Figure 7.4) clearly show that the thermal decomposition of virgin PVC is a two-step process.

In addition to the thermogravimetry experiments, batch pyrolysis experiments continuously monitoring HCl formation were performed with PVC to determine the optimum temperature for HCl formation. Under conditions of maximum HCl formation, PVC was pyrolyzed with and without oxygen in a fluidized bed reactor and the formation of polychlorinated dibenzodioxins (PCDDs) and polychlorinated dibenzofurans (PCDFs) measured. Avoiding the formation of these highly toxic compounds would be a critical element in any waste stream processing scheme.

In addition to these techniques, analytical pyrolysis experiments were performed where 0.5-mg samples were batch pyrolyzed under flowing helium gas in a tube furnace connected to a liquid nitrogen cold trap. By warming the cold trap, the pyrolysis products were transferred directly to a GC/MS system for identification.

Several important design guidelines for processing aluminum scrap, plastic waste, and combinations of the two were elucidated by these studies. For instance, thermal decomposition of PVC in the presence of oxygen (combustion) generated 10 to 1000 times as much PCDD and PCDF as did thermal decomposition in the absence of oxygen. Because anaerobic thermal decomposition of PVC does not cause PCDD and PCDF emission problems, simpler emissions scrubbing steps can be employed. Most of the organic fraction of aluminum scrap can be removed by pyrolysis below the melting point of the aluminum. If the plastic fraction of

the aluminum scrap contains a considerable amount of PVC, it is more economical to incinerate the pyrolysis products on-site, in combination with HCl removal and heat recovery. In the case of other plastics, it is possible to get a valuable pyrolysis oil.

7.2.2.3 Pyrolysis of Sewage Sludge

Disposal of sewage sludge has become a major environmental problem, particularly in areas of dense population. The increase in metals content in soil and the potential presence of toxic organic compounds have thrown the traditional utilization of sewage sludge on farmlands into question. Thermal decomposition of the sewage sludge, followed by sanitary landfill disposal of the resultant slag and ashes, represents an alternative to the agricultural use, but one must then be concerned with the fate of the inorganic and organic constituents during the thermal treatment and final disposal. A laboratory-scale pyrolysis reactor was used to determine the process conditions for a minimum flux of metals to the environment from the anaerobic thermal decomposition (pyrolysis) of sludge and subsequent disposal of the pyrolysis products.¹⁶

Sewage sludge containing less than 20% water was dried in 600-g batches to less than 1% water. A fraction of each batch (30 to 40 g) was analyzed for organic matter and metals (Cr, Ni, Cu, Zn, Cd, Hg, and Pb), and the rest was pyrolyzed at selected temperatures (350, 505, 625, and 750°C) for 1 h, with the off-gases being passed through traps and filters.

Analysis of the solid residue (char) and the various traps and filters showed that, at all temperatures, more than 97% of the Hg was evaporated completely from the sludge. At 505°C, all of the Cd remained in the char, but at 750°C, all of the Cd was volatilized. At 625°C, the partitioning of Cd between the gas phase and the solid phase depended upon the residence time at the pyrolysis temperature. Essentially all of the other metals remained in the char at all pyrolysis temperatures.

This study demonstrated that the best temperature for the pyrolysis of sewage sludge with respect to the metals content is in the range of 500 to 600°C. Higher temperatures, which leave less char, are less desirable because at $T > 600^{\circ}\text{C}$, Cd and other metals with relatively high vapor pressures are transferred to the gas phase. Since Hg is very difficult to scrub from the off-gas stream and is completely volatilized at even the lowest temperatures, the most economical approach with respect to Hg seems to be to limit the input of Hg to the sewer system.

In another study,¹⁷ an apparatus consisting of a primary pyrolyzer (Pyroprobe 1000) combined with a secondary reactor was used to study the thermal decomposition of three different chemical sewage sludges. The pyrolysis gases were swept directly into a gas chromatograph for analysis. Yields of 12 pyrolysis products were determined (methane, ethylene, ethane, propylene, propane, methanol, acetic acid, acetaldehyde, C_4 -hydrocarbons, CO, CO_2 , and water). The temperatures could be adjusted in the two-stage process such that nearly all of the organic material was converted to CO, CO_2 , and water at temperatures that retained the heavy metals (except for Cd and Hg) in the final residue.

7.3 APPLICATIONS RELATED TO WATER

7.3.1 WASTEWATER

7.3.1.1 Measuring the Organic Carbon in Wastewater

In 1970, Nelson et al.¹⁸ described the use of a newly designed instrument for measuring the total organic load in sewage treatment plant wastewater samples. This instrument employed flash pyrolysis followed by quantitation of the total pyrolyzate with a flame ionization detector (FID). Two tests of the organic load in wastewater, chemical oxygen demand (COD) and biological oxygen demand (BOD), are used to provide data for making adjustments to processes within sewage treatment plants. Because COD tests take 2 h and BOD tests can take up to 5 days, this pyrolysis-FID (Py-FID) technique was proposed as a rapid alternative procedure to provide the needed information.

The design of the pyrolysis reactor was such to convert all of the organic material, either suspended or dissolved, in a 50- μ l wastewater sample, to volatile organic compounds that would then be measured as a single peak by the FID. A standard mixture of glucose and glutamic acid was pyrolyzed to calibrate the unit. By entering the BOD value of the standard mixture into the final calculation, the results obtained by Py-FID could be directly compared with the BOD values for the same samples.

The relative percent differences between the organic loads measured by Py-FID and BOD for raw sewages, and for primary treated effluents, were 4.1 and 5.6%, respectively. Apparently, the organic material in both of these wastewaters was mostly biodegradable, judging from the close agreement between the Py-FID and BOD values. A comparison of Py-FID and BOD values for secondary treated effluents, however, yielded values nearly twice as high by Py-FID. Apparently, the bacterial degradation of organic material during the secondary treatment shifts the total organic material to a higher ratio of nonbiodegradable organic matter. Since Py-FID measures the total organic material and BOD only the biodegradable, this large difference is understandable.

Among other techniques, Py-GC/MS was used recently to study the nature of the residual organic matter in wastewater from a sewage treatment plant.¹⁹ As in the earlier study, it was found that as the total load of organic material decreased during biological treatment of the waste stream, the percentage of the total remaining organic material that was resistant to chemical or biological hydrolysis increased. The analysis of this refractory organic matter by Py-GC/MS did not lead to a clear understanding of the chemical nature or origin of this material but did provide the basis for some interesting speculations.

7.3.1.2 Analysis of Pulp Mill Effluents Entering the Rhine River

van Loon et al.²⁰ used Py-MS and Py-GC/MS as analytical techniques for examining the high molecular weight dissolved organic fraction from pulp mill effluents entering the Rhine River. The study had as its objectives: (1) to optimize the analytical method of ultrafiltration combined with Py-MS (which had been reported earlier), (2) to analyze qualitatively the chlorolignins and lignosulfonates in pulp mill efflu-

ents entering the Rhine River in order to find structurally specific pyrolysis products for quantitative analysis in river water, and (3) to obtain an overview of the amounts of adsorbable organic halogens discharged by these pulp mills.

Portions of the effluent samples were treated to remove the nondissolved materials and then subjected to ultrafiltration to remove the materials with molecular weights less than 1000 Daltons. With repetitive treatments, water and lower molecular weight organic and inorganic materials were removed, effectively concentrating and de-salting the high molecular weight dissolved organic carbon (DOC) fractions. Volatile organic fractions were collected by vapor stripping followed by trapping on charcoal tubes, and nonpolar and moderately polar organic compounds were collected by adsorption/elution using XAD-4 resin columns.

The high molecular weight DOC samples were analyzed by Py-MS using the in-source platinum filament pyrolysis technique. The filament, bearing a 1- to 20- μg sample, was heated at $15^{\circ}\text{C}/\text{sec}$ to a final temperature of 800°C . The mass spectrometer collected one scan/sec over the m/z range of 20 to 800 amu for 1.5 min.

The Py-GC/MS analysis was performed with 20- μg samples, a Curie-point temperature of 610°C , and a pyrolysis time of 4 sec. The resulting pyrolyzate was then swept onto a capillary GC column (50 m long \times 0.32 mm I.D., with a 1- μm film of methyl silicones) heated from 30 to 300°C at $4^{\circ}\text{C}/\text{min}$ for a total analysis time of about 1 h.

A discussion of the many interesting and important topics presented in this paper is well beyond the scope of this handbook. However, the inclusion, in detail, of some of the Py-MS, Py-GC/MS, and GC/MS data might provide some thought-provoking material for those interested in the usefulness of these techniques for the examination of such a complex organic matrix as pulp mill effluent.

Figure 7.5, for instance, shows the Py-MS spectra of the high molecular weight DOC isolated from samples from three pulp mills. A distinctive feature of the spectra is the presence of intense signals from small pyrolysis products containing sulfur or chlorine ($m/z = 34$, hydrogen sulfide; 48, methyl sulfide; 62, dimethyl sulfide; 64, sulfur dioxide; 76, carbon disulfide; 50, methyl chloride; and 36, hydrogen chloride). Also noteworthy are the relatively low intensities of lignin pyrolysis products. These features are explained as being due to the highly sulfonated, chlorinated, and oxidized nature of the chlorolignins and lignosulfonates, which leads to macromolecules with relatively low aromatic content and high aliphatic functional group content. Comparing these spectra with the Py-MS spectra of standard materials (sodium lignosulfonate, lignosulfonic acid, sodium polystyrenesulfonate, and polystyrenesulfonic acid) provided some insights into mechanisms for the formation of the small pyrolysis products containing sulfur or chlorine.

Figure 7.6 presents the Py-GC/MS profile of the high molecular weight DOC from pulp mill effluent B. The peak numbers refer to the compound identifications shown in Table 7.3, a listing of all of the compounds found in the pulp mill effluents. Most likely the peak identifications in Table 7.3 were presumptive identifications obtained by matching spectra against known spectra in a computer database, and likely some of the identifications were incorrect; for instance, peaks 78 and 86 were both identified as 4-methylguaiacol. Nevertheless, the types of compounds identified and the relative amounts of the various types of compounds allowed the authors

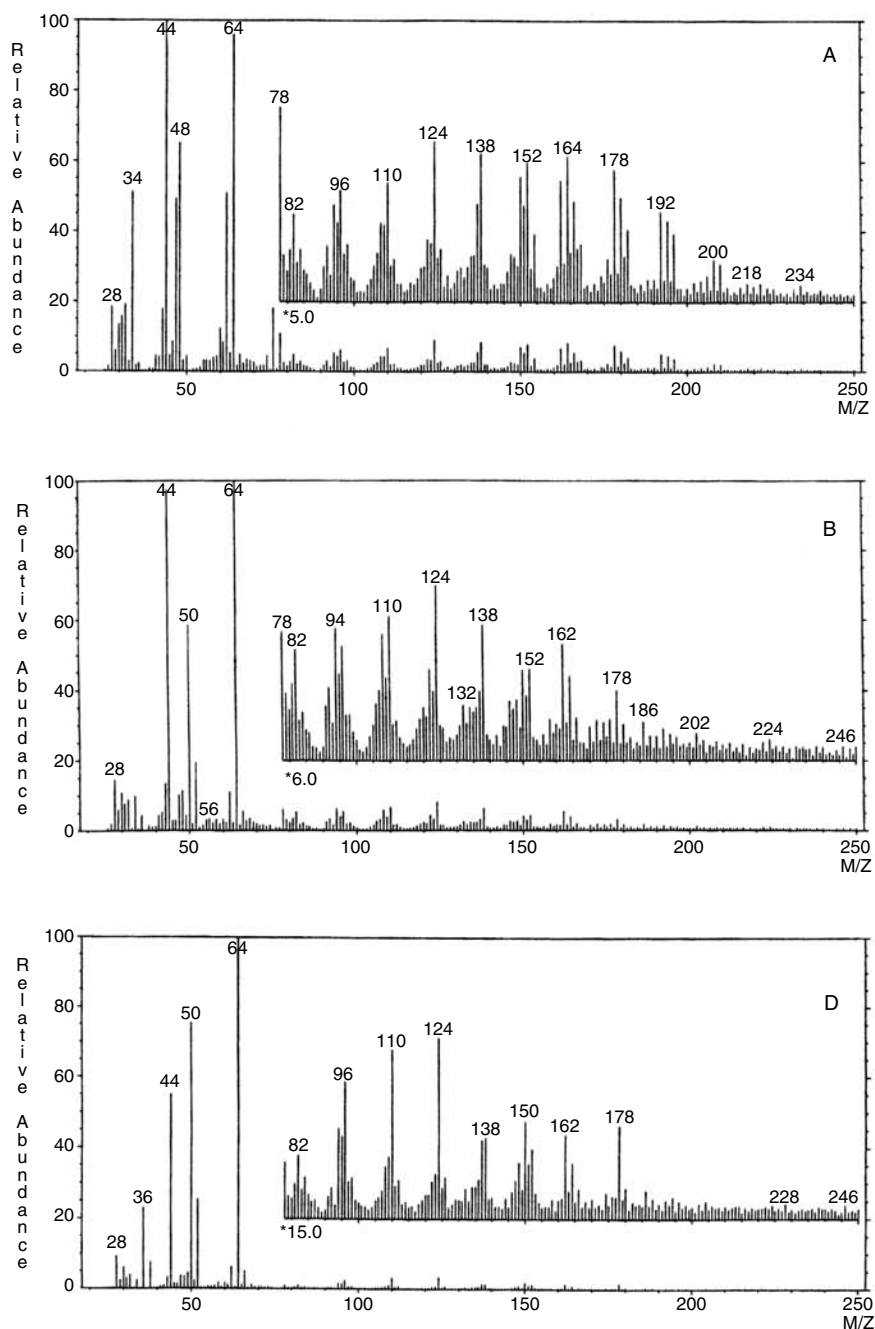


FIGURE 7.5 Pyrolysis-mass spectra of high molecular weight material (MW > 1000) isolated from pulp mill effluents A, B, and D. (From van Loon, W.M.G.M. et al., *J. Anal. Appl. Pyrol.*, 20: 275 (1991). With permission.)

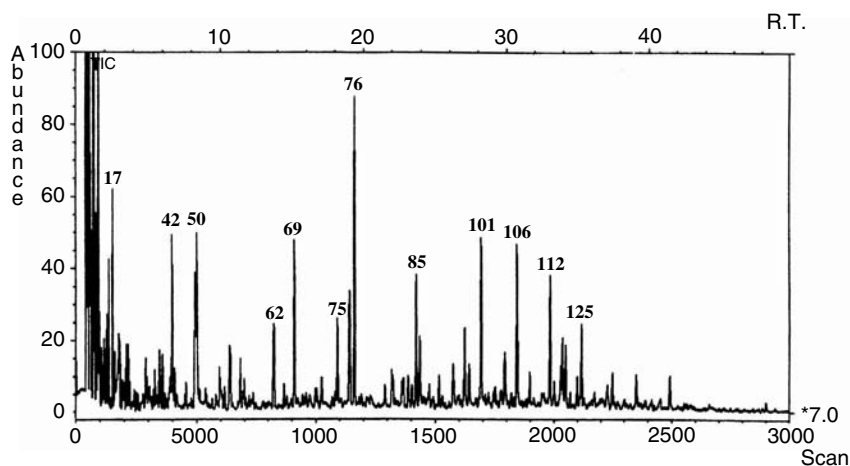


FIGURE 7.6 Curie-point pyrolysis-GC/MS total ion current profile of high molecular weight material (MW > 1000) from pulp mill effluent B. (From van Loon, W.M.G.M. et al., *J. Anal. Appl. Pyrol.*, 20: 275 (1991). With permission.)

to reach some useful conclusions about the chemical composition of the high molecular weight DOC. The original table presented considerably more information than that shown in Table 7.3 (such as relative retention times, the m/z of the base peak and molecular ions in each spectrum, and the pulp mill effluents found to contain each compound).

It is interesting to compare the compounds found in the pyrolyzate of the high molecular weight DOC (Table 7.3) with the types of compounds identified by GC/MS analysis of the low molecular weight DOC (Table 7.4). Many of the same compounds are present, leading to the observation that pyrolytic and chemical degradation can lead to monomeric products with a high structural similarity.

This chapter presents a good example of how the two techniques, Py-MS and Py-GC/MS, can be used in a complementary fashion to elucidate various aspects of a very complex analytical problem. Each method has its particular strengths and weaknesses. Py-MS, for instance, does not provide the wealth of detail concerning the various individual compounds that constitute the pyrolyzate of the material studied but has the great advantage of speed and simplicity. If a particular feature of the Py-MS spectrum represents a marker for a component of interest, many samples can be examined for this marker in a relatively short time. The authors suggest that sulfur dioxide may be such a marker that could be used to determine lignosulfonates in river water. (For further reading in this area, consult References 21, 22, 23, 24, and 25.)

7.3.2 SURFACEWATER: ANALYSIS OF NATURAL ORGANIC MATTER

The 1980s and early 1990s have been referred to as the golden age of environmental analytical chemistry in the U.S.²⁶ This era saw the development of relatively inexpensive, very powerful GC/MS systems and the widespread use of GC/MS in

TABLE 7.3
Curie-Point Py-GC/MS Pyrolysis Products of High Molecular Weight
Material in Pulp Mill Effluent of Mills A, B, C, D, and E^a

Peak No.	Compound	Peak No.	Compound
1	Carbon dioxide	75	2-Methylphenol
2	Sulfur dioxide	76	4-Methylphenol
3	Methyl chloride	77	Guaiacol
4	Acetaldehyde	78	4-Methylguaiacol
5	Butene	79	Dimethylphenol-isomer
6	Methanethiol	80	Dimethylphenol-isomer
7	Acetonitrile	81	1-Methyl-1-formyl-1H-imidazole
8	2-Propenal	82	1-Methyl-1H-indene
9	2-Propanone	83	Ethylphenol-isomer
10	Furan	84	Ethylphenol-isomer
11	Dimethylsulfide	85	Dimethylphenol-isomer
12	Acetic acid, methyl ester	86	4-Methylguaiacol
13	Carbon disulfide	87	Monochloroguaiacol-isomer
14	Cyclopentadiene	88	Naphthalene
15	1-Butanal	89	Methylguaiacol
16	2-Methyl-2-propenal	90	1,2-Dihydroxybenzene
17	2,3-Butanedione	91	Monochloroguaiacol-isomer
18	2-Butanone	92	4-Vinylphenol
19	2-Methylfuran	93	Dimethylguaiacol
20	3-Methylfuran	94	Methoxydihydroxybenzene
21	Propionic acid, methyl ester	95	Methyldihydroxybenzene-isomer
22	2-Butenal	96	Methyldihydroxybenzene-isomer
23	3-Methylbutanal	97	Monochloroguaiacol-isomer
24	Acetic acid, methyl ester	98	4-Ethylguaiacol
25	2-Methylbutanal	99	Monochloroguaiacol-isomer
26	Benzene	100	Methyldihydroxybenzene
27	Thiophene	101	Monochloroguaiacol-isomer
28	Hydrochloric acid	102	4-Vinylguaiacol
29	Methylisothiocyanate	103	Chloro-4-methylguaiacol
30	2,3-Pentadione	104	2-Methylnaphthalene
31	4-Thiol-3-buten-2-one	105	Syringol
32	1-Thiol-2-propanone	106	4-(1-Propenyl)guaiacol
33	2,5-Dimethylfuran	107	4-Formylguaiacol
34	Acetic acid	108	Chloro-1,2-dimethoxybenzene
35	(Methylthio)methanol	109	Chloro-4-methylguaiacol
36	2-Vinylfuran	110	4-(2-Propenyl)guaiacol
37	1-Methyl-1H-pyrrole	111	Chloro-1,2-dihydroxybenzene
38	2,3-Dihydro-3-methylfuran	112	4-Methylsyringol
39	2-Methylpyrrole	113	4-(2-Propenyl)guaiacol
40	Pyridine	114	1,2-Dimethoxy-4-benzaldehyde
41	Dimethyldisulfide	115	Chloro-4-ethylguaiacol

Continued.

TABLE 7.3 (Continued)

Curie-Point Py-GC/MS Pyrolysis Products of High Molecular Weight Material in Pulp Mill Effluent of Mills A, B, C, D, and E^a

Peak No.	Compound	Peak No.	Compound
42	2-Butenoic acid, methyl ester	116	4-Propylguaiaicol
43	Toluene	117	Dichlorguaiaicol-isomer
44	3,4-Dihydro-2H-pyran	118	4-Ethanalguaiaicol
45	Methylthiophene	119	4-C ₃ H ₃ -Guaiaicol
46	2,3-Dihydrofurfural	120	4-C ₃ H ₃ -Guaiaicol
47	3-Furaldehyde	121	4-(1-Propenone)guaiaicol
48	3-Acetylfuran	122	Chloro-4-vinylguaiaicol-isomer
49	2,5-Dimethyl-1,4-dioxane	123	4-(3-Hydroxypropenyl)guaiaicol
50	Dimethylsulfoxide	124	4(2-Propanone)guaiaicol
51	2-Furaldehyde	125	4-Ethylsyringol
52	Methyl-1H-pyrrole	126	4(1-Propanone)guaiaicol
53	Methyl-1H-pyrrole	127	Chloro-4-vinylguaiaicol-isomer
54	4-Methylpyridine	128	Tetrachloro-compound
55	Ethylbenzene-isomer	129	Trichloroguaiaicol-isomer
56	Ethylbenzene-isomer	130	4-(Propane-1,2-dione)guaiaicol
57	Dimethylbenzene-isomer	131	Trichloroguaiaicol-isomer
58	2,4-Dimethylthiophene	132	4-(2-Chloro-2-ethanone)guaiaicol
59	CH ₃ -S-CO-SH	133	4-Vinylsyringol
60	3-Methyl-2-cyclopenten-1-one	134	4-(1-propenyl)syringol
61	Dimethylbenzene-isomer	135	Chloro-4-propenylguaiaicol
62	2-Acetylfuran	136	4-Ethyoxylguaiaicol
63	5-Methyl-2-furaldehyde	137	4-Formylsyringol
64	2,3-Dimethylpyrazine	138	3-Methoxy-2-naphthalenol
65	Methoxybenzene	139	Chloro-4-(2-propanone)guaiaicol
66	CH ₃ -SO-CH ₂ -CO-CH ₃	140	4-C ₃ H ₃ -Syringol
67	3-Methyl-2-cyclopenten-1-one	141	Biphenol-isomer
68	5-Methyl-2-furaldehyde	142	C ₃ H ₃ -Syringol
69	2-Furancarboxylic acid, methyl ester	143	Trichloroguaiaicol-isomer
70	Phenol	144	4-(1-Propenyl)syringol
71	Benzofuran	145	4-(Prop-1-en-3-al)guaiaicol
72	Trimethylbenzene	146	4-Ethanal-syringol
73	2-Hydroxy-3-Methyl-2-cyclopenten-1-one	147	4-(2-Propanone)syringol
74	1H-Indene	148	C ₁₆ -Fatty acid methyl ester
		149	1,2-Diguaiaicylthene

^a Pulp mill identities are provided in the text.

Source: Adapted from van Loon, W.M.G.M. et al., *J. Anal. Appl. Pyrol.*, 20: 275 (1991). With permission.

TABLE 7.4**Low Molecular Weight Compounds Identified with GC/MS in Effluent from Pulp Mills A, B, C, and D^a**

Peak No.	Compound	Peak No.	Compound
1	Benzene	26	4-Formylguaiaicol
2	Pentanol	27	Syringol
3	Toluene	28	1,7,7-Trimethyl-bicyclo[2.2.1]heptan-2-ol
4	Dimethylfuran	29	C ₁₁ -Alkane
5	2-Furancarboxaldehyde	30	1,1,1-Trichloro-2-propanone
6	Dimethylsulfide	31	4-Propenylguaiaicol
7	2-Methanolfuran	32	4-Ethanalguaiaicol
8	Hexanal	33	4-Acetylguaiaicol
9	2-Acetylpyrrole	34	C ₁₂ -Alkane
10	5-Methyl-2-furancarboxaldehyde	35	4-(2-Propanone)guaiaicol
11	Trichloromethane	36	4-(Ethanoic acid)guaiaicol
12	C ₃ -Benzene	37	C ₁₃ -Alkane
13	Guaiaicol	38	Dichloroguaiaicol (3 isomers)
14	2-Acetylfuran	39	1,1,3,3-Tetrachloro-2-propanone
15	C ₄ -Benzene	40	Trichlorophenol
16	4-Propylphenol	41	C ₁₄ -Alkane
17	C ₁₀ -Alkane	42	4-(2-Propanone)syringol
18	Dichlorobenzene	43	C ₁₅ -Alkane
19	4-Vinylguaiaicol	44	4-(Propanedione)syringol
20	4,6,6-Trimethyl-bicyclo-[3.3.1]hept-3-en-2-one	45	C ₁₆ -Alkane
21	1,7,7-Trimethyl-bicyclo-[2.2.1]heptan-2-one	46	C ₁₄ -Fatty acid
22	1,7,7-Trimethyl-bicyclo-[2.2.1]heptan-2-ol	47	C ₁₇ -Alkane
23	1,3,3-Trimethyl-bicyclo-[2.2.1]heptan-2-one	48	C ₁₈ -Alkane
24	2,6,6-Trimethyl-bicyclo-[3.1.1]heptan-3-one	49	Tetrachloroguaiaicol
25	4-Ethylguaiaicol		

^a Pulp mill identities are provided in the text.Source: Adapted from van Loon, W.M.G.M. et al., *J. Anal. Appl. Pyrol.*, 20: 275 (1991). With permission.

laboratories that formerly had been using only GC. During this same period, Py-GC/MS became one of the routine analytical tools applied to the study of natural organic material (NOM) in water. An extensive discussion of the use of Py-GC/MS for the examination of NOM is well beyond the scope of this chapter, but the studies cited below will lead the interested reader into studies of NOM in surface waters around the world: rivers in France;²⁷ nine different unspecified water sources in Norway;²⁸ comparison of the Mediterranean with the Black Sea;²⁹ estuarine water on

the border between the Netherlands and Germany;³⁰ lake water in Germany;³¹ Keddara dam reservoir water in Algeria;³² reservoir water in Australia;³³ lake water in Finland;³⁴ and in the U.S., freshwater wetlands water in Florida³⁵ and 17 drinking water sources in Alaska.³⁶ In addition, the NOM in seawater from off the coast of Florida was examined using Py-MS,³⁷ and the NOM in the lake water in Germany was investigated using pyrolysis-field ionization mass spectrometry (Py-FIMS) and pyrolysis-gas chromatography-combustion-isotope ratio mass spectrometry (Py-GC-C-IRMS).³¹

Generally speaking, NOM in water is the organic material that derives from nonanthropomorphic sources. One of the complexities in examining this material is that the organic materials range in size from relatively simple organic molecules to quite complex biopolymers, and these materials may be dissolved or suspended in the water or adsorbed upon inorganic suspended particulates in the water. The raw water samples can be processed in a variety of ways to yield a variety of organic fractions that can be examined by a variety of techniques, one of which is frequently Py-GC/MS. In the studies cited above, particular types of compounds found in the pyrolyzates are used to infer the presence of various classes of biopolymers in the original sample (e.g., polysaccharides, proteins, N-acetylamino sugars, polyhydroxyaromatics, and lignins).

7.3.3 ANALYSIS OF GROUNDWATER CONTAMINATION

Voorhees et al.³⁸ described an environmental application that is not a pyrolysis application per se, but rather an environmental application of pyrolysis equipment that seemed too clever not to mention here.

Groundwater contamination by organic chemicals is frequently measured by drilling wells into aquifers to obtain samples of the groundwater for subsequent purge-and-trap GC/MS analysis. When used in a reconnaissance mode, this process can be very expensive. These organic chemicals can migrate vertically to the surface as vapors, but their concentrations are often too low for direct measurement. The trapping procedure described by these authors, however, provides a viable approach.

Static traps were prepared by coating about 1 cm of the end of 358°C Curie-point pyrolysis wires with finely powdered activated charcoal. After being precleaned by being heated to the Curie point under vacuum, the traps were transported to the field test site in sealed culture tubes. At the field test site (a site known for groundwater contamination by tetrachloroethylene (PCE)), the static traps were placed in 25- to 35-cm-deep holes, covered with inverted aluminum cans, and the soil replaced in the holes. After 3 days the traps were removed for analysis.

Analysis was performed by desorbing the organics from the traps with a Curie-point pyrolyzer unit in series with a quadrupole mass spectrometer. The data produced were similar to Py-MS data, although, quite likely, thermal desorption was taking place rather than pyrolysis. The typical mass spectrum obtained from the contaminated areas was dominated by the major ions of PCE. Table 7.5 shows the various compounds that were identified in spectra obtained from the 25 samples spaced around the contaminated area. Table 7.6 shows the compounds identified by static trapping from a particular location and by purge-and-trap GC/MS analysis of water from an adjacent well.

TABLE 7.5
Compounds Identified by Static
Trapping/MS Analysis for a Denver
Industrial Site

Benzene	Dichlorobenzene
Toluene	Chloroform
Xylene	Trimethylbenzene
Phenol	Naphthalene
Trichloroethylene	Carbon tetrachloride
Tetrachloroethylene	

Source: Adapted from Table I of Voorhees, K.J. et al., *Anal. Chem.*, 56: 2604 (1984). With permission.

TABLE 7.6
Compounds Identified by Static Trapping/MS and by
Purge-and-Trap GC/MS

Compound	Static Trapping/MS Above Well 23179 (Ion Counts)	Purge-and-Trap GC/MS Well 23179 ($\mu\text{g/l}$)
Dichloroethylene	ND	12
Benzene	ND	22.1
Toluene	1052	<2
Xylene	853	4.3
Trichloroethylene	352	9.5
Tetrachloroethylene	616	75.2
Chloroform	— ^a	3440
Carbon tetrachloride	110	<3

Note: ND = not detected.

^a Other compounds interfered with $m/z = 83$ and 85 ; identification could not be made.

Source: Adapted from Table II of Voorhees, K.J. et al., *Anal. Chem.*, 56: 2604 (1984). With permission.

This static trapping technique could be an excellent reconnaissance technique for many volatile organic compounds. In this study, the ion counts for the PCE were proportional to the surface fluxes from the plume contamination, falling off sharply at the plume edges. An attractive feature of the technique is the short analysis time — a few minutes per sample. However, as pointed out by the authors, the technique is limited in some instances by the lack of separation of the adsorbed components prior to the measurement by mass spectrometry. Apparently, the overlapping ions from the mixture of components can make some components unidentifiable in the

mixed spectrum. This can be a serious limitation in some cases; for instance, in the comparison shown in Table 7.6, a very high chloroform concentration in the purge-and-trap GC/MS analysis was undetected in the static trapping/MS analysis due to a high background of ions from other substances masking the chloroform ions. The authors suggest that combining this Py-MS technique with Py-GC or Py-GC/MS could be an improvement.

7.4 ANALYSIS OF SOIL AND SEDIMENT

7.4.1 THERMAL DISTILLATION-PYROLYSIS-GC

The use of thermal distillation-pyrolysis-GC (TD-Py-GC) and GC/MS to examine marine sediments and suspended particulates for anthropogenic input was reported by Whelan et al.^{39,40} The TD-Py-GC technique differed from typical Py-GC in that the temperature of the sample was raised slowly (e.g., 60°C/min) to 800°C, evolving two distinct peaks of organic material, well separated in time. The first, a low-temperature peak (P_1), in the range of 100 to 200°C, contained unaltered, absorbed volatile organic compounds; the second pyrolyzate peak (P_2), which emerged in the 350 to 600°C range, consisted of compounds thermally “cracked” from high molecular weight organic materials. The TD-Py-GC apparatus is shown diagrammatically in Figure 7.7.

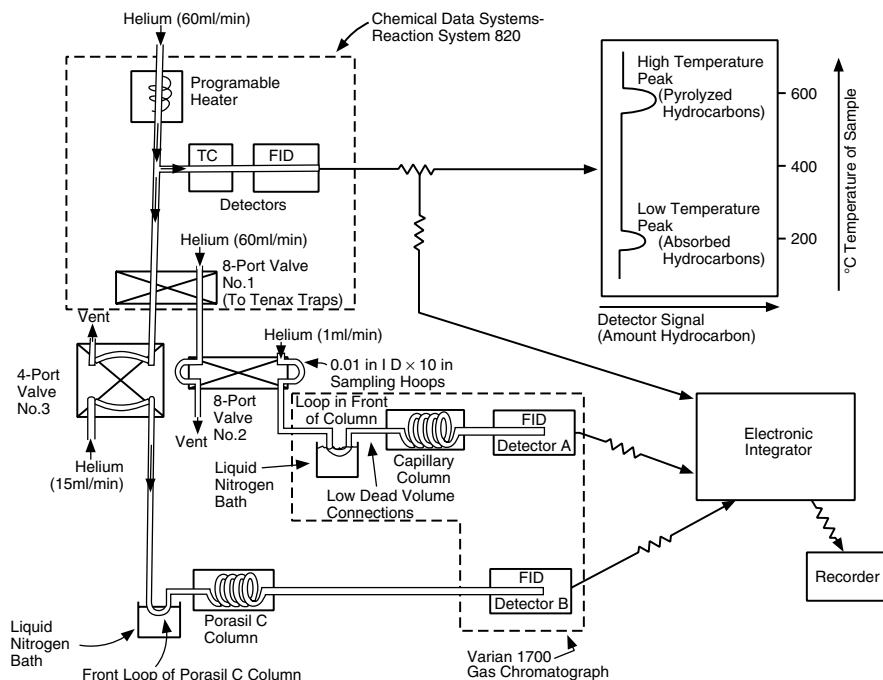


FIGURE 7.7 Diagram of the thermal distillation-pyrolysis-GC apparatus. (From Whelan, J.K. et al., *J. Anal. Appl. Pyrol.*, 2: 79 (1980). With permission.)

As described in the first report,³⁹ a 0.5- to 50-mg sample of wet (or frozen) sediment was placed in a quartz tube that was then placed in the platinum coil of a pyrolysis probe. The probe was inserted into the cooled interface chamber of the reaction system, which was then purged with helium carrier gas. The interface chamber was heated to 250°C and the pyrolysis probe temperature ramp started. About 10% of the helium carrier stream was split off to a thermal conductivity-flame ionization detector series, which provided profiles of products evolved from the sample. The main portion of the helium carrier flow was directed via switchable multiport valves through a pair of Tenax traps for the appropriate time periods to trap the P_1 and P_2 groups of evolved organic materials.

The GC-FID analysis of the Tenax-trapped portions of P_1 and P_2 was accomplished sequentially. By flash desorbing the adsorbed organics from each of the Tenax traps in turn, P_1 and P_2 were sent sequentially to the GC for analysis. One column (a micropacked column, 3 m long with a 3% OV-17 stationary phase coated on a 160–180 mesh support material) of a dual-column, dual-FID GC connected to the system was used for this analysis. To improve chromatographic peak shape, the desorbed organic materials were cryofocused with liquid nitrogen prior to being transferred to the GC column. Qualitative analysis of the low molecular weight portions of P_1 and P_2 that were not trapped by the Tenax traps (e.g., C_1 to C_5 hydrocarbons) was accomplished by sweeping the helium effluent from the interface chamber through the Tenax traps (via switchable multiport valves) to a liquid nitrogen trap on the first coil of the other column of the GC (*n*-octane/Porasil C, 6 ft long \times 0.085 in. I.D.).

Rather than analysis by GC-FID, the P_1 and P_2 fractions could be analyzed by GC/MS by being trapped on small Tenax traps. These traps would then be desorbed by being placed in the heated inlet of the GC of the GC/MS system, with the desorbed organics cryofocused with liquid nitrogen at the head of the GC column.

In the later work,⁴⁰ the micropacked GC column was replaced with a 50-m-long narrow-bore capillary column with probably more than 10 times as many theoretical plates. Comparing the P_2 profile (micropacked GC column) in Figure 7.8 with the P_2 profile (narrow-bore capillary GC column) in Figure 7.9 illustrates the tremendous additional amount of detail that can be obtained through the use of high-resolution capillary columns for the separation of pyrolyzates.

Whether they were generated using a packed column or a narrow-bore capillary column, the GC profiles from the TD-Py-GC technique proved quite useful for examining the distribution of organic materials in the various compartments of the marine ecosystem. Due to the relatively small size sample required, the method was especially useful for examining organic matter in several types of samples, such as marine particles and parts of small marine animals. Analysis of sediments and various particles, including sewage sludge, from the Boston Harbor area provided interesting insights into sediment deposition processes in this area and the fate of the anthropogenic organic matter.

7.4.2 FLASH PYROLYSIS-GC AND GC/MS

Several groups of researchers noticed that nonpolymeric organic compounds that are reasonably volatile at elevated temperatures do not fragment upon pyrolysis but

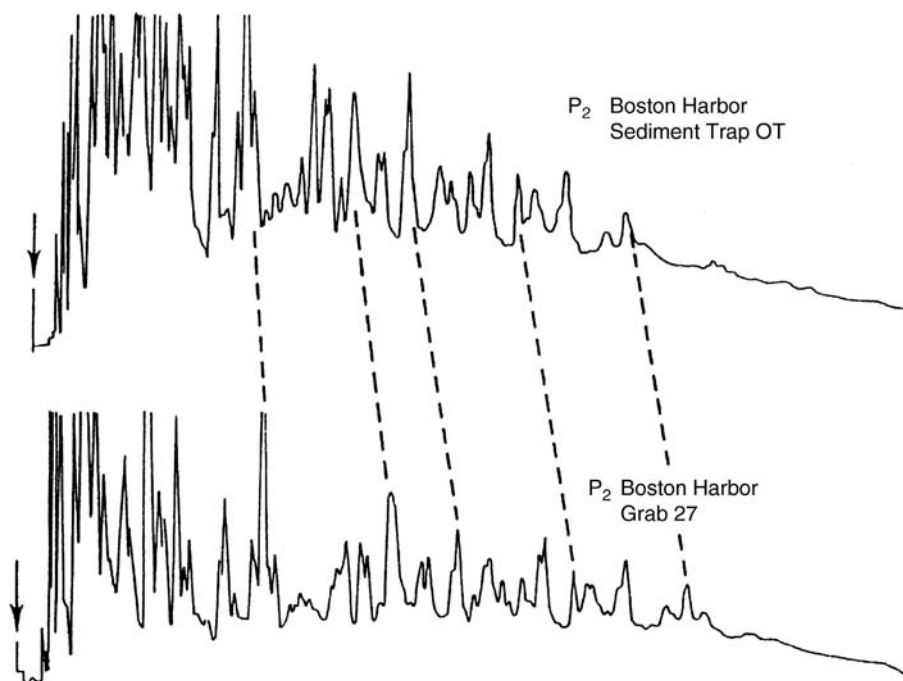


FIGURE 7.8 Micropacked GC analyses of P2 peaks from Boston Harbor particles. OT is a midwater sediment trap sample; GRAB 27 is a surface sediment sample. (From Whelan, J.K. et al., *J. Anal. Appl. Pyrol.*, 2: 79 (1980). With permission.)

simply volatilize.^{41,42} They realized that pyrolysis could be a rapid way of extracting these compounds from a complex sample matrix and transferring them directly into the analytical system, thus providing a rapid screening method and avoiding the often lengthy extraction and cleanup procedures. One group⁴² referred to this procedure as flash evaporation pyrolysis (EV-Py). This technique differs from TD-Py, described above, in that the sample is elevated to the pyrolysis temperature in milliseconds rather than the slow temperature ramp used in TD-Py.

McMurtrey et al.⁴¹ evaluated EV-Py-GC/MS as a rapid method for screening soils for polychlorinated biphenyls (PCBs). Five-milligram samples of dried lake sediment spiked with PCB (Aroclor 1254) were pyrolyzed at 1000°C for 10 sec with a probe pyrolyzer and the evolved organics swept onto an 80°C packed GC column (3% OV-1, 6 ft long × 2 mm I.D.) that was then temperature programmed to 275°C. This method proved easily capable of demonstrating the presence of the spiked PCB at the 10 ppm level using the MS in the full scan mode. Although they did not do the experiments, the authors theorized that the detection limit could be reduced considerably by operating the MS in the selected ion monitoring mode. They realized that Py-GC using the much more sensitive electron-capture detector would be a more attractive screening method for PCBs than Py-GC/MS, but their preliminary attempts in that direction did not seem very promising because pyrolysis

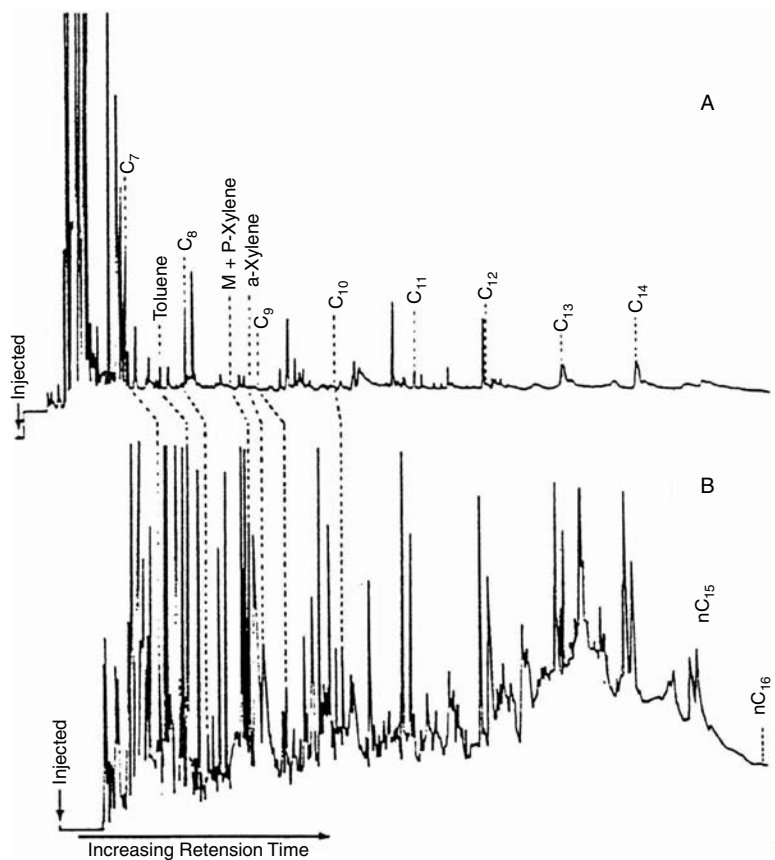


FIGURE 7.9 P2 capillary GC patterns: seston (A) and sediment trap particles (B). (From Whelan J.K. et al., *Environ. Sci. Technol.*, 17: 292 (1983). With permission.)

of sediments released so much electron-capturing material that the peak patterns of the PCBs were obscured and hence unrecognizable.

de Leeuw et al.⁴² demonstrated the usefulness of EV-Py-GC/MS as a rapid screening technique for polycyclic aromatic hydrocarbons (PAHs), halogenated organics, aliphatic hydrocarbons, heteroaromatics, elemental sulfur, cyanides, and pyrolysis products of synthetic polymers. A 200- μ g sample (either polluted soil or sediment) was heated to 510°C with a Curie-point pyrolyzer and the evolved organics swept onto a high-resolution capillary column (CP-SIL 5, 25 m long \times 0.22 mm I.D.) at 0°C. The GC temperature was programmed to 275°C at 3°C/min. The MS scanned the range 50 to 550 amu at 1.5 sec/scan.

Figure 7.10 displays a total ion current profile (TICP) of EV-Py-GC/MS analysis of a polluted soil sample. A central portion of the TICP has been expanded eight times to emphasize the wealth of compounds present (upper trace). The numbers in the mass chromatograms (lower third of the figure) represent the m/z values indicative of the following classes of compounds: 104, 118, 132 (C_0 to C_2 styrenes); 116, 130 (C_0 to C_1 indenenes); 128, 142, 156, 170 (C_0 to C_3 naphthalenes); 134, 148, 162 (C_0 to C_2 benzo[b]thiophenes); 154 (biphenyl and acenaphthene); 168, 182, 196 (C_1 to C_2 biphenyls and C_0 to C_2 dibenzofurans); 166, 180 (C_0 to C_1 fluorenes and 9-fluorenone); 184 (dibenzothiophene); 202 (fluoranthene and pyrene); 228 (benzo[c]phenanthrene, benz[a]anthracene, chrysene, and triphenylene); and 252 (benzo[e]pyrene and benzo[a]pyrene). The x axes of the mass chromatograms correspond exactly with the appropriate parts of the TIC x axis directly above them (e.g., the major peak in the mass chromatogram of $m/z = 168$ corresponds with peak 41 in the total ion current profile). The peak numbers in Figure 7.10 correspond to the peak numbers of the presumptively identified compounds listed in Table 7.7. Relating the response for phenanthrene (peak 63) and benzo[a]pyrene (peak 73) to the 200 μ g applied to the pyrolysis wire, it was estimated that the detection limit for PAHs using this method was about 5 ppm.

The authors pointed out that because no pretreatment of the samples was carried out, the peaks present in the TICP reflected both components generated by pyrolysis of primary sample compounds (real pyrolysis products) and components that were present as such in the sample and simply evaporated (free products). In this soil sample, for instance, they saw four different groups of anthropogenic compounds: HCN and dicyanogen (pyrolysis products), elemental sulfur (present as such), PAH (mainly unsubstituted, present as such), and styrenes and phenyl ethers (pyrolysis products). They then went on to speculate about the previous industrial activities that took place in the area where the soil sample was collected that might have led to the suite of compounds identified by the EV-Py-GC/MS analysis.

The authors presented an analytical scheme (Figure 7.11) to use flash evaporation pyrolysis with a variety of detectors in addition to MS to provide greater selectivity and sensitivity for common classes of pollutants, but data only for MS were presented in this report.

Over the years this technique (usually referred to simply as Py-GC or Py-GC/MS) has proven very useful for the examination of soils and sediments to determine the nature of the natural organic materials or the degree of contamination by anthropomorphic organic materials.⁴³⁻⁵⁰ One study⁵¹ analyzed river sediments and

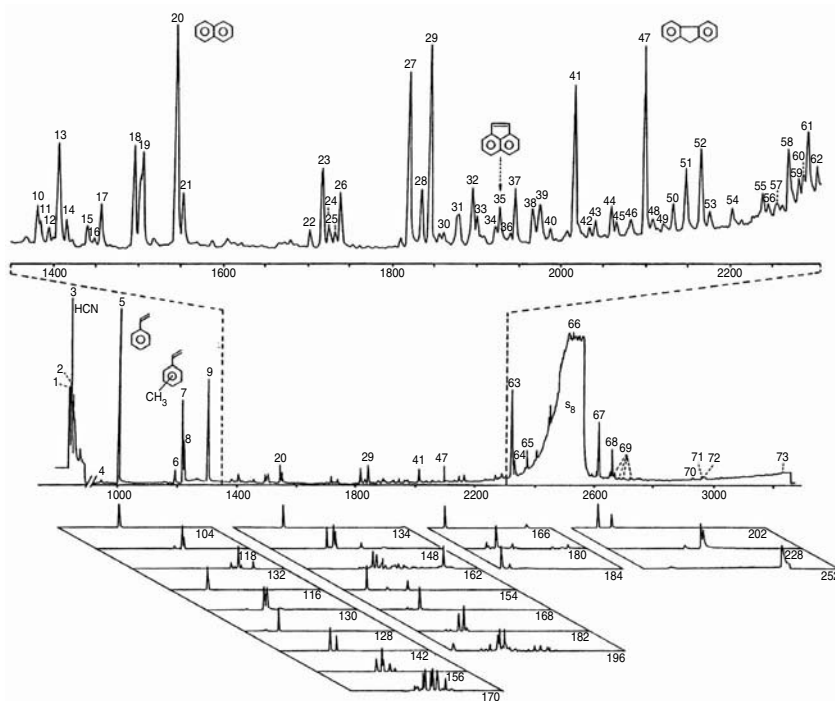


FIGURE 7.10 TIC of EV-Py-GC/MS analysis of polluted soil sample. The upper trace represents a part of the TIC magnified eight times. The number in the mass chromatograms represents the m/z values indicative of the following classes of compounds: 104, 118, 132 (C_0 to C_2 styrenes); 116, 130 (C_0 to C_1 indenenes); 128, 142, 156, 170 (C_0 to C_3 naphthalenes); 134, 148, 162 (C_0 to C_1 benzo[b]thiophenes); 154 (biphenyl and acenaphthene); 168, 182, 196 (C_1 to C_2 byphenyls and C_0 to C_2 dibenzofurans); 166, 180 (C_0 to C_1 fluorenes and 9-fluorenone); 184 (dibenzothiophene); 202 (fluoranthene and pyrene); 228 (benzo[c]phenanthrene, benz[a]anthracene, chrysene, and triphenylene); and 252 (benzo[e]pyrene and benzo[a]pyrene). The x axes of the mass chromatograms correspond exactly with the appropriate parts of the TIC x axis directly above them (e.g., the major peak in the mass chromatogram of $m/z = 168$ corresponds with peak 41 in the total ion current profile). (From de Leeuw, J.W. et al., *Anal. Chem.*, 58: 1852 (1986). With permission.)

sewage sludges by pyrolysis gas chromatography using an atomic emission detector (Py-GC/AED) and compared the results with Py-GC/MS analysis. Multielement detection focused on C, N, S, O, and Cl was shown to be a useful tool for specifying the distribution of organic heteroatom compounds.

7.4.3 TD-PY-FID APPLIED TO MARINE SEDIMENTS

Kennicutt et al.⁵² described the use of Py-FID for assessing the areal distribution of drilling fluids in surficial marine sediments around drilling platforms. Unlike the Py-FID, which utilized flash pyrolysis (described in Section 7.3.3), their technique subjected the samples to a $30^\circ\text{C}/\text{min}$ temperature ramp from ambient to 700°C , with

TABLE 7.7
Identified Evaporation and Pyrolysis Products of the Soil Sample

Peak No.	Compound	Peak No.	Compound
1	H ₂ S, CO ₂ , CO	37	(C ₁ -Phenyl)ethyl tert-butyl ether (tentative)
2	Dicyanogen	38	(C ₁ -Phenyl)ethyl tert-butyl ether (tentative)
3	Hydrogen cyanide	39	Acenaphthene + 4-methylbiphenyl
4	Ethylbenzene	40	3-Methylbiphenyl
5	Styrene	41	Dibenzofuran
6	α -Methylstyrene	42	C ₃ -Naphthalene
7	3-Methylstyrene	43	C ₃ -Naphthalene
8	4-Methylstyrene	44	C ₃ -Naphthalene
9	Indene	45	C ₃ -Naphthalene
10	α ,3-Dimethylstyrene	46	C ₃ -Naphthalene
11	3-Ethylstyrene	47	Fluorene
12	α ,4-Dimethylstyrene	48	C ₃ -Naphthalene + dimethylbiphenyl
13	3,5-Dimethylstyrene	49	Dimethylbiphenyl
14	α ,2- or 2,5- or 2,4-Dimethylstyrene	50	Unknown organic sulfur compound
15	Phenyl ethyl ether	51	Methylbenzofuran
16	2,3-Dimethylstyrene	52	Methylbenzofuran
17	3,4-Dimethylstyrene	53	Methylbenzofuran
18	Methylindene	54	α -1-Phenyl ethyl ether (tentative)
19	Isomeric methylidenes	55	2-Methylfluorene
20	Naphthalene	56	1-Methylfluorene
21	Benzo[b]thiophene	57	C ₂ -Benzofuran
22	Methylbenzo[b]thiophene	58	9-Fluorenone
23	2-Methylnaphthalene	59	C ₂ -Benzofuran
24	Methylbenzo[b]thiophene	60	C ₂ -Benzofuran
25	Methylbenzo[b]thiophene	61	Dibenzothiophene
26	1-Methylnaphthalene	62	C ₂ -Benzofuran
27	1-Phenylethyl tert-butyl ether (tentative)	63	Phenanthrene
28	Biphenyl	64	Anthracene
29	Unknown organic sulfur compound	65	Bis(1-phenylethyl)thioether (tentative)
30	1-Ethyl-naphthalene + dimethylbenzo[b]thiophene	66	Elemental sulfur
31	2,6- or 2,7-Dimethylnaphthalene	67	Fluoranthene
32	1,3-Dimethylnaphthalene	68	Pyrene
33	1,7- and/or 1,6-Dimethylnaphthalene	69	Isomeric naphthobenzofurans
34	2,3- and/or 1,4-Dimethylnaphthalene	70	Benzo[c]phenanthrene
35	Acenaphthalene	71	Benzo[a]anthracene
36	1,2-Dimethylnaphthalene	72	Chrysene + triphenylene
		73	Benzo[a]pyrene + benzo[c]pyrene

Source: Adapted from Table I of de Leeuw, J.W. et al., *Anal. Chem.*, 58: 1852 (1986). With permission.

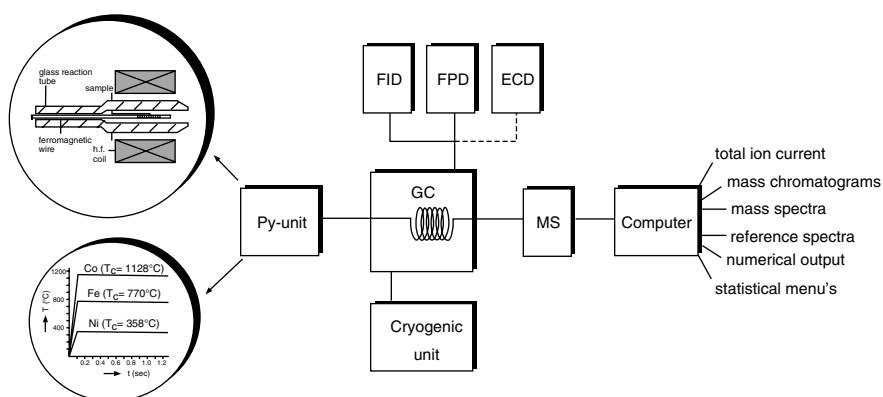


FIGURE 7.11 Instrumental setup for screening analysis by evaporation/pyrolysis gas chromatography. (From de Leeuw, J.W. et al., *Anal. Chem.*, 58: 1852 (1986). With permission.)

the evolved organic compounds swept into an FID for measurement. This technique would better be described as thermal distillation pyrolysis-FID (TD-Py-FID) rather than Py-FID.

Freeze-dried, ground, and sieved surficial sediment samples (upper few centimeters) were heated from ambient temperature to 700°C at 30°C/min in a helium atmosphere, and the evolved organics were swept into an FID with the area under the resulting or peaks integrated and digitized. The resulting FID area units were normalized by being divided by the organic carbon content (measured by combustion in an oxygen atmosphere — after carbonate removal — and measurement of the evolved CO₂) of the sample, expressed as nanograms, to produce values referred to as pyrolysis ratios (PRs).

The data presented clearly demonstrated that different materials, such as planktonic debris, ancient shales, leaves, and wood, show widely different PRs. Just what the ratio between the amount of organic carbon as measured by TD-Py-FID and the amount of organic carbon as measured by an oxidative technique actually represented was not clear. Nevertheless, the isopleths showing PRs as a function of the distance from drilling platforms indicated that PRs could be used to delineate the areal extent of materials added to surficial sediments by drilling operations.

7.4.4 ROCK EVAL PYROLYSIS

Rock eval pyrolysis from its inception in 1977(referred to in Luniger and Schwark⁵³) has become a widely used technique for geochemical characterization of organic matter in sediments. Two references have been included here that will lead interested persons into the rich literature in this area.^{53,54} One of these studies in particular⁵³ describes the method in some detail.

Rock eval pyrolysis is similar to Py-FID (described in Section 7.3.3) in that the organic material from the sample passes directly to an FID for measurement without separation by GC, and is similar to TD-Py-GC (described in Section 7.4.1) in that two organic profiles are obtained: one from a low-temperature treatment of the

sample and one from the subsequent high-temperature pyrolysis of the sample. As described in Luniger and Schwark,⁵³

In this technique, bulk dried samples are heated in an inert helium atmosphere, where upon thermo-vaporization and pyrolysis, hydrocarbons are quantified by flame-ionisation detection. Compounds occurring as free gases and liquids in sediments are separated from those that occur in bound form, or as particulate organic matter by temperature control. The S₁-detector signal records free hydrocarbons, which are thermo-vaporizable at 300°C, and the S₂-detector signal measures those compounds liberated during programmed pyrolysis from 300 to 550°C.

Manipulation of the S₁ and S₂ data provides a measure of the hydrogen richness and oxygen content of the organic matter, parameters that can be used to assess the biological origin of the organic matter and the degree of microbial reworking or abiotic oxidation.

7.4.5 TMAH-PYROLYSIS-GC/MS

A report from a forensic science laboratory in 1989 described a technique to pyrolyze synthetic polymer samples and simultaneously chemically derivatize (methylate) the pyrolysis products prior to analysis by capillary GC and GC/MS, a technique that was referred to as simultaneous pyrolysis methylation-capillary gas chromatography (SPM-GC) and SPM-GC/MS.⁵⁵ The methylation is caused to take place *in situ* by the simple expedient of adding a few microliters of methanol containing tetramethyl ammonium hydroxide (TMAH) to the sample in the sample holder of the pyrolysis device. When applied to sediment samples for characterization of the organic matter, this technique is referred to as TMAH-Py-GC/MS.^{56,57} The methylation procedure quite likely allows measurement of many compounds that otherwise would pass undetected. Table 7.8 shows a list of compounds that were identified in programs of river and lake sediments subjected to analysis by TMAH-Py-GC/MS.⁵⁷

7.5 OTHER ENVIRONMENTAL APPLICATIONS

7.5.1 ANCIENT LIMESTONE: EXAMINATION BY PY-GC AND PY-GC/MS

Py-GC and Py-GC/MS analysis played an interesting role in the characterization of a green layer of material 1 mm below the surface of the limestone on the south-facing exterior wall of a 14th-century building in Tongeren, Belgium.⁵⁸ This green layer consisted of a discrete band (of about 0.2- to 0.5-mm thickness) beneath the surface of the limestone, following the surface contours of the stone. Various bits of evidence suggested that this green layer comprised a cryptoendolithic ecological niche filled by a moss and two species of cyanobacteria. Presumably, these photosynthetic organisms gained some protection from the covering limestone surface but were able to use the moisture and light that passed through it.

A small portion of the green layer was ground to a powder, applied to the wire of a Curie-point pyrolysis unit, and heated within 0.1 sec to 610°C for 10 sec. The

TABLE 7.8
Identification of Peaks from TMAH-Py-GC/MS

Peak No.	Compound	Peak No.	Compound
1	Phosphonic acid, dimethyl ester	46	Pentadecanoic acid, methyl ester
2	Stryene	47	1-Octadecene
3	Phosphoric acid, trimethyl ester	48	1-(Dimethoxyphenyl)-1,2,3-trimethoxypropane
4	Diethylene glycol dimethyl ether	49	Tetradecanoic acid, 12-methyl-, methyl ester
5	Benzaldehyde	50	1,2,4-Benzenetricarboxylic acid, trimethyl ester
6	Methylstyrene	51	2-Propenoic acid, 3-(3,4-dimethoxyphenyl)-, methyl ester
7	(Methoxymethyl)benzene	52	Hexadecanoic acid, methyl ester
8	1-Methoxy-4-methylbenzene	53	N,N-Dimethyloctadecylamine
9	2-Butendioic acid, dimethyl ester	54	Heptadecanoic acid, methyl ester
10	Butanoic acid, methyl ester	55	Octadecenoic acid, methyl ester
11	Benzoic acid, methyl ester	56	N,N-Dimethyloctadecylamine
12	Octanoic acid, methyl ester	57	Octadecanoic acid, methyl ester
13	1,4-Dimethoxybenzene	58	Tetracosane
14	Decanal	59	Eicosanoic acid, methyl ester
15	Triethylene glycol dimethyl ether	60	Dehydroabietic acid?
16	3,4-Dimethoxytoluene	61	Pentacosane
17	4-Methoxybenzaldehyde	62	Heneicosanoic acid, methyl ester
18	1-Methylindole	63	Hexacosane
19	Lignine derivative (m/z = 98)	64	Dicosanic acid, methyl ester
20	Decanoic acid, methyl ester	65	Heptacosane
21	Proteinaceous derivative (m/z = 98)	66	Tricosanoic acid, methyl ester
22	1,2,4-Trimethoxybenzene	67	Docosanoic acid, 2-methoxy-, methylester
23	4-Methoxybenzoic acid, methyl ester	68	Octacosane
24	2-Propenoic acid, 3-phenyl-, methyl ester	69	Tetracosanoic acid, methyl ester
25	Dodecanal	70	Tricosanoic acid, 2-methoxy-, methyl ester
26	3-Methoxy-4,7-dimethyl-1H-isoindole	71	Sterol 1
27	1,3,5-Trimethoxybenzene	72	Sterol 2
28	1,2-Benzenedicarboxylic acid, dimethyl ester	73	Nonacosane
29	3,4-Dimethoxybenzaldehyde	74	Tetracosanoic acid, 2-methoxy, methyl ester
30	1,4-Benzenedicarboxylic acid, dimethyl ester	75	Triacontane
31	Dodecanoic acid, methyl ester	76	Hexacosanoic acid, methyl ester
32	Nonanedioic acid, dimethyl ester	77	5 β -Cholesterol
33	Ethanone, 1-(3,4-dimethoxyphenyl)	78	C ₂₇ -Stanol

Continued.

TABLE 7.8 (Continued)
Identification of Peaks from TMAH-Py-GC/MS

Peak No.	Compound	Peak No.	Compound
34	3,4-Dimethoxybenzoic acid, methyl ester	79	3 β -Methoxycholest-5-ene
35	1-Hexadecene	80	Sterol 3
36	3,4,5-Trimethoxybenzaldehyde	81	5 α -Cholestanol
37	Benzeneacetic acid, 3,4-dmethoxy-, methyl ester	82	C ₂₈ -Stanol
38	4,5-Dimethoxy-2-(2-propenyl)phenol	83	Octaconsanoic acid, methyl ester
39	Ethanone, 1-(3,4,5-trimethoxyphenyl)	84	Sterol 4
40	2-Propenoic acid, 3-(4-methoxyphenyl)-, methyl ester	85	C ₂₉ -5 β -, 3 β -, 3 α -stanol
41	3,4,5-Trimethoxybenzoic acid, methyl ester	86	C ₂₉ -Stanol
42	Tetradecanoic acid, methyl ester	87	24S-Stigmast-5-en-3.beta.ol
43	2-Propenoic acid, 3-phenyl-, ethyl ester	88	Sterol 5
44	4-Acetyl-2,3,6-trimethoxytoluene	89	Sterol 6
45	1-(Dimethoxyphenyl)-1,2,3-trimethoxypropane		

Source: Adapted from Mansuy, L., Bourezgui, Y., Garnier-Zarli, E., Jarde, E., and Reveille, V., *Org. Geochem.*, 32: 223 (2001). With permission.

resulting pyrolysis products were separated on a 25-m-long \times 0.32-mm-I.D. capillary GC column temperature programmed from 0 to 310°C at 3°C/min. The mixture of compounds volatilized from the sample or generated during the pyrolysis was resolved into more than 150 separate peaks by the capillary GC, yielding a pyrogram (not shown here) not greatly dissimilar in appearance from some of those shown earlier in this chapter. Table 7.9, however, lists the compounds presumptively identified from this mixture by Py-GC/MS. The list of compounds, deriving from the pyrolysis of living material, is quite unlike the lists shown in the earlier tables in this chapter.

The substances identified support the assertion that the green layer contained biogenic material, because the vast majority of the evaporation/pyrolysis products obtained were related to polysaccharides, proteins, and lipids, substances that are the main cellular components of organisms such as cyanobacteria and mosses.

7.5.2 OUTDOOR BRONZE MONUMENTS: EXAMINATION OF CORROSION PATINAS BY PY-GC/MS

Samples of the corrosion layers from six outdoor Italian bronze monuments were examined by Py-GC/MS, leading to the identification of organic compounds deriving from both environmental pollution and protective organic coatings.⁵⁹ In addition to direct pyrolysis, some of the samples were subjected to SPM-Py-GC/MS (described in Section 7.4.5). For SPM, 5 μ l of 25% tetramethyl ammonium hydroxide in

TABLE 7.9

Compounds Identified from Pyrolysis of a Green Layer in Limestone from a Building in Tongeren, Belgium

Peak No.	Compound	Peak No.	Compound
1	Sulfur dioxide	72	n-Dodec-1-ene
2	1,3-Butadiene + but-1-ene	73	n-Dodecane
3	Methanethiol	74	Methylbenzylcyanide
4	trans-But-2-ene	75	VAL-VAL sequence + C ₃ -alkylphenol
5	Acetone	76	C ₃ -Alkylphenol + C ₂ -alkylindene
6	Furan	77	VAL-VAL sequence
7	Cyclopentadiene	78	C ₂ -Alkylindene
8	2-Methylpropanal	79	Quinoline
9	2,3-Butanedione	80	Methylnaphthalene
10	2-Butanone	81	C _{5:1} -Alkylbenzene
11	2-Methylfuran	82	C ₃ -Alkylphenol
12	3-Methylfuran	83	C _{5:1} -Alkylbenzene + methylnaphthalene
13	2-Butenal	84	C _{5:1} -Alkylbenzene
14	3-Methylbutanal	85	n-Tridec-1-ene
15	Benzene	86	n-Tridecane
16	2-Methylbutanal	87	VAL-ILEU sequence
17	Pentane-3,4-dione	88	ILEU-VAL sequence
18	Cyclopentanone	89	VAL-LEU sequence + C _{5:1} -alkylbenzene
19	Pentane-2,3-dione	90	VAL-ILEU sequence
20	2,5-Dimethylfuran	91	VAL-LEU sequence
21	2,4-Dimethylfuran	92	ILEU-VAL sequence
22	Vinylfuran	93	LEU-VAL sequence
23	N-Methylpyrrol + pyridine	94	C _{6:1} -Alkylbenzene
24	Toluene	95	LEU-VAL sequence
25	3-Furaldehyde	96	C _{6:1} -Alkylbenzene
26	2-Furaldehyde	97	Methylindole
27	2-Methyl-2,3-dihydrofuran-3-one	98	C _{6:1} -Alkylbenzene
28	Ethylbenzene	99	C ₁₄ -Aldehyde
29	m/p-Xylene	100	n-Tetradec-1-ene
30	1-Acetoxypentan-2-one	101	ILEU-ILEU sequence
31	Styrene	102	n-Tetradecane
32	o-Xylene	103	ILEU-LEU sequence
33	2-Methyl-2-cyclopenten-1-one	104	ILEU-ILEU sequence
34	C ₃ -Alkylfuran	105	ILEU-LEU sequence + LEU-ILEU sequence
35	C ₃ -Alkylfuran	106	LEU-LEU sequence
36	C ₃ -Alkylfuran	107	LEU-ILEU sequence
37	C ₃ -Alkylfuran	108	LEU-LEU sequence
38	Benzaldehyde	109	C ₈ -Alkylbenzene
39	C ₃ -Alkylbenzene	110	Levogluconane
40	5-Methyl-2-furaldehyde	111	C _x -Methylketone

Continued.

TABLE 7.9 (Continued)**Compounds Identified from Pyrolysis of a Green Layer in Limestone from a Building in Tongeren, Belgium**

Peak No.	Compound	Peak No.	Compound
41	3-Methyl-2-cyclopenten-1-one	112	1,2-Diphenylethane
42	C ₃ -Alkylbenzene	113	n-Pentadec-1-ene
43	C ₃ -Alkylbenzene	114	n-Pentadecane
44	α-Methylstyrene	115	Isoprenoid hydrocarbon
45	Benzofuran	116	Methyl-pentadecane
46	C ₃ -Alkylbenzene	117	Dodecanoic acid
47	n-Dec-1-ene	118	n-Hexadec-1-ene
48	Phenol	119	n-Hexadecane
49	n-Decane	120	1,3-Diphenylpropane
50	C ₃ -Alkylbenzene	121	Methylhexadecane
51	C _{3:1} -Alkylbenzene	122	Biphenyl
52	C ₃ -Alkylbenzene	123	9,10-Dihydroanthracene
53	Indene + 2-hydroxy-3-methyl-2-cyclopenten-1-one	124	1,3-Diphenyl-3-methyl-1-propene
54	Cyanopyridine	125	n-Heptadec-1-ene
55	C ₄ -Alkylbenzene	126	n-Heptadecane
56	C ₄ -Alkylbenzene + C _{4:1} -alkylbenzene	127	Prist-1-ene
57	Tolualdehyde	128	7-Methylheptadecane
58	m/p-Cresol	129	Tetradecanoic acid
59	C ₄ -Alkylbenzene	130	Pristane
60	p-Cresol	131	n-Octadec-1-ene
61	n-Undec-1-ene	132	n-Octadecane
62	n-Undecane	133	Dialkyl phthalate
63	Benzylcyanide + C ₄ -alkylbenzene	134	Phytadiene
64	C ₄ -Alkylfuran	135	Phyt-1-ene
65	Methylindene	136	Pentadecanoic acid
66	Methylindene	137	Phytadiene
67	Ethylphenol	138	Phytadiene
68	C ₂ -Alkylphenol	139	n-Nonadecane
69	C ₄ -Alkylbenzene	140	Dialkyl phthalate
70	Naphthalene	141	Hexadecanoic acid
71	C ₂ -Alkylphenol	142	n-Eicosane

Source: Adapted from Table 3 of Saiz-Jimenez, C. et al., *Sci. Total Environ.*, 94: 209 (1990). With permission.

methanol was added to the dry sample inside the quartz pyrolysis tube. This methylation procedure was especially useful in improving the chromatographic behavior of fatty acids present in the sample. Analytical results varied considerably among monuments, variously showing the presence of nitrogen compounds (pyridine, benzonitrile, cyanopyridine, dicyanobenzene), oxygenated compounds (phenol, benzoic acid, phthalic anhydride), fatty acids, and alkanes.

The ease with which the sample analysis could be accomplished allowed the collection of multiple samples from each monument. The comparison of results from protected portions of monuments to other areas more directly in contact with wind and rain allowed some interesting speculations about the weathering process.

7.5.3 DIGESTED AND UNDIGESTED POLLENS: DISCRIMINATION

BY PY-MS

The so-called yellow rain occurrences in Southeast Asia in the early 1980s led to this application of Py-MS. A high pollen count was reported for some of the yellow samples, and it was suggested that pollens might be used as a support or carrier for the distribution of chemical agents. As part of the investigations, it became important to be able to distinguish between pollen and bee feces (undigested and digested pollen, respectively). Because Py-MS had been used extensively for the characterization of biological and other polymeric materials and, combined with pattern recognition techniques, had been successful for providing compositional information for a number of different types of materials, a study was undertaken to evaluate whether Py-MS analysis coupled with pattern recognition data analysis procedures could distinguish between bee feces and pollen samples.⁶⁰

The U.S. Army Chemical Research and Development Center provided 11 Southeast Asian samples for this study as unknowns, that is, with no sample history or identification known to the analysts at the time of analysis. The analytical task was to determine whether these samples were pollen, bee feces, or some other unrelated material. For purposes of comparison, a set of known materials was constructed consisting of bee feces, pollens, beeswax, and honey — 20 samples of different origins obtained from various sources.

The samples were applied to Curie-point wires as methanol suspensions of about 10 mg/ml and pyrolyzed at 610°C with a rise time of 100 msec. The pyrolyzer was interfaced to a quadrupole mass spectrometer set to accumulate low-energy (15 eV) electron-impact ionization spectra across the scan range of 45 to 245 amu, with a scan speed of 1200 amu/sec. For the subsequent data analysis, 30 spectra were summed together to produce a Py-MS spectrum for each sample. The 31 samples were run three times, as three sets of 31, with each set arranged in random order before the beginning of analysis.

The four Py-MS spectra — for pollen, bee feces, and two of the unknowns — presented as a figure in this report (but not shown in this chapter) clearly showed distinct differences, but the authors found that the complexity present in the 93 spectra made visual classification of the samples impossible. A discussion of the data analysis techniques used for the classification of these samples is beyond the scope of this chapter, but a brief summary of the results can be made. (Those readers with interest in statistical methods for analysis of data generated by analytical pyrolysis-mass spectrometry should find this paper interesting and may also want to read more recent work in this area.^{61,62})

Unsupervised learning (that is, factor analysis and nonlinear mapping) showed that the Py-MS data contained enough distinguishing chemical information that digested and undigested pollens could be differentiated. Also, samples that were

quite different from pollen, such as waxes and honeys, were identified as nonpollen samples through unsupervised learning techniques. Discriminant analysis was the most successful supervised statistical procedure used. Employing blind digested and undigested pollen standards, a classification success rate of 95% was achieved. Of the 11 Southeast Asian samples submitted blind, the 4 of known composition were correctly classed as either digested or undigested pollen. Of the five yellow rain samples in the set, three were classified as digested pollens (bee feces) and two as undigested pollen.

7.5.4 SPRUCE NEEDLES: EXAMINATION BY PY-FIMS

Field ionization mass spectrometry (FIMS) was initially developed for molecular weight determinations and mixture analyses. This soft ionization technique is particularly well suited for the mass spectrometric examination of the extremely complex mixture of compounds resulting from the pyrolysis of macromolecules because predominantly characteristic, high-mass molecular ions are produced.⁶³

As part of a research project on forest damage, spruce needles were examined by pyrolysis-field ionization mass spectrometry (Py-FIMS) using high-resolution mass spectrometry, time-resolved high-resolution mass spectrometry, and Curie-point Py-GC/MS.⁶⁴ Subsequent chemometric analysis of the data using pattern recognition techniques led to the conclusion that, in the geographical region studied, the impact of acids and water stress was the major cause of the observed tree damage.¹ Presentation and discussion of the data obtained from the elegant analytical mass spectrometric techniques utilized for these studies are beyond the scope of this chapter. However, for those with access to the necessary instrumentation, Py-FIMS appears to offer unique insights into difficult environmental problems.

7.5.5 FOREST SOILS: EXAMINATION BY PY-MBMS

Impressed by the information provided by Py-FIMS, another research group developed pyrolysis-molecular beam mass spectrometry (Py-MBMS) by coupling a quartz pyrolysis chamber to the inlet of a triple-quadrupole mass spectrometer.⁶⁵ This group wished to study the organic matrix of forest soils and saw two limitations for the application of Py-FIMS to their study: first, that the very small sample used in Py-FIMS might not be representative of the macro soil sample, and second, that the time required for each sample analysis by Py-FIMS was relatively long if one wished to examine and compare a large number of soil samples.

In their Py-MBMS instrument, about 0.1 g of each soil sample was heated to 500°C in the pyrolysis chamber containing flowing helium gas, and the pyrolysis vapors passed into the ion source of the mass spectrometer (the sampling orifice of the MS was located inside the end of the pyrolysis chamber). Although details of the sample introduction process were sketchy, a typical profile of soil pyrolysis product evolution for eight samples run in a period of 14 min was shown.

As with the Py-FIMS technique, presentation and discussion of the data obtained by Py-MBMS is beyond the scope of this chapter, but the resulting pyrolysis mass spectra were very complex and information rich. With the use of chemometric

techniques, the data obtained from whole soil samples taken from four sites at three depths successfully characterized changes in the chemical composition of the soil organic matter.

7.5.6 ANALYSIS OF INTRACTABLE ENVIRONMENTAL CONTAMINATION

In the U.S., most of the field investigation, remediation, and monitoring of environmental chemical contamination utilizes specific analytical methodologies, primarily those set forth by the U.S. Environmental Protection Agency (USEPA). These methods are directed almost entirely to measuring the presence and amounts of the several hundred chemical elements and compounds on the various USEPA lists of chemicals of concern. Most of the methods for organic compounds involve a primary extraction followed by a concentration step, or dissolution followed by dilution, with subsequent separation of the organic mixtures by gas chromatography prior to measurement with any one of a variety of detectors.

These methods not only fail to identify or measure most synthetic polymer materials, but also are sometimes greatly hampered by the presence of these materials within the sample matrix. Probably every environmental laboratory has suffered from this problem, although it may have gone unrecognized. The experience of having a single sample suddenly “trash” an analytical system, rendering it incapable of meeting analytical quality assurance criteria without a major system overhaul, unfortunately, is not uncommon. Many of these occurrences are probably due to synthetic polymers that do not pass through the analytical system as the volatile and semivolatile analytes do, but rather “coat” the system and change its analytical performance characteristics.

Py-GC and Py-GC/MS could find useful places in the routine environmental analytical laboratory to help with the nonroutine samples. Abandoned drums of “goo” or the collected containers of household waste chemicals that no longer bear labels possibly could be handled with some sort of thermal vaporization/pyrolysis analytical scheme.

Using analytical pyrolysis for such samples would be just one component of a systems approach to multimedia analysis, a multifaceted approach to the examination of environmental samples centered upon the use of a purge-and-trap/head-space/pyrolysis/gas chromatography system utilizing multiple detection systems. Although the development of such an analytical scheme was under discussion more than 10 years ago,⁶⁶ no analytical method using Py-MS, Py-GC, or Py-GC/MS has yet been promulgated.

REFERENCES

1. N. Simmleit and H.-R. Schulten, *J. Anal. Appl. Pyrol.*, 15: 3 (1989).
2. R. Tsao and K.J. Voorhees, *Anal. Chem.*, 56: 368 (1984).
3. K.J. Voorhees and R. Tsao, *Anal. Chem.*, 57: 1630 (1985).
4. A. Alajbeg, *J. Anal. Appl. Pyrol.*, 12: 275 (1987).
5. T.P. Wampler, *J. Anal. Appl. Pyrol.*, 16: 291 (1989).

6. T.P. Wampler, *J. Chromatogr.*, 842: 207 (1999).
7. S.C. Moldovenau, *J. Microcolumn Sep.*, 13: 102 (2001).
8. A. Alajbeg, *J. Anal. Appl. Pyrol.*, 9: 255 (1986).
9. W. Klusmeier, P. Vogler, K.-H. Ohrback, H. Weber, and A. Kettrup, *J. Anal. Appl. Pyrol.*, 14: 25 (1988).
10. K.J. Voorhees, W.D. Schulz, L.A. Currie, and G.A. Klouda, *J. Anal. Appl. Pyrol.*, 14: 83 (1988).
11. A. Plewka, K. Müller, and H. Herrmann, *Proceedings from the EUOTRaC-2 Symposium 2000*, Springer-Verlag Berlin, Heidelberg 2000.
12. A.P. Snyder, A. Tripathi, W.M. Maswadeh, J. Ho, and M. Spence, *Field Anal. Chem. Technol.*, 5: 190 (2001).
13. K. Laniewski, H. Boren, A. Grimvall, and M. Ekelund, *J. Chromatogr. A*, 826: 201 (1998).
14. A. Yasuhara and M. Morita, *Environ. Sci. Technol.*, 22: 646 (1988).
15. A.B.J. Oudhuis, P. De Wit, P.J.J. Tromp, and J.A. Moulijn, *J. Anal. Appl. Pyrol.*, 20: 321 (1991).
16. R.C. Kistler, F. Widmer, and P.H. Brunner, *Environ. Sci. Technol.*, 21: 70 (1987).
17. J.A. Caballero, R. Front, A. Marcilla, and J.A. Canesa, *J. Anal. Appl. Pyrol.*, 40/41: 433 (1997).
18. K.H. Nelson, I. Lysyj, and J. Nagano, *Water Sewage Works*, 117: 14 (1970).
19. M.-F. Dignac, P. Ginestet, D. Rybacki, A. Bruchet, V. Urbain, and P. Scribe, *Water Res.*, 34: 4185 (2000).
20. W.M.G.M. van Loon, J.J. Boon, and B. de Groot, *J. Anal. Appl. Pyrol.*, 20: 275 (1991).
21. D. van de Meent, J.W. de Leeuw, and P.A. Schenck, *J. Anal. Appl. Pyrol.*, 2: 249 (1980).
22. W.M.G.M. van Loon and J.J. Boon, *Anal. Chem.*, 65: 1728 (1993).
23. E.R.E. van der Hage, M.M. Mulder, and J.J. Boon, *J. Anal. Appl. Pyrol.*, 25: 149 (1993).
24. M. Kleen and G. Lindblad, *J. Anal. Appl. Pyrol.*, 25: 209 (1993).
25. W.M.G.M. van Loon and J. J. Boon, *Trends Anal. Chem.*, 13: 169 (1994).
26. W.L. Budde, *Analytical Mass Spectrometry: Strategies for Environmental and Related Applications*, Oxford University Press, Oxford (2001).
27. L. Cotrim da Cunha, L. Serve, F. Gadel, and J.-L. Bazi, *Sci. Total Environ.*, 256: 191 (2000).
28. A.A. Christy, A. Bruchet, and D. Rybacki, *Environ. Int.*, 25: 181 (1999).
29. Y. Coban-Yildiz, D. Fabbri, D. Tartari, S. Tugrul, and A.F. Gaines, *Org. Geochem.*, 31: 1627 (2000).
30. J.D.H. van Heemst, L. Megens, P.G. Hatcher, and J.W. de Leeuw, *Org. Geochem.*, 31: 847 (2000).
31. H.-R. Schulten and G. Gleixner, *Water Res.*, 33: 2489 (1999).
32. A. Aouabed, R. Ben Aim, and D.E. Hadj-Boussaad, *Environ. Technol.*, 22: 597 (2001).
33. D.W. Page, J.A. van Leeuwen, K.M. Spark, and D.E. Mulcahy, *Mar. Freshwat. Res.*, 52: 223 (2001).
34. N. Paaso, J. Peuravuori, T. Lehtonen, and K. Pihlaja, *Environ. Int.*, 28: 173 (2002).
35. X.Q. Lu, N. Maie, J.V. Hanna, D.L. Childers, and R. Jaffe, *Water Res.*, 37: 2599 (2003).
36. D.M. White, D.S. Garland, J. Narr, and C.R. Woolard, *Water Res.*, 37: 939 (2003).
37. B. Little and J. Jacobus, *Org. Geochem.*, 8: 27 (1985).
38. K.J. Voorhees, J.C. Hickey, and R.W. Klusman, *Anal. Chem.*, 56: 2604 (1984).
39. J.K. Whelan, J.M. Hunt, and A.Y. Huc, *J. Anal. Appl. Pyrol.*, 2: 79 (1980).

40. J.K. Whelan, M.G. Fitzgerald, and M. Tarafa, *Environ. Sci. Technol.*, 17: 292 (1983).
41. K.D. McMurtry, N.J. Wildman, and H. Tai, *Bull. Environ. Contam. Toxicol.*, 31: 734 (1983).
42. J.W. de Leeuw, E.W.B. de Leer, J.S. Sinninghe Damsté, and P.J.W. Schuyf, *Anal. Chem.*, 58: 1852 (1986).
43. M.A. Kruger, P.K. Mukhopadhyay, and C.F.M. Lewis, *Org. Geochem.*, 29: 1797 (1998).
44. E.A. Guthrie, J.M. Bortiatynski, J.O.H. van Heemst, J.H. Richman, K.S. Hardy, E.M. Kovach, and P.G. Hatcher, *Environ. Sci. Technol.*, 33: 119 (1999).
45. D.M. White, H. Luong, and R.L. Irvine, *J. Cold Reg. Eng.*, 12: 1 (1998).
46. D. Fabbri, C. Trombini, and I. Vassura, *J. Chromatogr. Sci.*, 36: 600 (1998).
47. D.S. Garland, D.M. White, and C.R. Woolard, *J. Cold Reg. Eng.*, 14: 24 (2000).
48. D. Fabbri, *J. Anal. Appl. Pyrol.*, 58/59: 361 (2001).
49. B. Tienpont, F. David, F. Vanwalleghe, and P. Sandra, *J. Chromatogr. A*, 911: 235 (2001).
50. Y. Zegouagh, S. Derenne, C. Largeau, P. Bertrand, M.-A. Sicre, A. Saliot, and B. Rousseau, *Org. Geochem.*, 30: 101 (1999).
51. P. Faure, F. Vilmin, R. Michels, E. Jarde, L. Mansuy, M. Elie, and P. Landais, *J. Anal. Appl. Pyrol.*, 62: 297 (2002).
52. M.C. Kennicutt II, W.L. Keeney-Kennicutt, B.J. Bresley, and F. Fenner, *Environ. Geol.*, 4: 239 (1983).
53. G. Luniger and L. Schwark, *Sediment. Geol.*, 148: 275 (2002).
54. M. Yamamoto, H. Kayanne, and M. Yamamuro, *Geochem. J.*, 35: 385 (2001).
55. J.M. Challinor, *J. Anal. Appl. Pyrol.*, 16: 323 (1989).
56. A.P. Deshmukh, B. Chefetz, and P.G. Hatcher, *Chemosphere*, 45: 1007 (2001).
57. L. Mansuy, Y. Bourezgui, E. Garnier-Zarli, E. Jarde, and V. Reveille, *Org. Geochem.*, 32: 223 (2001).
58. C. Saiz-Jimenez, J. Garcia-Rowe, M.A. Garcia Del Cura, J.J. Ortega-Calvo, E. Roekens, and R. Van Grieken, *Sci. Total Environ.*, 94: 209 (1990).
59. G. Chiavari, A. Colucci, R. Mazzeo, and M. Ravanelli, *Chromatographia*, 49: 35 (1999).
60. S.J. DeLuca, K.J. Voorhees, and E.W. Sarver, *Anal. Chem.*, 58: 2439 (1986).
61. R.S. Sahota and S.L. Morgan, *Anal. Chem.*, 65: 70 (1993).
62. R. Goodacre, A.N. Edmonds, and D.B. Kell, *J. Anal. Appl. Pyrol.*, 26: 93 (1993).
63. H.-R. Schulten, N. Simmleit, and R. Müller, *Anal. Chem.*, 59: 2903 (1987).
64. H.-R. Schulten, N. Simmleit, and R. Müller, *Anal. Chem.*, 61: 221 (1989).
65. K.A. Magrini, R.J. Evans, C.M. Hoover, C.C. Elam, and M.F. Davis, *Environ. Pollut.*, 116: S255 (2002).
66. J.E. Bumgarner, personal communication, 1993.

8 Examination of Forensic Evidence

John M. Challinor

CONTENTS

8.1	Introduction	176
8.1.1	The Analysis Challenge	176
8.1.2	Types of Evidence.....	176
8.1.3	Development of Py-GC.....	176
8.1.4	Pyrolysis Derivatization: Modifications to the Pyrolysis Process.....	177
8.2	Paint.....	177
8.2.1	Automotive Paint.....	177
8.2.1.1	Repainted Vehicles.....	178
8.2.1.2	Alkyd-Based Enamels	179
8.2.2	Architectural Paint	180
8.2.3	Industrial Paints.....	182
8.3	Adhesives	183
8.3.1	Intraclass Differentiation.....	185
8.4	Rubbers.....	185
8.5	Plastics.....	185
8.6	Motor Vehicle Body Fillers	187
8.7	Fibers	188
8.8	Oils and Fats	189
8.9	Cosmetics	192
8.10	Natural Resins: Ancient and Modern Applications	193
8.11	Inks	196
8.12	Miscellaneous.....	197
8.13	Case Study.....	197
8.14	Conclusions	197
	References.....	198

8.1 INTRODUCTION

8.1.1 THE ANALYSIS CHALLENGE

The chemical characterization of forensic evidence from a crime scene or the criminal has some different requirements from that of many other types of chemical analysis. High sensitivity is important because the quantity of material for examination is often limited to minute traces found at the scene. The material under scrutiny must be characterized as comprehensively as possible to ensure maximum discrimination from other material in the same class. Forensic laboratories are multi-instrument facilities required to deal with many types of evidence found at a crime scene; therefore, the routine methods used should preferably employ relatively inexpensive instrumentation. In order to protect integrity, samples should be analyzed "as received" if possible and any workup minimized. The method should preferably not be labor intensive. Pyrolysis-gas chromatography (Py-GC) and pyrolysis-gas chromatography-mass spectrometry (Py-GC/MS) have proven to be an effective means of satisfying these requirements in many forensic science laboratories.¹⁻³

8.1.2 TYPES OF EVIDENCE

Py-GC/MS is an appropriate characterization technique for such crime scene material as paint from burglaries and hit-and-run traffic accidents or adhesives from insulation tapes and improvised explosive devices. Rubbers in auto tires and foams in carpets and clothing, fibers from garments, or plastics from household goods and auto parts are examples of commodities that may be identified and compared. Other applications are as diverse as the identification of blood stains,⁴ propellants in ammunition,⁵ human hair,⁶ or chewing gum.⁷ The numerous uses of analytical pyrolysis, including forensic applications, have been reviewed in a selected bibliography.⁸ The technique is essential for the effective operation of any crime laboratory required to examine these and other organic materials found as evidence.

8.1.3 DEVELOPMENT OF PY-GC

Py-GC was adopted by forensic scientists in the 1970s.⁹ Packed Carbowax phase GC columns were accepted as the standard in many forensic science laboratories.¹⁰ Reproducible pyrograms enabled a reliable database to be established. However, packed columns had a limited life span and were unsatisfactory for the chromatographic examination of very polar and higher molecular weight compounds. These compounds are often diagnostic for many polymers of forensic interest. However, as a comparative technique, Py-GC was excellent.^{2,11-13} The limitations of packed-column GC prompted the use of capillary GC columns, particularly high-resolution vitreous silica types. A simple system for interfacing a Curie-point pyrolyzer to a gas chromatograph equipped with a medium-polarity phase capillary column and forensic applications were reported, and comparison was made with the results obtained from a packed column.¹⁴ The pyrolysis capillary column GC has become the standard method adopted in most forensic science laboratories, and discussion of the applications in this chapter will be restricted to this technique.

8.1.4 PYROLYSIS DERIVATIZATION: MODIFICATIONS TO THE PYROLYSIS PROCESS

In order to obtain greater information about the composition of polymers and macromolecular material, modifications to the analytical pyrolysis process have been developed. These have included on-line pyrolysis hydrogenation of polyolefines using hydrogen carrier gas and a palladium catalyst.¹⁵ Polyacetals have been pyrolyzed in the presence of a cobalt catalyst to produce cyclized compounds that afford greater information about the structure of the polymer.¹⁶

Another relatively recent development in pyrolysis techniques developed by Challinor¹⁷ has involved high-temperature chemolysis and derivatization reactions that provide more information about the structure of polymers. In the pyrolysis derivatization process, a tetraalkyl ammonium hydroxide, in particular tetramethyl ammonium hydroxide (TMAH), when reacted at elevated temperatures with polymers having hydrolyzable groups, gives alkyl derivatives that reflect the composition of the polymer. Resins used in drying oil-modified alkyl enamels and saturated or unsaturated polyesters are particularly amenable to this procedure. The chromatographic profiles are generally simplified and are easier to interpret in terms of chemical composition. The precursors of the polymer or other resin components may be identified, providing data about the polymer that are often unattainable by conventional Py-GC. The reaction has been termed thermally assisted hydrolysis and methylation (THM), initially referred to as simultaneous pyrolysis methylation (SPM). The term *SPM* was abandoned, as it led to misunderstandings of the mechanism of the reaction.

The pyrolysis products in conventional Py-GC may sometimes be obscure, particularly in the pyrolysis of some step-growth polymers, and are not easy to interpret in terms of the polymer composition. However, THM results in the formation of products that clearly identify the composition of these polymers and adds another dimension to the analytical capability of the pyrolysis technique.

8.2 PAINT

Paint, because of its variability and complexity, can provide strong evidence in a forensic investigation.¹⁸ The resin/binder may vary widely within a class. There are, for example, numerous different monomers used in acrylic paint formulations, which are difficult to identify by other analytical techniques such as infrared spectroscopy. Py-GC/MS is an effective method for identifying and differentiating the organic binder of paint. In some cases, additives may be detected and identified. The Py-GC/MS identification of organic pigments in a resin matrix is a challenging prospect for the future.

The Py-GC examination of paint, in the context of an overall forensic analysis of this type of evidence, has been described.¹⁹

8.2.1 AUTOMOTIVE PAINT

Motor vehicle-related crime can include hit-and-run, willful damage, and homicide incidents. Automotive paint binder types can be identified on microgram-sized samples

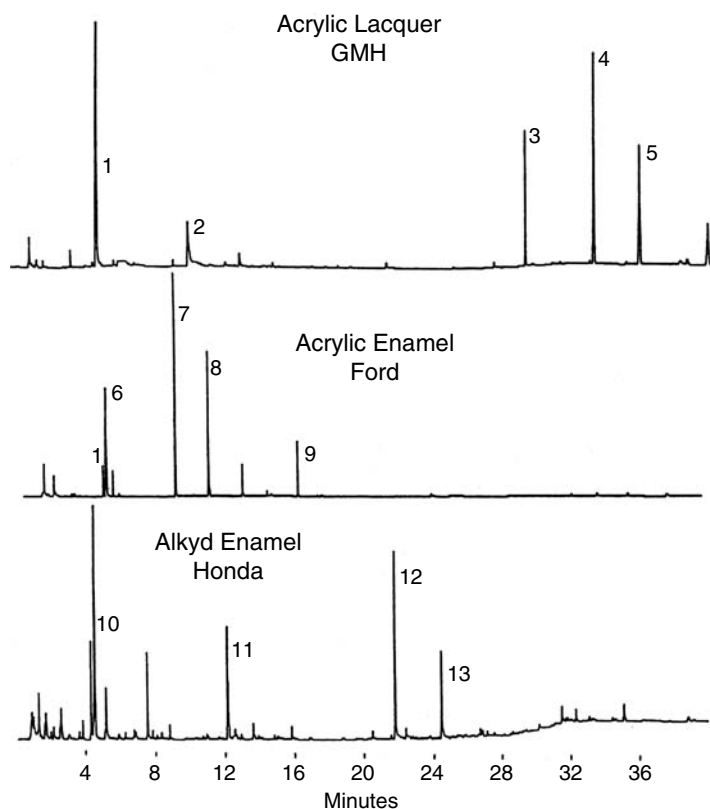


FIGURE 8.1 Pyrograms of an acrylic lacquer, acrylic enamel, and alkyd enamel used in some original automotive topcoat paint systems. 1 = methyl methacrylate, 2 = methacrylic acid, 3 = dibutyl phthalate, 4 = butyl cyclohexyl phthalate, 5 = butyl benzyl phthalate, 6 = butanol, 7 = styrene, 8 = butyl methacrylate, 9 = 2-ethylhexyl acrylate, 10 = isobutanol, 11 = vinyltoluene, 12 = phthalic anhydride, and 13 = phthalimide.

of topcoat.^{20–22} Some examples of typical pyrograms of acrylic lacquer, acrylic enamel, and alkyd enamel types found in original paint systems are shown in Figure 8.1.

The variability in the pyrolysis profiles of the different classes of coatings is self-evident. The interpretation of the composition revealed is as follows: The acrylic lacquer (General Motors) is a methyl methacrylate/methacrylic acid copolymer plasticized with dibutyl-, butyl cyclohexyl-, and butyl benzyl phthalates. The acrylic enamel (Ford) is a styrene/ethylhexyl acrylate/methyl methacrylate terpolymer. The alkyd enamel (Honda) pyrolysis profile indicates that the paint resin is an orthophthalic alkyd containing a butylated-amino resin cross-linking component.

8.2.1.1 Repainted Vehicles

Acrylic lacquer paints are frequently used for refinishing vehicles after accident damage. The formulations are often based on methyl methacrylate monomer and

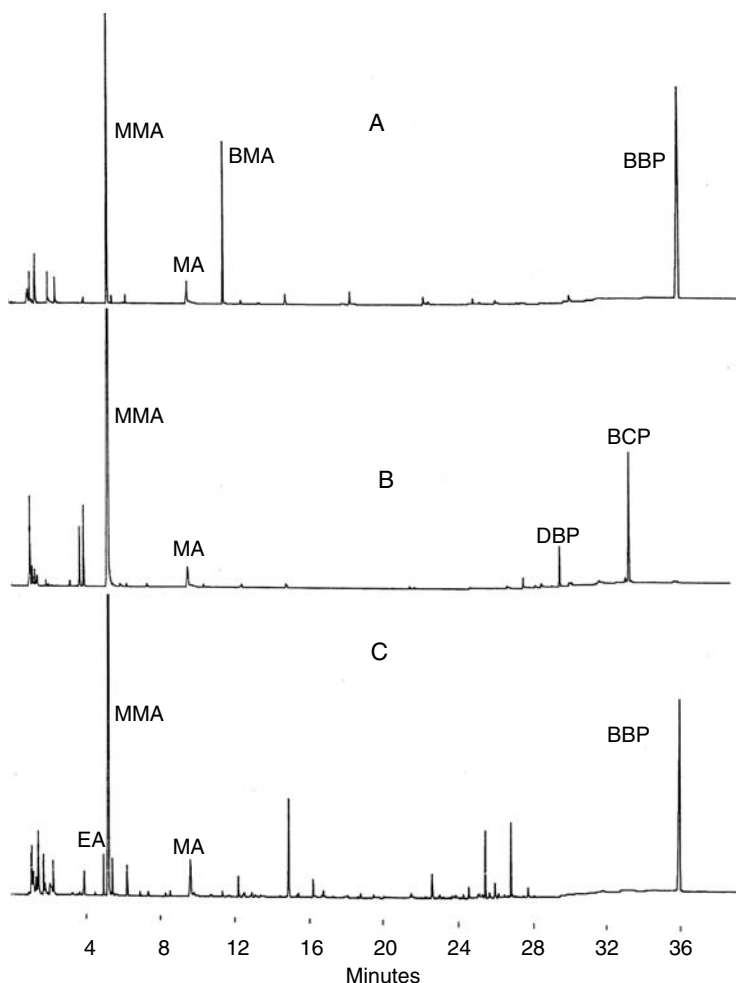


FIGURE 8.2 Pyrograms of three refinishing acrylic lacquers of different composition. (A) Methyl methacrylate (MMA)-butyl methacrylate (BMA)-methacrylic acid (MA) terpolymer plasticized with butyl benzyl phthalate (BBP). (B) MMA-MA copolymer plasticized with a mixture of dibutyl phthalate (DBP) and butyl cyclohexyl phthalate (BCP). (C) MMA-EA (ethyl acrylate) long-chain methacrylate type polymer plasticized with BBP.

are plasticized by the incorporation of monomers that produce “softer” polymers such as butyl methacrylate or external plasticizers such as the phthalates. The pyrograms of three different refinishing acrylic lacquers are shown in Figure 8.2.

8.2.1.2 Alkyd-Based Enamels

Alkyd enamels occurring as original baked enamels or spraying enamels may be identified by the THM pyrolysis derivatization modification of the Py-GC technique.²³ These alkyd polyesters are converted to methyl derivatives of their polyol,

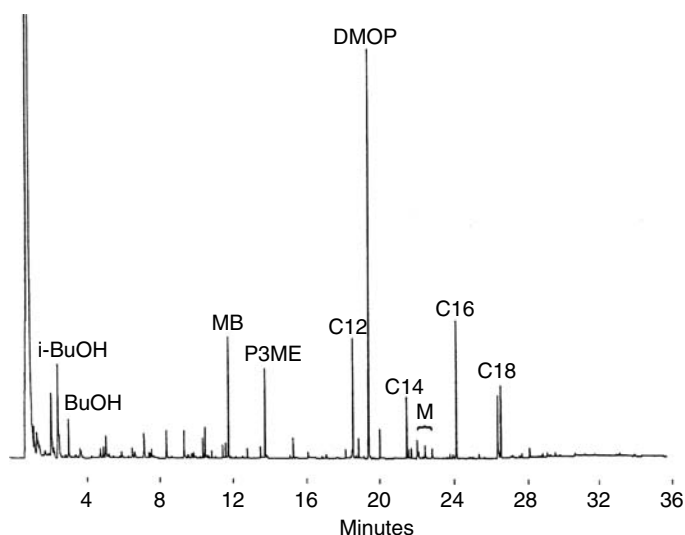


FIGURE 8.3 THM chromatogram of the baked alkyd enamel paint smear. i-BuOH = isobutanol, BuOH = butanol, MB = methyl benzoate, P3ME = pentaerythritol trimethyl ether, DMOP = dimethyl orthophthalate, M = triazines from melamine, C₁₂, C₁₄, C₁₆, and C₁₈ = respective fatty acid methyl esters.

polybasic acid, and drying oil. More chemical structure information can be gained from the THM-GC analysis of alkyd resins than from conventional Py-GC. For example, Figure 8.3 shows the THM chromatogram of a blue paint smear found on a crowbar that had been allegedly used to damage a blue automobile. The paint is a baked alkyd enamel.

From the THM chromatogram it is evident that the paint is a pentaerythritol-orthophthalic acid baked alkyd enamel having a coconut nondrying oil cross-linked with a butylated melamine formaldehyde resin.

8.2.2 ARCHITECTURAL PAINT

Break-in tools used to gain access to premises may well carry traces of paint that have abraded from painted surfaces at the point of entry. Commonly encountered household paint types include polyvinyl acetate (PVA), acrylics, alkyd enamels, epoxies, and chlorinated rubbers. Py-GC can distinguish between these different classes (Figure 8.4).

Furthermore, their polymer class and composition may be determined. The PVA type has a vinyl acetate/2-ethylhexyl acrylate copolymer binder. The acrylic is a methyl methacrylate/butyl acrylate copolymer. The alkyd enamel is an orthophthalic alkyd type, and the epoxy is a bisphenol A type.

In some cases, paint additives may be identified. The presence of a latex coalescing agent, trimethyl pentanediol mono-isobutyrate (Texanol), may also be detected (peak 5).

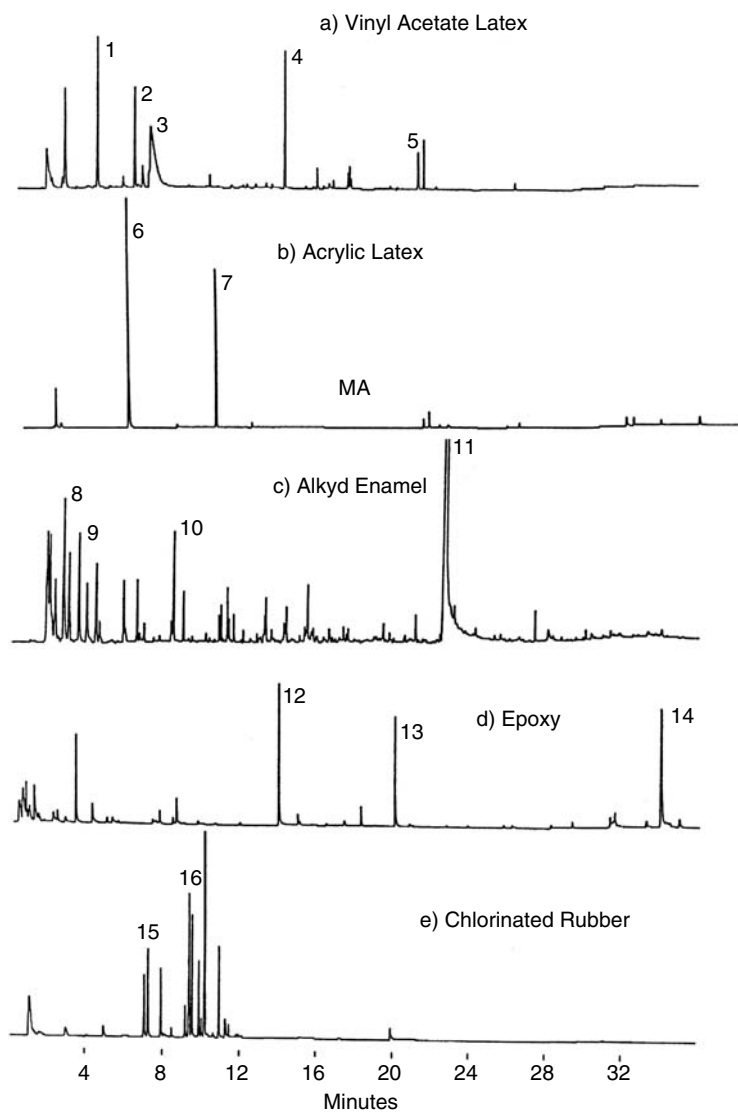


FIGURE 8.4 Pyrograms of vinyl acetate, acrylic, alkyd enamel, epoxy, and chlorinated rubber type architectural paints. 1 = benzene, 2 = isooctene, 3 = acetic acid, 4 = 2-ethylhexyl acrylate, 5 = 2,2,4-trimethyl 1,3-pentanediol mono-isobutyrate, 6 = methyl methacrylate, 7 = butyl methacrylate, 8 = acrolein, 9 = methacrolein, 10 = hexanal, 11 = phthalic anhydride, 12 = phenol, 13 = isopropenylphenol, 14 = bisphenol A, 15 = xylenes, 16 = trimethylbenzenes.

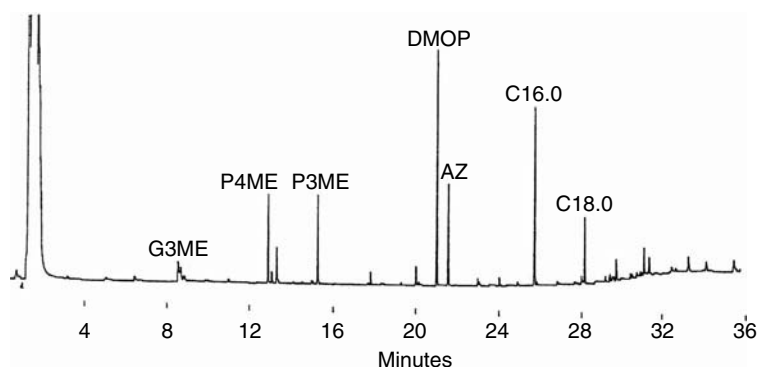


FIGURE 8.5 THM chromatogram of an architectural alkyd enamel. G3ME = glycerol trimethyl ether, P4ME = pentaerythritol tetramethyl ether, P3ME = pentaerythritol trimethyl ether, DMOP = dimethyl orthophthalate, AZ = methyl azelate, C_{16.0} = methyl palmitate, C_{18.0} = methyl stearate.

Studies on the differentiation between alkyd enamels by conventional Py-GC have been carried out.^{24,25} As discussed previously, more structural information about alkyd enamels may be obtained by the THM technique.²³ Polybasic acid, polyhydric alcohol, drying oil composition, oil length, degree of cure, and any rosin modification can be determined. The discrimination between alkyd enamels is therefore improved. For example, the alkyd enamel whose pyrogram is shown in Figure 8.4 gives the THM profile shown in Figure 8.5.

In this case, the paint can be identified as a pentaerythritol o-phthalic alkyd consistent with having a high proportion of a soya bean drying oil (from the C_{16.0}:C_{18.0} ratio). The total absence of unsaturated C₁₈ acid methyl esters and significant azelaic acid indicates that the paint has a high degree of cure. No rosin or other modification is detected.

8.2.3 INDUSTRIAL PAINTS

Industrial coatings are generally used on goods manufactured on a factory production line. They include domestic appliances, furniture, tools, and products derived from sheet metal. Their organic binders are either heat cured, air dried, catalyzed air dried, or radiation cured. Heat-cured coatings or baking or stoving enamels are the most commonly found industrial coatings. These binders can be alkyd enamels, thermosetting acrylics, polyesters, epoxies, silicone acrylics, vinyls, and heat-resistant polyimides and fluorocarbons. The air-dried coatings include acrylic, vinyl and nitrocellulose lacquers, alkyd resins, urethanes, and latex types. Polyurethanes and epoxy resins are examples of catalyzed air-dried binders.

Circumstances where these coatings occur as evidence involve items such as crowbars, tire levers, baseball bats, domestic appliances, and furniture.

Typical examples of Py-GC characterization of two of the wide variety of these coatings using THM are shown in Figure 8.6.

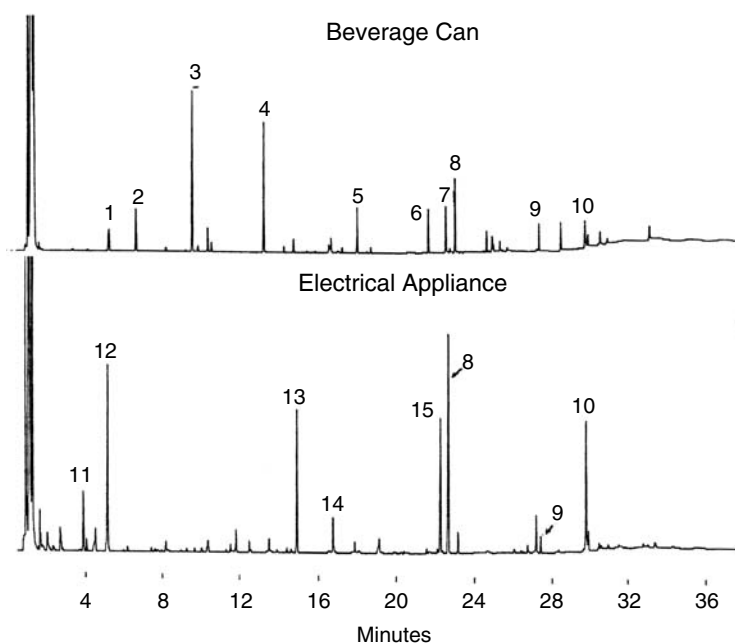


FIGURE 8.6 THM chromatograms of two industrial finishes from a beverage can and an electrical appliance. 1 = methyl methacrylate, 2 = neopentylglycol dimethyl ether, 3 = neopentylglycol monomethyl ether, 4 = ethylhexyl alcohol, 5 = dimethyl adipate, 6 = methyl laurate, 7 = dimethyl orthophthalate, 8 = dimethyl isophthalate, 9 = methyl palmitate, 10 = methyl stearate, 11 = isobutanol, 12 = n-butanol, 13 = methyl benzoate, 14 = pentaerythritol trimethyl ether, 15 = N-methyl phthalimide.

It can be concluded that the beverage can coating is a methyl methacrylate/ethylhexyl acrylate copolymer modified polyester. The polyester is an adipic acid-modified neopentyl glycol iso-/orthophthalic acid type. The electrical appliance coating is a butylated amino resin cross-linked pentaerythritol-orthophthalic thermosetting alkyd enamel.

Conventional Py-GC of these coatings gives either a misleading diagnosis or data from which it is impossible to obtain useful structural information. THM provides more useful data about their composition.²⁶

Other applications of Py-GC to synthetic resins include the identification of photocopy toners and surface coatings on currency notes.

8.3 ADHESIVES

There is a wide diversity of commercial adhesives available to the retail trade and for industrial applications.²⁷ Synthetic adhesives have tended to replace animal- and vegetable-based glues, such as casein and starch types.

Forensic case situations involving adhesives are abundant and various. The identification of adhesive components in improvised explosive devices has been

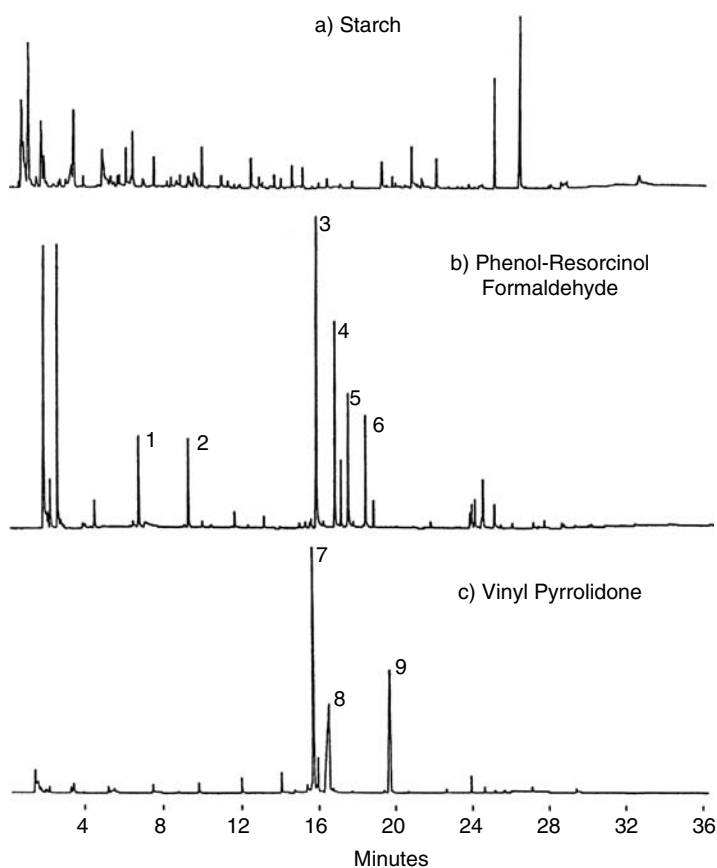


FIGURE 8.7 Pyrograms of (a) starch-based, (b) phenol-resorcinol formaldehyde, and (c) vinylpyrrolidone type adhesives. 1 = toluene, 2 = xylene, 3 = phenol, 4 = ortho-cresol, 5 = para-cresol, 6 = xylenol, 7 = vinyl pyrrolidone, 8 = pyrrolidone, 9 = caprolactam.

reported.²⁸ Fraudulently resealed packages and mail may be examined for the presence of foreign adhesive used for resealing purposes. Adhesives and sealers are becoming more frequently used in automotive construction and could hence occur in traffic-related crime. Hot-melt adhesives are now common in the sealing of various types of packaging. Pyrolysis mass spectrometry has also been used for the identification of adhesives.²⁹

The pyrograms of some typical adhesives obtained by Curie-point pyrolysis using a medium-polarity phase vitreous silica column are shown in Figure 8.7.

The major diagnostic pyrolysis products found in common adhesives are tabulated as follows:

Adhesive Resin	Diagnostic Pyrolysis Products
Vinyl acetate	Acetic acid

Adhesive Resin	Diagnostic Pyrolysis Products
Acrylic	Ethyl acrylate, methyl methacrylate, butyl acrylate, 2-ethylhexyl acrylate, 2-ethylhexyl alcohol, isooctene
Epoxy	Phenol, isopropenyl phenol, bisphenol A
Polyindene	Indene, vinyl toluene
Polyisoprene	Dipentene, isoprene, dimethylvinylcyclohexene
Neoprene-Novolac	Chloroprene oligomers, substituted phenols
Phenol formaldehyde	Phenols, cresols, dimethyl phenols
Silicone	Methyl-substituted cyclic siloxanes
Starch	Furans, levoglucosan
Vinylpyrrolidone	Vinylpyrrolidone, caprolactam

8.3.1 INTRAClass DIFFERENTIATION

Within-class discrimination is an important factor in the forensic examination of materials, and Py-GC is an appropriate technique to distinguish closely related polymers. Vinyl acetate polymers, for example, may be plasticized internally or externally. Copolymers include ethylhexyl acrylate, while phthalate plasticizers, such as dibutyl or di-isooctyl phthalate, may be used as external plasticizers in commercial products.

8.4 RUBBERS

Rubbers have physical characteristics and a chemical composition that precludes their successful identification by infrared spectroscopy due to their inherent elasticity and highly filled composition. In contrast, no such difficulties are encountered with Py-GC. Crime scene rubber evidence from automotive tires and rubber vehicle components is found in hit-and-run cases and in soles of shoes worn by offenders in offenses against property. Discrimination of vehicle bumper rubbers by Py-GC has been reported.³⁰ Volatile and polymeric components of rubbers and other polymers have been analyzed by Py-GC and the inorganic residue recovered for subsequent analysis.³¹ The technique may also be used to quantitate rubber blends by measuring the ratios of characteristic pyrolysis products. Figure 8.8 shows examples of the pyrograms of three common types of rubber.

Peak ratios of 2 (from butadiene) and 3 and 4 (from polyisoprene) reflect the relative proportions of butadiene, styrene, and isoprene in the rubber blend.

8.5 PLASTICS

Motor vehicles, fire scene debris, and household utensils from crime scenes are materials that may contain plastics. Their identification and comparison are often necessary to further the criminal investigation. A wide range of thermoplastic and thermosetting plastics may be encountered as crime scene evidence. These include polyolefines, polyacrylates, polyamides, polyesters, epoxies, and vinyl polymers. Pyrograms of some of these types are shown in Figure 8.9.

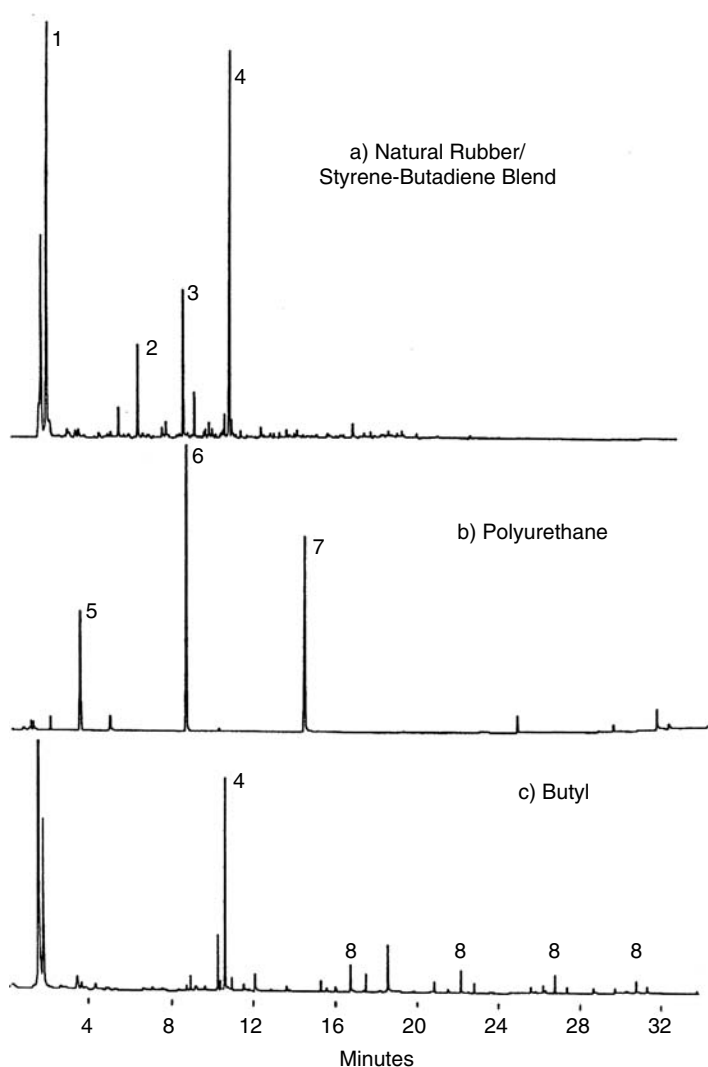


FIGURE 8.8 Pyrograms of (a) natural rubber/styrene butadiene blend, (b) polyurethane, and (c) butyl rubbers. 1 = isoprene, 2 = vinylcyclohexene, 3 = styrene, 4 = dipentene, 5 = tetrahydrofuran, 6 = cyclopentanone, 7 = butanediol, 8 = isobutene oligomers.

The pyrogram of polyethylene was obtained on a nonpolar methyl silicone phase capillary column.

Additional structural information can also be derived by Py-GC. Information on stereoisomerism, crystallinity, and sequence distribution data is sometimes able to be obtained. Isotactic and syndiotactic polypropylene may be identified by the ratio of oligomeric components.³² High- and low-density polyethylene can also be determined by the proportion of branch chain alkane pyrolysis products¹⁵ using a novel pyrolysis hydrogenation technique.

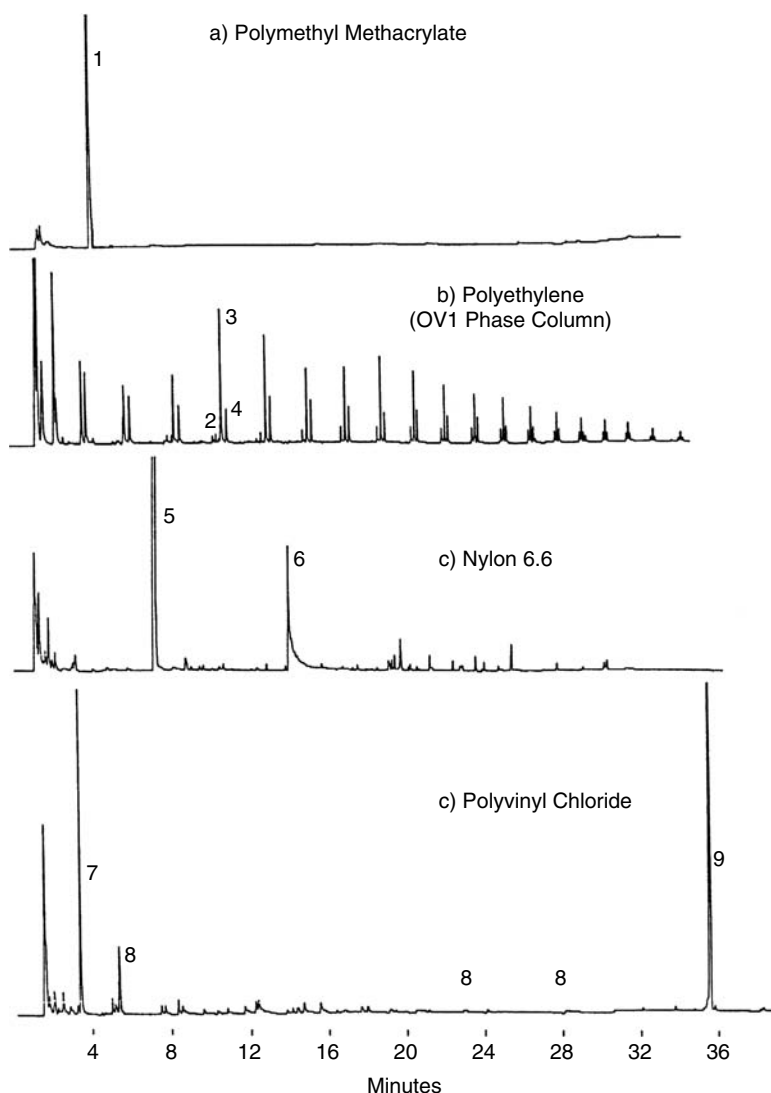


FIGURE 8.9 Pyrograms of (a) polymethyl methacrylate, (b) polyethylene, (c) nylon 6.6, and (d) polyvinyl chloride. 1 = methyl methacrylate, 2 = *a,w*-decadiene, 3 = 1-decene, 4 = decane, 5 = cyclopentanone, 6 = hexamethylene diamine, 7 = benzene, 8 = toluene, 9 = butyl benzyl phthalate.

8.6 MOTOR VEHICLE BODY FILLERS

Body fillers from repainted vehicles in traffic accidents may be left at the crime scene. Identification and subsequent comparison to material from the vehicle of the offender may be required to establish that the vehicle was at the accident scene. Auto body fillers are usually a mixture of easily sanded inorganic fillers and sty-

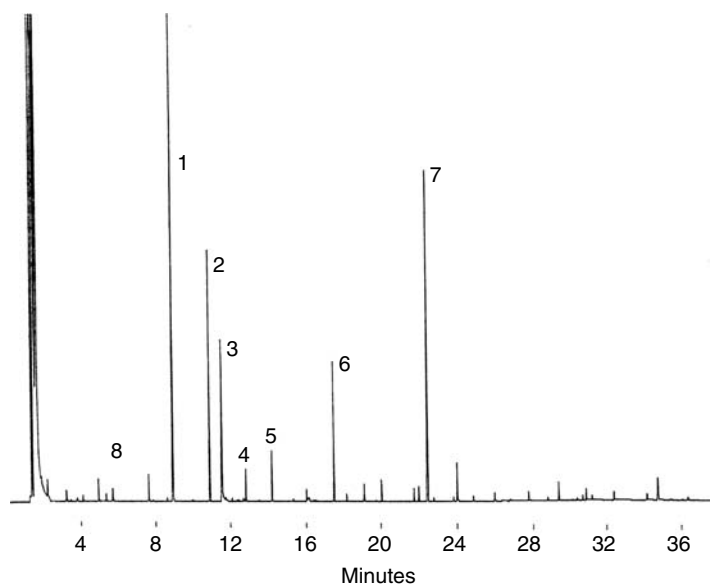


FIGURE 8.10 THM chromatogram of an automotive body filler. 1 = styrene, 2 = diethylene glycol dimethyl ether, 3 = diethylene monomethyl ether, 4 = dimethyl adipate, 5 = methyl benzoate, 6 = dimethyl adipate, 7 = dimethyl isophthalate.

renated unsaturated polyester resins. The composition of the resins may vary according to the application, resin supplier, and relative cost of raw materials at the time of manufacture. The resins may vary in polyol, polybasic acid, or additive composition. The THM-GC procedure provides the most diagnostic information about the structure of the resin. A pyrogram of a typical body filler is shown in Figure 8.10.

From these data it is apparent that the resin in the body filler is a styrenated diethylene glycol-isophthalic acid polyester cross-linked with maleic anhydride/fumaric acid and modified with adipic acid to give the resin flexibility.

It might be expected that it would be possible to determine the degree of cure by monitoring the concentration of residual maleic anhydride/fumaric acid, detected as dimethyl maleate in the THM procedure.

In a survey of body fillers³³ it was found that the resin composition varies between products in the proportion of styrene, the phthalic acid isomer, and the presence of adipic acid. Most resins contained diethylene glycol and in some cases propylene glycol.

8.7 FIBERS

Textile fibers can provide strong evidence in criminal activity because of the wide variety in color, dye, and organic structure found in their composition. Fibers may be transferred between garments in person-to-person contact during assaults, transferred to vehicles in hit-and-run traffic incidents, and encountered as ropes or twine in cases of kidnapping or deprivation of liberty.

The forensic examination of natural and synthetic fibers employs optical and scanning electron microscopy for characterizing color, morphology, surface features, and elemental composition. The organic composition of fibers can be determined by Fourier-transform infrared spectroscopy and Py-GC. A single fiber is often sufficient to obtain an identification of the polymer class by both techniques. The Py-GC technique has been criticized for lack of sensitivity. However, with contemporary pyrolyzers and efficient gas chromatographic systems, it is often possible to identify submicrogram quantities of fibers by this method. Using THM and selected ion monitoring-mass spectrometry techniques, it is possible to lower the limit of detection by an order of magnitude.

The application of Py-GC to the forensic examination of textile fibers has been reviewed.³⁴ Examples of the selectivity of Py-GC to several fiber types were described. The limitations in sensitivity of the technique and the action to be taken to alleviate this restriction and possible solutions were outlined.

Py-GC can therefore be used as an effective means of determining the chemical composition of man-made homopolymer and copolymer fibers, natural fibers, fiber blends, or partly degraded fibers. Pyrograms of polyester, acrylic, and cotton fibers show how these fibers can readily be identified (Figure 8.11).

Polyester fibers are composed of linear chains of polyethylene terephthalate (PET), which produces benzene, benzoic acid, biphenyl, and vinyl terephthalate on pyrolysis. Acrylic fibers comprise chains made up of acrylonitrile units, usually copolymerized with less than 15% by weight of other monomers, e.g., methyl acrylate, methyl methacrylate, or vinylpyrrolidone. Thermolysis results in the formation of acrylonitrile monomer, dimers, and trimers with a small amount of the copolymer or its pyrolysis product. In this case, the acrylic is Orlon 28, which contains methyl vinyl pyridine as comonomer. Residual dimethyl formamide solvent from the manufacturing process is also found in the pyrolysis products. Cotton, which is almost pure cellulose, comprises chains of glucose units. The pyrolysis products of cellulose, identified by GC/MS, include carbonyl compounds, acids, methyl esters, furans, pyrans, anhydrosugars, and hydrocarbons. The major pyrolysis products are levoglucosan (1,6-anhydro-B-D-glucopyranose) and substituted furans.

Further, Py-GC examination of synthetic polymer fibers can often provide more data than other techniques in cases where there are minor differences in composition within a class. In contrast, fibers that are chemically very similar are difficult to differentiate by IR and Py-GC. Cotton and viscose rayon, polyesters based on PET and wool and regenerated protein, are examples of the use of these methods.

The pyrolysis derivatization approach may also be used. THM results in the formation of dimethyl terephthalate when PET fibers are subjected to the procedure. Tetrabutyl ammonium hydroxide may be used to replace TMAH in the reaction to confirm the presence of vinyl acetate in acrylonitrile-vinyl acetate copolymer acrylic fibers. The derivatized product is butyl acetate.¹⁷

8.8 OILS AND FATS

Vegetable oils and animal fats are found alone or combined with other ingredients in many proprietary products. They are usually identified and compared as their fatty

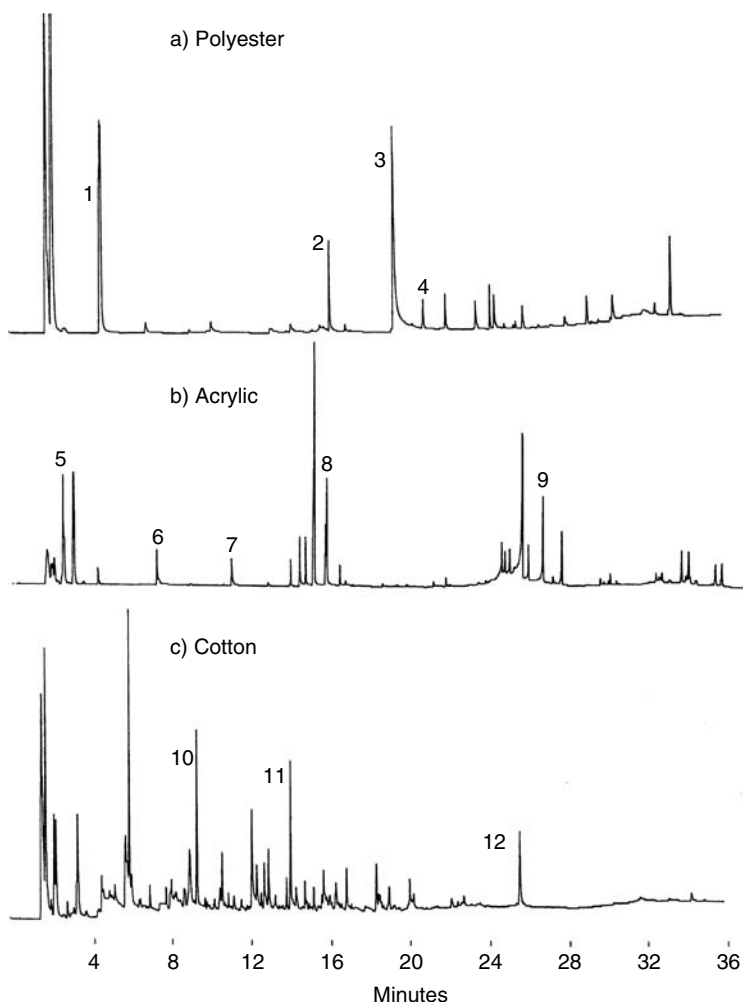


FIGURE 8.11 Pyrograms of (a) polyester, (b) acrylic, and (c) cotton fibers. 1 = benzene, 2 = vinyl benzoate, 3 = benzoic acid, 4 = biphenyl, 5 = acrylonitrile, 6 = dimethyl formamide, 7 = methyl vinyl pyridine, 8 = acrylonitrile dimers, 9 = acrylonitrile trimers, 10 = 2-furaldehyde, 11 = dihydromethylfuranone, 12 = levoglucopyranose.

acid derivatives or their triglycerides. The well-established methods usually depend on GC as a means of identification. THM procedures developed more recently²⁶ provide a related method for characterizing these materials. Microgram quantities of the triglycerides are reacted with tetramethyl ammonium hydroxide (TMAH) at high temperature to yield fatty acid methyl esters without the need to employ multistep procedures. The method has proved to be reliable, reproducible, and particularly suitable for forensic samples.

Vegetable oils can be considered to belong to classes that include oleic-, linoleic-, linolenic-, and ricinoleic-rich types. Examples of THM-GC of these types indicate

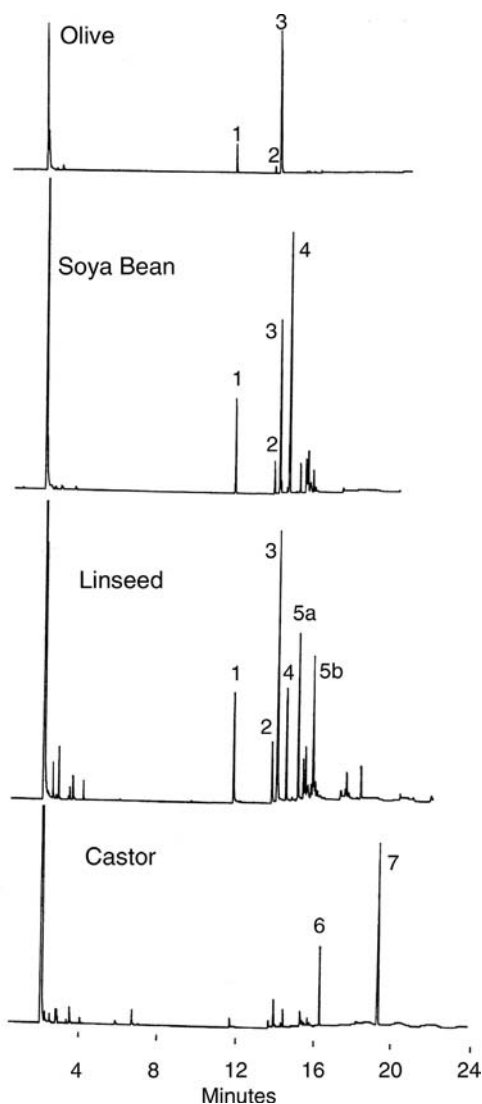


FIGURE 8.12 THM-GC profiles of olive oil (oleic rich), soya bean oil (linoleic rich), linseed oil (linolenic rich), and castor oil (ricinoleic rich) using a cyanopropyl (50%)-methyl silicone phase capillary column.

the degree of discrimination that can be achieved on submicrogram quantities without prior sample preparation (Figure 8.12). A high-polarity capillary column and 100°C oven starting temperature were used for the GC separations.

Olive oil and other oleic-rich oils are recognized by their relatively high content of oleic acid, detected as its fatty acid methyl ester (FAME) (peak 3). Palmitic and stearic acid FAMES (peaks 1 and 2) are also detected. Soya bean oil and similarly safflower, sunflower, and dehydrated castor oils contain approximately 60% linoleic

acid, detected as the FAME (peak 4). Linseed oil is characterized by its high linolenic FAME (peak 5) concentration. Some thermal isomerization of the polyunsaturated fatty acids takes place when TMAH is employed for the THM procedure. These artifacts are not produced when TMAH is replaced by the commercially available reagents MethPrep 1 and MethPrep 2, which are trifluoromethylphenyl trimethyl ammonium hydroxide solution in water and methanol. Castor oil, which contains a high proportion of ricinoleic acid (9-hydroxy octadecenoic acid) in triglyceride form, may be identified by the presence of its free hydroxy FAME (peak 7) or as the methoxy derivative (peak 6), in which both the hydroxy and the carboxylic acid groups are methylated. While these examples are not intended to give a comprehensive description of the determination of fatty acids in vegetable oils, they do indicate the degree of differentiation that it is possible to obtain by the technique.

8.9 COSMETICS

Traces of cosmetics such as lipstick smears, face creams, and body lotions can provide valuable evidence to link an offender to a victim at the scene of a crime.

Lipstick bases comprise a blend of waxes, oils, and emollients. While the dyes and pigments present may be identified by techniques such as thin-layer and high-performance liquid chromatography and electron microscopy, Py-GC techniques may be used to characterize the lipstick bases.³⁵ THM-GC is useful for the identification of triglycerides and polyols formulated into the product. Fatty acids in the triglycerides are converted to methyl esters, while aliphatic alcohols are converted to their methyl ethers. The triglyceride of ricinoleic acid is the major component of castor oil, the most common medium found in lipstick bases. Saponification and derivatization of the triglyceride by the THM process are necessary to facilitate its identification. Using the pyrolysis apparatus to volatilize the organic components of the cosmetic product into the Py-GC facilitates the identification of mineral oils, aliphatic alcohols, and simple fatty acid esters used as emollients. Figure 8.13 shows the Py-GC and THM-GC profiles of a typical lipstick base.

Volatilization of the lipstick using the Py-GC process indicates the presence of cetyl acetate (CA) and isopropyl myristate (IPM). Heptanal (C-7AL), a pyrolysis product of castor oil, is a major product. The THM profile in this case is more complex and gives more information about the composition of the product. Cetyl acetate is converted to the methyl ether of cetyl alcohol (C-16-OME), while IPM is partly converted to the methyl ester. The major components, RIC-OME and RIC, are identified as the methyl ether of ricinoleic acid methyl ester and ricinoleic acid methyl ester having a free OH group, respectively. These compounds result from hydrolysis and complete or partial methylation of the major component of castor oil. C8.0 and C10.0 are fatty acid methyl esters that indicate the presence of coconut oil in the formulation. This product was differentiated from more than 60 lipsticks examined in the study, on the basis of the composition of the organic components.

Body lotions usually comprise oil/water emulsions that may contain long-chain fatty alcohols, glycerol, long-chain fatty acids, vegetable oils, mineral oils, and emollients. Approximately 50 body lotions have been characterized by these techniques,³⁵ and it has been possible to differentiate all of these products. Figure 8.14

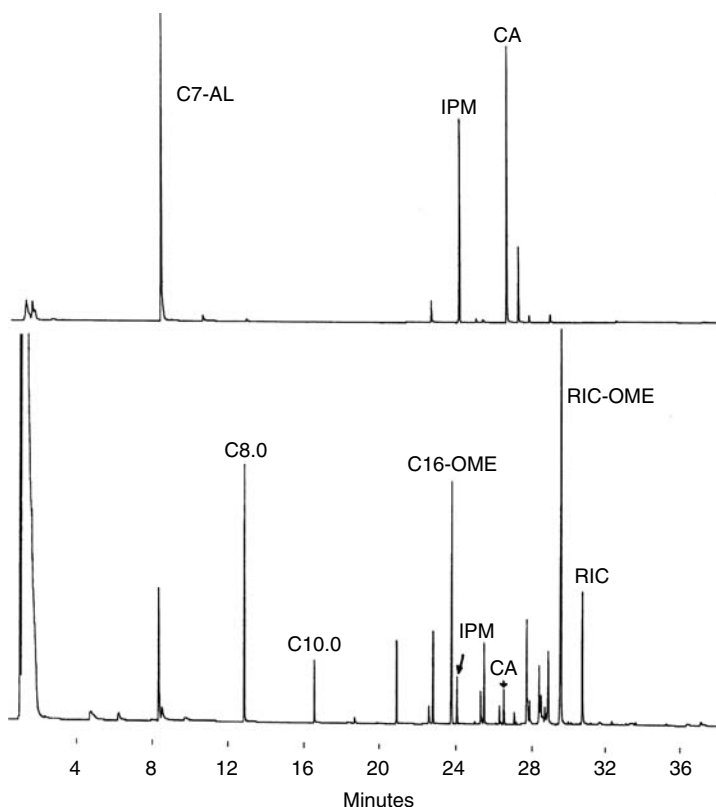


FIGURE 8.13 Py-GC (upper) and THM-GC (lower) profiles of a lipstick base.

shows a THM-GC profile of a body lotion, identified from traces that were found at a crime scene.

The fatty acid methyl esters C16.0, C18.0, and C18.2 indicate the presence of a vegetable oil. However, the detection of isopropyl palmitate (IPP) and isopropyl stearate (IPS) in the Py-GC experiment (not shown) means that there would also be a contribution of their fatty acids to this pyrogram. The methyl ethers of cetyl alcohol (C16-OME) and stearyl alcohol (C18-OME) suggest the presence of the respective free fatty alcohols, and this is confirmed by an inspection of the pyrogram from the Py-GC experiment (not shown). Myristyl alcohol methyl ether (C14-OME) and myristic acid methyl ester (C14.0) originate from myristyl myristate used in the formulation.

8.10 NATURAL RESINS: ANCIENT AND MODERN APPLICATIONS

To establish authenticity of oil paintings and works of art, an examination of the surface-coating resin and pigment may be required. In older objects, resins may be oleoresins, wood rosin, amber, dammar, shellac, oriental lacquers, or other natural resins.

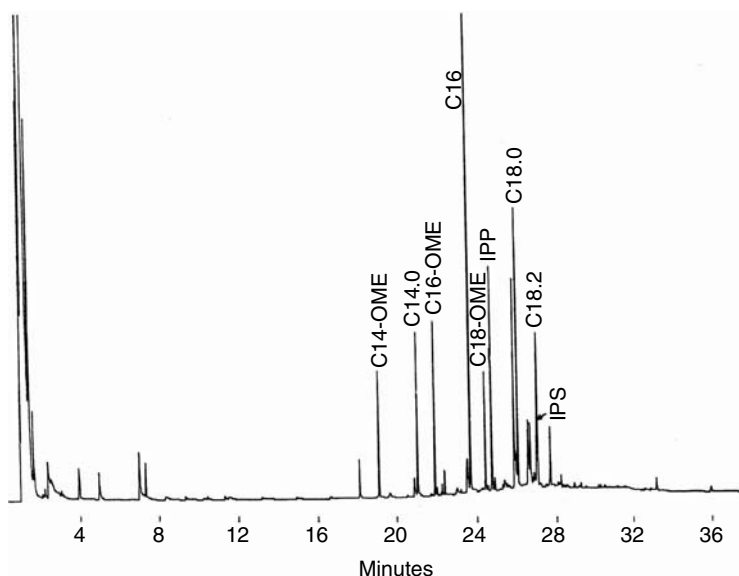


FIGURE 8.14 THM-GC profile of a body lotion.

Oleoresinous varnishes contain vegetable drying oils such as linseed and tung oils. Wood rosin comprises a mixture of rosin acids. Shellac is the flaked form of purified lac, the natural secretion of the insect *laccifer lacca kerr*. It contains 46% aleuritic acid, a trihydroxy-substituted hexadecanoic acid, and 27% shelloic acid, a dihydroxy polyacyclic aliphatic dicarboxylic acid, together with other components, many of which are undetermined. The main components of oriental lacquer are urushiol, laccol, and thitsiol, which are C_{15} - and C_{17} -alkyl and alkenyl-substituted benzene-1,2 diol compounds. Printing inks on questioned document letterheads may also contain natural resins in combination with contemporary synthetic modifiers, including phenol-formaldehyde resins.

Considering the polar nature of these constituents, it is not surprising that THM-GC would be an appropriate technique to characterize these resins.^{35,36} THM-GC pyrolysis profiles of shellac, a Burmese lacquer, and a printing ink resin are shown in Figure 8.15.

Shellac displays a THM profile distinctly different from the Py-GC pyrogram (not shown), indicating a largely hydrolyzable component in the resin. There is some evidence of C_{14} -, C_{16} -, and C_{18} -FAMES (peaks 1 to 2), 6-hydroxy C_{18} -FAME (peak 3), an oxirane group containing FAME (peak 4), and a polymethoxy-substituted C_{18} -FAME (peak 5) in the products.

THM-GC analysis of the cured Burmese lacquer results in a series of straight-chain and branched-chain alkyl benzenes ranging from toluene to dodecyl benzene, and C_6 - to C_{17} -alkanes and alkenes. These products are similar in composition to the products obtained by conventional pyrolysis. Compounds corresponding to peaks marked with an asterisk are FAMES that are products of the THM reaction and

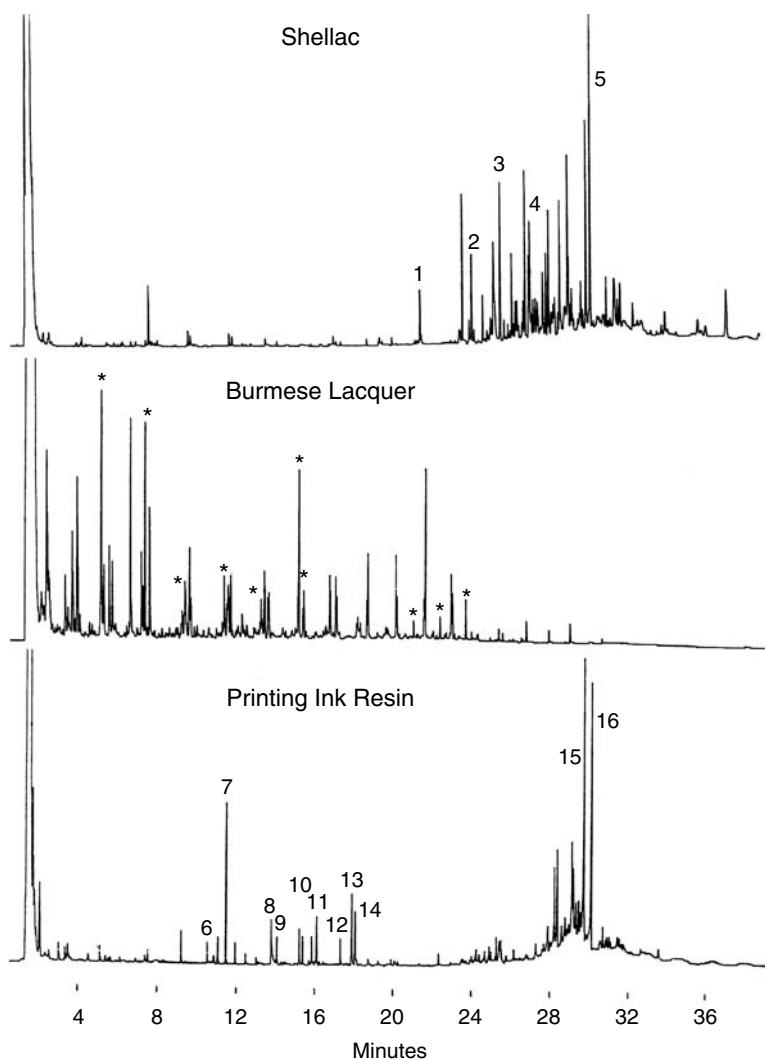


FIGURE 8.15 THM-GC profiles of shellac, a Burmese lacquer, and a printing ink resin.

become apparent as the lacquer cures. These two natural resins are therefore clearly distinguished by this method.

In the THM-GC profile of the printing ink resin,³⁶ dimethyl fumarate (peak 6) is detected, suggesting the presence of maleic or fumaric acid. Pentaerythritol is indicated by the presence of the tetra- and trimethyl ethers (peaks 7 and 8, respectively). Tertiary butyl phenol and methyl and dimethyl tertiary butyl phenols are detected as their methyl ethers (peaks 9, 10, and 11, respectively). Rosin acid methyl esters are detected with dehydroabietic acid and abietic acid methyl esters predominating (peaks 15 and 16, respectively). This resin is therefore diagnosed

as a tertiary butyl phenol-formaldehyde condensate-modified pentaerythritol rosin maleic ester type.

8.11 INKS

Forensic document examiners are asked to identify altered ballpoint ink writing and, in some cases, to determine when such an entry was made. Ballpoint inks are composed of an intimate blend of resin, pigment or dye, and solvent.

In principle, the age of a ballpoint ink entry may be determined by its dye component composition. With a sufficiently wide historical database of such information, it has been possible to “date” a ballpoint entry. An alternative approach to determine the composition and relative age is by Py-GC methodology.

Py-GC using the THM technique has shown some potential for identifying both solvent composition and resin type.³⁶ A THM-GC profile of a typical ballpoint ink is shown in Figure 8.16.

From these data the solvents are identified as phenoxy ethanol (PE), benzyl alcohol (BA), and propylene glycol (PG). The methyl ethers, which are also detected, are suffixed by ME. It would appear that the resin is a polyvinyl pyrrolidone type, as indicated by the detection of the dimer (PVP2) and trimer (PVP3). Mass spectral data suggest that the peak marked DIAZ is derived from a diazo dye.

The relative age of the ink on the document can be assessed by monitoring the reduction in concentration of individual solvent components; however, these solvents evaporate rapidly from the document entry, and so the method has limited application. In alkyd resin binder inks, it may be possible to determine the age of the ink entry by monitoring changes in the fatty acid composition due to curing, as discussed previously.

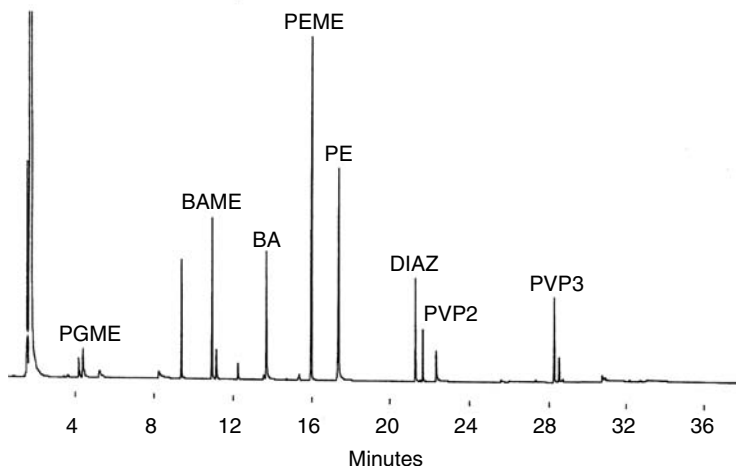


FIGURE 8.16 THM-GC profile of a typical ballpoint ink.

8.12 MISCELLANEOUS

A discussion of the applications of Py-GC to forensic chemistry would not be complete without including the role of the technique in the characterization of proprietary drugs and other organic substances used illegally. This topic has been adequately described by Irwin.³ In spite of the advantages, Py-GC has not been widely adopted for this purpose in forensic laboratories. The pyrolysis derivatization techniques previously described have potential for identifying drugs in the form of esters and carboxylic acids (such as Ibuprofen) and their excipients, including vegetable oils, sugars, and preservatives.²⁶

Soils containing high levels of organic matter may be characterized by Py-GC techniques. The presence of humic acids in soils infers that there should be potential for soil differentiation by THM techniques.

The identification and comparison of wood are an area of forensic interest. Microscopy methods on the basis of morphology are generally used for this purpose. However, developments in the mid-1990s indicate that there is potential for the chemical taxonomy of wood species by THM³⁷ and also by the pyrolysis of TMAH extractives.³⁸

8.13 CASE STUDY

During the police investigation of the scene of a multiple murder at the home of the victims, a greasy substance was found on a bedroom door and a fingerprint was found on the grease.

The forensic laboratory was asked to identify the substance so that appropriate fingerprint development techniques could be used to visualize the print. Some of the greasy substance was carefully removed from the door and analyzed by THM-GC. The substance was a cosmetic body lotion (see Figure 8.14). The print matched that of a person known to have been in the house several days previously and was therefore not necessarily incriminatory.

However, this was considered to be suspicious, and the laboratory asked for swabs from three of the victims to be forwarded for comparison, as some sexual activity had been known to have taken place. Methylene chloride extracts of the swabs were taken and evaporated onto the pyrolysis wires, and the experiments were repeated. The results were compared with those of the body lotion taken from the door.

There was a high degree of correspondence between the composition of the body lotion on the door and the composition of the components in the swabs, taking into account that some adsorption of some of the components could have taken place on the skin surfaces. The link between the suspect's fingerprint and the victims was established. As a result, the suspect was questioned again and confessed to all aspects of the crime.

8.14 CONCLUSIONS

It is evident that Py-GC may be used to characterize many different types of material likely to be associated with a crime scene. It is a versatile and discriminatory technique that may be used for the forensic examination of materials by the following:

High-temperature pyrolysis to determine the structure of macromolecular materials. This may lead to products that do not directly relate to the parent polymer as a result of dehydration and decarboxylation mechanisms, for example. This is particularly so where the polymer is derived from polar monomers such as polyesters.

Elevated temperature reaction pyrolysis in which the analyte is reacted with a chemical reagent. The method is appropriate for those materials that contain hydrolyzable bonding or free reactive groups, e.g., acids, alcohols, and phenols. Usually, the pyrograms more clearly reflect the composition of the parent material. A review of the technique describes applications to nonforensic materials.³⁹

A system for thermally desorbing chemical compounds from the sample. This is useful for introduction by volatilization of the total sample to the GC system and compounds adsorbed on an adsorbent such as activated charcoal or porous polymer. The latter method can be used for the analysis of hydrocarbon accelerants from fire scenes in cases of arson or environmental or toxicological monitoring.

An effective interpretation of data cannot be made without a knowledge of the identity of the pyrolysis products, and hence with good fortune, a diagnosis of the composition of the original polymer can be made. Therefore, every effort should be made to identify and interpret the significance of at least the major products by mass spectrometry, relative retention times, or infrared spectroscopy (in the case of GC-FTIR).

While this discussion has been limited to Py-GC, other pyrolysis techniques should not be forgotten. Py-MS in its simplest form (in contrast to other more sophisticated techniques, such as field ionization-MS, laser ablation-MS, and fast atom bombardment) provides data that can give useful information about chemical structure.

Future directions include the application of other separation techniques, such as supercritical fluid chromatography⁴⁰ and the development of novel high-temperature chemolytic methods that may yield even more information about the structure of macromolecules.

REFERENCES

1. B.B. Wheals, *J. Anal. Appl. Pyrolysis*, 2: 277 (1980).
2. B.B. Wheals, *J. Anal. Appl. Pyrolysis*, 8: 503 (1985).
3. W.J. Irwin, *Analytical Pyrolysis: A Comprehensive Guide*, Chromatographic Series Vol. 22, Marcel Dekker, New York (1982).
4. P.K. Clausen and W.F. Rowe, *J. Forens. Sci.*, 25: 765 (1980).
5. R.O. Keto, *J. Forens. Sci.*, 34: 74 (1989).
6. T.O. Munson and J. Vick, *J. Anal. Appl. Pyrolysis*, 8: 493 (1985).
7. J.B.F. Lloyd, K. Hadley, and B.R. Roberts, *J. Chromatogr.*, 101: 417 (1974).
8. T.P. Wampler, *J. Anal. Appl. Pyrolysis*, 16: 291 (1989).
9. P.R. De Forest, *J. Forens. Sci.*, 19: 113 (1974).

10. R.W. May, E.F. Pearson, and D. Scothern, *Pyrolysis Gas Chromatography*, Analytical Science Monograph 3, The Chemical Society (1977).
11. T.P. Wampler and E.J. Levy, *Crime Lab. Dig.*, 12: 25 (1985).
12. A. Parabyk, The Characterization of Plastic Automobile Bumper Bars Using FTIR, PGC and SEM-EDX, master of science in forensic science thesis, George Washington University (1988).
13. R. Saferstein, in *Polymer and GC Analysis*, S.A. Liebman and E.J. Levy, Eds., Marcel Dekker, New York, p. 339 (1985).
14. J.M. Challinor, *Forens. Sci. Int.*, 21: 269 (1983).
15. S. Tsuge, Y. Sugimura, and T. Nagaya, *J. Anal. Appl. Pyrolysis*, 1: 221 (1980).
16. Y. Ishida, K. Abe, H. Ohtani, and S. Tsuge, *Macromolecules*, 28: 6528 (1995).
17. J.M. Challinor, *J. Anal. Appl. Pyrolysis*, 16: 323 (1989).
18. J.I. Thornton, in *Forensic Science Handbook*, R. Saferstein, Ed., Prentice Hall, Englewood Cliffs, NJ, p. 529 (1982).
19. J.M. Challinor, in *Expert Evidence, Advocacy and Practice*, I. Freckleton and H. Selby, Eds., Law Book Company, Melbourne, Australia, p. 90 (1994).
20. P.J. Cardosi, *J. Forens. Sci.*, 27: 695 (1982).
21. K. Fukuda, *Forens. Sci. Int.*, 29: 227 (1985).
22. D. McMinn, T.L. Carlson, and T.O. Munson, *J. Forens. Sci.*, 30: 1064 (1985).
23. J.M. Challinor, *J. Anal. Appl. Pyrolysis*, 18: 233 (1991).
24. J.M. Challinor, *Proceedings of the 13th Meeting of the International Association of Forensic Sciences*, Oxford, 1984.
25. J.W. Bates, T. Allinson, and T.S. Bal, *Forens. Sci. Int.*, 40: 25 (1989).
26. J.M. Challinor, *J. Anal. Appl. Pyrolysis*, 20: 15 (1991).
27. I. Skeist, *Handbook of Adhesives*, 2nd ed., Van Nostrand Reinhold Company, New York (1977).
28. N.L. Bakowski, E.C. Bender, and T.O. Munson, *J. Anal. Appl. Pyrolysis*, 8: 483 (1985).
29. J.C. Hughes, B.B. Wheals, and M.J. Whitehouse, *Forens. Sci.*, 10: 217 (1977).
30. R.D. Blackledge, *J. Forens. Sci.*, 26: 557 (1981).
31. J. Chian Hu, *J. Chromatogr. Sci.*, 19: 634 (1991).
32. S. Tsuge and H. Ohtani, in *Analytical Pyrolysis, Techniques and Applications*, K.J. Vorhees, Ed., Butterworths, London, p. 407 (1984).
33. J.M. Challinor, unpublished work.
34. J.M. Challinor, in *The Forensic Examination of Fibres*, 2nd ed., J. Robertson and M. Grieve, Eds., Ellis Horwood: London, p. 223 (1999).
35. J.M. Challinor, *J. Anal. Appl. Pyrolysis*, 25: 349 (1993).
36. J.M. Challinor, *Proceedings of the 12th International Association of Forensic Sciences*, Adelaide, Australia, 1990.
37. J.M. Challinor, *J. Anal. Appl. Pyrolysis*, 35: 93 (1995).
38. J.M. Challinor, *J. Anal. Appl. Pyrolysis*, 37: 1 (1996).
39. J.M. Challinor, *J. Anal. Appl. Pyrolysis*, 61: 3 (2001).
40. P.R. DeForest et al., in *Gas Chromatography in Forensic Science*, I. Tebbett, Ed., Ellis Horwood: Chichester, p. 165 (1992).

9 Characterization of Microorganisms by Pyrolysis-GC, Pyrolysis-GC/MS, and Pyrolysis-MS

*Stephen L. Morgan, Bruce E. Watt,
and Randolph C. Galipo*

CONTENTS

9.1	Introduction	201
9.2	Microbial Chemotaxonomy	203
9.3	Practical Aspects	208
9.3.1	Microbial Sample Handling	208
9.3.2	Analytical Pyrolysis Techniques for Microorganisms	210
9.3.3	Chromatographic Separation and Mass Spectrometric Detection of Pyrolysis Products from Microorganisms	213
9.4	Selected Applications	216
9.4.1	Discrimination of Gram Positive and Gram Negative Bacteria	216
9.4.2	Analysis of Gram Positive Organisms	220
9.4.3	Analysis of Gram Negative Organisms	224
9.4.4	Analysis of Fungi	227
9.5	Conclusions	227
	References	229

9.1 INTRODUCTION

Detecting, identifying, and characterizing microorganisms is vital to solving important environmental, biological, and medical problems. In monitoring a food production process for pathogenic microorganisms or surveying a battlefield for biological warfare agents, detection may require recognizing that microbial species other than those expected in the normal environment are present. A diagnosis of pneumonia for a patient may require the ability to classify a microbial sample as one of several closely related species. Microorganisms play a central role in soil biodegradation

processes; analysis and characterization of environmental microbial communities can contribute to the design and control of waste bioremediation processes. Characterization of different organisms might also provide supporting evidence for or against relatedness of species for taxonomic purposes.

*Bergey's Manual of Determinative Bacteriology*¹ catalogs over 250 bacterial genera. Traditional microbiological identification of bacterial species is based on appearance under a microscope (shape, size, presence of particular structures), response to staining (e.g., the classic Gram stain), or indirect characteristics (growth under aerobic or anaerobic conditions, generation of specific enzymes or biochemical products, etc.). Morphology is closely related to taxonomy, but its use for microbial characterization is not definitive.^{2,3} Structural characteristics of Gram type (e.g., thick peptidoglycan in Gram positive organisms vs. lipopolysaccharide in Gram negative organisms) do not always correlate with the results of the Gram stain. Other cell types (such as acid-fast species) also exist.^{4,5} The presence of specific enzymes, the response of an organism to growth substrates, or the susceptibility of an organism to specific antibiotics is often due to metabolism rather than structure. Although valuable for identification, the use of these largely phenotypic characteristics requires culturing and isolation of viable cells, which can be time consuming and may even fail for fastidious organisms.⁶

The complex mixture of microbial cellular and extracellular components is an appealing target for chemotaxonomic analysis by gas chromatography (GC), mass spectrometry (MS), or the combination of the two techniques (GC/MS). Such instrumental methods focus on chemical structures present in a sample and are not dependent, as are biological tests, on the microorganism being viable. Additionally, since only microgram amounts of sample are required, instrumental methods offer enhanced sensitivity.

Chemical components characteristic of specific microorganisms or microbial groups are usually enclosed in or part of a polymeric cellular matrix. Such nonvolatile and intractable biological samples present some difficulties for their direct characterization by GC, MS, or GC/MS. For these techniques to be useful, chemical components characteristic of the microbial sample must be released intact or a related compound must be generated before GC or MS analysis. Depolymerization is usually performed off-line by acid hydrolysis, methanolysis, saponification, or other reactions. One or more chemical derivatization steps might then be employed to produce volatile and thermally stable derivatives suitable for GC or MS.

When analytical pyrolysis is applied to a microbial sample, depolymerization and volatilization of bacterial components are accomplished simultaneously. The volatile thermal products may be separated on-line by capillary GC with flame ionization detection (Py-GC-FID), separated by GC and detected by MS (Py-GC/MS), or detected directly by MS (Py-MS). In contrast to derivatization-based methods and like other direct approaches, microbial characterization by analytical pyrolysis requires minimal sample pretreatment and short total analysis times.

The use of analytical pyrolysis for biomedical taxonomy was proposed by Zemany⁷ in 1952. A single strain of an unidentified microorganism was used in fundamental studies of pyrolysis temperatures and residence times by Oyama⁸ in 1963. The first comprehensive work was that of Reiner,⁹ who used pyrolysis-GC in

1965 to identify different strains of *Escherichia coli*, *Shigella* sp., *Streptococcus pyogenes*, and *Mycobacteria*. Although most early work was performed with packed columns and nonselective flame ionization detection, the potential of analytical pyrolysis for making sensitive discriminations between various microorganisms samples was well established by the late 1970s.

In 1979, Gutteridge and Norris¹⁰ reviewed the application of pyrolysis methods to the identification of microorganisms. Significantly, this review appeared in a bacteriology journal and listed 148 references. Meuzelaar et al.¹¹ discussed pyrolysis-MS methods for biomaterials in their 1982 text, describing nearly 30 applications in clinical microbiology, quality control, and other biological areas. Irwin¹² included a chapter on microbial taxonomy in his comprehensive 1982 guide to analytical pyrolysis and listed 124 references. The use of analytical pyrolysis in clinical and pharmaceutical microbiology was described by Wieten et al.¹³ in 1984, and over 100 references were cited. Also in 1984, Bayer and Morgan¹⁴ reviewed the analysis of biopolymers by pyrolysis-GC and listed 80 literature citations on microorganisms. In 1985, Fox and Morgan⁶ discussed a chemotaxonomic approach to characterizing microorganisms based on analysis of chemical signatures detected by analytical pyrolysis and derivatization GC/MS. Wampler's 1989 bibliography of analytical pyrolysis references¹⁵ listed 29 microbial applications along with other examples of biopolymer analysis. Analytical methods for microorganisms, including pyrolysis, were also surveyed by Eiceman et al.¹⁶ More recently, Morgan et al.^{17,18} reviewed their work on identification of chemical markers for microbial differentiation produced by pyrolysis.

Improvements in analytical capability for the analysis of complex pyrolysate mixtures have appeared during the last decade: high-resolution capillary GC with more polar and selective stationary phases coated on inert fused-silica columns; coupling of capillary GC with sensitive, selective, and lower-cost mass spectrometric detectors; enhanced pyrolysis-MS techniques; hyphenated analysis methods, including GC-Fourier-transform infrared spectroscopy (GC/FTIR) and tandem MS; and better strategies for handling complex multidimensional pyrolysis data. The present chapter reviews the known chemotaxonomy of microorganisms, summarizes practical considerations for the use of pyrolysis in microbial characterization, and critically discusses selected applications of analytical pyrolysis to microbial characterization.

9.2 MICROBIAL CHEMOTAXONOMY

Chemotaxonomy is the study of chemical differences in organisms and the use of those differences to identify and classify them. As suggested in the last section, direct chemical analysis provides a powerful supplement to the more traditional methods of classifying microorganisms by morphological and biochemical characteristics. Although variations in growth, treatment, and sampling conditions can influence their structure and composition, microorganisms also exhibit many invariant structures that can be employed for differentiation.

Bacteria and other prokaryotes lack the complex intracellular structures (endoplasmic reticulum, Golgi apparatus, lysosomes, mitochondria, etc.) found in plant and animal cells (eukaryotes). Bacterial morphology (shape and size) is limited to

a few simple forms, such as rods, cocci, chains, and spirals.^{5,19} The chemical composition of the cell walls, outer membranes, and capsules of bacteria is sufficiently diverse to offer potential for taxonomic discrimination.^{3,4} For example, the chemical makeup of a single colon bacillus (*E. coli*) has been estimated to contain 2000 to 4500 different types of small molecules distributed as 120 different amino acids and their precursors and derivatives; 250 different carbohydrates and their precursors; 50 different fatty acids and their precursors; 100 different nucleotides and their precursors and derivatives; and 300 quinones, polyisoprenoids, porphyrins, vitamins, and other small organic molecules.²⁰ Many of these molecules are common to all organisms and not well suited for discrimination among microorganisms. Some of these molecules are specific to various major groups of organisms and can serve as chemical markers for their detection or identification.

The cell envelope usually consists of a cell membrane, a cell wall, and an outer membrane.^{21,22} Figure 9.1 shows schematic representations of the structure of Gram positive and Gram negative cell envelopes. The cell wall consists of the peptidoglycan (PG) layer and associated structures. PG is the only substance common to almost all bacteria (except *Mycoplasma* and *Chlamydia*) and not present in nonbacterial matter.²³ PG and its associated chemical components may account for up to 10 to 40% of the dry weight of the cell.⁵ As seen in Figure 9.2, PG consists of a polysaccharide backbone that is a repeating polymer of N-acetylglucosamine and N-acetylmuramic acid. Attached covalently to the lactyl group of muramic acid are tetra- and pentapeptides (composed of repeating L- and D-amino acids) cross-linked by peptide bridges. The amino sugar muramic acid (3-O- α -carboxethyl-D-glucosamine) is a fairly definitive marker for bacteria. Other chemical markers in PG include D-alanine, D-glutamic acid, and diaminopimelic acid.^{24,25} The D-amino acids are sometimes found in other bacterial components but are not synthesized by mammals. Different bacteria may vary in the sequence of the amino acids in the peptide side chains and cross bridges.

The PG layer is thicker in Gram positive bacterial cell envelopes than in Gram negative bacteria (Figure 9.1A). As a result, chemical markers for PG are found in higher amounts in Gram positive cells. Teichoic acids (with ribitol or glycerol phosphate backbones and side chains of variable amino acid composition) are covalently bound to the thick peptidoglycan layer in some Gram positive species.²⁶ Lipoteichoic acids (LTAs) composed of glycerophosphate polymers terminated in glycolipid are not bound to the cell wall but are sometimes linked through the cell wall to muramic acid.^{5,26} Teichuronic acids (glucuronic acid polymers with variable side chains) and neutral polysaccharides are also bound to PG.

Gram negative cell envelopes usually have a thin PG layer (Figure 9.1B). PG is attached to the outer membrane by lipoprotein containing phospholipids and other hydrophobic substances. A variety of phospholipids and proteins are found on the inner side of the outer membrane, some of these (porins) spanning the outer membrane. The external surface of the outer membrane of Gram negative bacteria contains its primary endotoxin, a unique lipopolysaccharide (LPS), consisting of an outer O-antigen, a middle core, and an inner lipid A region.²⁷ The lipid A region contains a glucosamine disaccharide with covalently bound 2- and 3-hydroxy fatty acids. Glucosamine is common, but 3-hydroxy and 2-hydroxy fatty acids are unusual. Although

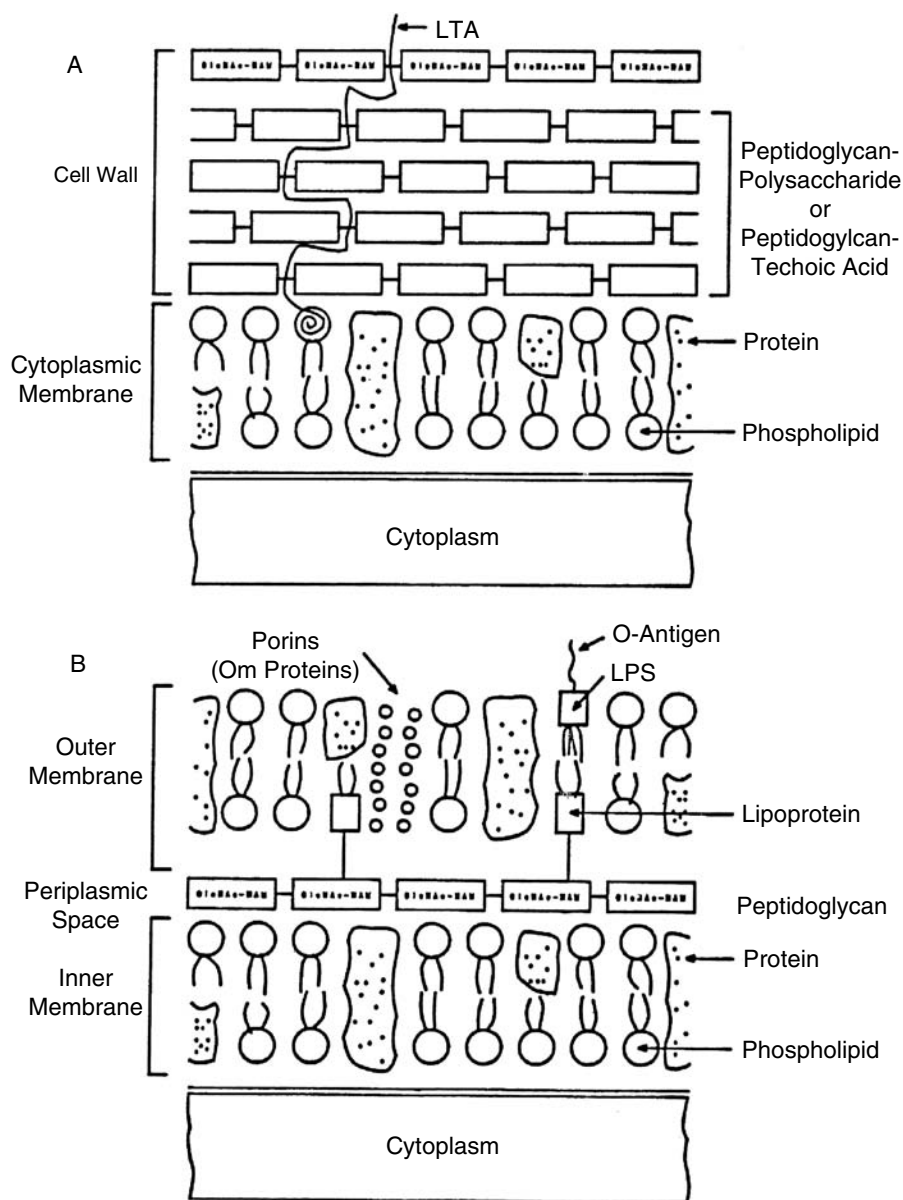


FIGURE 9.1 Generalized structure of bacterial cell envelope. (A) Gram positive organism. (B) Gram negative organism.

the fatty acid composition of LPS varies among Gram negative bacteria, -hydroxy-myristic acid is a chemical marker for LPS.

Fatty acid profiling by GC is routine in some clinical reference laboratories, particularly for identification of anaerobic bacteria.^{28,29} Fatty acids and lipids are bonded to proteins, carbohydrates, or other chemical entities in microbial cell walls and membranes. Fatty acids of chain length from C₉ to C₂₀ are useful for identifying Gram negative organisms at the species and genus levels. Perhaps the only automated GC-based microbial characterization system that is commercially available is a microbial analysis system based on derivatization GC of fatty acid methyl esters (Microbial ID, Inc., Newark, NJ).³⁰

The core region in the LPS of Gram negative bacteria contains two unusual sugars, ketodeoxyoctonic acid (KDO) and L-D-glycero-mannoheptose. KDO and heptoses are not commonly found in structures other than LPS and are potential markers for Gram negative organisms. Levels and types of sugars (e.g., rhamnose and fucose) within the core and O-antigen regions of LPS differ among bacterial species. Carbohydrate profiling using derivatization followed by GC/MS is an excellent tool for bacterial differentiation.³¹

Various groups of Gram positive bacteria also contain cell wall-associated carbohydrates. For example, rhamnose-containing polysaccharides are major components of streptococcal cell walls and are used for their serological classification (Lancefield grouping). The group A-specific polysaccharide consists of a polyrhamnose backbone with single N-acetylglucosamine side chains, while the group B-specific polysaccharide consists of a backbone of rhamnose and glucitol phosphate residues with trisaccharide side chains composed of rhamnose, galactose, and N-acetylglucosamine.³²

Mycobacteria, nocardiae, corynebacteria, and some related organisms have unusual cell envelopes. Not all *Mycoplasma* contain peptidoglycan,⁵ and PG in *Chlamydia* does not contain muramic acid.³³ Although mycobacteria and nocardiae stain as Gram positive organisms, some resist decolorization by acid alcohol after staining (acid-fastness). Acid-fastness is believed to be related to the presence of long-chain mycolic acids.⁵ Mycolic acids are α -alkyl, β -hydroxy fatty acids ranging in size from C₃₀ to C₈₆ and may constitute up to 60% of the dry weight of these bacterial envelopes. Mycolic acids in corynebacteria are relatively short chained. Mycolic acids have a variety of structural forms within the cell envelope, and some mycolic acids are covalently bound to PG by a polysaccharide. Other compounds that contain mycolic acid form a thick waxy layer around the outside of the cell wall.

Under certain circumstances, many bacteria produce capsules outside their cell envelopes. Capsules are usually made of polysaccharide; however, some *Bacillus* capsules are composed of D-glutamic acid polypeptide. Certain Gram positive bacteria, most notably strains of *Bacillus* and *Clostridium*, produce modified cells (endospores) capable of surviving in adverse environments.⁵ Spore PG is found between an inner and outer membrane and differs from that in the normal vegetative cell: muramic acid is mostly in the lactam form; the spore PG has fewer peptide cross-links; and the cell exterior is coated with keratin. The spore also contains large quantities of calcium dipicolinate, a substance involved in microbial heat resistance.

Poly- β -hydroxybutyrate (PHB), a polymer of 3-hydroxybutyric acid, serves as a major energy and carbon storage compound. Diverse bacteria usually accumulate PHB in intracellular granules having an approximate composition of 98% PHB and 2% proteins and small amounts of lipids. In genetically competent bacteria, PHB is in the plasma membrane or covalently linked to extracellular polysaccharides. Some *Bacillus* and *Pseudomonas* species accumulate up to 30% of their weight as PHB.⁵

Many of the characteristic components mentioned in this section are common to diverse bacterial species. For example, chemical markers for peptidoglycan (muramic acid, etc.) are ubiquitous in bacteria. Other chemical components have the potential to be chemical markers whose presence or absence differentiates dissimilar (or even closely related) microbial species. The bacterial cell envelope (membrane, surrounding wall, and outer membrane) in particular offers a rich assortment of unusual polymers that have distinctive monomeric constituents. Whether any of these chemical components from specific microorganisms generates identifiable and unique pyrolysis signatures has been the focus of much research over the past decade.

9.3 PRACTICAL ASPECTS

When analytical pyrolysis is subjected to the same rigorous controls and quality checks as any other analytical technique, reproducible results can be achieved both within and between laboratories. Biological variability and heterogeneity of sampling tend to have deleterious effects on reproducibility — these problems will plague any analytical technique applied to microorganisms. Because of the great intraspecies variability of bacteria, it is important to employ representative samples of more than one strain of each organism if possible. Ruggedness, simplicity, and ease of interpretation of results are other performance characteristics relevant in developing pyrolysis methods for microbial characterization.

9.3.1 MICROBIAL SAMPLE HANDLING

The first step in the handling of any microbial sample, whether it is taken from a clinical specimen or from the environment, is usually to culture the organism in growth media under controlled conditions. This step serves several purposes: the number of cells of the organisms is increased, thereby increasing the detectability, and the organisms present may be isolated as nearly pure strains, thus increasing the chances for identification. Such cleanup or isolation of strains can be important. Cultures containing mixed populations of microorganisms can present difficulties for identification schemes, even those based on chemotaxonomic markers.

The formulation of growth media, inoculation, incubation times and temperatures, and sampling of a microorganism should be carefully standardized and controlled so as not to introduce undesired variability into later attempts at characterization. Media should be formulated in a standardized manner and of a known composition. Inoculation of the microbial cells into the culture media should be done with the same quantity of cells in the same growth stage. All strains should then be cultured for the same period of time and at the same temperature to provide

uniformity. Ideally, organisms should be grown under exactly the same conditions (media, temperature, stage of growth). Unfortunately, this is not always practical. More often, the isolation of an unknown microbiological sample might require a battery of different media appropriate for different growth types. Related strains can be grown under identical conditions to the same growth stage. Organisms having very different physiological requirements for growth clearly can not be grown under the same conditions (e.g., obligate anaerobes and aerobes). In any case, standardization and quality control are required.

Changes in the type or composition of growth media may influence the production of extracellular components (enzymes, metabolic products, etc.) as well as some cellular components. For example, Gutteridge and Norris³⁴ studied the effects of different growth conditions on the discrimination of three different bacteria by Py-GC. Pyrograms of the same organism grown on different media were more different from one another than pyrograms of different organisms grown on the same media. The effect of culture time and incubation temperature was less obvious, producing variations for two organisms but not for the other organism. Engman et al.³⁵ also examined the effect of growth media, incubation time, and sample storage time on the pyrograms of five bacterial species of the genus *Flavobacterium*. Pyrograms of organisms grown on two different but similar media such as *Flavobacterium* medium and Trypticase Soy Agar (both consisting of a protein hydrolysate agar with no added carbohydrate) showed few differences. When glucose was added to the growth medium, however, several new peaks appeared in the pyrograms. Samples incubated for different times also showed few differences except for two peaks that increased in height upon longer incubation. It is desirable, of course, for differences in the amounts of discriminating pyrolysis products to be representative of relatively stable genetic or structural differences between organisms that do not vary appreciably with culture conditions.

Depending on its origin, incubation time may affect the levels of a particular pyrolysis product. Watt et al.³⁶ profiled the production of (*trans*) 2-butenic acid, a pyrolysis product of poly- β -hydroxybutyrate (PHB), as a function of incubation time for *Legionella pneumophila*. The amount of 2-butenic in the pyrograms followed the expected growth curve for PHB. PHB is found in the plasma membrane of *E. coli* and is only present in high amounts when growth is limited and cells are genetically competent. Pyrolysis products of PHB were not found in *E. coli* pyrograms, perhaps because the growth conditions were not optimal to force production of PHB.

After harvesting bacteria, it is usually desirable to wash the samples several times with sterile distilled water to remove possible contamination from the media. Samples are often autoclaved or heat-killed (at 60 to 120°C in air, depending on the susceptibility of the organism) for safety reasons, then lyophilized (freeze-dried) to a dry powder. Heating may be performed under an inert gas to avoid the possibility of oxidation. Since the sample is exposed to much more energetic degradation conditions during pyrolysis, most researchers have assumed that heat-killing and lyophilization do not appreciably change the chemical structure of the microbial sample. Organisms should be prepared and killed in a similar fashion whenever possible. Preparing samples in widely different fashions may not permit hypotheses

concerning observed pyrolysis patterns to be tested. The sample may then be refrigerated for storage before analysis.

In addition to being cultured in a well-defined manner, strains should also be systematically characterized by traditional microbiological tests. Only in this manner can quality control be assured. Traditional microbiological characterization should be performed before killing, as most of these tests require viable cells. In a pyrolysis study of streptococci, a sample labeled as a group F strain was found to contain a chemical marker (due to glucitol phosphate) previously detected only in group B organisms.³⁷ Routine tests (hippurate hydrolysis and serological grouping) identified the organism as a group B streptococcus. It was later confirmed that this sample had been incorrectly identified by the originating laboratory. Bacteria are not simple pure chemical substances; incorrect assignments and sample contamination are not uncommon when routine microbiological control is not carried out. This is not a criticism of interlaboratory studies as much as a comment on the complexity of adequate sample and information transmittal between laboratories.

Knowledge of chemical composition with respect to relevant carbohydrate, amino acid, or fatty acid chemical markers is often critical for proper interpretation of the pyrolysis of a microbial sample. Sometimes this information is already available in the literature regarding specific bacteria. More often, however, complementary analyses for that particular class of components by an independent GC, GC/MS, or spectroscopic method may be needed.

Finally, researchers working with potentially pathogenic microorganisms should be aware of local and government regulations pertaining to operating a safe and healthy workplace.³⁸ In the U.S., this involves compliance with the Occupational Safety and Health Act of 1970 and regulations of the Department of Labor, including OSHA document 29 CFR 1910.³⁹ Employers are required to inform and train employees regarding the specific hazards associated with their work. Safety techniques and devices should be used to isolate personnel from biohazards. Specific examples include use of protective laboratory clothing, aseptic techniques to avoid environmental spread of pathogenic agents, and safety cabinets to minimize spread of aerosols. Containment considerations also include use of nonporous surfaces for laboratory bench tops, type of door used to separate the laboratory from public areas, type of ventilation system in use, and accessibility of autoclaves for sterilization. Biohazard labels should be affixed to waste containers, refrigerators, freezers, and transport containers holding potentially infectious materials. Specific procedures for storage, decontamination, and disposal of biohazardous agents should also be documented.

9.3.2 ANALYTICAL PYROLYSIS TECHNIQUES FOR MICROORGANISMS

Ease of sample handling is often cited as an advantage in pyrolysis-based methods. This advantage generally refers to the fact that lengthy sample pretreatment, derivatization, or cleanup steps are not required. As pointed out by Windig,⁴⁰ biological samples are often heterogeneous, and the preparation of a representative suspension involving microgram amounts of bacteria can be tedious. Additionally, Montaudo⁴¹ points out that the assumption that any sample pretreatment should be avoided is

naive. Indeed, if the characteristic discriminating information for a microbial application is known *a priori* to reside in a certain cellular component, a carefully designed pretreatment step may be able to provide a suitable isolated cell fraction. This approach will generally give better reproducibility because the background of extraneous chemical components not relevant to decision making is eliminated.

To prepare a microbial sample for analysis, an amount of the lyophilized powder is weighed and added to a measured volume of water to give a solution of known concentration (e.g., 10 $\mu\text{g}/\mu\text{l}$). The solution should be vortexed or sonicated to produce a homogeneous suspension before sampling on the pyrolysis sampling device.

Alternatively, a microbial sample may be transferred by a plastic inoculation loop directly from the culture media into a quartz sampling tube or onto a metal wire. Care should be taken to avoid carrying media with the sample; blank pyrolysis runs on media alone should also be done to check for background contamination. Sample homogeneity (composition, shape, and amount) is desirable for reproducible results, and this may be difficult to achieve. In some instances, however, analytical pyrolysis may be conducted directly on original samples with little or no sample pretreatment. Gilbert et al.⁴² discriminated group B streptococci from groups A, C, F, and G following swabbing of the samples directly from sheep blood agar plates and suspension of the samples in distilled water to a consistent opacity.

When a resistively heated filament pyrolyzer (e.g., the Pyroprobe from CDS Analytical, Inc., Oxford, PA) is used, the sample may be placed directly on a platinum filament or in a quartz tube or boat inside a platinum coil. In either case, the placement of sample with respect to the sampling tube or the ribbon should be the same for all samples. For liquid sample suspensions placed on a ribbon or in a coil, the solvent is evaporated prior to pyrolysis. Solid microbial samples can be sandwiched between quartz wool plugs inside the quartz sampling tube so as to reduce extraneous nonvolatile material from leaving the sampling tube during pyrolysis. With quartz, the sample never comes into direct contact with the pyrolyzer filament, as it does when sample is coated directly on a thin ribbon filament. Ribbon filaments sometimes exhibit a memory effect (particularly with polar components), are harder to clean, and typically have a shorter lifetime. Quartz tubes may be reused after cleaning.

The temperature actually experienced by the sample in a resistively heated probe may be different from the pyrolysis temperature setting. Factors influencing the sample temperature include sample amount, positioning of sample, and whether a quartz sampling tube is employed. To achieve reproducibility, sample sizes for analytical pyrolysis should be in the lower microgram range. Large sample sizes (more than 100 μg) make controlled heat transfer and uniform heating difficult to achieve; secondary reactions are promoted, resulting in more complicated and less reproducible pyrograms. Small sample sizes allow formation of thin films and permit effective and rapid heat transfer from the heat source.⁴³ If analytical profiling is the goal, sample amounts applied to the tube are typically in the range of 10 to 100 μg . Acquisition of quality mass spectra for all peaks (including minor pyrolysis products) may require samples of several hundred micrograms.

With Curie-point pyrolysis, the active heating element is a ferromagnetic metal wire (0.5 mm in diameter). The sample (10 to 20 μg) may be coated on the wire by

depositing drops (5 μl each) of suspension (2 to 4 $\mu\text{g}/\mu\text{l}$) and then dried while rotating the wire.¹¹ As mentioned already, placement of sample should be done reproducibly to reduce variability in pyrolysis results. Carbon disulfide has been recommended as a solvent for sampling onto Curie-point wires, as it evaporates easily and leaves no detectable residue.⁴⁴ Sampling factors influencing Curie-point techniques in Py-MS have been extensively studied.⁴⁵⁻⁴⁷ The deposition of unpyrolyzed sample or nonvolatile residue onto the walls of the pyrolysis interface increases with the amount of sample loaded on Curie-point wires, with optimal loading between 1 and 20 μg .^{11,45}

Following loading of sample, the filament probe or Curie-point wire is inserted into a heated interface connected to the GC injection port or Py-MS vacuum. In the original design of filament pyrolysis systems from CDS Analytical, the ribbon or coil is an element in a Wheatstone bridge circuit. The bridge is set so that it is balanced at the set point temperature, and a capacitor is discharged to rapidly heat the filament (up to 20°C/msec and 1000°C). Although resistively heated filament pyrolyzers are generally calibrated by the manufacturer, the actual temperature of the pyrolyzer element can be determined by appropriate calibration.⁴⁸

Curie-point pyrolysis involves placing the sample wire into a radio frequency field that induces eddy currents in the ferromagnetic material and causes a temperature rise. When the wire reaches the Curie-point temperature, it becomes paramagnetic and stops inducing power. The temperature at which the wire stabilizes (the Curie point) is a function of the type of metal. For example, the Curie points of cobalt, iron, and nickel are 1128, 770, and 358°C, respectively. Wires made from alloys of these metals produce intermediate temperatures. For example, the commonly used nickel-iron wire has a Curie point of 510°C.¹¹ Differences between filament and Curie-point pyrolyzers depend on the pyrolysates examined and may be obscured by other instrumental differences, including the design of the transmission system to the detector.

Long-term reproducibility is affected by eventual deterioration of resistive filaments or sample wires. All components exposed to sample during pyrolysis (GC injection port liners and quartz sample tubes if used) often require acid cleaning, solvent washing, and oven drying. Active pyrolyzer elements (coils and ribbons in filament pyrolyzers) can be heated without sample to remove contamination (1000°C for 2 sec is usually adequate). Curie-point wires are inexpensive enough to be discarded after use.

Preliminary experiments are usually required to choose pyrolysis conditions. The pyrolysis literature may guide the researcher, but optimal conditions for a particular sample must be determined empirically. The question of appropriate heating rates and final temperatures has been addressed by other authors.^{11,12} Pyrolysis heating conditions interact with sample size, and effects are usually system dependent (i.e., resistive heating vs. Curie point, wires vs. ribbons vs. quartz tubes). With microorganisms, temperatures that produce pyrolysates characteristic of the parent sample may range from 400 to 800°C or even 1000°C. Generally, lower pyrolysis temperatures induce less fragmentation and decrease the total amount of pyrolysates produced. Higher temperatures ensure more complete fragmentation, and thus might reduce the structural information obtained. Extremely low pyrolysis

temperatures may not produce significant amounts of volatile fragments from intractable biomaterials and may lead to the accumulation of nonvolatile residues contaminating the analytical system. Pyrolysis at a variety of different temperatures may provide selective information about degradation patterns and thereby reveal different aspects of structure. A time profile of volatile products generated at different temperatures by linear programmed thermal degradation may also provide characteristic structural information.⁴⁹

9.3.3 CHROMATOGRAPHIC SEPARATION AND MASS SPECTROMETRIC DETECTION OF PYROLYSIS PRODUCTS FROM MICROORGANISMS

Once the sample has been pyrolyzed, volatile fragments are swept from the heated pyrolysis/injection port by carrier gas into the GC or GC/MS system. In Py-MS, it is likewise desired to transfer pyrolysis products to the ionization source of the MS without appreciable degradation, condensation loss, or recombination. Designs of Curie-point Py-MS systems have incorporated glass reaction tubes, expansion chambers, heated walls, and positioning of the pyrolysis reactor directly in front of the ion source.¹¹

In Py-GC, if the column is kept relatively cold at the start of the run (e.g., as in a programmed temperature run), pyrolysates will be focused at the head of the column until eluted by the increasing temperature. The amount of pyrolysis products transferred to the chromatographic column is dependent on whether a split injection or a direct injection without splitting is employed. For highest sensitivity, direct flow without splitting is preferred; good chromatography may dictate using a reasonable split ratio (e.g., 10 to 20 parts split flow, 1 part column flow).

In their profiling of oral streptococci, French and coworkers^{50,51} used 1.5-m × 4-mm columns packed with a porous polymer (Chromosorb 104) combined with isothermal chromatographic conditions for fast repetitive analysis. Porous polymer columns are suitable for analysis of low molecular weight volatile pyrolysates but provide only limited higher molecular weight information. Although some conventional packed columns have been used in pyrolysis studies of microorganisms, over the past decade GC applications have converted completely to the use of fused-silica open tubular capillary columns. Because microbial pyrolysates are often labile polar species, the column material and chromatographic column should be as inert as possible. Fused-silica capillary columns coated with bonded phases satisfy these needs. Fused-silica columns offer improved resolution, increased inertness, and better analytical precision than packed columns. Superior resolution per unit time available with capillary columns means that adequate resolution can often be achieved using short (5- to 10-m) columns. With optimized conditions, analysis times are usually less than 10 to 30 min. Engman et al.,³⁵ in studying the pyrolysis of *flavobacteria*, employed fast temperature programs to shorten analysis times when using selected ion monitoring (SIM). Despite the resultant loss of resolution, capillary pyrograms were found to retain discriminating information. Another advantageous approach is to directly interface short (1- to 5-m) capillary columns to low-pressure MS ion sources. The decrease in analysis time, maintenance of resolution,

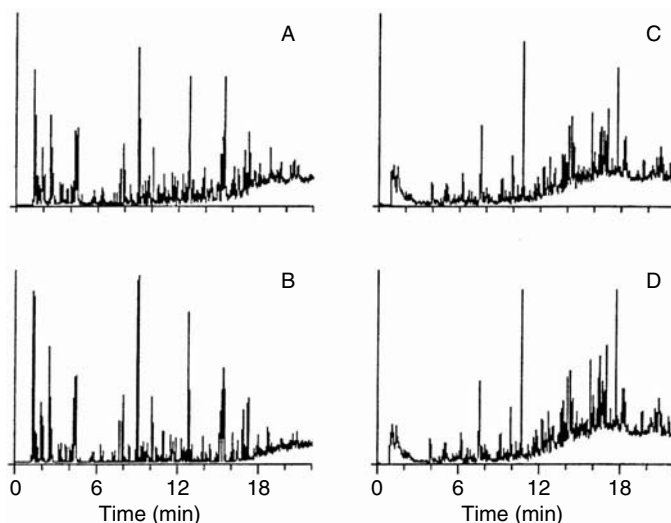


FIGURE 9.3 Pyrolysis of *B. anthracis* strain VNR-1-D1 at two different temperatures and analyzed by two different columns. (A, B) Replicate pyrograms produced by pyrolysis at 650°C with pyrolysates separated on a 1- μ film-thickness DB-1701 fused-silica column (J&W Scientific). (C, D) Replicate pyrograms produced by pyrolysis at 800°C with pyrolysates separated on a 0.25- μ film-thickness FFAP fused-silica column (Quadrex).

and elution of labile components at reduced temperatures have been described by Trehy et al.⁵² and applied to microbial pyrolysis by Snyder et al.⁵³

Choice of chromatographic stationary phases for fused-silica capillary columns can range from nonpolar (e.g., 100% methyl silicone) to polar (e.g., polyethylene glycol) phases. A particular stationary phase is employed, of course, to affect elution order of components chromatographed. Figure 9.3A and B shows replicate pyrolysis-GC/MS analyses of *B. anthracis* strain VNR-1-D1. These pyrograms were obtained using a fused-silica capillary column coated with a 1- μ film thickness of DB-1701 (moderate polarity, 14% cyanopropylphenyl–86% methyl silicone). Figure 9.3C and D shows replicate pyrograms of the same strain on a different fused-silica capillary column coated with a 0.25- μ film thickness of free fatty acid phase (FFAP; polar, polyethylene glycol acid modified). Correlation of peaks between the two sets of chromatograms on different columns is extremely difficult without an additional dimension of information (e.g., mass spectra for all peaks). Nevertheless, replicate chromatograms on the same phase are reproducibly identical. The different stationary phases employed here process the mixture of pyrolysis products differently. Both stationary phases provide a characteristic and reproducible signature for the microorganism. In the same way, chromatographic systems (instrument plus column) with differing active metal or other sorption sites may preferentially filter polar or reactive components from the chromatogram.

Contamination in GC systems is a continual problem in analytical pyrolysis. Early reports^{54,55} recognized that production of a residue from a sample during pyrolysis may be unavoidable, particularly with biological samples. Extraneous

peaks that mysteriously appear in some pyrograms have determinate causes that, if understood, can be eliminated.⁵⁶ Contamination in pyrolysis is often due to carryover of higher molecular weight, polar, or less volatile material produced during pyrolysis that remains behind in the interface, connecting tubing, or other parts of the chromatographic system. Tarry products or smoke may be produced by many samples and build up inside the system after a period of use, confounding long-term reproducibility. During temperature programming, small amounts of the contaminating materials are flushed from the system. Possible troubleshooting solutions include investigating different pyrolysis temperatures and times to pyrolyze the sample more effectively and evaluating the pyrolysis elements for possible contamination. Wiping the inner surfaces of the pyrolysis interface with a cotton swab will reveal if residue accumulation is the problem. If residue is present, the pyrolysis interface and GC interface should be cleaned using various solvents, including dilute nitric acid, hexane, chloroform, and acetone, in that order. Irwin¹² recommends overnight heating (600 to 700°C) of solvent-washed pyrolysis elements, heating in a water-saturated stream of hydrogen at 550°C, or chemical polishing followed by washing with acetone and heating. Direct flame heating should be avoided, as it may oxidize metal, contaminating surfaces and changing heat transfer characteristics. Quartz sample tubes should be cleaned in dilute nitric acid at 100°C overnight, rinsed with methanol and acetone, then dried in an oven.

Sample sizes that are too large (approaching 1 mg) may contaminate the column. If residue from pyrolysis cannot be avoided, using less sample may reduce contamination and extend column life. However, contamination becomes even more obvious when small samples are involved. Occasionally with increased usage, contamination may be visibly detected on the first few centimeters of a column. A rather drastic but appropriate solution is to clip off the initial section of column. Removal of a section of contaminated column does not have a great effect on resolution and may restore performance to a degraded system. Cross-linked or bonded phase columns can sometimes be rejuvenated by rinsing with organic solvent such as methylene chloride and then reconditioning. Mitchell and Needleman⁵⁷ described a disposable precolumn with backflushing capability to remove contaminants from a pyrolysis-GC system. Sugimura and Tsuge⁵⁸ designed a splitter system for pyrolysis with capillary GC that may be used to reduce column contamination without decreasing chromatographic performance. More recently, Halket and Schulten⁵⁹ modified a Curie-point inlet system for capillary columns to permit better identification of all products, including less volatile products left behind in a quartz pyrolysis chamber.

In Py-GC or Py-MS systems, contamination may be caused by a cold spot that is trapping less volatile residue. To see if any temperature zones are set too low, temperature settings should be increased by small increments (without exceeding temperature limits of the column or instrument) and the results checked. Wrapping connecting tubing with heating tape or insulation may eliminate cold spots. Condensation losses due to cold spots can also severely limit the ability to observe higher molecular weight and less volatile components. Flexible fused-silica columns can be inserted directly into the pyrolysis interface near the pyrolyzer element at one end and threaded straight through to the FID flame tip or the MS ion source at the

other end. Contact with active surfaces is minimized, and more complete transfer of the pyrolysis products from the pyrolysis interface to the detector is achieved.

Similar considerations are important in Py-MS: cold spots and wall contact in the Py-MS vacuum systems can also affect transmission of pyrolysates.¹¹ Py-MS produces a pyrogram of all compounds in the pyrolysis product mixture superimposed in a single mass spectrum. For that reason, interpretation of Py-MS results from a complex sample can be more difficult than interpretation of a Py-GC/MS pyrogram, in which pyrolysis products are chromatographically separated before MS detection. As pointed out by Snyder et al.,⁵³ Py-MS with relatively cold pyrolysis interface walls or with expansion chambers tends to provide only low mass range analysis (under $m/z = 200$). When direct Py-MS is performed with the pyrolysis reactor close to the ion source, so as to detect larger mass pyrolysis products ($m/z = 200$ to 1000), the ion source tends to contaminate rather quickly, jeopardizing reproducibility.

Long-term reproducibility of pyrograms in Py-GC or Py-GC/MS depends on the lifetime of chromatographic columns. Fused-silica columns coated with polar bonded phases (such as the DB-1701 and FFAP columns mentioned above) have been used in our laboratory for periods longer than 1 year without appreciable degradation.

In any pyrolysis work, a valuable habit to acquire is the analysis of a standard sample at regular intervals between other samples. When “ghost peaks” appear in a pyrogram, analysis of the standard sample as a quality check, coupled with one or more of the ideas described above, may help resolve the contamination problem.

9.4 SELECTED APPLICATIONS

A summary of experimental conditions for selected analytical pyrolysis studies of microorganisms is given in Table 9.1. The literature review included here is not intended to be comprehensive but is designed to summarize selected recent applications of analytical pyrolysis to the analysis of microorganisms.

9.4.1 DISCRIMINATION OF GRAM POSITIVE AND GRAM NEGATIVE BACTERIA

Perhaps the simplest and most basic distinction made of microbial cells is that of Gram type, and numerous studies have assessed the value of analytical pyrolysis for this task. Early systematic studies included those of Simmonds⁶⁰ and Medley et al.,⁶¹ who correlated the formation of specific pyrolysis products with their site of origin in the microorganism. Pyrolysis products were assigned to protein, carbohydrate, nucleic acid, lipid, and porphyrin sources in the cell. Acetamide was identified in pyrograms of whole cells, and it was speculated that acetamide was produced from the N-acetyl groups on the glycan backbone of peptidoglycan (see Figure 9.2). Model compounds with chemical structures similar to substructures of PG were pyrolyzed by Hudson et al.⁶² and Eudy et al.⁶³ Only very low amounts of acetamide were found in pyrograms of glucosamine, muramic acid, and trialanine. Acetylated compounds such as N-acetyl glucosamine, N-acetyl muramic acid, and muramyl dipeptide produced much larger amounts of acetamide when pyrolyzed. It was not suggested that PG is the only source of acetamide in microbes, only that it is a major source. Levels

TABLE 9.1
Summary of Selected Experimental Conditions for Pyrolysis-GC and Pyrolysis-GC/MS of Microorganisms

Organism/Components	Pyrolysis Conditions	Stationary Phase	Column and Material	Detector	Reference
<i>Bacillus</i> species	Curie point, 510°C	—	—	VG Pyromass 8-80 Py-MS	80
Bacilli	CDS Pyroprobe, 650°C, 10-sec fast ramp	DB-1701	30 m × 0.329 mm id, 1-μ film fused silica	Hewlett-Packard MSDEI GC/MS	83
<i>B. cereus</i> , <i>B. globigii</i> spores, <i>B. subtilis</i> , MS-2 aldolase, <i>E. coli</i> , <i>Secale cereale</i> , coliphage, fog oil, diesel and wood smoke, pollen, type X, dry yeast	CDS Pyroprobe, 800°C, 5-sec fast ramp	FFAP	25 m × 0.25 mm id, 0.25-μ film fused silica	Hewlett-Packard MSDEI GC/MS	36
<i>B. cereus</i> , <i>B. licheniformis</i> , <i>B. subtilis</i> , <i>E. coli</i> , <i>S. aureus</i>	Curie point, 610°C	—	—	Extrel ELQ400; Extrel EL-400 triple-quadrupole MS, EI 79, 82	97
<i>B. subtilis</i> , <i>E. coli</i> , <i>M. tuberculosis</i>	Curie point, 610°C	—	—	Extrel EL-400 triple-quadrupole MS, EI	93
	Curie point, 358, 510, and 610°C	BP-1	12 m × 0.22 mm id, 0.15-μm film, fused silica	Perkin Elmer 8500 GC; Finnigan 700 MAT ion trap MS	98
<i>B. cereus</i> , <i>B. licheniformis</i> , <i>B. subtilis</i> , <i>B. thuringiensis</i> , <i>E. coli</i> , <i>S. aureus</i>	Curie point, 610°C	007-1, Quadrex methyl silicone	15 m × 0.250 mm id, 100%	Extrel EL-400 triple-quadrupole MS, EI; Varian 4000 GC	

Continued.

TABLE 9.1 (Continued)
Summary of Selected Experimental Conditions for Pyrolysis-GC and Pyrolysis-GC/MS of Microorganisms

Organism/Components	Pyrolysis Conditions	Stationary Phase	Column and Material	Detector	Reference
<i>B. anthracis</i> , <i>B. cereus</i> , <i>B. licheniformis</i> , <i>B. thuringiensis</i> , <i>B. subtilis</i> , <i>E. coli</i> , <i>P. fluorescens</i> , <i>S. albus</i> , <i>S. aureus</i>	CDS Pyroprobe, 1000°C, 20-sec fast ramp	BP-1	5 m × 0.25 m film, capillary	HP 5890 GC; Finnigan- MAT 700 ion trap MS	95
<i>B. cereus</i> , <i>B. subtilis</i> , <i>E. coli</i>	Curie point, 510°C	Methyl silicone	4 m × 0.25 mm id, fused silica	Extrel triple-quadrupole MS, CI	81
<i>Bacteroides gingivalis</i>	Curie point, 358 and 510°C	—	—	FOM Institute quadrupole MS	100
Biomaterials	Curie point, 500°C	DB-1	30 m × 0.32 mm id, 0.25- µm film, fused silica	Varian 3700 GC; Finnigan MAT 212 MS, EI/FID, FID	59
<i>E. coli</i> HB101, HB101(pSLM204)	Curie point 530°C	—	—	Horizon Instruments PYMS-200X quadrupole MS, EI	102
Flavobacterium	CDS Pyroprobe, 900°C, 10-sec fast ramp	Methyl silicone or SE-52	20 m × 0.21 mm id fused silica or 8-m glass capillary	Hewlett-Packard 5985 EI GC/MS	35

Gram positive, Gram negative, bacteria, and cell walls	CDS Pyroprobe, 800°C fast ramp	Carbowax 20M or Superox-4	20 m × 0.25 mm id glass capillary or 25 m × 0.2 mm id fused silica	Hewlett-Packard 5992 EI GC/MS; Finnigan EI GC/MS	62–64
Capsular polysaccharide from <i>Klebsiella</i>	CDS Pyroprobe, 650°C, 10 sec	DB-1701	30 m × 0.329 mm id, 1-μm film fused silica	Finnigan MAT GC/MS, EI/CI	87
Lipids, lipopolysaccharides, fatty acids	Direct CI, 570°C	—	—	Scientific Res. Instruments CI MS	99
<i>Listeria monocytogenes</i>	Curie point, 358°C	—	—	Spectral quadrupole MS	88
<i>Mycobacterial</i> /lipids	Curie point, 610°C	SE-30	5 m × 0.32 mm id fused silica	Finniganion trap GC/MS	94
		BP-1	5 m, 0.25 mm i.d., 1-μm film		
<i>Mycobacterial</i> /methyl mycolates	Curie point, 358°C	OV-1	3% (w/w) packed column, 1 m × 3 mm id	Hitachi EI GC/MS	90
Methylated microbial fatty acids	Curie point, 510°C	DB-5	7.2 m × 0.2 mm id fused silica, 0.11-μm film	Hewlett-Packard MSD, EI GC/MS, FID	92
<i>Penicillium italicum</i> /polysaccharides	DCI pyrolysis	—	—	Finnigan MAT HSQ-30	105
<i>Pseudomonas</i> and <i>Xanthomonas</i> bacteria	Curie point, 510°C	—	—	Extrel quadrupole MS	101
Streptococci/glucitol phosphate	CDS Pyroprobe, 800°C fast ramp	FFAP	25 m × 0.25 mm id fused silica EI GC/MS	Hewlett-Packard MSD	18, 37, 42, 75, 76

of acetamide were greater in pyrograms of Gram positive bacteria than in those of Gram negative bacteria.^{18,62,63} These results correlate well with the higher levels of PG found in Gram positive cells.^{18,64} A second pyrolysis product, propionamide, was also seen to originate in part from the lactyl-peptide bridge region of PG.⁶³ This pyrolysis product is not produced in sufficient amount and probably has other sources of origin in the microbial cell, so as not to be valuable for differentiating Gram type.¹⁸

Furfuryl alcohol has been suggested to derive in minor amounts from carbohydrates and in major amounts from RNA and DNA in microorganisms.^{60,61,63} As Gram negative bacteria have relatively thin cell walls compared with Gram positive bacteria, the higher levels of furfuryl alcohol in pyrograms of Gram negative bacteria may be due to intracellular DNA being more readily released from Gram negative bacteria.¹⁸ Although not directly related to Gram typing, a pyrolysis-GC/MS method for measuring DNA content of cultured cells was recently compared with results from an established colorimetric method based on reaction with diphenylamine.⁶⁵ The single-step procedure used cell samples containing 0.1 to 25 μg of DNA and had a detection limit of about 100 ng of DNA. Furfuryl alcohol from DNA was also found to be the source peak in pyrograms of virally transformed mammalian cells that could discriminate them from their normal counterparts.^{66,67} This was not surprising, as DNA levels are known to be higher in cancer cells.

Figure 9.4 shows relative amounts of acetamide and furfuryl alcohol measured in the GC/MS pyrograms of a group of microorganisms.¹⁸ Replicate pyrolysis results are connected by lines to indicate their reproducibility. Fungal samples included in this study as a control produced low levels of both pyrolysis products. Gram positive bacteria cluster toward higher levels of acetamide and moderate levels of furfuryl alcohol. Gram negative bacteria produced higher levels of furfuryl alcohol and moderate levels of acetamide. Diagonal lines (with no statistical significance) can be drawn separating the Gram positive and Gram negative groups. The data from some organisms are close to the dividing lines. Obviously, acetamide and furfuryl alcohol have other sources within cells and are not generally useful as specific chemical markers for bacterial PG. Morgan et al.¹⁸ concluded that it remains to be seen if individual bacteria can be Gram typed by analytical pyrolysis.

Adkins et al.⁴⁹ reported ions at $m/z = 166$ in negative ion mass spectra following pyrolysis of N-acetylglucosamine, chitin, and *B. subtilis* peptidoglycan. It has been speculated that larger pyrolysis products more specific for bacterial PG might be generated by pyrolysis, but a comprehensive study with diverse Gram positive and Gram negative bacteria has not validated this possibility. However, recent pyrolysis results from Voorhees⁶⁸ indicate that Gram typing may be more readily demonstrated with the higher selectivity of the triple-quadrupole MS.

9.4.2 ANALYSIS OF GRAM POSITIVE ORGANISMS

Streptococci have been popular targets for analytical pyrolysis,^{18,37,42,69–76} perhaps because their chemical composition has been well characterized by other techniques. One of the first papers describing additivity of pyrograms of individual components in a complex microbial pyrogram was published by Huis In't Veld et al.⁶⁹ The pyrogram of a streptococcal strain containing a polysaccharide cell wall antigen was

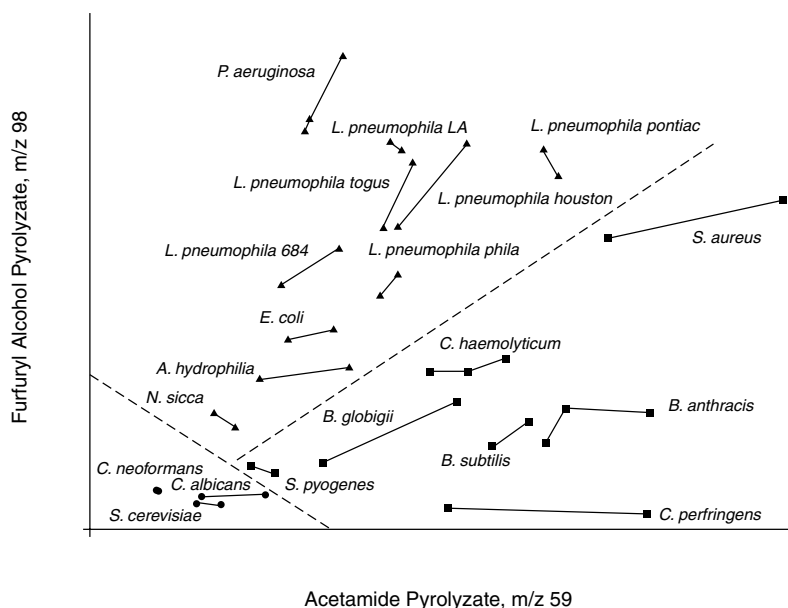


FIGURE 9.4 Plot of relative amounts of acetamide and furfuryl alcohol in a diverse group of microorganisms. Amounts are measured as the integrated reconstructed ion intensity ($m/z = 59$ for acetamide, $m/z = 98$ for furfuryl alcohol) at the appropriate retention time as a percentage of the total ion intensity. Gram positive bacteria are represented by squares, Gram negative bacteria by triangles, and fungi by circles. (Reproduced with permission from Morgan, S.L. et al., in *Analytical Microbiology Methods: Chromatography and Mass Spectrometry*, Fox, A. et al., Eds., Plenum Press, New York, 1990, chap. 12, pp. 179–200. Copyright 1990 Plenum Publishing Corporation.)

the sum of the pyrogram of its streptococcal mutant lacking this antigen and the pyrogram of the isolated antigen.

In a study involving 14 different strains, Smith et al.⁷⁵ found that group B streptococci (*Streptococcus agalactiae*) could be differentiated from group A streptococci by a single peak. Electron impact (EI) mass spectra of model compounds, including group B polysaccharide antigen and glucitol, suggested that the distinctive peak in the pyrogram of group B organisms was derived from glucitol phosphate residues in the group-specific polysaccharide. This carbohydrate-derived chemical marker for group B streptococci was identified by EI and methane CI MS as a dehydration product of glucitol-6-phosphate, dianhydroglucitol.¹⁸ Figure 9.5 shows this differentiation using selected ion monitoring to focus on the characteristic $m/z = 86$ ion of the dianhydroglucitol marker. Later studies using 29 different strains differentiated groups A, B, C, F, and G streptococci from one another.^{37,42,76} Group B pyrograms were clearly distinguishable from the other groups, and samples from groups A and F were usually classified correctly.³⁷ That group C and G strains were indistinguishable was not surprising because no commercial available system was capable of distinguishing these groups. The discrimination by pyrolysis was judged as good as that achievable by any technique except serogrouping.

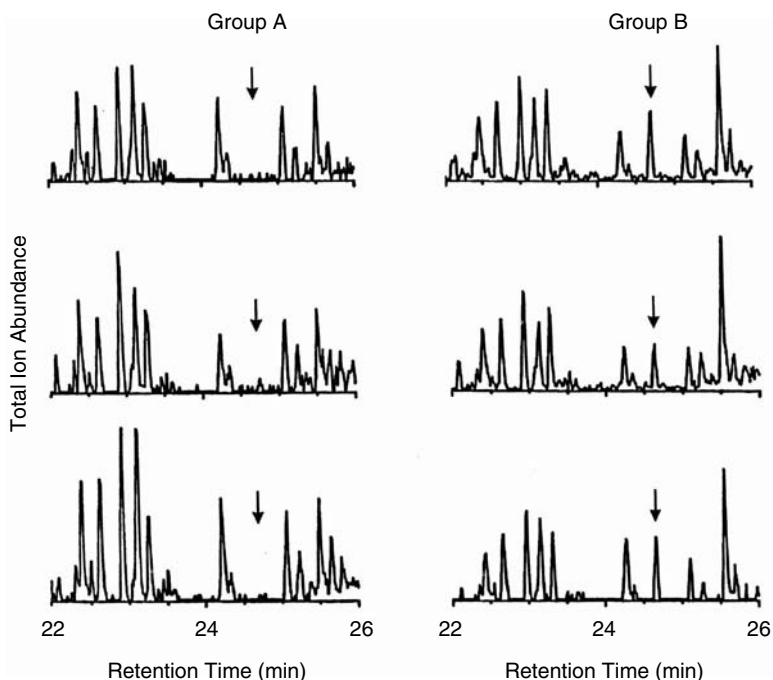


FIGURE 9.5 Discrimination of group A and group B streptococci shown in an expanded view of total ion abundance pyrograms in the region from 22 to 26 min. Pyrograms from three different samples of group A and group B isolates are shown. The peak marked with an arrow is dianhydroglucitol. Pyrolysis conditions: CDS model 120 Pyroprobe, 80- μ g sample, pyrolysis settings at 800°C and 75°C/msec. Chromatographic conditions: 25 m \times 0.24 mm FFAP fused-silica capillary, Hewlett-Packard model 5880A GC coupled to a model 5970 mass selective detector. (Reproduced with permission from Smith, C.S. et al., *Anal. Chem.*, 59, 1410–1413, 1987. Copyright 1987 American Chemical Society.)

Identification of staphylococci tends to be slow and irreproducible, and a commercially available system (APIStaph) only reduces identification time to 24 h.⁷⁷ Hindmarch and Magee⁷⁸ analyzed a total of 451 strains of staphylococci from a clinical investigation by Curie-point pyrolysis-GC. Samples were pyrolyzed at 610°C and packed GC columns were used to acquire pyrograms. After discarding some results from anomalous strains, discrimination by pyrolysis for only 60 of 415 strains was in disagreement with biochemical testing. At least a third of the misidentified strains were atypical.

Samples of a single *S. aureus* strain were pyrolyzed in an air atmosphere tube furnace and in a vacuum Curie-point pyrolyzer connected to a triple-quadrupole mass spectrometer.⁷⁹ Pyrograms of *S. aureus* were distinguishable from those of *E. coli* and *Bacillus* strains. Peaks related to fatty acids were identified in the mass pyrograms.

Curie-point pyrolysis MS was applied to the identification of selected *Bacillus* species by Shute et al.⁸⁰ Fifty-three strains of *B. subtilis*, *B. pumilus*, *B. licheniformis*, and *B. amyloliquefaciens* in both a sporulating and nonsporulating state were pyro-

lyzed at 510°C using a PyroMass 8-80 instrument (VG Gas Analysis, Middlewich, Cheshire, U.K.). The four strains could be differentiated by Py-MS from nonsporulated cultures. With sporulated cultures, the pyrograms were more similar and only *B. licheniformis* could be completely differentiated.

Adkins et al.⁴⁹ presented temperature-resolved pyrolysis mass spectra of cell fractions from Gram positive bacteria of the genus *Bacillus*. Culture conditions were found to play a major role in determining exact pyrolysis profiles. Figure 9.6 shows two pyrolysis mass spectra of *B. subtilis* samples grown under different conditions. Pyrolysis products were identified from amino sugars in peptidoglycan as well from teichoic acids present in the bacilli. In one of the first pyrolysis triple-quadrupole MS analyses of bacteria, Voorhees et al.⁸¹ compared Curie-point pyrograms of *B. cereus*, *B. subtilis*, and *E. coli*. Parent ion scans of daughter ions selected by pattern recognition were found to give the best identification of the three species. Morgan et al.¹⁷ reported that dipicolinic acid from sporulating organisms produces pyridine upon pyrolysis and found a pyridine peak to differentiate spore-forming and vegetative strains of *B. anthracis*. Voorhees et al.⁸² have also recently used pyrolysis-tandem MS to analyze samples of *B. subtilis*, *B. globigii*, *E. coli*, and other possible interferents (fog oil, diesel smoke, dry yeast, and pollen). Four useful markers for biological substances were identified: adenine from nucleic acids, diketopiperazine and indole from proteins, and pyridine from picolinic acid in sporulating bacteria.

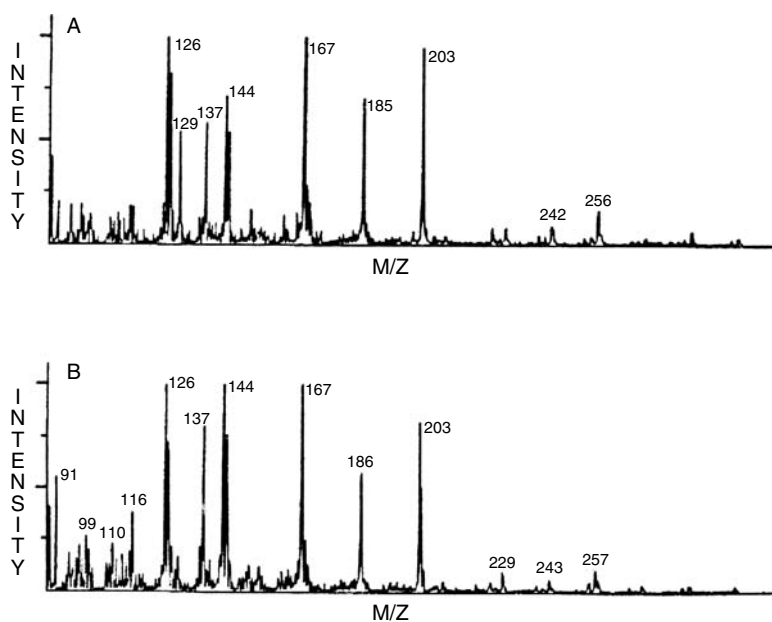


FIGURE 9.6 Pyrolysis mass spectra of *B. subtilis* grown (A) on minimal media and (B) in penassay broth. (Reproduced with permission from Adkins, J.A. et al., *J. Anal. Appl. Pyrol.*, 7, 15–33, 1984. Copyright 1984 Elsevier Science Publishers.)

A pyrolysis product of galactose was identified in *B. anthracis* by Fox et al.⁸³ The anhydrosugar 1,6-anhydro-galactopyranose was found in pyrograms of *B. anthracis* and was absent in pyrograms of *B. cereus*. The presence of galactose in *B. anthracis* was confirmed by an alditol acetate derivatization GC/MS method. The results support the assertions of Helleur et al.⁸⁴⁻⁸⁷ that analytical pyrolysis can be used for rapid carbohydrate profiling of complex biological samples such as microorganisms.

Samples of the Gram positive cocobacillus *Listeria monocytogenes* from infected patients and food sources were analyzed by Py-MS.⁸⁸ Samples within the serogroup could be differentiated to the extent that the strain obtained from the food was ruled out as a possible source for human infections. The independence of Py-MS from the labor-intensive use of reagent probes for classification of these organisms was noted by these researchers.

9.4.3 ANALYSIS OF GRAM NEGATIVE ORGANISMS

During the 1980s, organisms classified in the family Legionellaceae grew rapidly as new serogroups of *Legionella*-like organisms were identified. Pyrolysis-GC/MS with selected ion monitoring was used to differentiate 21 strains of *Legionella* organisms.⁶ Replicate samples (100 µg) were pyrolyzed at 800°C using a model 120 Pyroprobe (CDS Analytical), and 15 pyrolyzates were monitored by SIM GC/MS. The pyrograms of *Legionella pneumophila*, *Tatlockia micdadei*, and *Fluoribacter* could be distinguished from one another. In a Py-MS study of *Legionella* species, Kajioka and Tang⁸⁹ suggested that differences in ion profiles could be used to distinguish the various species from one another. Samples were pyrolyzed in a Curie-point pyrolyzer at 358°C and analyzed by a quadrupole mass spectrometer. Specific and reproducible pyrograms providing distinctive fingerprints for *Legionella* strains were obtained by Py-MS.

A pyrolysis fragment, 2-butenic acid, from the lipid substance poly-β-hydroxybutyrate present in microbial samples was identified by Watt et al.³⁶ The use of this pyrolysis product as a chemical marker was validated by correlating results from an extraction, hydrolysis, and derivatization GC/MS method; by growth trials that profiled PHB content as a function of culture age; and by comparative pyrolysis studies of a diverse group of organisms. PHB was shown to be common at moderate to high levels in the family Legionellaceae. Only background to low levels of PHB were in organisms of the family Enterobacteriaceae. Figure 9.7 compares total ion abundance GC/MS pyrograms and reconstructed ion $m/z = 86$ pyrograms for two organisms, *L. pneumophila* and *P. vulgaris*. In common with many other bacilli, *B. anthracis* was also found to contain PHB.

The bacterium *Klebsiella* is known to possess capsular polysaccharides. Helleur⁸⁷ studied isolated capsular polysaccharides from *Klebsiella* by pyrolysis-GC/MS. The polysaccharide is composed of repeating three glucopyranosyl units, one galactopyranosyl unit, one galactofuranosyl unit, one rhamnopyranosyl unit, and one glucouronosyl unit. Specific anhydrosugars produced upon pyrolysis for each type of saccharide unit were identified and quantified (Figure 9.8).

Pyrolysis-GC/MS of 32 species of mycobacteria for classification based upon the methyl ester fatty acid profiles was performed by Kusaka and Mori.⁹⁰ The

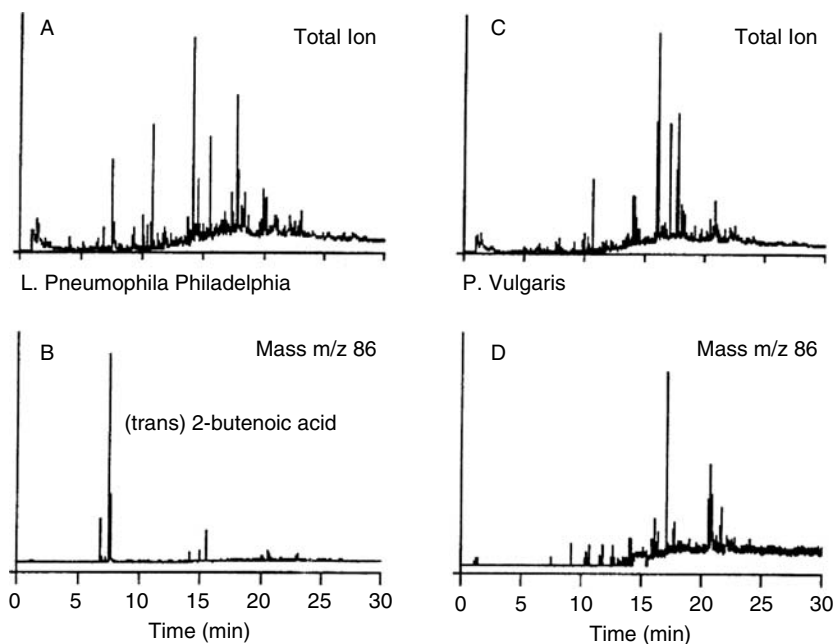


FIGURE 9.7 (A) Total ion abundance pyrogram of *L. pneumophila* Philadelphia. (B) Reconstructed ion pyrogram for ion mass $m/z = 86$ of *L. pneumophila* Philadelphia. Peak 3 is *trans*-2-butenic acid. (C) Total ion abundance pyrogram of *P. vulgaris*. (D) Reconstructed ion pyrogram for ion mass $m/z = 86$ of *P. vulgaris*. (Adapted with permission from Watt, B.E. et al., *J. Anal. Appl. Pyrol.*, 20, 237–250, 1991.)

mycobacteria were successfully classified into four groups: 22-group, C_{20} to C_{24} fatty acids with C_{22} predominating; 24-group, C_{22} to C_{24} fatty acids with C_{24} predominating; 24'-group, C_{22} to C_{26} fatty acids with C_{24} predominating; and 26-group, C_{22} to C_{26} fatty acids with C_{26} predominating.

Curie-point pyrolysis coupled with short-column GC interfaced to an ion trap mass spectrometer was employed by Snyder et al.^{53,91} to identify lipid components of microorganisms. A portion of the lipid component was further distinguished as dehydrated mono- and diacylglycerides. Discrimination of diverse microorganisms (four different bacilli, *S. aureus*, *E. coli*, and *L. pneumophila*) was performed by visual comparison of total ion chromatograms and selected reconstructed ion chromatograms.

Holzer et al.⁹² employed Curie-point pyrolysis to analyze microbial fatty acid by *in situ* methylation with trimethylanilinium hydroxide (TMAH). The fatty acid methyl ester profiles produced during pyrolysis of the whole cell agreed well with the analysis of lipid extracts from the same microorganism. Dworzanski et al.⁹³ also used pyrolytic methylation-GC to profile fatty acids in whole cells of *E. coli*, *Mycobacterium tuberculosis*, and *B. subtilis*. Curie-point pyrolysis coupled to GC/ion trap MS was used by Snyder et al.⁹⁴ to characterize 14 strains representing 9 bacterial species for their lipid biomarker content. A quartz tube Pyroprobe from

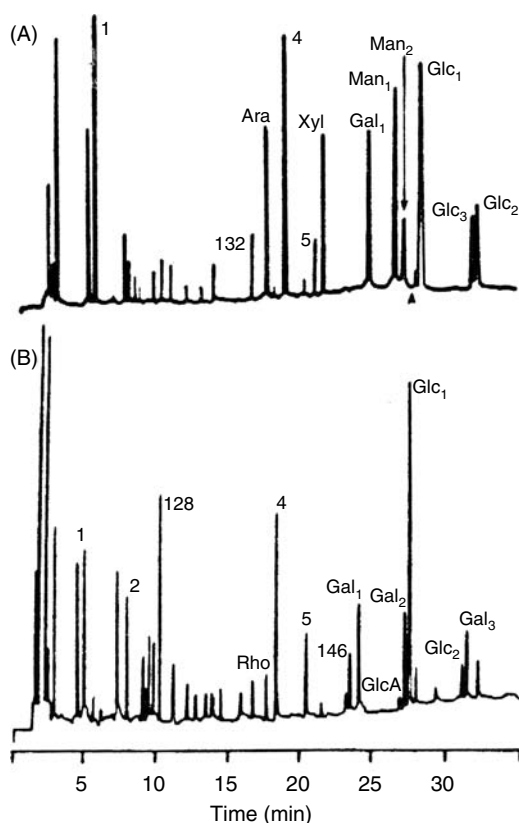


FIGURE 9.8 Capsular polysaccharides identified by pyrolysis GC/MS from *Klebsiella* K41 strains. (Reproduced with permission from Helleur, R.J., *J. Anal. Appl. Pyrol.*, 11, 297–311, 1987. Copyright 1987 Elsevier Science Publishers.)

CDS Analytical was used with GC/ion trap MS by Smith and Snyder⁹⁵ to analyze lipid and fatty acid components in a variety of bacteria with a total analysis time under 10 min. Snyder et al.⁹⁶ also used 13 strains of 8 bacterial species to demonstrate the use of Curie-point wire and quartz tube pyrolysis coupled to short-column GC/MS for the detection of biological warfare agents. Lipid and nucleic acid components were the primary target for discrimination purposes. Two articles by DeLuca et al.^{97,98} studied Curie-point pyrolysis-tandem MS for direct analysis of bacterial fatty acids. Py-MS results correlated well with previous Py-GC/MS data on the same bacteria. Interestingly, better classification results were obtained when just Py-MS fatty acid profiles were employed rather than total ion spectra.

Adkins et al.⁹⁹ also produced temperature-resolved pyrolysis results for cell envelope fractions and whole cells of *Salmonella typhimurium* and for several *Salmonella* LPS samples. Model compounds (fatty acids, phospholipids, cholines, etc.) for LPS structures were also pyrolyzed using linear-programmed thermal degradation strategies. Common ions were found in the Py-MS fingerprints of cell wall components and the model compounds. Boon et al.¹⁰⁰ applied Py-MS to the analysis

of samples from *Bacteroides gingivalis* isolated from dental patients. Pyrolysis mass spectra were dominated by volatile components, but clear differences were detected between related *Bacteroides* strains. A rule-building expert system was shown to be able to classify pyrolysis mass spectra from Gram negative *Pseudomonas* samples vs. samples containing *Xanthomonas*, a plant pathogen.¹⁰¹ Goodacre et al.¹⁰² demonstrated the use of Py-MS to detect the fimbrial adhesive antigen F41 from *E. coli* and to discriminate between bacteria that differ genotypically in that regard.

9.4.4 ANALYSIS OF FUNGI

Pyrolysis-GC fingerprints were obtained for fungal spores by Papa et al.¹⁰³ using packed-column chromatography with Carbowax 20M on 80–100 mesh Supelcoport. Papa et al.¹⁰⁴ also characterized several fungi, including *Agaricales*, *Boletus*, *Russula*, *Amanita*, *Lepiota*, *Agaricus*, and *Lycoperdon*. Pyrolysis coupled to capillary GC/MS was used to identify discriminating components. Among other results, it was noted that pyrograms of *B. calopus* and *B. bovinus* contained saturated and unsaturated aliphatic hydrocarbons and toluene. *B. bovinus* pyrograms contained esadecanoic acid.

Pyrolysis-direct CI MS was employed by Tas et al.¹⁰⁵ to detect ions related to polysaccharides in pyrograms of fungal *Penicillium italicum* strains. A series of Py-MS ions at $m/z = 167, 185, 187$, and 210 were identified as originating from N-acetylglucosamine residues, present at higher levels in the strain cultured in the presence of imazalil fungicide. Tas et al.¹⁰⁶ also used pyrolysis-direct CI MS to investigate differences between *Candida albicans* and *Ophiostoma ulmi* fungi. Hexoses, deoxyhexose, N-acetylglucosamine from chitin, and sterols in treated yeast samples could be detected in the pyrograms.

9.5 CONCLUSIONS

In his 1982 text on analytical pyrolysis, Irwin¹² described the ideal taxonomic method for the analysis of microorganisms: universally applicable to diverse microorganisms, capable of differentiating groups of organisms, reproducible independent of operator and system, rapid, sensitive, and capable of being both automated and interpreted in biochemical or chemical terms. At the time, Irwin also noted that “no comprehensive taxonomic scheme based on pyrograms of mass pyrograms had been proposed.”

The identification of pyrolysis products and their sources in intact organisms was not widespread in pyrolysis studies until the last decade. Classification and differentiation of organisms were often based on the relative peak heights of one or more peaks at a given retention time in the pyrogram. This simplistic approach can lead to erroneous conclusions when the chemical identities of pyrolysis products and their origin are unknown.

When pyrolysis is applied to a microbial sample, a complex mixture of thermal degradation products is produced. Analytical pyrolysis is often performed in a fingerprinting mode using sophisticated pattern recognition methods. However, if the chemical basis of pattern differences is not defined, pyrograms are so complex

that minor variations in instrumental conditions cause sufficient changes in patterns that making comparisons over extended time and between laboratories is a formidable task.

Ideally, pyrolysis products retain much of the structural integrity and chemical uniqueness of the original monomer so that their origin can be determined. Simple scission fragments may not retain as much chemical uniqueness of the parent structure as products such as those from dehydration, simple rearrangements, or generated by newer soft ionization methods and detected directly by MS. Many pyrolysis products are common organic compounds that could potentially be derived from multiple sources. Some pyrolysis products, although their origin may be well defined, may not be useful as chemical markers for bacterial discrimination.

By identifying specific chemicals in pyrograms as originating from taxonomically relevant microbial structures, discrimination may be based on well-defined features, simplifying this process dramatically. Invariant chemical features of the organism will provide effective discrimination if distinctive pyrolysis products can be generated under a wide range of experimental conditions. Furthermore, the discrimination thus achieved should be reproducible between different instruments and different laboratories. While quantitative amounts of pyrolysates generated may vary, the absence or presence of pyrolysis products due to a true chemotaxonomic marker should not depend dramatically on the choice of pyrolysis system.

Appropriate groups of organisms for chemotaxonomic studies involving pyrolysis can often be chosen on the basis of *a priori* information concerning microbial chemical structures. Interpretation is simplified by selecting groups of organisms, or cell fractions, that differ in defined structural characteristics. Analysis of bacteria possessing unrelated differences may not permit significance of a particular pyrolysis product to be evaluated. Organisms not containing particular known chemical structures act as a blank, indicating background levels produced from other sources. Analysis of multiple strains also confirms the consistency of correlations established among results from different organisms.

Automation of sampling is more readily accomplished using Py-MS than Py-GC/MS; however, better and automated sampling methods are needed for all forms of analytical pyrolysis. Absence of standard reference materials for many microbial components makes peak validation difficult and is a hindrance to systematic studies. Improved high-resolution capillary GC with inert polar phases capable of separating the complex mixture of pyrolysis products from microbial samples is needed. A new generation of MS techniques are evolving and being applied to microbiological problems: laser and plasma desorption, fast-atom bombardment, new chemical ionization approaches, and tandem MS. Many of these advances in MS detection will find their way into pyrolysis applications. Multiple detectors coupled in "hyphenated" modes will allow more thorough characterization of the microbial pyrolysis product mixture. Finally, advances in small computers are also driving data analysis techniques closer to the analytical instrument. The future may bring us closer to Irwin's ideal taxonomic method for the analysis of microorganisms.

REFERENCES

1. R.E. Buchanan and N.E. Gibbons, Eds., *Bergey's Manual of Determinative Bacteriology*, 8th ed., Williams and Wilkins, Baltimore (1974).
2. C.S. Cummins, in *Analytical Microbiology Methods: Chromatography and Mass Spectrometry*, A. Fox, S.L. Morgan, L. Larsson, and G. Odham, Eds., Plenum Press, New York, chap. 3, pp. 53–57 (1990).
3. S.L. Morgan, A. Fox, and J. Gilbert, *J. Microbiol. Methods*, 9: 57–69 (1989).
4. A. Fox, J. Gilbert, and S.L. Morgan, in *Analytical Microbiology Methods: Chromatography and Mass Spectrometry*, A. Fox, S.L. Morgan, L. Larsson, and G. Odham, Eds., Plenum Press, New York, chap. 1, pp. 1–17 (1990).
5. W.K. Joklik, H.P. Willet, and D.B. Amos, Eds., *Zinsser Microbiology*, 17th ed., Appleton-Century-Crofts, New York (1980).
6. A. Fox and S.L. Morgan, in *Instrumental Methods for Rapid Microbiological Analysis*, W.H. Nelson, Ed., VCH Publishers, Deerfield Beach, FL, chap. 5, pp. 135–164 (1985).
7. P.D. Zeman, *Anal. Chem.*, 24: 709 (1952).
8. V.I. Oyama, *Nature (London)*, 200: 1058 (1963).
9. E. Reiner, *Nature*, 206: 1272 (1965).
10. C.S. Gutteridge and J.R. Norris, *J. Appl. Bacteriol.*, 47: 5 (1979).
11. H.L.C. Meuzelaar, J. Haverkamp, and F.D. Hileman, *Pyrolysis Mass Spectrometry of Recent and Fossil Biomaterials*, Elsevier, Amsterdam (1982).
12. W.J. Irwin, *Analytical Pyrolysis: A Comprehensive Guide*, Marcel Dekker, New York (1982).
13. G. Wieten, H.L.C. Meuzelaar, and J. Haverkamp, in *Gas Chromatography/Mass Spectrometry Applications in Microbiology*, G. Odham, L. Larsson, and P.-A. Maardh, Eds., Plenum, New York, chap. 10, pp. 335–380 (1984).
14. F.L. Bayer and S.L. Morgan, in *Pyrolysis and GC in Polymer Analysis*, E.J. Levy and S. Liebman, Eds., Marcel Dekker, New York, chap. 6, pp. 277–337 (1985).
15. T.P. Wampler, *J. Anal. Appl. Pyrol.*, 16: 291–322 (1989).
16. G.A. Eiceman, W. Windig, and A.P. Snyder, in *Gas Chromatography: Biochemical, Biomedical, and Clinical Applications*, R.E. Clement, Ed., John Wiley & Sons, New York, chap. 12, pp. 327–347 (1990).
17. S.L. Morgan, A. Fox, J.C. Rogers, and B.E. Watt, in *Modern Techniques for Rapid Microbiological Analysis*, W.H. Nelson, Ed., VCH Publishers, New York, chap. 1, pp. 1–18 (1991).
18. S.L. Morgan, B.E. Watt, K. Ueda, and A. Fox, in *Analytical Microbiology Methods: Chromatography and Mass Spectrometry*, A. Fox, S.L. Morgan, L. Larsson, and G. Odham, Eds., Plenum Press, New York, chap. 12, pp. 179–200 (1990).
19. J. Postgate, *Microbes and Man*, 3rd ed., Cambridge University Press, Cambridge, U.K. (1992).
20. J.D. Watson, N.H. Hopkins, J.W. Roberts, J.A. Steitz, and A.M. Weiner, *Molecular Biology of the Gene*, 4th ed., The Benjamin/Cummings Publishing Company, Menlo Park, CA, pp. 101 (1987).
21. H.J. Rogers, *Bacterial Cell Structure*, Van Nostrand Reinhold Co. Ltd., Wokingham, Berkshire, U.K. (1983).
22. H.J. Rogers, H.R. Perkins, and J.B. Ward, *Microbial Cell Walls and Membranes*, Chapman & Hall, London (1980).
23. K.H. Schliefer and O. Kandler, *Bacteriol. Rev.*, 36: 407 (1972).

24. K. Ueda, S.L. Morgan, A. Fox, A. Sonesson, L. Larsson, and G. Odham, *Anal. Chem.*, 61: 265–270 (1989).
25. A. Fox, K. Ueda, and S.L. Morgan, in *Analytical Microbiology Methods: Chromatography and Mass Spectrometry*, A. Fox, S.L. Morgan, L. Larsson, and G. Odham, Eds., Plenum Press, New York, chap. 6, pp. 89–99 (1990).
26. J. Baddiley, in *Essays in Biochemistry*, Vol. 8, P.N. Campbell and F. Dickens, Eds., Academic Press, London, pp. 35–78 (1972).
27. O. Luderitz, O. Westphal, A.M. Staub, and H. Nikaido, in *Microbial Endotoxins*, Vol. 4, G. Weingbaum, S. Kadis, and S.J. Ayl, Eds., Academic Press, London, pp. 145–223 (1971).
28. C.W. Moss, in *Analytical Microbiology Methods: Chromatography and Mass Spectrometry*, A. Fox, S.L. Morgan, L. Larsson, and G. Odham, Eds., Plenum Press, New York, chap. 4, pp. 59–69 (1990).
29. V. Holdeman, E.P. Cato, and W.C. Moore, *Anaerobe Laboratory Manual*, 4th ed., Virginia Polytechnic Institute and State University, Anaerobe Laboratory, Blacksburg (1977).
30. L. Miller and T. Berger, Bacteria identification by gas chromatography of whole cell fatty acids, *Hewlett-Packard Application Note* 228: 41 (1985).
31. A. Fox, S.L. Morgan, and J. Gilbert, in *Analysis of Carbohydrates by GLC and MS*, C.J. Bierman and G. McGinnis, Eds., CRC Press, Boca Raton, FL (1989).
32. D.G. Pritchard, B.M. Gray, and H.C. Dillon, *Arch. Biochem. Biophys.*, 235: 385 (1984).
33. A. Fox, J.C. Rogers, J. Gilbert, S.L. Morgan, C.H. Davis, S. Knight, and P.B. Wyrick, *Infect. Immun.*, 58: 835–837 (1990).
34. C.S. Gutteridge and J.R. Norris, *Appl. Environ. Microbiol.*, 40: 462 (1980).
35. H. Engman, H.T. Mayfield, T. Mar, and W. Bertsch, *J. Anal. Appl. Pyrol.*, 6: 137 (1984).
36. B.E. Watt, S.L. Morgan, and A. Fox, *J. Anal. Appl. Pyrol.*, 20: 237–250 (1991).
37. C.S. Smith, S.L. Morgan, C.D. Parks, and A. Fox, *J. Anal. Appl. Pyrol.*, 18: 97–115 (1990).
38. *NIH Biohazards Safety Guide*, U.S. Department of Health, Education, and Welfare, Washington, DC (1974).
39. Occupational Safety and Health Administration, U.S. Department of Labor, *Occupational Safety and Health Standards for General Industry (29 CFR Part 1910)*, Commerce Clearing House, Chicago (1969).
40. W. Windig, *J. Anal. Appl. Pyrol.*, 17: 283–289 (1990).
41. G. Montaudo, *J. Anal. Appl. Pyrol.*, 13: 1–7 (1988).
42. J. Gilbert, A. Fox, and S.L. Morgan, *Eur. J. Clin. Microbiol.*, 6: 715–723 (1987).
43. T.P. Wampler and E.J. Levy, *J. Anal. Appl. Pyrol.*, 12: 75–82 (1987).
44. H.L.C. Meuzelaar and R.A. In't Veld, *J. Chromatogr. Sci.*, 10: 213–216 (1972).
45. W. Windig, P.G. Kistemaker, J. Haverkamp, and H.L.C. Meuzelaar, *J. Anal. Appl. Pyrol.*, 1: 39–52 (1979).
46. W. Windig, P.G. Kistemaker, J. Haverkamp, and H.L.C. Meuzelaar, *J. Anal. Appl. Pyrol.*, 2: 7–18 (1980).
47. A. van der Kaaden, R. Hoogerbrugge, and P.G. Kistemaker, *J. Anal. Appl. Pyrol.*, 9: 267 (1986).
48. G. Wells, K.J. Voorhees, and J.H. Futrell, *Anal. Chem.*, 52: 1782 (1980).
49. J.A. Adkins, T.H. Risby, J.J. Scocca, R.E. Yasbin, and J.W. Ezzell, *J. Anal. Appl. Pyrol.*, 7: 15–33 (1984).
50. G.L. French, I. Phillips, and S. Chin, *J. Gen. Microbiol.*, 125: 347 (1981).

51. G.L. French, H. Talsania, and I. Philips, *Med. Microbiol.*, 29: 19 (1989).
52. M.L. Trehy, R.A. Yost, and J.G. Dorsey, *Anal. Chem.*, 58: 14 (1986).
53. A.P. Snyder, W.H. McClennen, and H.L.C. Meuzelaar, in *Analytical Microbiology Methods: Chromatography and Mass Spectrometry*, A. Fox, S.L. Morgan, L. Larsson, and G. Odham, Eds., Plenum Press, New York, chap. 13, pp. 201–217 (1990).
54. P.A. Quinn, *J. Chromatogr. Sci.*, 12: 796–806 (1974).
55. H.L.C. Meuzelaar, H.G. Ficke, and H.C. den Harink, *J. Chromatogr. Sci.*, 13: 12–17 (1975).
56. J.E. Purcell, H.D. Downs, and L.S. Ettre, *Chromatographia*, 8: 605–616 (1975).
57. A. Mitchell and M. Needleman, *Anal. Chem.*, 50: 668–669 (1978).
58. Y. Sugimura and S. Tsuge, *Anal. Chem.*, 50: 1968–1972 (1978).
59. J.M. Halket and H.-R. Schulten, *J. High Resolut. Chromatogr. Chromatogr. Commun.*, 9: 596–597 (1986).
60. P.G. Simmonds, *Appl. Microbiol.*, 20: 567 (1970).
61. E.E. Medley, P.G. Simmonds, and S.L. Mannatt, *Biomed. Mass Spectrom.*, 2: 261 (1975).
62. J.R. Hudson, S.L. Morgan, and A. Fox, *Anal. Biochem.*, 120: 59–65 (1982).
63. L.W. Eudy, M.D. Walla, J.R. Hudson, S.L. Morgan, and A. Fox, *J. Anal. Appl. Pyrol.*, 7: 231–247 (1985).
64. L.W. Eudy, M.D. Walla, S.L. Morgan, and A. Fox, *Analyst*, 110: 381–385 (1985).
65. R.S. Sahota, S.L. Morgan, and K.E. Creek, *J. Anal. Appl. Pyrol.*, 24: 107–122 (1992).
66. R.S. Sahota and S.L. Morgan, *Anal. Chem.*, 64: 2383–2392 (1992).
67. R.S. Sahota, S.L. Morgan, K.E. Creek, and L. Pirisi, unpublished manuscript (1994).
68. K.J. Voorhees, Department of Chemistry and Geochemistry, Colorado School of Mines, Golden, CO, personal communication (1994).
69. J.H.J. Huis In't Veld, H.L.C. Meuzelaar, and A. Tom, *Appl. Microbiol.*, 26: 92–97 (1973).
70. M.V. Stack, H.D. Donoghue, J.E. Tyler, and M. Marshall, in *Analytical Pyrolysis*, C.E.R. Jones and C.A. Cramers, Eds., Elsevier, Amsterdam, p. 57 (1977).
71. M.V. Stack, H.D. Donoghue, and J.E. Tyler, *Appl. Environ. Microbiol.*, 35: 45 (1980).
72. G.L. French, I. Phillips, and S. Chin, *J. Gen. Microbiol.*, 125: 347 (1981).
73. M.V. Stack, H.D. Donoghue, and J.E. Tyler, *J. Anal. Appl. Pyrol.*, 3: 221 (1981/1982).
74. G.L. French, H. Talsania, and I. Phillips, *Med. Microbiol.*, 29: 19 (1989).
75. C.S. Smith, S.L. Morgan, C.D. Parks, A. Fox, and D.G. Pritchard, *Anal. Chem.*, 59: 1410–1413 (1987).
76. A. Fox, J. Gilbert, B. Christensson, and S.L. Morgan, in *Rapid Methods and Automation in Microbiology and Immunology*, A. Balows, R.C. Titon, and A. Turano, Eds., Brixia Academic Press, Brescia, Italy, pp. 379–388 (1989).
77. Y. Brun, J. Fleurette, and F. Forey, *J. Clin. Microbiol.*, 8: 503–508 (1978).
78. J.M. Hindmarch and J.T. Magee, *J. Anal. Appl. Pyrol.*, 11: 527–538 (1987).
79. S.J. DeLuca and K.J. Voorhees, *J. Anal. Appl. Pyrol.*, 24: 211–225 (1993).
80. L.A. Shute, C.S. Gutteridge, J.R. Norris, and R.C.W. Berkeley, *J. Gen. Microbiol.*, 130: 343–355 (1984).
81. K.J. Voorhees, S.L. Durfee, J.R. Holtzclaw, C.G. Enke, and M.R. Bauer, *J. Anal. Appl. Pyrol.*, 14: 7 (1988).
82. K.J. Voorhees, S.J. DeLuca, and A. Noguerola, *J. Anal. Appl. Pyrol.*, 24: 1–21 (1992).
83. A. Fox, G. Black, K. Fox, and S. Rostovtseva, *J. Clin. Microbiol.*, 31: 887–894 (1993).
84. D.R. Budgell, E.R. Hayes, and R.J. Helleur, *Anal. Chim. Acta*, 192: 243 (1987).
85. R.J. Helleur, E.R. Hayes, J.S. Craigie, and J.L. MacLachlan, *J. Anal. Appl. Pyrol.*, 8: 349 (1985).

86. R.J. Helleur, D.R. Budgell, and E.R. Hayes, *Anal. Chim. Acta*, 192: 367 (1987).
87. R.J. Helleur, *J. Anal. Appl. Pyrol.*, 11: 297–311 (1987).
88. R. Kajioka and M.A. Noble, *J. Anal. Appl. Pyrol.*, 22: 29–38 (1991).
89. R. Kajioka and P.W. Tang, *J. Anal. Appl. Pyrol.*, 6: 59–68 (1984).
90. T. Kusaka and T. Mori, *J. Gen. Microbiol.*, 132: 3403 (1986).
91. A.P. Snyder, W.H. McClennen, J.P. Dworzanski, and H.L.C. Meuzelaar, *Anal. Chem.*, 62: 2565–2573 (1990).
92. G. Holzer, T.F. Bourne, and W. Bertsch, *J. Chromatogr.*, 468: 181 (1989).
93. J.P. Dworzanski, L. Berwald, and H.L.C. Meuzelaar, *Appl. Environ. Microbiol.*, 56: 1717–1724 (1990).
94. A.P. Snyder, W.H. McClennen, J.P. Dworzanski, and H.L.C. Meuzelaar, *Anal. Chem.*, 62: 2565–2573 (1990).
95. P.B. Smith and A.P. Snyder, *J. Anal. Appl. Pyrol.*, 24: 23–38 (1992).
96. A.P. Snyder, P.B.W. Smith, J.P. Dworzanski, and H.L.C. Meuzelaar, in *Mass Spectrometry for the Characterization of Microorganisms*, ACS Symposium Series 541, C. Fenselau, Ed., American Chemical Society, Washington, DC, chap. 5, pp. 63–84 (1994).
97. S.J. DeLuca, E.W. Sarver, P. De B. Harrington, and K.J. Voorhees, *Anal. Chem.*, 62: 1465–1472 (1990).
98. S.J. DeLuca, E.W. Sarver, and K.J. Voorhees, *J. Anal. Appl. Pyrol.*, 23: 1–14 (1992).
99. J.A. Adkins, T.H. Risby, J.J. Scocca, R.E. Yasbin, and J.E. Ezzell, *J. Anal. Appl. Pyrol.*, 7: 35–51 (1984).
100. J.J. Boon, A. Tom, B. Brandt, G.B. Eijkel, P.G. Kistemaker, F.J.W. Notten, and F.H.M. Mikx, *Anal. Chim. Acta*, 163: 193–205 (1984).
101. P.B. Harrington, T.E. Street, K.J. Voorhees, F.R. Brozolo, and R.W. Odom, *Anal. Chem.*, 61: 715–719 (1989).
102. R. Goodacre, R.C.W. Berkeley, and J.E. Beringer, *J. Anal. Appl. Pyrol.*, 22: 19–28 (1991).
103. G. Papa, P. Balbi, and G. Audisio, *J. Anal. Appl. Pyrol.*, 11: 539–548 (1987).
104. G. Papa, P. Balbi, and G. Audisio, *J. Anal. Appl. Pyrol.*, 15: 137 (1989).
105. A.C. Tas, A. Kerkenaar, G.F. LaVos, and J. Van der Greef, *J. Anal. Appl. Pyrol.*, 15: 55–70 (1989).
106. A.C. Tas, H.B. Bastiaanse, J. Van der Greef, and A. Kerkenaar, *J. Anal. Appl. Pyrol.*, 14: 309–321 (1989).

10 Analytical Pyrolysis of Polar Macromolecules*

Charles Zawodny and Karen Jansson

CONTENTS

10.1 Introduction	233
10.2 Synthetic Polymers	234
10.2.1 Poly(methacrylates).....	234
10.2.2 Polyesters	237
10.3 Surfactants.....	240
10.4 Sulfur-Containing Macromolecules	243
10.5 Natural Polymers.....	244
10.5.1 Cellulose.....	244
10.5.2 Chitin and Chitosan	245
10.5.3 Proteins.....	246
10.6 Summary	246
References.....	248

10.1 INTRODUCTION

There is a wide range of polymers that are polar in their compositional makeup. These macromolecules can be produced in numerous ways, including chain growth polymerization and step growth polymerization.¹ Chain growth polymerization involves a rapid macromolecule formation that suddenly stops. Step growth polymerization exhibits condensation kinetics. It includes not only small molecule removal, but also reactions in which there is no small molecule removal. Analytical pyrolysis can be a useful qualitative as well as quantitative tool in the characterization of these macromolecules.

Pyrolysis of these macromolecules produces characteristic pyrogram (pyrolysis chromatogram) profiles that are indicative of the polymers. Individual fragments help in the deconstruction or deformation of the polymer. Many polar macromolecular systems produce high yields of monomer by pyrolysis, which aids in the qualification and the quantitation of polymers as well as copolymer systems. This type of information can be valuable not only in terms of characterizing the polymer, but also in

* This chapter was based on the original work of the late John W. Washall.

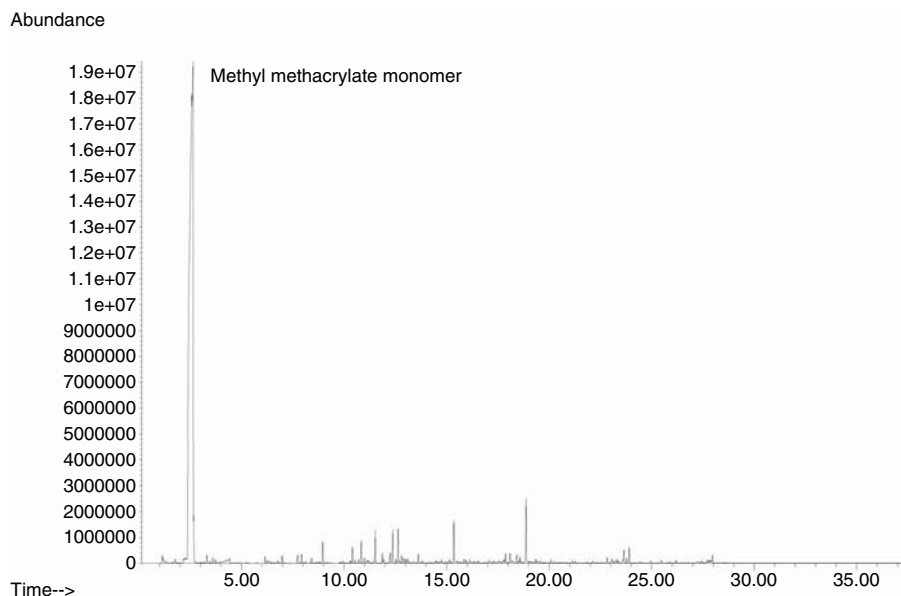


FIGURE 10.1 Pyrolysis of poly(methyl methacrylate) at 750°C.

performing degradation studies. This chapter will briefly discuss synthetic polymers as well as natural polymers and the information that can be obtained using pyrolysis.

10.2 SYNTHETIC POLYMERS

10.2.1 POLY(METHACRYLATES)

Poly(methacrylates) fit into a class of polymers that tend to undergo depolymerization under pyrolysis conditions. When poly(methyl methacrylate) (PMMA) is pyrolyzed, it yields primarily the monomer, methyl methacrylate. This process begins by initial cleavage of the skeletal backbone of the polymer, forming two free radical ends. Subsequent beta scissions produce an unwinding effect as sequential monomer units are formed. Once initiated, this process proceeds down the entire length of the polymer and is known as unzipping. Figure 10.1 shows a typical pyrogram of poly(methyl methacrylate) pyrolyzed at 750°C for 15 seconds. From this pyrogram, it is clearly evident how extensively the depolymerization process works.

Figure 10.2 shows the mechanistic description of depolymerization initiation and product formation for methacrylate polymers. From the literature concerning monomer yields for poly(methyl methacrylate), typical values are 92 to 98% recovery of methyl methacrylate monomer.

These recovery values are fairly consistent regardless of pyrolysis temperature and heating rates. It seems that in the case of PMMA, as long as there is sufficient energy delivered to the sample in order to break a C–C bond, depolymerization occurs readily.

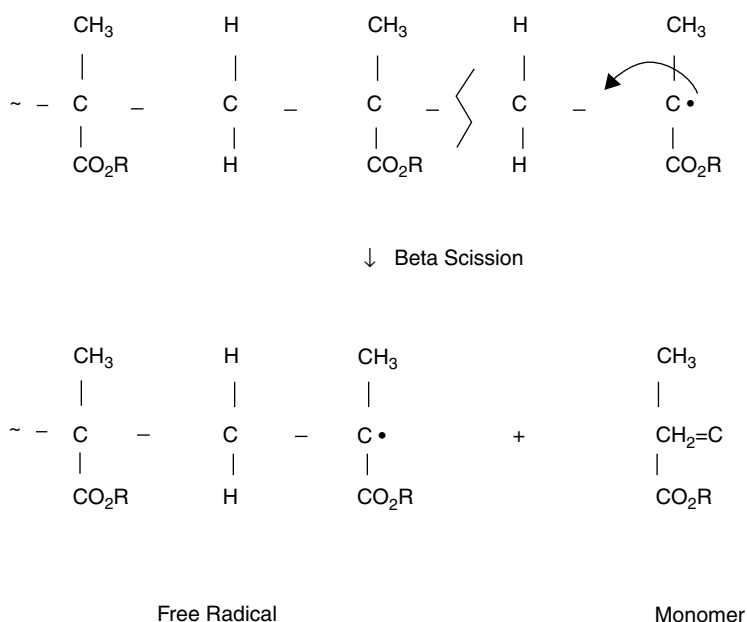


FIGURE 10.2 Depolymerization mechanism for poly(methacrylates).

Pyrolysis of methacrylate polymers tends to get more complex as the length of the R group increases. Because of increasing length and increased steric interactions, the amount of depolymerization may be reduced. This increases the probability that products other than the monomer will be produced. For instance, the pyrogram of poly(butyl methacrylate) (PBMA) is shown in Figure 10.3. The monomer yield for PBMA is in the 93 to 95% range. Minor products include 1-butanol, butyl acrylate, 1-propene, 2-methyl-1-propene, and butanal. Among these minor products, 1-butanol is the most abundant and is formed as a result of cleavage of the ethereal C–O bond of the ester group.

The last methacrylate polymer example is poly(lauryl methacrylate) (PLMA). This polymer is interesting because it contains an extremely long R group. Having such a long hydrocarbon chain dangling from the polymer backbone makes it much easier to cleave. The result is a pyrolyzate composed not only of lauryl methacrylate monomer, but also of many unsaturated hydrocarbons as the result of random scission reactions in the chain of the C₁₂ group. Figure 10.4 shows an example of PLMA pyrolyzed at 750°C. There is quite a noticeable repeating series of peaks between 10 and 16 minutes in the pyrogram, corresponding to the various monounsaturated hydrocarbons. In this particular example, the yield for lauryl methacrylate was 68%. This value is much lower than those obtained for PMMA and PBMA, which may be attributed to the length of the R group.

The qualitative aspect of methacrylate polymer pyrolysis and the quantitative determination of recovered monomer have been described. What remains to be discussed is a quantitative assessment of monomeric composition in a copolymer

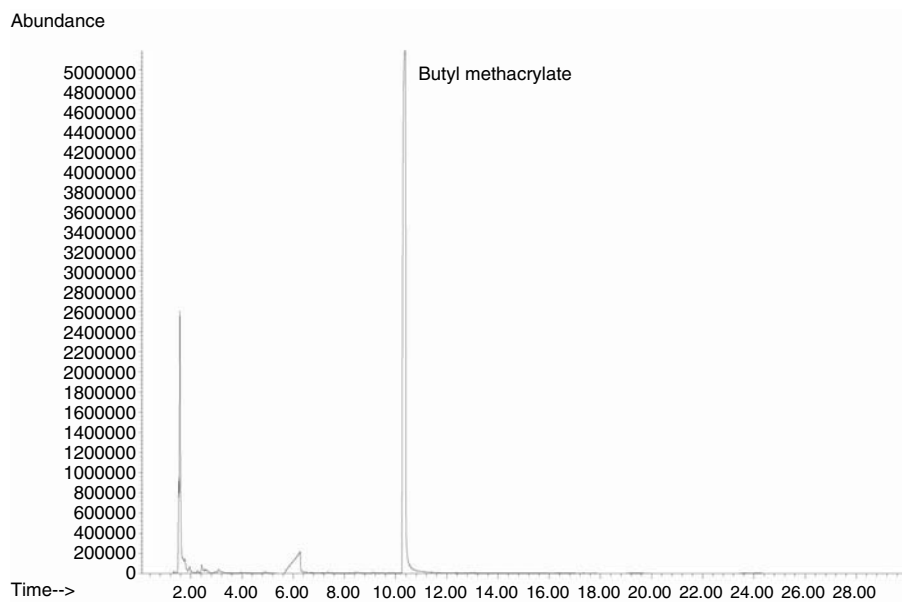


FIGURE 10.3 Pyrogram of poly(butyl methacrylate) pyrolyzed at 750°C. The small peak at > 6 minutes is methacrylic acid.

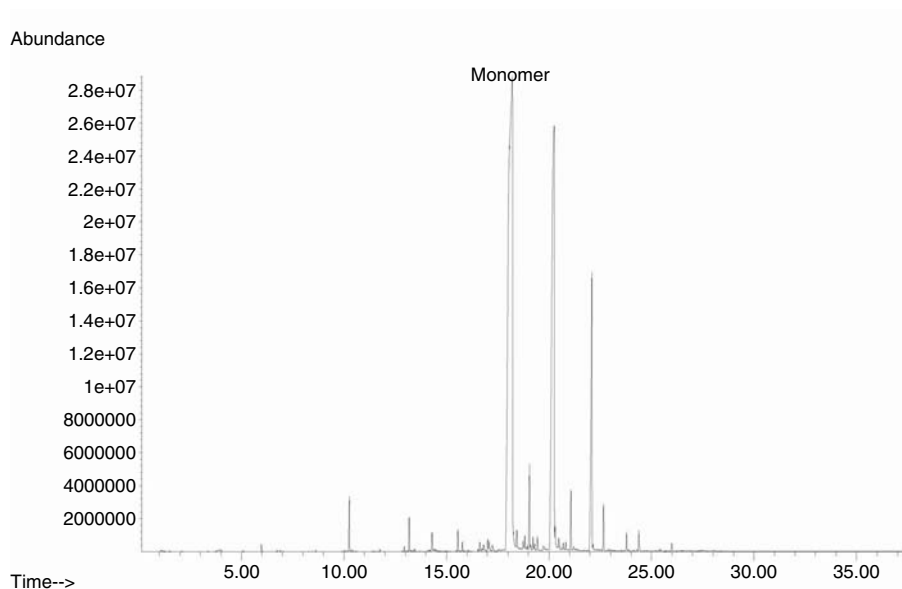


FIGURE 10.4 Pyrolysis of poly(lauryl methacrylate) at 750°C.

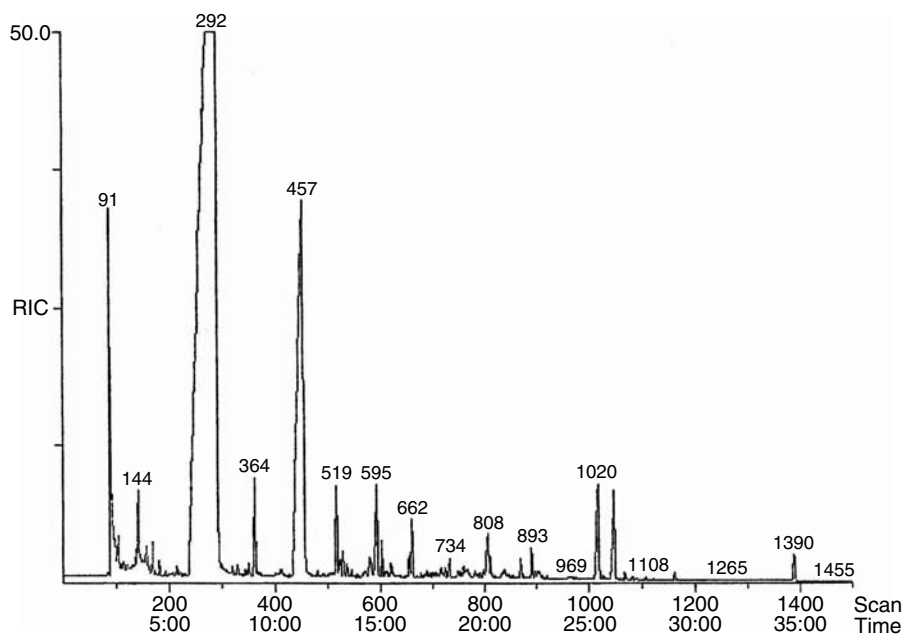


FIGURE 10.5 Pyrolysis of copolymer (30% methyl methacrylate, 70% butyl acrylate) at 600°C.

sample. It is often helpful for quality purposes to know the composition of a copolymer product. One copolymer system that has been studied extensively using pyrolysis is poly(methyl methacrylate/butyl acrylate). A pyrogram of this copolymer is shown in Figure 10.5. The two primary peaks in this pyrogram correspond to the respective monomers. A series of such copolymers with varying concentrations of monomers can be pyrolyzed in order to obtain a calibration curve by plotting the peak area ratios for compounds generated from each of the monomers vs. concentration. A typical calibration curve is shown in Figure 10.6, plotting the area ratio of the methyl methacrylate peak to the butanol peak against the concentration of methyl methacrylate. Proper calibration of the pyrolyzer makes it possible to obtain linear quantitative relationships for most polymeric systems.

10.2.2 POLYESTERS

Pyrolysis of polyesters shows some interesting thermal degradation mechanisms. Polyesters can be made from a variety of monomers, a common example being polyethylene terephthalate (PET; made from ethylene glycol and phthalic acid). This material produces a number of primary products upon pyrolysis,² which are shown in Figure 10.7. Benzene and biphenyl are by far the most abundant products from the pyrolysis of PET at 600°C for 15 seconds. The reaction mechanism for the formation of benzene proceeds first through an intramolecular rearrangement involving the carbonyl oxygen with a $-\text{CH}_2$ hydrogen atom (beta to the ethereal oxygen)

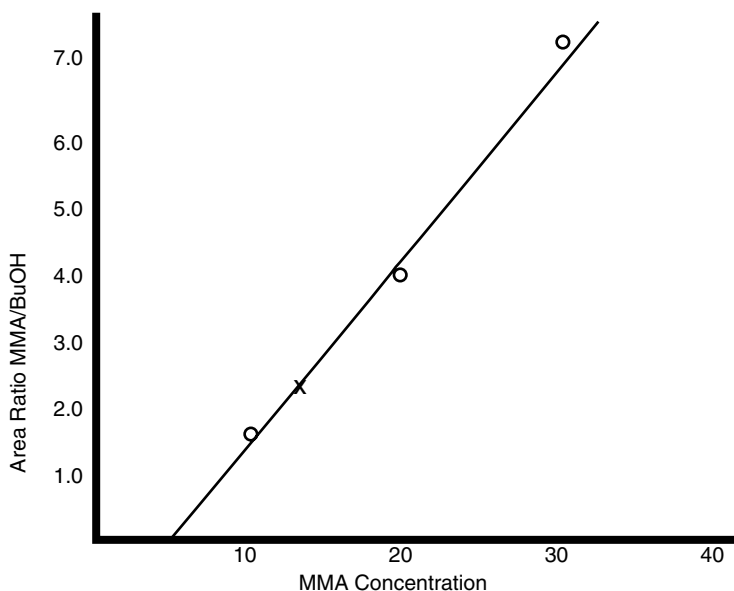


FIGURE 10.6 Graph of peak area ratio of methyl methacrylate monomer (from PMMA) to butanol (from PBA) vs. the concentration of methyl methacrylate in the copolymer.

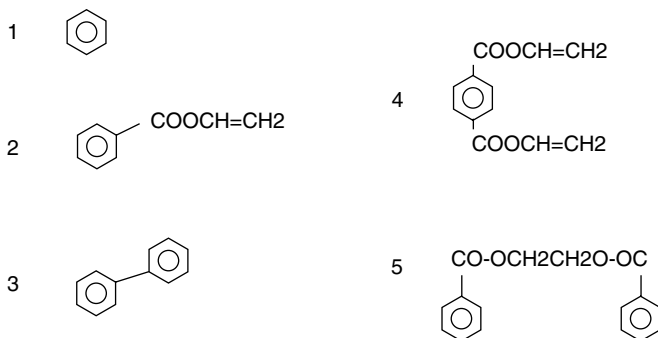


FIGURE 10.7 Five principal pyrolysis products from polyethyleneglycol terephthalate. (Adapted from Ref. 5.)

in a 1,5-hydrogen shift. Decarboxylation and subsequent random scission account for the formation of the very stable products benzene and biphenyl.

In the pyrolysis of polar macromolecules, stability of the final products plays a crucial role in determining the relative product abundances. With polyesters, the polymer generally unzips to give the original monomer unit. However, when ester copolymers are pyrolyzed, a number of other reactions are likely. For instance, a polyester prepared by the reaction of chlorinated norbornene dicarboxylic acid, maleic anhydride, and 1,2-propanediol in vacuum produces an unsaturated polyester. Pyrograms of this unsaturated polyester³ show the following major pyrolysis products: 1,2,3,4,5-pentachlorocyclopenta-1,3-diene and 1,2,3,4,5,5-hexachlorocyclopenta-1,3-

diene. The monomer yield in this case was very small. Product formation takes place via retro-Diels Alder reactions because of the presence of various polychloro-5-norbornene-dicarboxylic acid units in the backbone of the polymer.

In the case of styrene-cured unsaturated polyesters, these polymers showed increased quantities of toluene, ethylbenzene, and alpha-methylstyrene in their pyrograms. Interestingly, dimer formation was not seen under these circumstances. It is believed that chlorine radicals participate to prohibit dimer formation through transfer reactions. The result of this reaction is the formation of phenylalkyl chlorides.⁴

Structural determination often hinges on identification of higher-molecular-weight pyrolysis fragments. For this reason, it may be necessary to choose a pyrolysis temperature that gives a product distribution that favors formation of dimeric, trimeric, and higher units. This provides information on the arrangement of the various monomer units and will also provide an insight as to whether a copolymer is random or a block copolymer. For example, a styrene-glycidyl methacrylate copolymer shows monomer, dimer, and co-dimer fragments in the pyrogram.⁵

Many acrylic copolymers are currently used in the textile industry as binders for nonwoven fabrics. The purpose of these fibers is to stabilize the material. In many instances, these copolymers are used in conjunction with amino resins. Casanovas and Rovira⁵ have done a study of methyl methacrylate-ethyl acrylate-N-methylol-acrylamide by PY/GC-MS. Among the products identified were methane, ethylene, propene, isobutene, methanol, propionaldehyde, ethanol, ethyl acetate, methyl acrylate, methyl isobutyrate, ethyl acrylate, methyl methacrylate, n-propyl acrylate, and ethyl methacrylate. In this sample, clearly monomer reversion is the primary degradation process occurring; however, several other degradation mechanisms are at work. When the sample contains an amino resin in the mixture, acrylonitrile is observed in the pyrogram. Another effect of the amino presence was a marked increase in the amount of methanol detected. Other products detected were methoxyhydrazine, methyl isocyanate, and methyl isocyanide.

Thus far we have looked at a number of oxygenated polymers and copolymers. We have seen that depolymerization is the primary degradation mechanism for many acrylate polymers and polyesters. This mechanism is affected by the nature of the monomer unit; for instance, with methacrylate polymers, the product distribution varies as the length of the R group increases. The result is that random scission begins to be more of a factor as the alkyl chain gets longer. Next we will take a look at macromolecules that contain a nitrogen heteroatom. Before doing so, however, it might be helpful to look at smaller molecules in order to understand the chemistry surrounding a central nitrogen atom.

The first compounds that we will discuss are amino acids. Smaller compounds containing a central nitrogen atom are relatively simple chemically and offer some insight as to the pyrolytic behavior surrounding the nitrogen atom. Many alpha-amino acids, when exposed to pyrolysis conditions, undergo initial decarboxylation to form the amine fragment. With aliphatic amino acids this results in the amine as the primary pyrolysis product in the chromatogram. This is not at all surprising since CO₂ is highly stable and readily available in the amino acid. There are some bimolecular processes that can occur to give the formation of a nitrile upon pyrolysis of amino acids; these have been widely characterized in the literature.

Other products that form from the pyrolysis of amino acids are aldehydes, which contain one less carbon atom than the parent amino acid. This process occurs via an S_Ni deamination mechanism. Another process that can occur is side chain stripping involving chain homolysis. The result is the production of various saturated and unsaturated compounds. Many alpha-amino acids, when pyrolyzed, form an amine fragment, a nitrile fragment, and aldehydes that contain one less carbon atom than the parent amino acid. Also, a side stripping mechanism can result in various saturated and unsaturated compounds.⁶

With materials that contain nitrogen heteroatoms, the pyrolysis conditions are of extreme importance. Because of the thermally labile nature of many nitrogen-containing compounds, the thermal stability of the final product is paramount. Sample size can also dramatically affect the degradation mechanism and product formation. The larger the sample size, the greater the corresponding thermal gradient within the sample. Large sample sizes tend to push the product distribution in the direction of secondary degradation processes.

Pyrolysis of phenylalanine, for example, can proceed through several different pathways. Figure 10.8 shows the pyrograms of phenylalanine and tyrosine. In the case of phenylalanine, a primary degradation product is toluene. This product results from the cleavage of the carbon-carbon bond beta to the amine nitrogen atom. There is the need for a hydrogen radical migration to form the final product. Likewise, cleavage of the carbon-nitrogen bond leads to the formation of styrene. Ethylbenzene is another product of the pyrolysis of phenylalanine. Bibenzyl is also a major pyrolysis product of phenylalanine resulting from the reaction of two toluyl radicals.⁷

The nature of the pyrolysis products with nitrogen-containing macromolecules can be highly dependent on many analytical conditions, such as sample size, pyrolysis temperature, and inertness of the pyrolysis system. Many nitrogen-containing compounds are thermally labile and thus are sensitive to temperature and metal surfaces. Figure 10.8 shows the result of pyrolyzing phenylalanine using a glass-lined analytical system. Irwin⁶ reports on the differences resulting from the presence of stainless steel, quartz, and Pyrex in the same analysis. Although the pyrolysis products remain the same in all three experiments, the product distribution does change. For instance, in a stainless system, the amount of benzene produced is much higher than that of the Pyrex and quartz systems. Quartz, which is the most inert, has the highest level of styrene and ethylbenzene. Pyrolysis at 500°C provides the largest yield of Ph-CH₂CH₂-CN. As the temperature increases, the amount of the nitrile diminishes.⁷

Understanding the product formation from the pyrolysis of amino acids is the first step in comprehending pyrolysis behavior for more complex systems, such as proteins and nucleic acids, which comprise a large quantity of the material in biological systems. Later in this chapter, in Section 10.5, proteins are discussed in more detail.

10.3 SURFACTANTS

Surfactants are used in a wide variety of consumer and industrial uses. They are used not only in the detergent and cosmetic industries, but also in lubrication, as

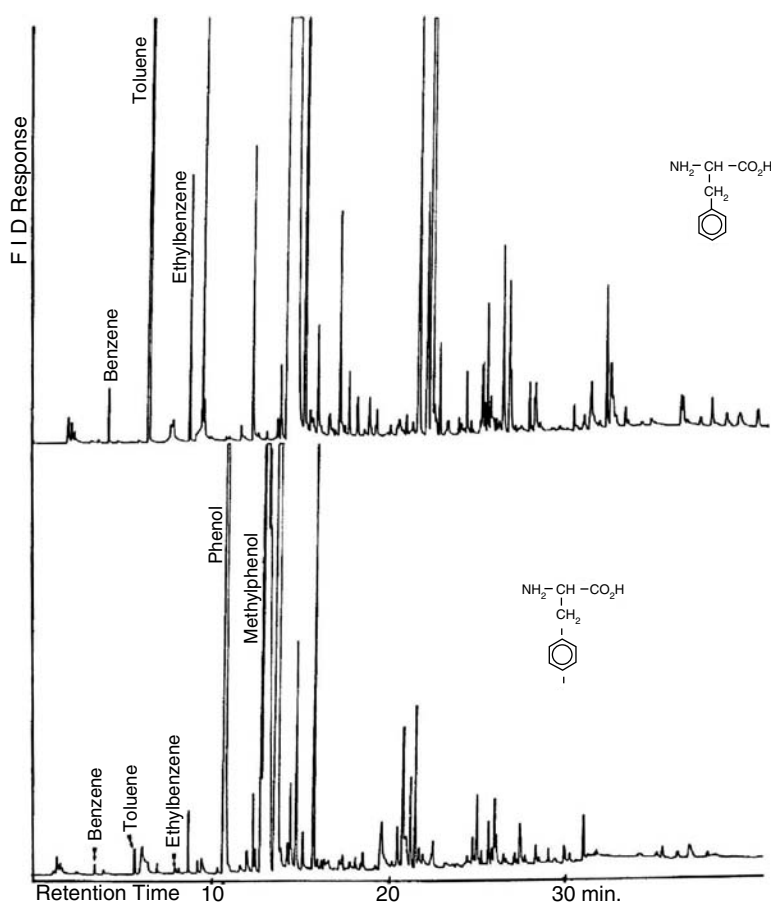


FIGURE 10.8 Pyrograms of phenylalanine (top) and tyrosine (bottom) (glass-lined system at 700°C for 10 s).

catalysts, and in drug delivery systems. Typically, surfactants are soluble surface agents that contain both hydrophilic and hydrophobic portions. The long-chain aliphatic part of the molecule is the hydrophobic portion. Upon aqueous dissociation, they can be categorized on the basis of the charge present on the hydrophilic portion of the molecule. There are anionic, nonionic, cationic, and amphoteric surfactants. For our purposes, only cationic surfactants will be discussed, although pyrolysis is appropriate in the investigation of anionic and nonionic surfactants as well.

Cationic surfactants generally contain a central heteroatom with four side groups extending from the central atom. A class of surfactants known as quaternary ammonium salts contain typically three small aliphatic or aromatic groups bonded to a central nitrogen atom. The cleansing properties arise from the presence of the fourth group, which is a long aliphatic chain. The length of this chain varies from C_{12} to C_{20} . The aliphatic chain, which is derived from the reaction of the amine with a fatty acid, is crucial to the formation of the micelle. Micelle formation is the mechanism

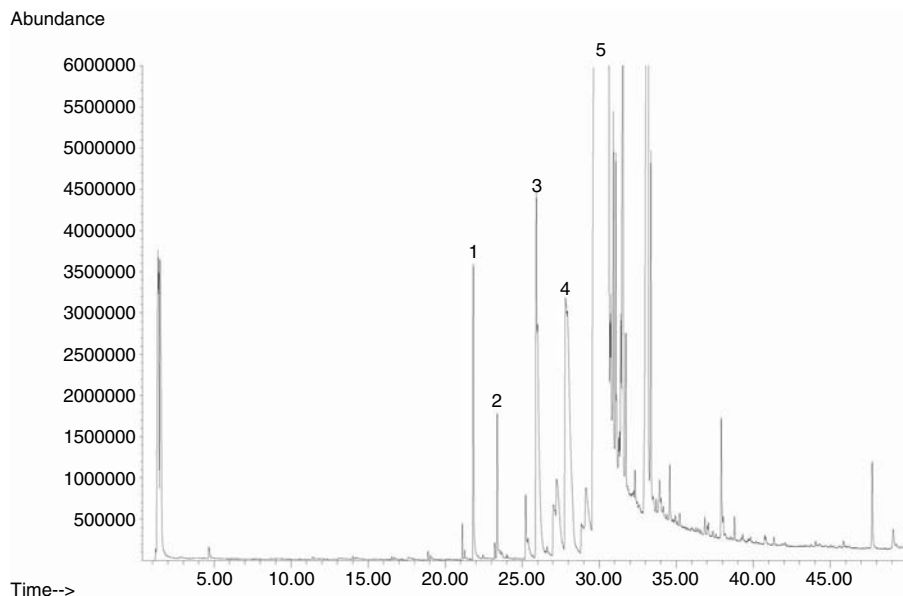
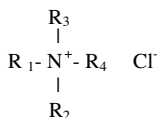


FIGURE 10.9 Pyrogram of hexadecyltrimethyl ammonium chloride at 600°C. Peaks: 1 = N,N-dimethyl dodecanamine, 2 = hexadecane, 3 = N,N-dimethyl tetradecanamine, 4 = N,N-dimethyl pentadecanamine, 5 = N,N-dimethyl hexadecanamine.

by which surfactants get their cleansing properties. Commercially available cleaning products contain a mixture of quaternary ammonium salts. To understand how pyrolysis can be used to analyze these materials, the pyrolysis products of the pure components may be examined. A generic quaternary ammonium salt with the following chemical structure



could undergo homolytic cleavage on the basis of bond strength.⁸ An R–N bond has a dissociation energy of 78 kcal/mole, whereas a C–C bond has one of 83 kcal/mole. A look at the pyrogram in Figure 10.9 shows that bond cleavage did occur at the C–N bond of the long aliphatic chain. The characterization of the peak at 23 minutes shows it to be hexadecene. A hydrogen transfer from the aliphatic free radical to the amine free radical forms the product methyl chloride, CH₃Cl. A series of homologous tertiary amines from C₁₂ to C₁₅ was also observed due to random cleavage of the C₁₆ aliphatic chain.

Similarly, when octadecyldimethylbenzyl ammonium chloride is pyrolyzed (Figure 10.10), the major products are octadecene and dimethylbenzyl amine. Other

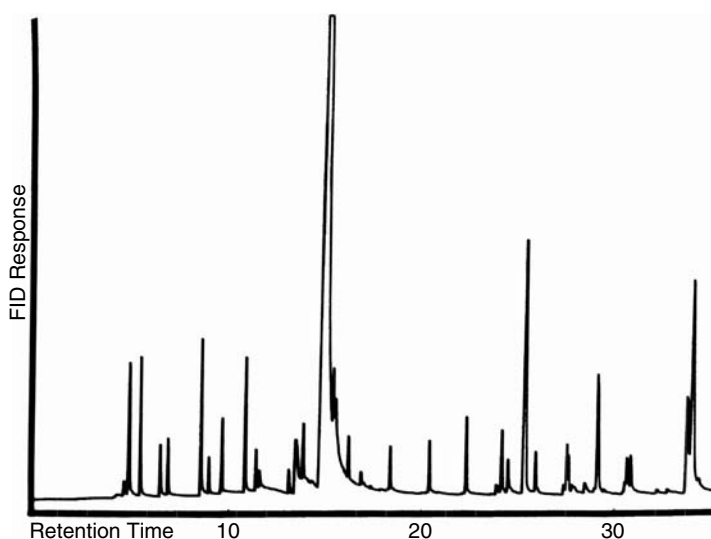


FIGURE 10.10 Pyrolysis of an octadecyldimethylbenzyl ammonium chloride at 750°C.

products include benzene, toluene, dimethyl amine, and unsaturated hydrocarbons with carbon numbers less than C_{18} .

The utility of pyrolysis for the analysis of surfactants can be shown by looking at aqueous solutions of these surfactants in dilute quantities. Analytical pyrolysis is frequently thought of as a technique that does not work well with trace quantities. However, dilute solutions of surfactants can be analyzed by applying the aqueous solution to the platinum ribbon of a filament pyrolyzer and allowing the water to evaporate. This procedure can be repeated to allow for the sensitivity needed. In Figure 10.11, a commercial surfactant at the low ppm level was analyzed by pyrolysis at 700°C. Among the products seen are benzene, toluene (the peaks at 5 and 8 minutes, respectively), and many olefinic hydrocarbons. This exercise brings about the prospect of using pyrolysis as a tool for analyzing sediments, high-molecular-weight organics, pesticides, and semivolatiles by pyrolysis-gas chromatography. Such work is currently underway by several research groups.

10.4 SULFUR-CONTAINING MACROMOLECULES

Sulfonamides are known for their ability to form antibacterial drugs, and the derivatives of 4-aminobenzene sulfonamide serve a number of medical applications. Analytical pyrolysis of these compounds proceeds in a manner similar to that of amino acids.

Pyrolysis generally occurs at the sulfonamido group, resulting in the liberation of sulfur dioxide. The other products will include aniline and a heterocyclic aromatic amine. The sulfonamide is generally characterized by the heterocyclic amine since aniline is always a product with these compounds.⁹ For example, in the pyrolysis of sulfadiazine, pyrolysis occurs at the sulfonamido nitrogen atom to form an

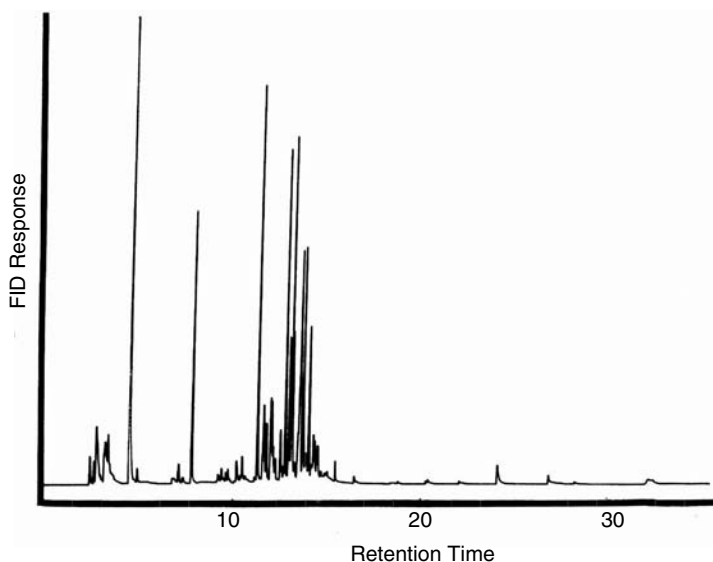


FIGURE 10.11 Pyrolysis of the residue of a 40 ppm solution in water of a quaternary ammonium chloride surfactant (800°C for 10 s).

unstable -SO_2 radical, which readily converts to sulfur dioxide. The other remaining products are aniline and 2-aminopyrimidine. The same process holds for the sulfonamides sulfamerazine and sulfadimidine. The only difference is that the heterocyclic products are 2-amino-4-methylpyrimidine and 2-amino-4,6-dimethylpyrimidine, respectively.⁶

These are very simple sulfur compounds in terms of pyrolytic behavior. The problem gets more sophisticated when the macromolecule is a polymer that may be cross-linked and have sulfur bridges. Many attempts have been made to address the topic of sulfur linkages in vulcanized cross-linked rubbers, with varying degrees of success. The problem that arises is that the sulfur bridges generally make up only a small portion of the polymer. This leads to difficulty because of sensitivity levels and the positive identification of pyrolysis fragments that can be attributed directly to the sulfur bridges. The chromatogram produced is often quite complex, not only because of the nature of the rubber itself, but also because of the sulfur bridging. The complexity of this situation may make it necessary to use statistical modeling of known cross-linked rubbers to be able to perform adequate quantitative analysis of the degree of cross-linking for these polymers.

10.5 NATURAL POLYMERS

10.5.1 CELLULOSE

The most abundant natural organic polymer on Earth is cellulose, which is basically composed of glucose units (a sugar). It is a major constituent of wood as well as plant

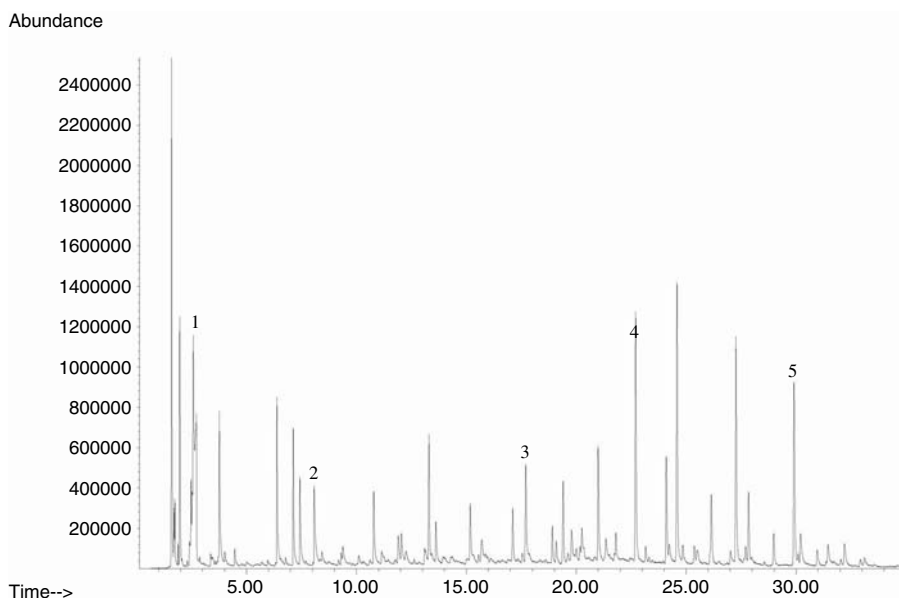


FIGURE 10.12 Pyrogram of oak wood pyrolyzed at 600°C. Peaks: 1 = acetic acid, 2 = furan carboxaldehyde, 3 = 2-methoxy-4-methyl phenol, 4 = 2,6-dimethoxy phenol, 5 = 2,6-dimethoxy-4-propenyl phenol.

leaves and stems. The vegetable fiber cotton is a very pure form of cellulose. In wood, a macromolecule called lignin binds the cellulose wood fibers together, essentially helping give wood its shape. It is interesting to note that the fibers of cellulose are exceptionally strong when they are in the dry state. Chemically, they are hydrophilic and become quite permeable when they are wet. The pyrolysis of wood yields a large number of organic compounds (see Figure 10.12) plus CO_2 and a considerable amount of nonvolatile char. The pyrolysate includes a number of substituted phenols, furans, and levoglucosan, as well as a large number of ketonic compounds.

10.5.2 CHITIN AND CHITOSAN

Chitin is one of the main components in the makeup of insect exoskeletons and those of other arthropods. It is a polysaccharide that is composed of units of acetyl glucosamine (N-acetyl-D-glucos-2-amine) that are linked together by a beta-1,4 bond. They are linked the same way that cellulose units are linked. Chitosan is a linear polysaccharide that contains randomly distributed (deacetylated) beta-1,4-D-glucosamine units and N-acetyl-D-glucosamine (acetylated) units. Figure 10.13 shows the pyrogram of saltwater shrimp exoskeleton. The typical chemical composition of the exoskeleton is approximately 15% chitin, with most of the remaining material made up of protein. The pyrogram of this exoskeleton shows the thermal elimination of acetic acid and acetamide. A number of nitrogenous heterocyclics were also detected, such as pyrrole, methylpyrrole, and 2,5-dimethylpyrrole.^{6,10}

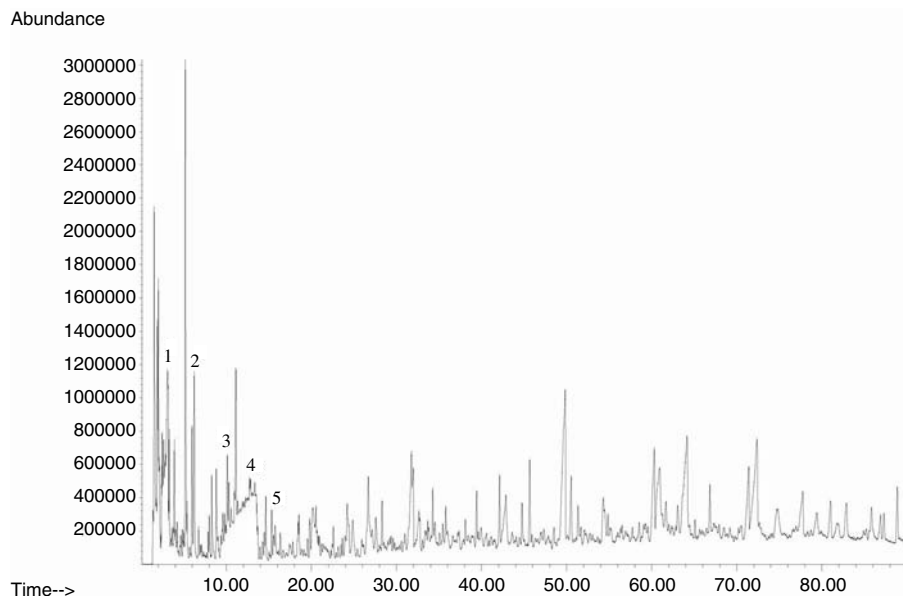


FIGURE 10.13 Pyrogram of the exoskeleton of a saltwater shrimp pyrolyzed at 750°C. Peaks: 1 = acetic acid, 2 = pyrrole, 3 = methyl pyrrole, 4 = acetamide, 5 = 2,5-dimethylpyrrole.

10.5.3 PROTEINS

Many macromolecules can be found in living organisms. Proteins, large polymeric peptides made up of amino acids, are a very important group. Materials like hair, wool, and feathers contain proteins called keratins. The chemical structure of wool shows that the cortex consists of at least 100 proteins with polypeptides made up of about 22 different amino acids with different structure and behavior. These amino acids are both structurally and chemically different — some are acidic, some are hydrophobic, and some contain sulfur. The pyrogram shown in Figure 10.14 was produced from wool and shows a peak for mercaptomethane and carbon disulfide indicative of the presence of the amino acid cystine. The pyrogram of a feather (Figure 10.15) shows the presence of sulfur dioxide, indicative of a sulfur-containing amino acid in the polypeptide. A homologous series of nitriles was also observed.

10.6 SUMMARY

The pyrolysis of polar macromolecules tends to be more complex from a mechanistic standpoint than that of nonpolar materials, since many of the products formed go through a cyclic intermediate. However, compounds such as polymethacrylates generally decompose via a depolymerization mechanism that produces mostly monomers. Analytical pyrolysis can be used to extract a great deal of information concerning nonvolatile samples, for instance, sample identification through fingerprinting, quantitative measurement of copolymers, and structural information related to branching and stereochemistry.

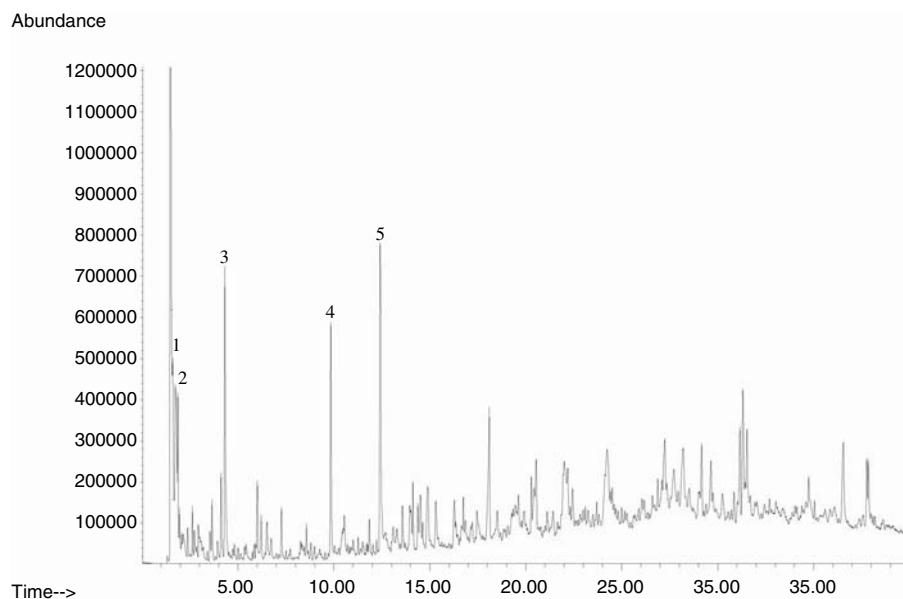


FIGURE 10.14 Pyrolysis of wool at 750°C. Peaks: 1 = mercaptomethane, 2 = carbon disulfide, 3 = toluene, 4 = phenol, 5 = methyl phenol.

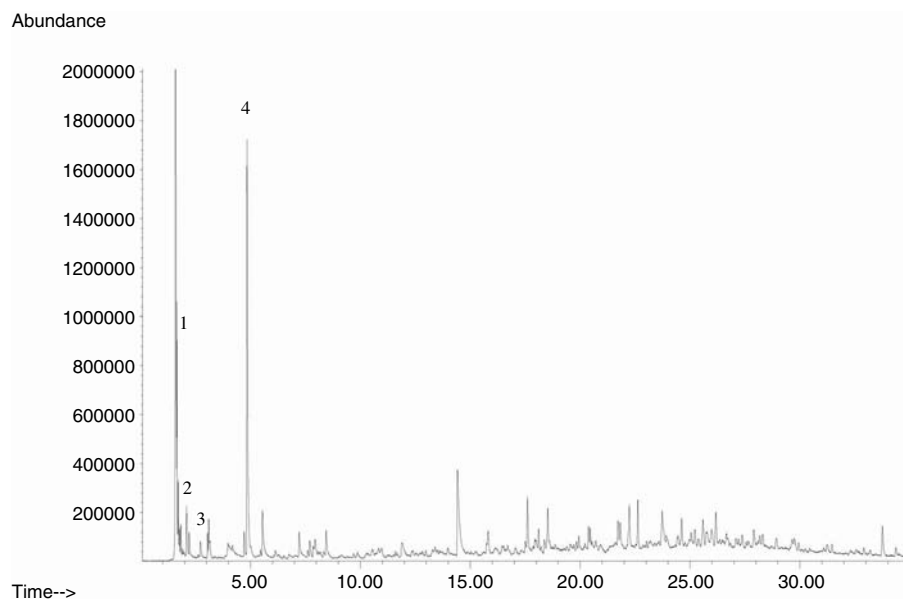


FIGURE 10.15 Pyrolysis of a feather from a wild turkey at 650°C. Peaks: 1 = sulfur dioxide, 2 = acetonitrile, 3 = propanenitrile, 4 = toluene.

It is clear from this brief overview that analytical pyrolysis can be a useful analytical tool for both qualitative and quantitative analysis of large macromolecules. Treatment of nonvolatile samples such as synthetic polymers and natural biopolymers using pyrolysis/GCMS can yield much information about volatiles and structure and provide a characteristic fingerprint of the macromolecule.

REFERENCES

1. Kumar, A. and Gupta, R.K., *Fundamentals of Polymers*, McGraw-Hill, New York (1998), pp. 1–24.
2. Sugimura, Y. and Tsuge, S., *J. Chromatogr. Sci.*, 17: 269–272 (1979).
3. Irzl, G.H., Vijayakumar, C.T., Fink, J.K., and Lederer, K., *J. Appl. Anal. Pyrol.*, 11: 277–286 (1987).
4. Irzl, G.H., Vijayakumar, C.T., and Lederer, K., *J. Appl. Anal. Pyrol.*, 13: 305–317 (1988).
5. Casanovas, A.M. and Rovira, X., *J. Appl. Anal. Pyrol.*, 11: 227–232 (1987).
6. Irwin, W.L., *Analytical Pyrolysis: A Comprehensive Guide*, Marcel Dekker, New York (1982).
7. Patterson, J.M., Haidar, N.F., Papadopoulos, E.P., and Smith, W.T., *J. Org. Chem.*, 38: 663–666 (1973).
8. Abraham, S.J. and Criddle, W.J., *J. Appl. Anal. Pyrol.*, 7: 337–349.
9. Irwin, W.J. and Slack, J.A., *Analytical Pyrolysis*, Elsevier, Amsterdam (1977), pp. 107–116 (1977).
10. Koll, P., Borchers, G., and Metzger, J., *J. Appl. Anal. Pyrol.*, 19: 119–128 (1991).

11 Characterization of Condensation Polymers by Pyrolysis-GC in the Presence of Organic Alkali

Hajime Ohtani and Shin Tsuge

CONTENTS

11.1	Introduction	249
11.2	Measuring System and Procedure	250
11.3	Applications	251
11.3.1	Fully Aromatic Polyester (Compositional Analysis).....	251
11.3.2	Aliphatic Polyesters (Compositional Analysis/ Biodegradability).....	252
11.3.3	Polycarbonate (Composition/End Group)	256
11.3.4	Thermally Treated Polycarbonate/Polyester (Branching and Cross-Linking)	259
11.3.5	UV-Cured Resin (Cross-Linking Network).....	266
11.3.6	Poly(Aryl Ether Sulfone).....	266
	References.....	269

11.1 INTRODUCTION

Pyrolysis-gas chromatography (Py-GC) has been widely applied to the characterization of various synthetic polymers. However, it is often difficult to characterize intractable condensation polymers such as aromatic polyesters by ordinary Py-GC, even using a high-resolution capillary GC system, because they usually degrade into a number of polar compounds along with considerable amounts of solid residues and chars.

Recently, modification to the pyrolysis process, which involves high-temperature chemical reactions other than conventional thermolysis of macromolecules, has often provided additional information on chemical structure for various organic

materials that is not readily obtainable by conventional analytical pyrolysis methods.¹ The representative process is pyrolysis in the presence of organic alkali, typically tetramethylammonium hydroxide ($(\text{CH}_3)_4\text{NOH}$; TMAH). This procedure is also called thermally assisted hydrolysis and methylation (THM) because the samples are hydrolytically decomposed and most of the products are almost simultaneously methylated by TMAH.

The THM reaction linked to GC, GC/mass spectrometry (MS), and MS has been successfully applied to the chemical characterization of a number of synthetic and natural products, including resins, lipids, waxes, wood products, soil sediments, and microorganisms.¹ This technique is also very effective for the detailed characterization of the synthetic polymeric materials, especially the condensation polymers, such as polyesters and polycarbonates, because many simplified pyrograms are usually obtained that consist of peaks of methyl derivatives from the constituents of the polymer samples almost quantitatively. In this chapter, the instrumental and methodological aspects of Py-GC in the presence of the organic alkali are briefly described, and then some typical applications to the precise compositional analyses and microstructural elucidation inclusive of the intractable cross-linking structures for various condensation type polymeric materials are discussed.

11.2 MEASURING SYSTEM AND PROCEDURE

Figure 11.1 illustrates a measuring system for Py-GC in the presence of organic alkali using a microfurnace pyrolyzer along with a typical reaction scheme for an ester and a carbonate linkage. This system is basically the same as that for the ordinary Py-GC. A weighed polymer sample is placed into a sample cup and TMAH reagent is added. The sample cup is then introduced into the pyrolyzer and the polymer sample is instantaneously decomposed in the flow of helium carrier gas. The polymer sample should be ground into a powder as fine as possible to obtain sufficient reaction efficiency with the organic alkali.

TMAH is generally added as a solution (typically 25 wt% in methanol or water). The amount of TMAH added should be at least several times higher than that of the hydrolyzable linkages in the polymer sample, although excess reagent might contaminate the pyrolysis device (typical combination is a 50 to 100 μg polymer sample and 1 to 2 μl of TMAH solution). The choice of the solvent usually depends on the compatibility with the sample. In the case of the methanol solution, it was reported that the solvent sometimes contributed to the methylation of the products to some extent.²

Compared with the general pyrolysis temperature for the ordinary Py-GC (500 to 700°C), a relatively low pyrolysis temperature (300 to 400°C) is commonly selected for Py-GC in the presence of organic alkali to suppress the contribution of random thermal cleavage of the polymer chain at higher temperatures, but high enough for the instantaneous THM reaction. The resulting products are transferred to the separation column, and the separated species are detected by a flame ionization detector (FID) or mass spectrometer (MS) to yield a pyrogram.

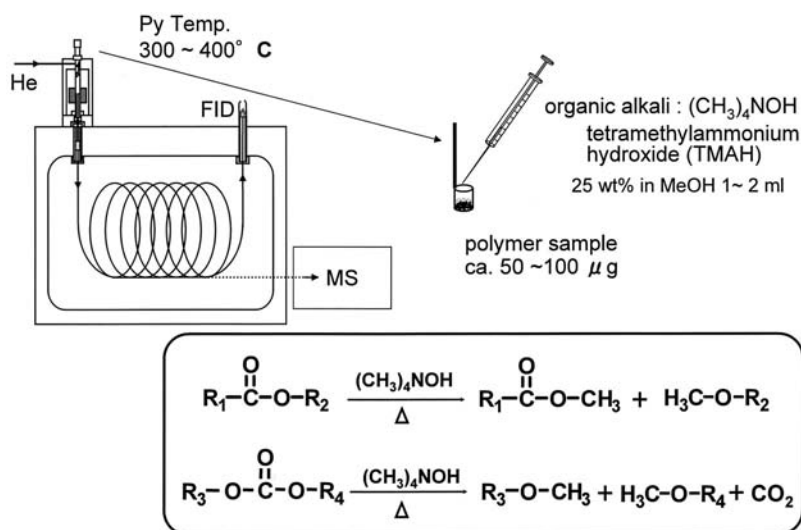


FIGURE 11.1 Typical measuring system for pyrolysis-GC in the presence of organic alkali.

11.3 APPLICATIONS

11.3.1 FULLY AROMATIC POLYESTER (COMPOSITIONAL ANALYSIS)

Fully aromatic liquid crystalline polyesters (LCPs) based on *p*-hydroxybenzoic acid (PHB) have recently been recognized as among the most promising high-performance engineering plastics, especially in fields where increasing thermal stability and mechanical strength are required. To modify the processability, copolymer type LCPs are industrially produced, and their precise compositional analysis is often required for the production management. However, ordinary spectroscopic analytical methods such as nuclear magnetic resonance (NMR) and infrared (IR), and even ordinary Py-GC, do not necessarily provide sufficient information about LCPs. On the other hand, Py-GC in the presence of TMAH is very effective for the precise compositional analysis of LCPs.³

Figure 11.2 shows the pyrograms of an LCP sample consisting of PHB (50 mol%), terephthalic acid (TA; 25 mol%), and biphenol (BP; 25 mol%), obtained (a) at 400°C in the presence of TMAH, and by ordinary pyrolysis (b) at 400°C and (c) at 600°C.³ At 400°C in the absence of the reagent (b), hardly any decomposition to volatile compounds took place owing to the highly thermal stability of the LCP sample: the majority of the sample remained as solid residue in the sample cup. Pyrolysis at 600°C without addition of TMAH (c) produced only small amounts of (nonmethylated) phenol and biphenol and about 30% of the sample remained in the cup. On the contrary, at 400°C in the presence of TMAH, three large peaks of the dimethyl derivatives of PHB, TA, and BP — methoxy *p*-methylbenzoate (MMB), dimethylterephthalate (DMT), and 4,4'-dimethoxybiphenyl (DMB), respectively — were observed after the elution of the products (methanol and trimethylamine) from TMAH, and nothing remained in the cup. This

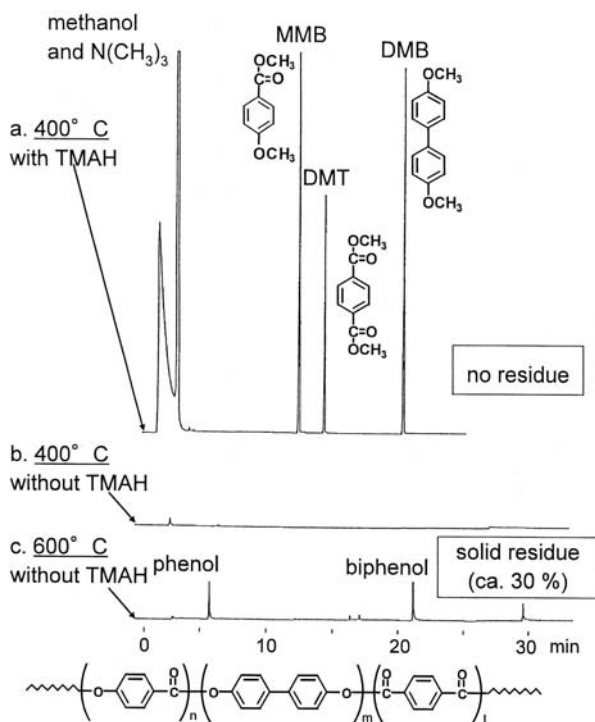


FIGURE 11.2 Pyrograms of LCP (a) at 400°C with TMAH, (b) at 400°C without TMAH, and (c) at 600°C without TMAH.³ Sample weight: 0.05 mg; reagent: 1 μ l of 25 wt % TMAH solution in methanol; separation column: fused silica capillary (30 m \times 0.25 mm i.d.) coated with 0.25 μ m of 5% diphenyl-95% dimethylpolysiloxane (J&W); column temp: 80–280°C at 8°C/min.

result suggested that TMAH did not methylate the volatile decomposition products but reacted directly with the ester linkages in the polymer chain, yielding the methyl derivative of each constituent.⁴ Figure 11.3 shows the most probable scheme of THM reaction at an ester linkage in LCP.

Table 11.1 summarizes the copolymer composition of various LCP samples estimated by this method together with that in feed. It is apparent that the observed molar ratios of the products are in quite good agreement with the original compositions in feed, with superior reproducibility (coefficient of variation [CV] less than 1.0%). This result demonstrates that Py-GC in the presence of TMAH is a powerful method for rapid and precise compositional analysis of LCPs.

11.3.2 ALIPHATIC POLYESTERS (COMPOSITIONAL ANALYSIS/BIODEGRADABILITY)

Recently, various aliphatic polyesters have become known to be the environmentally friendly materials with biodegradable nature or from a nonpetroleum origin. For example, a copolymer type poly(hydroxyalkanoate), poly(3-hydroxybutyrate-*co*-3-hydroxyvalerate) (P(3HB-*co*-3HV)), which is usually produced through the bacterial

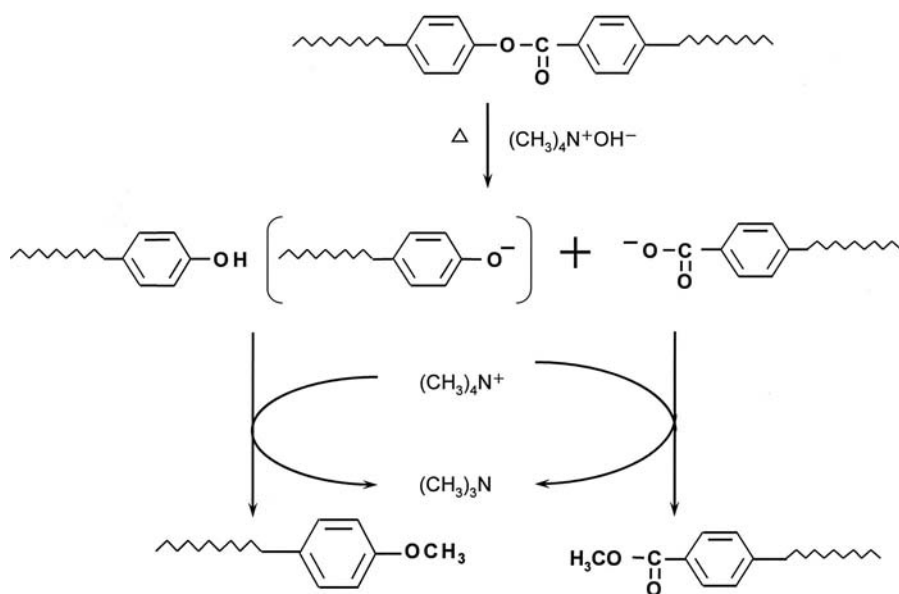


FIGURE 11.3 Typical scheme of TMAH reaction for an ester linkage in LPC.

TABLE 11.1
Composition of LCP Samples Determined
by Py-GC in the Presence of TMAH

sample	PHB	TA	BP	total
A	85.7 (84.6)	7.0 (7.7)	7.3 (7.7)	100
B	67.9 (66.7)	15.1 (16.7)	17.0 (16.7)	100
C	50.5 (50)	24.0 (25)	25.5 (25)	100
D	34.1 (33.3)	32.0 (33.3)	33.9 (33.3)	100

() : feed composition
reproducibilities : CV < 1.0 %

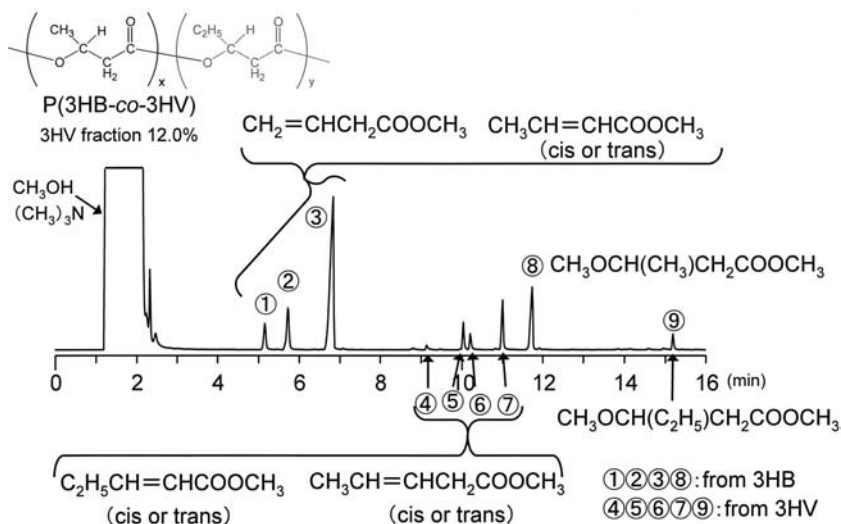


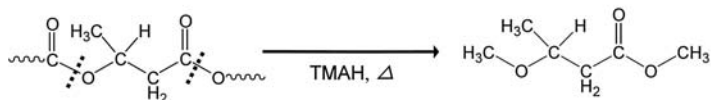
FIGURE 11.4 Pyrogram of P(3HB-co-3HV) at 350°C in the presence of TMAH [5]. Sample weight: 0.03 mg; reagent: 4 μl of 25 wt% TMAH solution in methanol; separation column: metal capillary (30 m \times 0.25 mm i.d.) coated with 0.25 μm of polydimethylsiloxane (Frontier Lab, Ultra ALLOY PY-1); column temp: 30°C (5 min)-230°C at 5°C/min.

fermentation by *Alcaligenes eutrophus*, generally shows good stiffness and toughness for practical use. The copolymer composition of P(3HB-co-3HV) strongly affects not only its physical properties but also the biodegradability, and it can be readily determined by Py-GC in the presence of TMAH.⁵

Figure 11.4 shows a typical pyrogram in the presence of TMAH of P(3HB-co-3HV) (3HV content is 12 mol%), in which nine major peaks are observed and identified, as shown.⁵ Figure 11.5 shows the reaction scheme around the 3HB unit to form the observed products. Typical products of P(3HB-co-3HV) through THM reaction should be methyl 3-methoxybutanoate (peak 8) from the 3HB unit and methyl 3-methoxypentanoate (peak 9) from the 3HV unit. On the other hand, the other major products in the pyrogram, such as methylbutenoates (peaks 1 to 3) and methylpentenoates (peaks 4 to 7), should be formed through not only THM reaction, but also the thermal cleavage at the ester bond through a six-membered cyclic transition state, as shown in Figure 11.5. Since the nine major products were attributed to either the 3HB or 3HV unit, the copolymer composition of P(3HB-co-3HV) was accurately determined based on the relative intensities of these peaks.⁵

Because of the highly sensitive nature of the Py-GC technique, requiring only trace amounts (ca. 0.1 mg or less) of sample, the local structural change in an aliphatic polyester sample during the biodegradation process can also be evaluated by Py-GC in the presence of organic alkali. For instance, the enzymatic degradation behavior of poly(ϵ -caprolactone) (PCL) with an α -benzoyloxy terminal by cholesterol esterase was studied by Py-GC in the presence of TMAH.⁶ Figure 11.6 shows the pyrograms of the PCL samples observed (a) before and (b) after the enzymatic degradation test. In both pyrograms, benzyl methyl ether (B) from the benzoyloxy terminal group and

A. hydrolysis (THM)



B. pyrolysis + THM

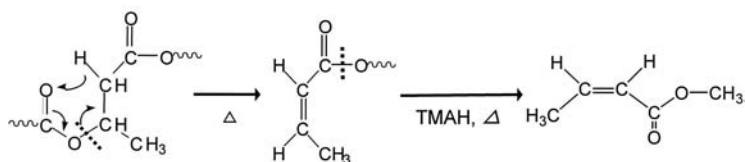


FIGURE 11.5 Typical scheme for decomposition at 3HB unit in the presence of TMAH.

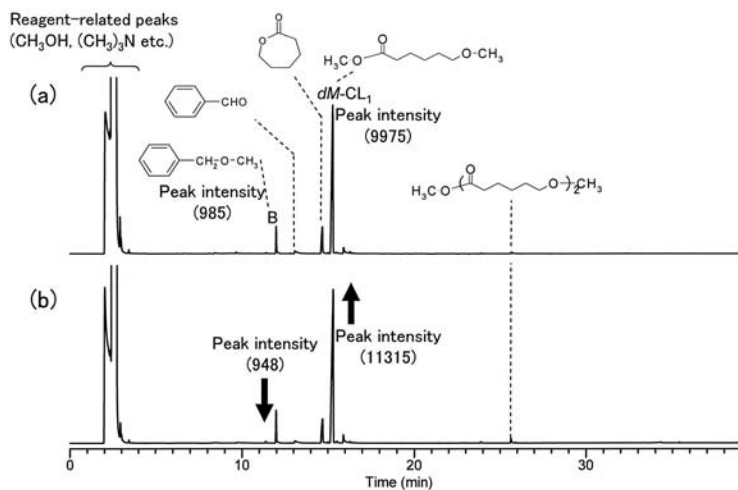


FIGURE 11.6 Pyrograms of PLC samples pyrolyzed at 400°C in the presence of TMAH, (a) control sample, (b) residual sample recovered after enzymatic degradation test for 36 h.⁶ Sample weight: 0.05 mg; reagent: 3 μ l of 25 wt% TMAH solution in methanol; separation column: metal capillary (30 m \times 0.25 mm i.d.) coated with 0.25 μ m of polydimethylsiloxane (Frontier Lab, Ultra ALLOY PY-1); column temp: 40°C (5 min)-300°C at 5°C/min.

the dimethyl derivative of hydroxycaproic acid ($dM\text{-CL}_1$) from the main chain formed through the THM reaction were commonly observed. It is interesting to note that the relative intensity of peak B slightly decreased after the enzymatic degradation, while that of peak $dM\text{-CL}_1$ comparatively increased. This result suggested that the enzymatic degradation of the PCL sample might proceed mainly in the exo-cleavage mode from the α -benzoyloxy terminal side under a given condition.⁶

11.3.3 POLYCARBONATE (COMPOSITION/END GROUP)

Polycarbonate (PC) is one of the most widely used engineering plastics owing to its excellent transparency and mechanical property. The main chain of ordinary PC molecules consists of bisphenol A (BPA) units linked together with carbonate linkages, while various terminal groups are formed depending on the polymerization process. The solution method (SM), in which *p*-*tert*-butylphenol is often used to control the molecular weight of the resulting polymer in addition to the main materials, such as sodium salt of BPA and phosgene, provides PC molecules end capped with *p*-*tert*-butylphenoxy groups. On the other hand, the melt method (MM), in which BPA and diphenylcarbonate are directly reacted through ester exchange, is known to yield PC molecules with either a phenoxy or a hydroxyl end group. Not only the identification but also the highly precise and sensitive determination of such terminal groups on PC can be achieved by Py-GC in the presence of organic alkali.⁷

Figure 11.7 shows the typical pyrograms of SM-PC observed (a) by conventional Py-GC at 600°C without adding TMAH and (b) at 400°C in the presence of TMAH.⁷ In the case of the conventional pyrolysis (a), various phenolic compounds such as phenol, cresols, and BPA were formed through the cleavages not only at carbonate linkages, but also at C–C bondings. On the other hand, as for pyrolysis in the presence of TMAH (b), there were only two main peaks from the PC sample: *p*-*tert*-butyl anisol from the end group and dimethylether of BPA from the main chain. This fact demonstrated that the PC polymer chains decomposed through THM reactions at carbonate linkages selectively and quantitatively to yield the methyl ethers of the components in the PC sample, as shown in Figure 11.8. Therefore, the content of the end groups can be accurately determined from the relative peak intensities between these two peaks after making the molar sensitivity correction for the FID response.

The number average molecular weight (M_n) was in turn estimated based on the relative content of the end group obtained by Py-GC in the presence of TMAH.⁷ Table 11.2 summarizes the M_n values for the fractionated SM-PC samples estimated by various methods, indicating that the values determined by this method were in fairly good agreement with those obtained by size exclusion chromatography (SEC) and NMR. Furthermore, highly precise results can be obtained by Py-GC, e.g., CV = 1.8% for S-2 and 0.6% for S-3 samples for five repeated measurements. On the other hand, the content of phenoxy end groups in the MM-PC samples can be similarly estimated very accurately by this technique.⁷

Recently, various kinds of copolymer type PCs have been produced as new functional engineering plastics having enhanced thermal and photo stability. As for

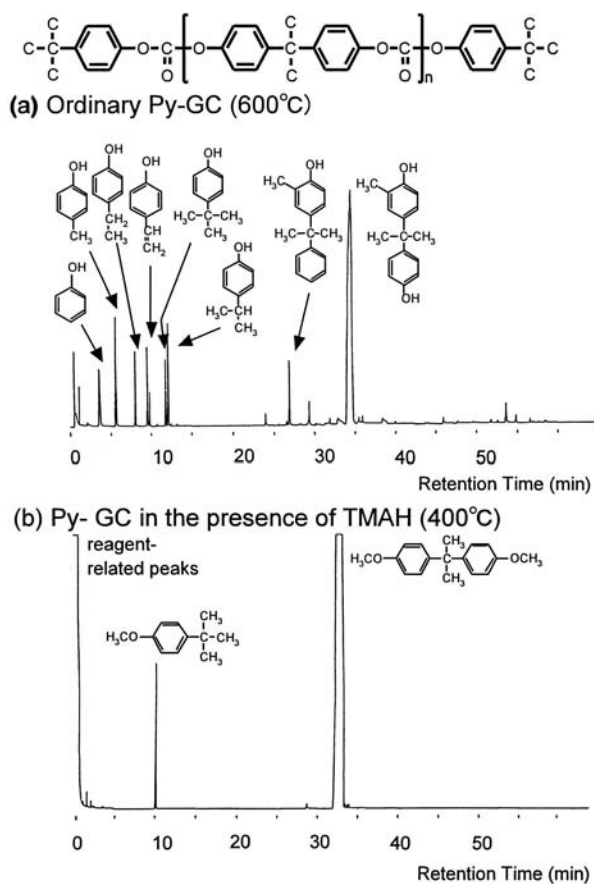


FIGURE 11.7 Pyrograms of polycarbonate sample (SM-PC) (a) at 600°C without TMAH, (b) at 400°C in the presence of TMAH.⁷ Sample weight: 0.05 mg; reagent: 1 μ l of 25 wt% TMAH solution in methanol; separation column: fused silica capillary (25 m \times 0.25 mm i.d.) coated with 0.25 μ m of polydimethylsiloxane (Quadrex MS); column temp: 50–300°C at 4°C/min.

these materials, however, not only their chemical composition but also their end groups have not been thoroughly clarified even by NMR because of the complexity of obtained spectra or insufficient sensitivity for the end groups, particularly in higher molecular weight polymers. For such copolymer type PCs, Py-GC in the presence of TMAH was also successfully applied to the compositional analysis and determination of the end groups.⁸

Typical examples were reported for two series of PC copolymers, thermally stabilized ones (PC-I) whose comonomer was 1,1'-bis-(4-hydroxyphenyl)-3,3,5-trimethylcyclohexane (BHTH; MW = 310) and light stabilized ones (PC-II) whose comonomer was 2,2'-methylenebis[6-(2H-benzotriazol-2-yl)-4-(1,1,3,3-tetramethylbutyl)phenol] (MBTP; MW = 656).⁸ The molecular structures for the PC-I and PC-II are shown in Figure 11.9. Figure 11.10 illustrates the typical pyrograms for (a) PC-I and (b) PC-II obtained in the presence of TMAH. In both cases, only three

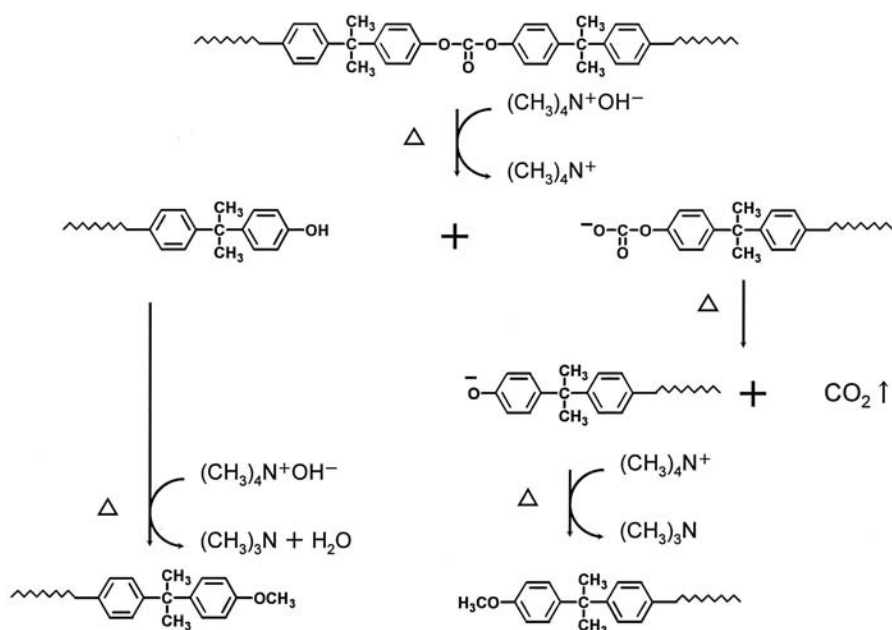


FIGURE 11.8 Typical scheme of TMH reaction for a carbonate linkage in PC. (From Tsuge et al., *Macromol. Symp.*, 195, 288–292 (2003). With permission.)

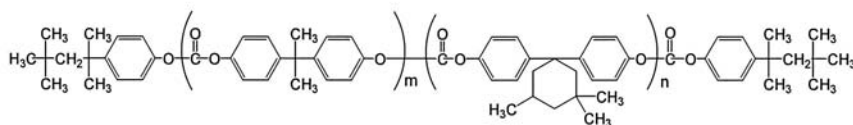
TABLE 11.2
Estimated Number Average Molecular
Weight of Fractionated SM-PC Samples

Fraction No.	Estimated M_n values		
	by SEC	by Py-GC*	by $^1\text{H-NMR}$
S-1	23,400	26,900	30,200
S-2	8,300	9,500	9,600
S-3	4,000	4,700	--

* :CV values: 0.5~2%

characteristic peaks were observed in the pyrograms. The peaks a, b, and c in pyrogram (a) were assigned to a methyl ether of *p*-*tert*-octylphenoxy terminal group moiety and dimethyl ethers of two comonomers (BPA and BHTH) formed through selective hydrolysis of carbonate linkages in the polymer chain followed by simultaneous methylation. On the basis of these molar peak intensities, the exact composition of the PC-I sample can be determined along with its accurate M_n . Similarly, pyrogram (b) reveals the same information for the PC-II sample. In this case, it should be noted that the bulky MBTP-related product (MW = 684) was detected by using a thermally stable metal capillary column at a high oven temperature up to 380°C.⁸

PC-I



PC-II

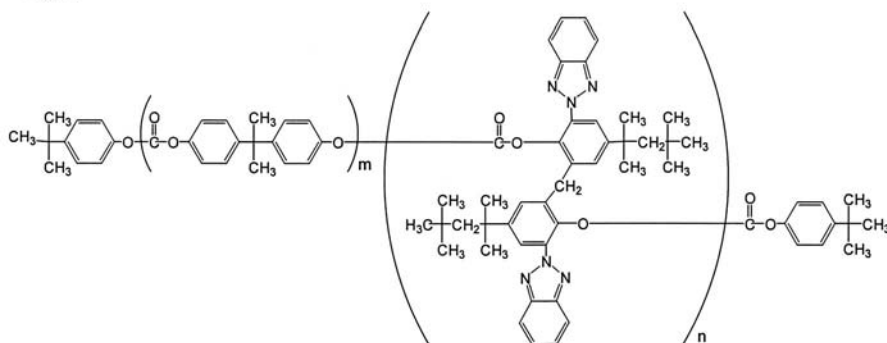


FIGURE 11.9 Molecular structure of a thermally stabilized PC-I and stabilized PC-II.

11.3.4 THERMALLY TREATED POLYCARBONATE/POLYESTER (BRANCHING AND CROSS-LINKING)

Because of the relatively higher polymerization temperatures around 200 to 300°C, MM-PC might contain the fraction with branching and insoluble cross-linking structures to some extent formed concomitantly during polymerization. Furthermore, PCs are often subjected to injection molding operations at higher temperatures around 300°C, also possibly causing branching and cross-linking formation. Characterization of these branching and cross-linking structures is often requested because these are closely associated with optical and mechanical properties of the PC materials. However, mainly because of their insoluble nature, their analyses are not an easy task even by NMR, which has been most extensively utilized for soluble polymeric materials.

It has been recently demonstrated that Py-GC in the presence of TMAH can also be applied to verify the branching or cross-linking structures, in both industrially available PC and its thermally treated samples.⁹⁻¹¹ In these reports, three kinds of PC samples listed in Table 11.3, that is, industrially synthesized SM-PC and MM-PC and an insolubilized PC (IS-PC) sample formed through thermal treatment of MM-PC, were examined. Figure 11.11 shows the pyrograms of the PC samples obtained in the presence of TMAH at 400°C. Table 11.4 summarizes the characteristic products on the pyrograms identified by Py-GC/MS in order of their retention times, together with their origin. In the pyrogram of every PC sample, the dimethyl ether of BPA (peak c), reflecting the main chain, and the ethers (peaks a and b)

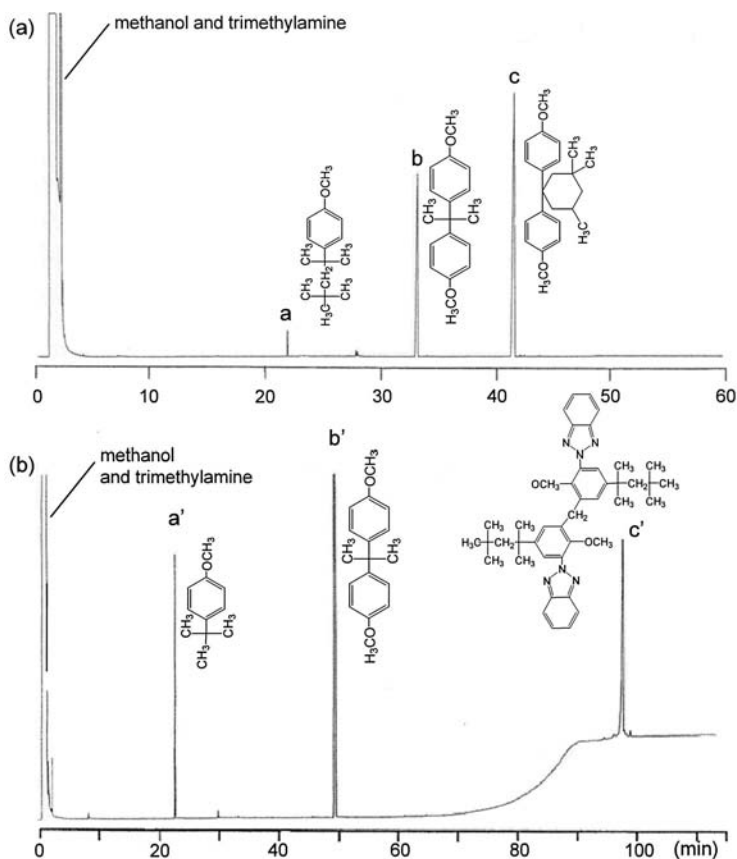
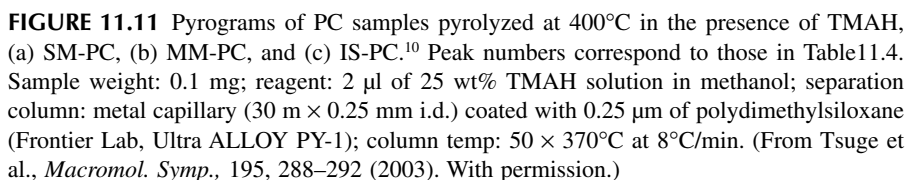


FIGURE 11.10 Pyrograms of PC samples pyrolyzed at 400°C in the presence of TMAH, (a) PC-I, (b) PC-II.⁸ Sample weight: 0.1 mg; reagent: 2 μl of 25 wt% TMAH solution in methanol; separation column: (a) fused silica capillary (30 m × 0.25 mm i.d.) coated with 0.25 μm of polydimethylsiloxane (Quadrex MS); column temp: 50–300°C at 5°C/min. (b) metal capillary (30 m × 0.25 mm i.d.) coated with 0.5 μm of polydimethylsiloxane (Frontier Lab, Ultra ALLOY PY-2); column temp: 50–380°C at 5°C/min.

originated from the end groups were clearly observed. Moreover, in the pyrograms of the MM-PC (b) and the related IS-PC (c) samples, peaks 1 to 5 were commonly observed and the additional peaks 6 to 10 were observed only on the pyrogram for IS-PC (c). Some of these peaks might reflect abnormal structures formed during the synthesis or thermal treatment at 300°C, since these peaks were scarcely observed in the pyrogram of SM-PC (a).

Among these products, the peak 5 component can be assigned to the dimethyl ether of BPA with a methoxycarbonyl group. Moreover, the appearance of this pyrolysis product in the pyrogram suggests that the original polymer samples contained the carboxylic branching structure to some extent. Figure 11.12 shows the most probable formation process of the carboxylic branching structure formed through the Kolbe–Schmitt or Fries rearrangement of the carbonate group, together



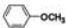
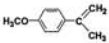
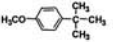
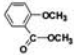
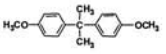
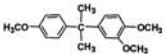
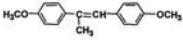
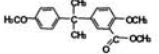
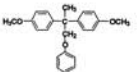
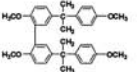
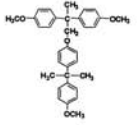
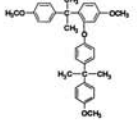
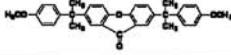
Sample name	Preparation method	Degree of branching and/or cross-linking structures
SM-PC	Solution method	Low
MM-PC	Melt method	Somewhat
IS-PC	Thermal insolubilization with MM-PC (at 300°C in air for 3 hours)	considerable

} industrial PC

SM-PC

MM-PC

TABLE 11.4
Identification of the Characteristic Peaks on the Pyrograms Shown in
Figure 11.11 and Their Classification

Peak no ^{a)}	Retention time (min.)	Structure	Classification for the corresponding structure in PC chain ^{b)}
a	5.1		I
1	10.1		III
b	10.2		I
2	11.9		III
c	20.5		I
3	21.8		II
4	22.6		III
5	23.6		II
6	27.5		III
7	32.7		II
8	33.6		II
9	34.3		II
10	39.5		III

a) Peak numbers correspond to those on the pyrograms in Fig. 11.11

b) I : Main chain or original terminal groups.

II : Branching or cross-linking structures formed during the thermal treatments.

III : Abnormal structures formed during the thermal treatment except for the branching and cross-linking structures.

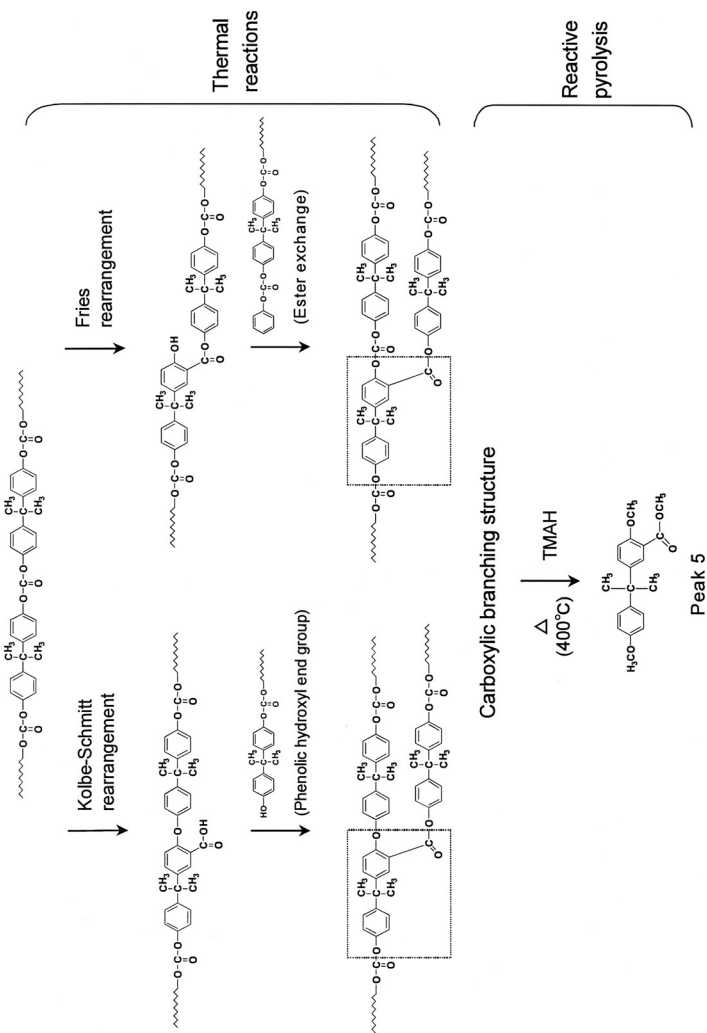


FIGURE 11.12 Possible formation pathway of carboxylic branching structure and its characteristic product (peak 5). (From Tsuge et al., *Macromol. Symp.*, 195, 288–292 (2003). With permission.)

with the formation pathway of the peak 5 component through the THM reaction of the branching moiety.⁹

In addition, since appreciable cleavage of the C–C bond would not occur under the given THM condition, the appearance of peak 1 (*p*-isopropenyl anisole) in the pyrograms suggests that the original polymer samples contained the isopropenyl end group structure to some extent in the MM-related PC samples, especially in the thermally treated PC sample (IS-PC), formed through the disproportionation reaction of a C(CH₃)-phenylene bond. In a similar manner, peak 2 reflected the disproportionation reaction of the C–C bond neighboring the carboxylic branching structure formed during the polymerization or thermal treatment of PC-2.

On the other hand, peaks 6 to 9, which were exclusively observed in the pyrogram of IS-PC (c), should be derived from other types of branching and cross-linking structures, such as CH₂–O (peaks 6 and 8), biphenyl (peak 7), and phenylene–O bridges, formed during thermal treatment.⁹ Furthermore, the identification of peak 10 confirms the existence of xanthone structures in IS-PC.¹⁰ On the basis of the results thus observed, a model structure of the thermally treated PC sample was speculated as shown in Figure 11.13.

Flame-retardant mechanisms of PC-containing silicone additives (FR-PC) were also elucidated by Py-GC in the presence of TMAH using a similar approach.¹² Recently, much attention has been paid to silicone additives as flame retardants because they generate particularly smaller amounts of toxic substances even in the case of extreme fire. In order to elucidate the structure change induced in the FR-PC system during thermal degradation, the FR-PC and its control PC samples before and after thermal treatment at 380°C (for 2 h) were comparatively subjected to the Py-GC measurement using TMAH at 400°C.

In the pyrogram of the control PC sample after thermal treatment, the peaks of 2-(4-methoxyphenyl)-2-phenylpropane and 2-(3-methoxycarbonyl-4-methoxyphenyl)-2-(4-methoxyphenyl)propane reflecting abnormal structures were observed and much more prominently appeared in pyrogram of the thermally treated FR-PC. This fact suggested that the formation of the related abnormal structures, including cross-linking, might be much more promoted in FR-PC material during its thermal treatment by the function of the silicone-based flame retardant. On the basis of the results observed for the FR-PC material, it was suggested that the cross-linking structure that was formed during an earlier stage of combustion induced in the presence of the silicone flame retardant might suppress the thermal decomposition of the PC materials at higher temperatures by confining the movements of the degradation products in the degrading material in the combustion zone.

Meanwhile, the abnormal structures in LCP, the 4-hydroxybenzoic acid (HBA)/2-hydroxy-6-naphthoic acid (HNA) copolymer, were also characterized by Py-GC in the presence of TMAH.¹³ In the pyrogram of the LCP sample thermally treated at 500°C, the peaks reflecting the branching and condensed structures were observed together with those of the methyl derivatives of HBA and HNA reflecting the main chain, and those originated from the end groups. Generally, the yields of all the characteristic products reflecting the abnormal structures increased with the rise of the thermal treatment temperature. Furthermore, it was confirmed that the

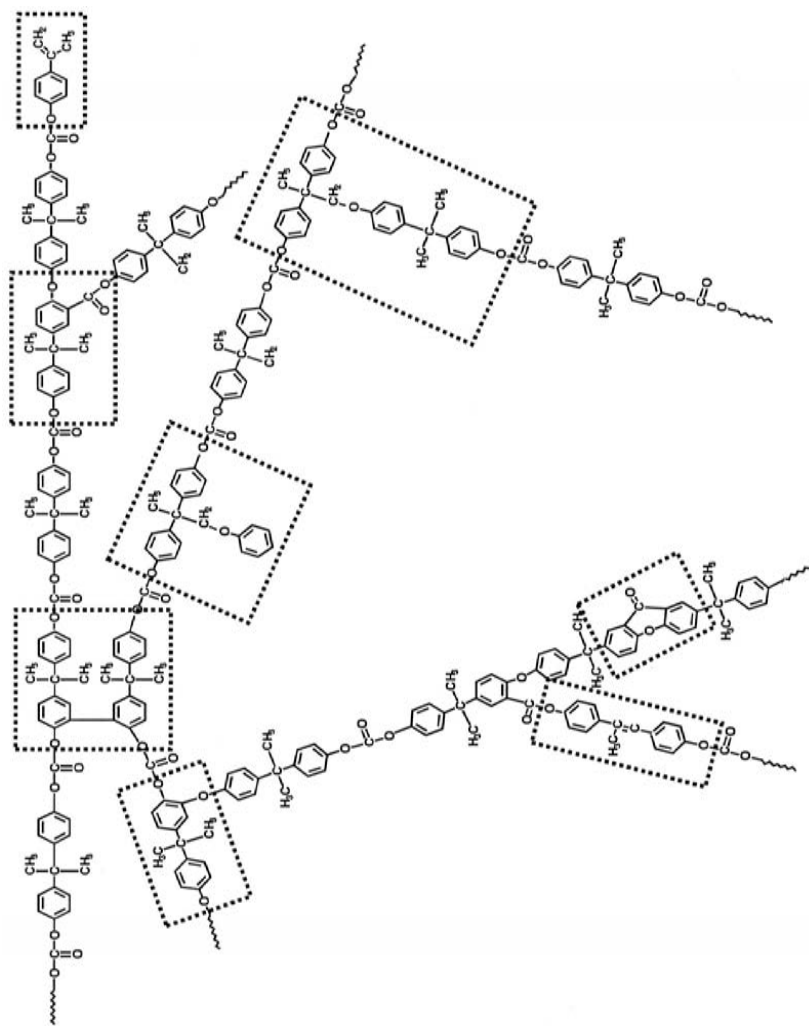


FIGURE 11.13 Model structure for IS-PC speculation based on Py-GC measurement using TMAH.

condensation reactions might occur in preference to the branching formations in the LCP sample at higher treatment temperatures around 500°C.

11.3.5 UV-CURED RESIN (CROSS-LINKING NETWORK)

Ultraviolet (UV)-cured photopolymerization is currently utilized in various industrial fields such as paints, adhesives, dental cements, coatings for optical fibers and disks, photoresistance, and three-dimensional stereolithography. To improve the performance of the UV-curable resins, it is desired to elucidate both the kinetics of photopolymerization and the chemical structures of the cured resins. However, their structural characterization is not an easy task because of the insoluble nature. Recently, Py-GC in the presence of TMAH was applied to the characterization of various UV-cured resins by focusing on the compositional analysis of multicomponent cured resins¹⁴ and the estimation of the original molecular weight of epoxy acrylate constituents in the cured resins.¹⁵ Moreover, this method was extensively utilized to study the network structures in the UV-cured acrylic ester resins prepared from polyethylene glycol diacrylate in the presence of a benzoyl type photoinitiator under UV irradiation.¹⁶ In this work, minor but characteristic peaks of methyl acrylate oligomer, observed in the pyrograms of the cured resin samples, were interpreted in terms of the chain distribution of the network junctions in the cured resins.

Figure 11.14 shows the typical pyrogram of the cured resin (expanded for the characteristic region mainly reflecting the network structure) and its model structure with possible pyrolysis pathways in the presence of TMAH. As shown in this reaction scheme, ester and ketone linkages in the cross-linked resin structure would be selectively cleaved and methylated by TMAH. In addition to the dimethyl ether of polyethylene glycols, therefore, methyl acrylate and the initiator fragment should be formed from unreacted acryloyl groups and initiator residues at the chain end of the cross-linking portion, respectively.

Moreover, from the cross-linking sequences consisting of methacryloyl groups linked together, various methyl acrylate oligomers should be clipped off depending on the degree of polymerization. In the observed pyrogram, various minor peaks were observed along with a series of main peaks of the dimethylethers of polyethylene glycol. Among these minor peaks, a series of methyl acrylate oligomers, from dimers to at least hexamers, were identified, which should directly reflect the distribution of cross-linking sequences in the cured resin.¹⁶

11.3.6 POLY(ARYL ETHER SULFONE)

In general, ether linkages in the polymer chains are less susceptible to the THM reactions than ester and carbonate bonds. In some cases, however, the ethers are also subjected to be hydrolyzed almost quantitatively by TMAH into methyl ethers, depending on the properties of the neighboring units to the ether linkages. The ether bonds in poly(aryl ether sulfones) (PSUs) are a typical example.¹⁷

Figure 11.15 shows typical pyrograms of poly(oxy-*p*-phenylenesulfonyl-*p*-phenylenoxy-*p*-phenyleneisopropylidene-*p*-phenylene), generally called polysulfone (PSF), observed in the absence (a) and presence (b) of TMAH.¹⁷ In the case of

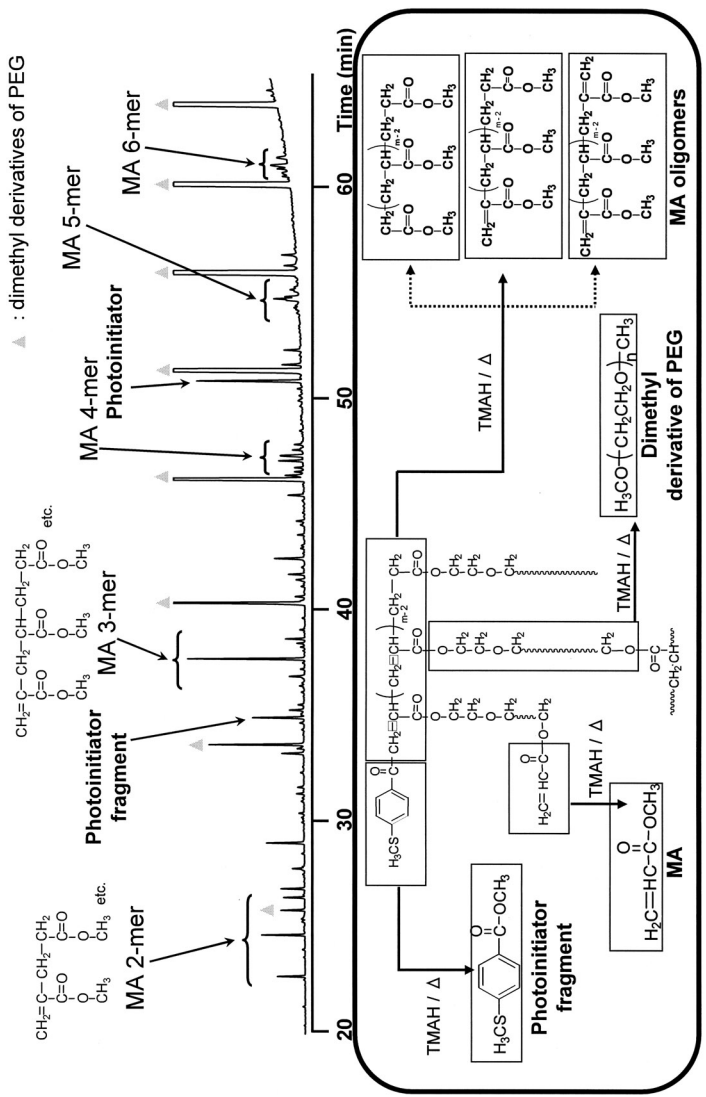


FIGURE 11.14 Pyrogram of UV-cured acrylic ester resin at 400°C in the presence of TMAH along with its possible cross-linking structure and formation pathway of products.¹⁶ Sample weight: 0.1 mg; reagent: 4 µl of 25 wt% TMAH solution in water; separation column: metal capillary (30 m × 0.25 mm i.d.) coated with 0.25 µm of 5% diphenyl-95% dimethylpolysiloxane (Frontier Lab, Ultra ALLOY ±5); column temp: 30 (5 min)-230°C at 5°C/min.

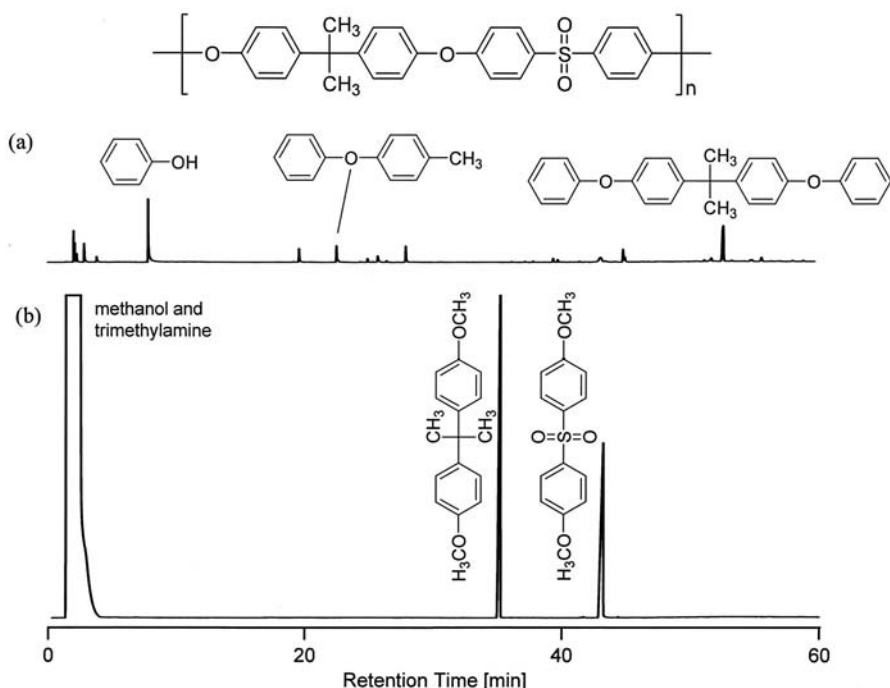


FIGURE 11.15 Pyrograms of polysulfone (a) at 700°C in the absence of TMAH, and (b) at 300°C in the presence of TMAH.¹⁷ Sample weight: 0.05 mg; reagent: 2 μl of 25 wt% TMAH solution in methanol; separation column: metal capillary (30 m \times 0.25 mm i.d.) coated with 0.5 μm of polydimethylsiloxane (Frontier Lab, Ultra ALLOY PY-1); column temp: 50–300°C at 5°C/min.

conventional pyrolysis at 700°C (a), small peaks of phenol and aromatic products containing diphenyl ether structure were barely observed, but no characteristic products containing sulfone groups were observed, due to the preferential elimination of SO_2 at the higher temperature. Moreover, the recovery of the observed products was relatively low and a considerable amount of carbonaceous residue remained in the sample cup even after pyrolysis.

In contrast, in the pyrogram obtained in the presence of TMAH at 300°C, the peaks of the constituents in the original PSF, BPA, and bis(4-hydroxyphenyl)sulfone (bisphenol S; BPS) were exclusively observed as their dimethyl ethers in almost quantitative recovery without any residues. In this case, the strong electron-withdrawing nature of the sulfone groups might promote the THM reaction at the ether linkages in PSF, retaining the sulfone structure almost completely. In a similar manner, the other type of commercially available PSU, poly(*p*-phenylenesulfonyl-*p*-phenylene) (poly(ether sulfone) (PES)), is also thoroughly decomposed into the dimethyl ether of BPS through THM reaction.¹⁷

REFERENCES

1. J.M. Challinor, *J. Anal. Appl. Pyrol.*, 61: 3 (2001).
2. Y. Ishida, H. Ohtani, and S. Tsuge, *J. Anal. Appl. Pyrol.*, 33: 167 (1995).
3. H. Ohtani, R. Fujii, and S. Tsuge, *J. High Resolut. Chromatogr.*, 14: 338 (1991).
4. J.W. de Leeuw and M. Baas, *J. Anal. Appl. Pyrol.*, 26: 175 (1993).
5. H. Sato, M. Hoshino, H. Aoi, T. Seino, Y. Ishida, K. Aoi, and H. Ohtani, *J. Anal. Appl. Pyrol.*, 74: 193 (2005).
6. H. Sato, Y. Kiyono, H. Ohtani, S. Tsuge, H. Aoi, and K. Aoi, *J. Anal. Appl. Pyrol.*, 68/69: 37 (2003).
7. Y. Ito, H. Ogasawara, Y. Ishida, H. Ohtani, and S. Tsuge, *Polym. J.*, 28: 1090 (1996).
8. Y. Ishida, S. Kawaguchi, Y. Ito, S. Tsuge, and H. Ohtani, *J. Anal. Appl. Pyrol.*, 40/41: 321 (1997).
9. K. Oba, Y. Ishida, Y. Ito, H. Ohtani, and S. Tsuge, *Macromolecules*, 33: 8173 (2000).
10. K. Oba, H. Ohtani, and S. Tsuge, *Polym. Degrad. Stab.*, 74: 171 (2001).
11. S. Tsuge, H. Ohtani, and K. Oba, *Macromol. Symp.*, 195: 287 (2003).
12. K. Hayashida, H. Ohtani, S. Tsuge, and K. Nakanishi, *Polym. Bull.*, 48: 483 (2002).
13. K. Oba, Y. Ishida, H. Ohtani, and S. Tsuge, *Polym. Degrad. Stab.*, 76: 85 (2002).
14. H. Matsubara, A. Yoshida, H. Ohtani, and S. Tsuge, *J. Anal. Appl. Pyrol.*, 64: 159 (2002).
15. H. Matsubara and H. Ohtani, *J. Anal. Appl. Pyrol.*, 75: 226 (2006).
16. H. Matsubara, A. Yoshida, Y. Kondo, S. Tsuge, and H. Ohtani, *Macromolecules*, 36: 4750 (2003).
17. H. Ohtani, Y. Ishida, M. Ushiba, and S. Tsuge, *J. Anal. Appl. Pyrol.*, 61: 35 (2001).

12 Index of Sample Pyrograms

Thomas P. Wampler

Each analyst will optimize the chromatography of his pyrolysis-gas chromatography (GC) system to provide the most pertinent information about the specific sample being analyzed. It is helpful, however, especially when first starting out, to have examples of typical analyses, giving some idea of what to expect in a pyrogram. This chapter includes capillary GC pyrograms of many different materials, all performed on readily available and typical columns. Although an analyst's samples will almost certainly be different in some way from the example materials shown here, it may be helpful to review results obtained on similar samples as a starting point in developing a specific pyrolysis method.

The examples are grouped roughly according to sample material type.

Pyrogram Number	Sample Material	Set Point, °C	Detector
Synthetic Polymers			
S-1	Kraton 1107 Kraton is a copolymer of styrene and isoprene.	800	FID
S-2	Polyester shirt thread	750	FID
S-3	Polychloroprene	750	FID
S-4	Polyethyl methacrylate	600	FID
S-5	Polymethyl methacrylate	600	FID
S-6	Polystyrene Peak numbers: 1 = monomer, 2 = dimer, 3 = trimer	750	FID
S-7	Polyvinyl chloride Peak number: 1 = benzene, 2 = toluene, 3 = naphthalene	600	FID
S-8	Polybutyl acrylate	750	MS
S-9	Polyvinylidene chloride	750	MS
S-10	Polyvinyl toluene	750	MS
S-11	Polystyrene butyl acrylate	750	MS
S-12	Polystyrene acrylonitrile	750	MS
S-13	Polyvinyl chloride	750	MS
S-14	Teflon	750	MS
S-15	Polyurethane	750	MS

Continued.

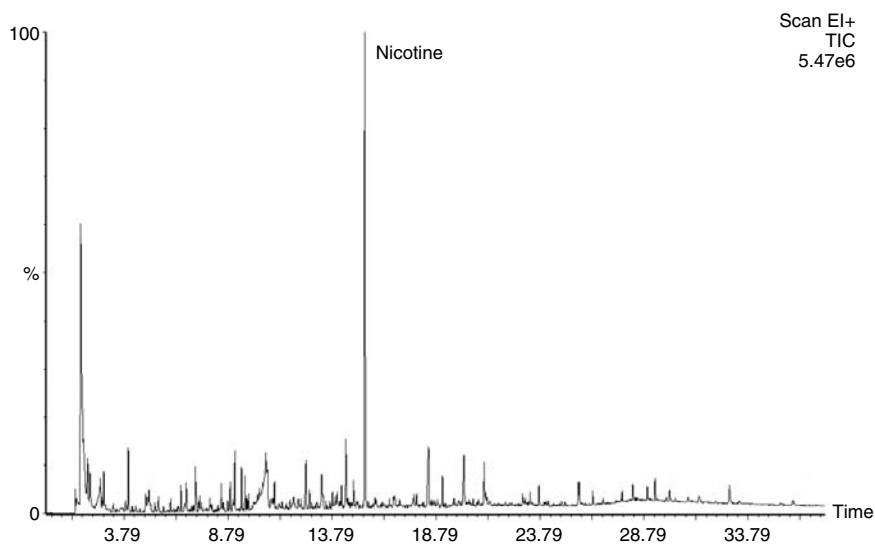
Pyrogram Number	Sample Material	Set Point, °C	Detector
Polyolefins			
O-1	Polyethylene	725	FID
O-2	Polypropylene, isotactic	700	FID
O-3	Polyisobutylene	800	FID
O-4	Polybutadiene	800	FID
O-5	Poly propylene-1-butene Copolymer (butene content = 47%)	750	FID
O-6	Polyethylene in air	650	FID
O-7	Polyethylene in air	750	FID
O-8	Polypropylene in air Heating rate = 100°/sec	800	FID
O-9	Polyisoprene	750	FID
O-10	Poly 1-butene	600	FID
O-11	Polypropylene, atactic	750	MS
O-12	Polyethylene (25%) propylene	750	MS
O-13	Ethylene (52%) propylene rubber	750	MS
Nylons			
N-1	Nylon 11	900	FID
N-2	Nylon 12	800	FID
N-3	Nylon 6/T	800	FID
N-4	Nylon 6/6	800	FID
N-5	Nylon 6/9	800	FID
N-6	Nylon 6/10	850	FID
N-7	Nylon 6/12	800	FID
N-8	Nylon 6	750	MS
Biological and Natural Materials			
B-1	Amber	650	FID
B-2	Baltic amber Peak marked <i>S</i> is succinic acid.	650	FID
B-3	Chitin from crab shells	450	FID
B-4	<i>E. coli</i> bacteria	650	FID
B-5	Gelatin	750	FID
B-6	Starch	650	FID
B-7	Phenylalanine Peak numbers: 1 = benzene, 2 = toluene, 3 = ethyl benzene	700	FID
B-8	Tyrosine Peak numbers: 1 = benzene, 2 = toluene, 3 = ethyl benzene, 4 = phenol, 5 = methyl phenol	700	FID
B-9	Animal glue From a 1500-year-old Egyptian artifact	500	FID
B-10	Human hair	750	FID
B-11	Lamb's wool	750	FID
B-12	Cotton thread	750	FID
B-13	Human fingernail	750	FID

Pyrogram Number	Sample Material	Set Point, °C	Detector
B-14	Kerogen	800	FID
B-15	Dried linseed oil	700	FID
B-16	Straw	750	FID
B-17	Oak leaf	750	FID
B-18	Natural rubber	800	FID
	Polyisoprene, cis configuration		
B-19	Oil shale	800	FID
	From rock sample heated at 60°C/min		
B-20	Oil shale	800	FID
	Total organic content = 1.2%, pulse heated		
B-21	Beeswax	500	FID
B-22	Silk	675	FID
B-23	Tobacco	750	MS
B-24	Tobacco (mentholated)	750	MS
B-25	Sucrose	750	MS
Manufactured Goods			
G-1	Unprinted newspaper	650	FID
G-2	White magazine paper	650	FID
G-3	White bond paper	750	FID
G-4	Bathroom cleaner product	650	FID
	Peak numbers: 1 = C ₁₉ , 2 = C ₁₆ hydrocarbons		
G-5	Disinfectant cleaner product	650	FID
	Peak numbers: 1 = benzene, 2 = toluene, 3 = C ₁₂ , 4 = C ₁₄ , 5 = C ₁₆ , 6 = C ₁₈ hydrocarbons		
G-6	Dishwashing liquid	700	FID
	Peak numbers: 1 = C ₁₀ , 2 = C ₁₁ , 3 = C ₁₂ hydrocarbons		
G-7	Ink, black, ballpoint pen	650	FID
G-8	Ink, black, ballpoint pen	650	FID
	Pyrolyzed intact with paper on which it had been written		
	Numbered peaks are from the paper; lettered peaks from the ink		
G-9	Ink, blue, ballpoint pen	650	FID
	Pyrolyzed intact with paper on which it had been written		
	Numbered peaks are from the paper; lettered peaks from the ink		
G-10	Printing ink	700	FID
	Formulation included linseed oil, wax, and petroleum resins.		
G-11	Petroleum resin	700	FID
G-12	Petroleum resin	700	FID
G-13	Kodak photocopy	650	FID
	Paper and toner material pyrolyzed together.		
	Peak numbers: 1 = methyl methacrylate, 2 = styrene		
G-14	Xerox photocopy	650	FID
	Peak numbers: 1 = styrene, 2 = butyl methacrylate		
G-15	Mascara	750	FID
	Peaks indicated with arrows result from beeswax.		

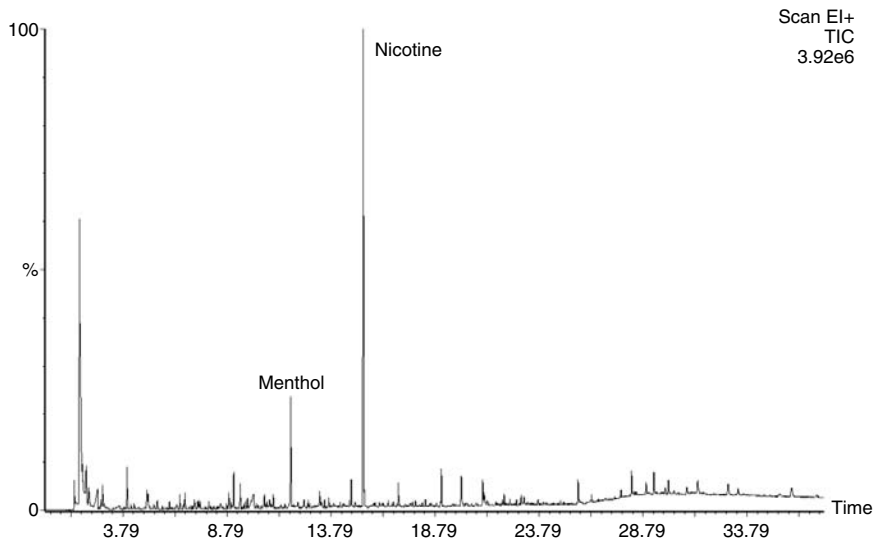
Continued.

Pyrogram Number	Sample Material	Set Point, °C	Detector
G-16	Mascara with acrylate Peaks indicated with arrows result from beeswax.	750	FID
G-17	Shirt thread 50/50 cotton/polyester blend fabric	750	FID
G-18	n-Tetracontane	650	FID
G-19	Silicone grease	900	FID
G-20	Epoxy paint	750	MS
G-21	Rayon	750	MS
G-22	Packaging PVA, PVC, styrene, MMA	750	MS
G-23	Automobile paint	750	MS
G-24	Automobile tire rubber	750	MS
G-25	Chewing gum	750	MS

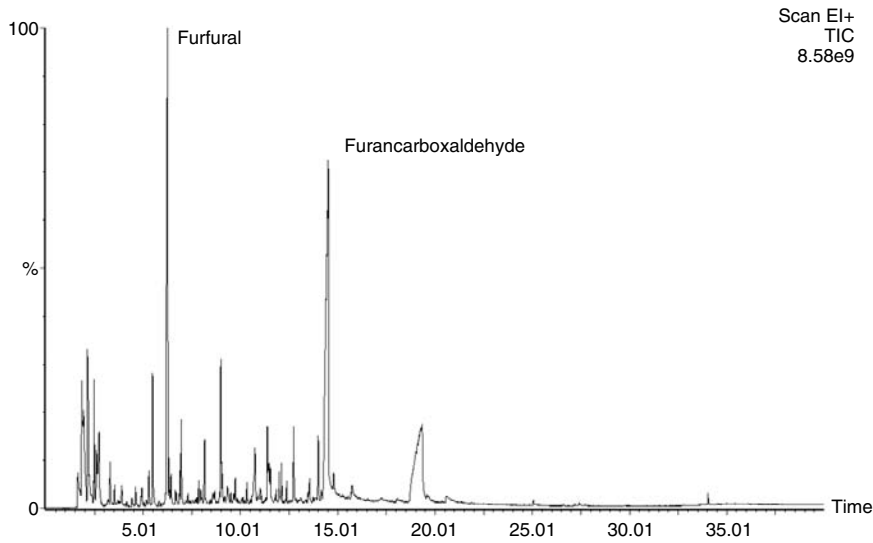
Note: FID = flame ionization detector; MS = mass spectrometry.



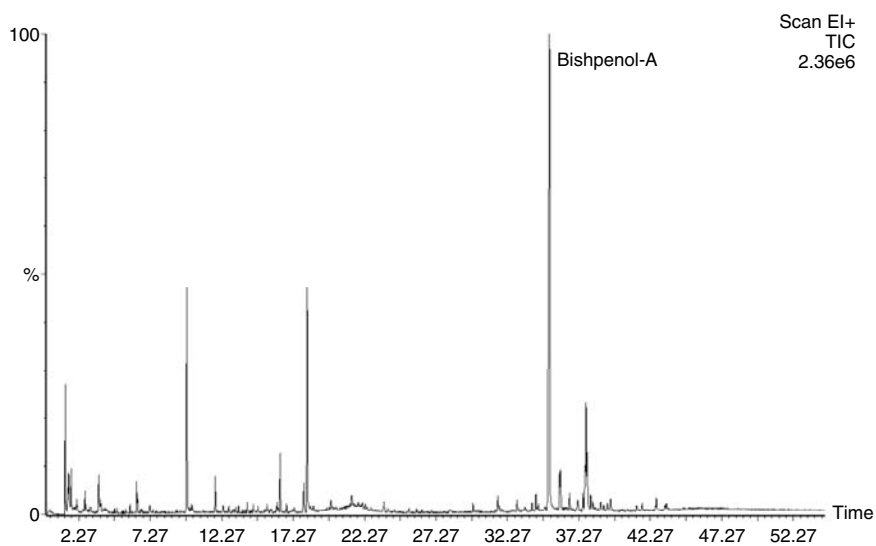
Pyrogram B-23: Tobacco.



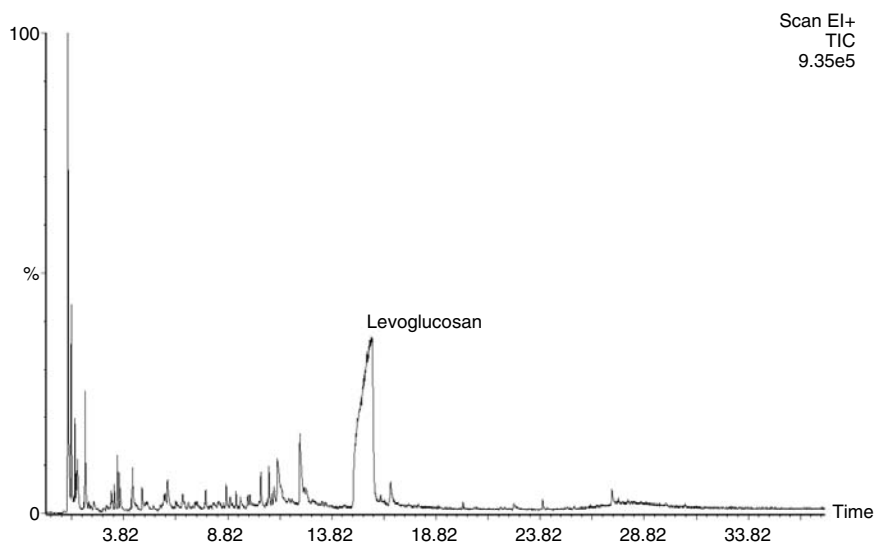
Pyrogram B-24: Tobacco (mentholated).



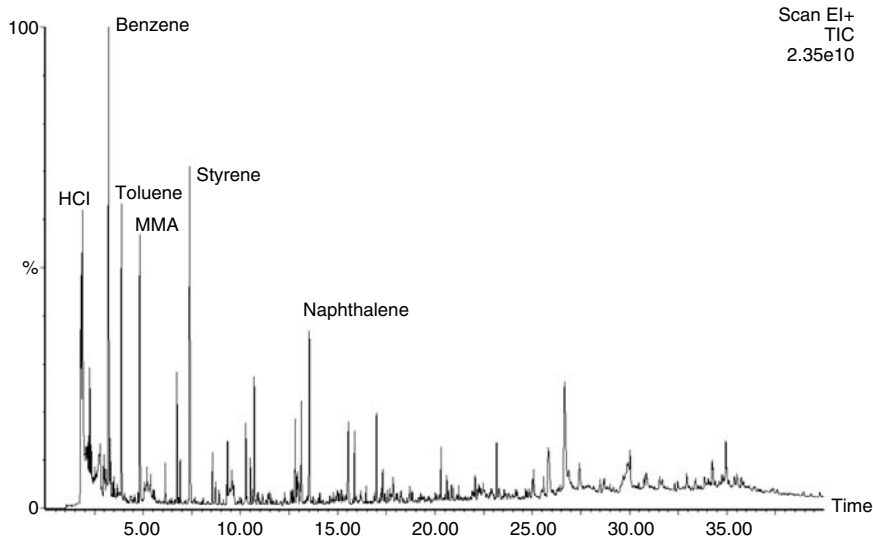
Pyrogram B-25: Sucrose.



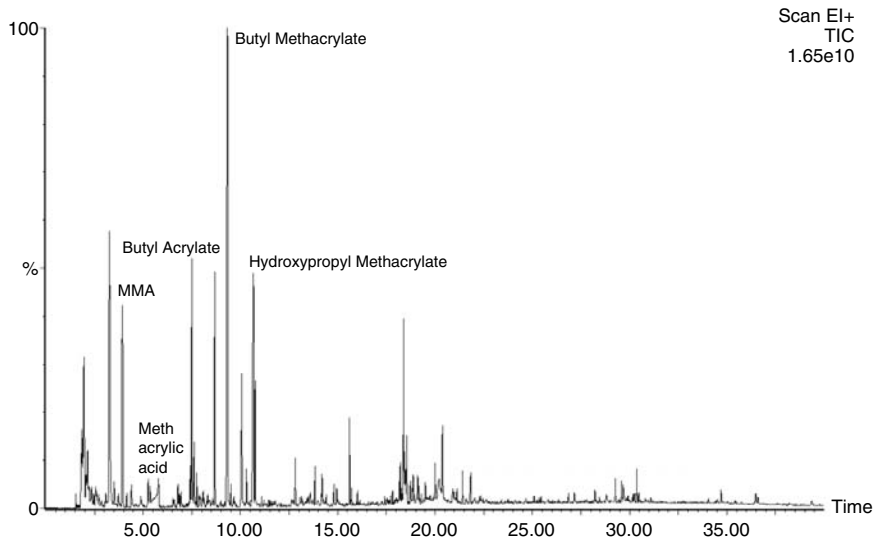
Pyrogram G-20: Epoxy paint.



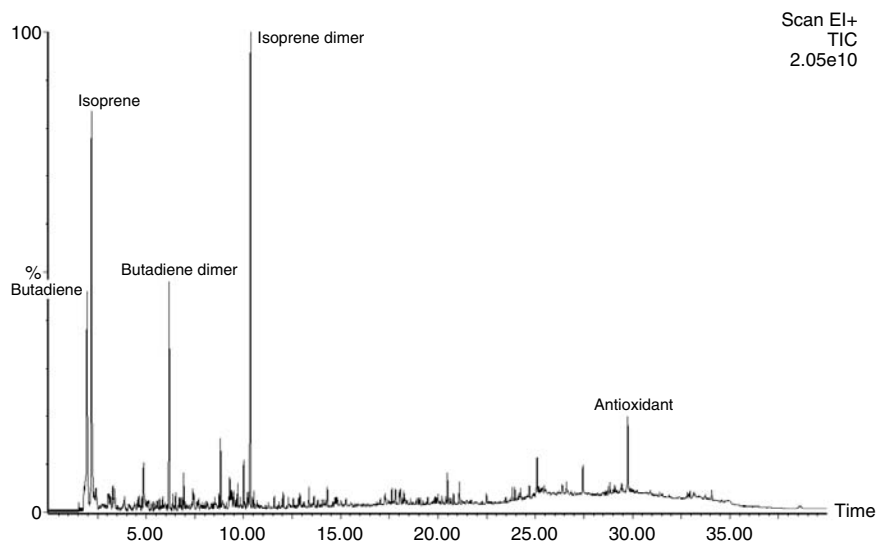
Pyrogram G-21: Rayon.



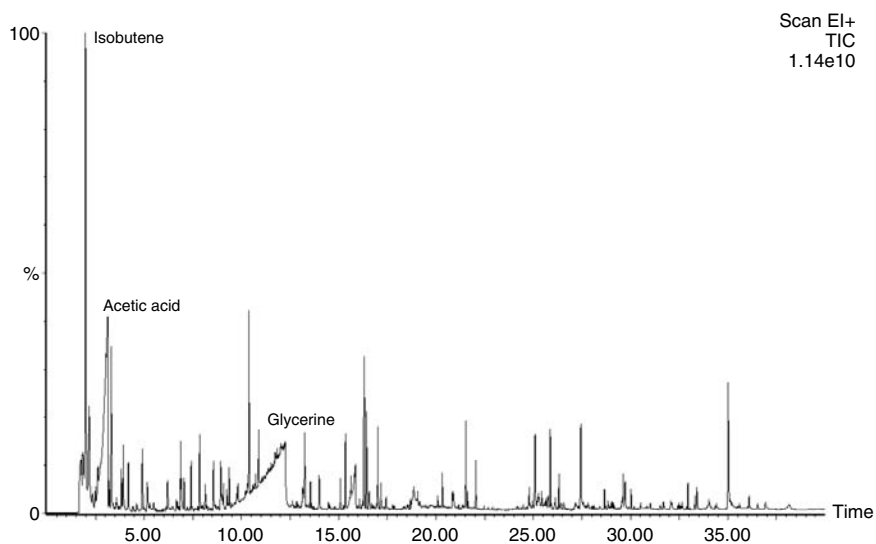
Pyrogram G-22: Packaging.



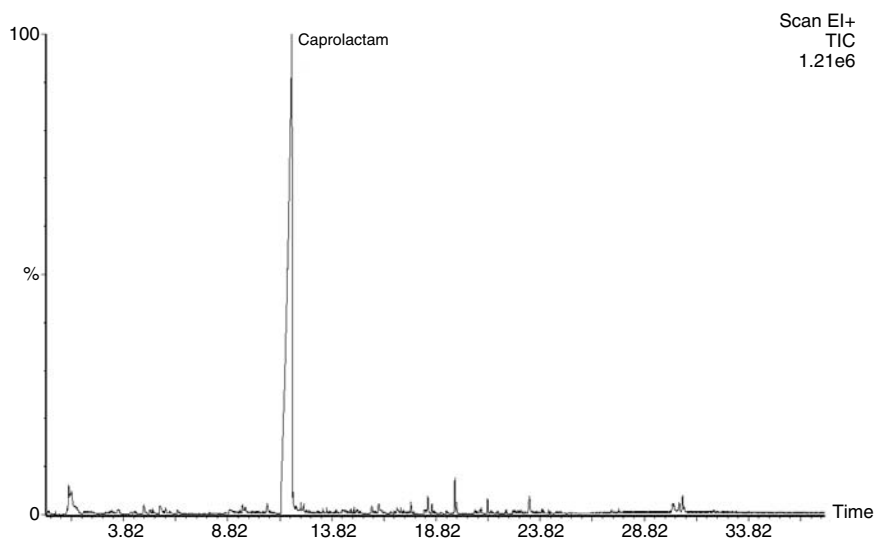
Pyrogram G-23: Automobile paint.



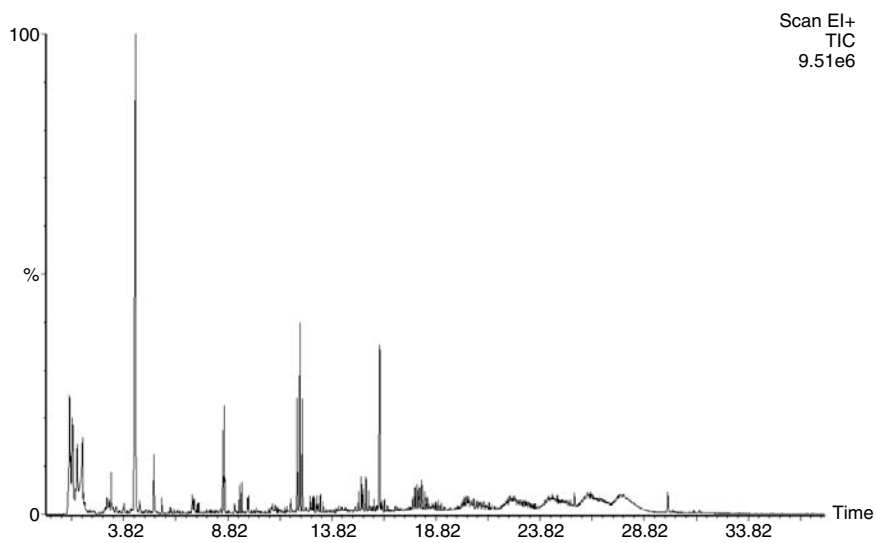
Pyrogram G-24: Automobile tire rubber.



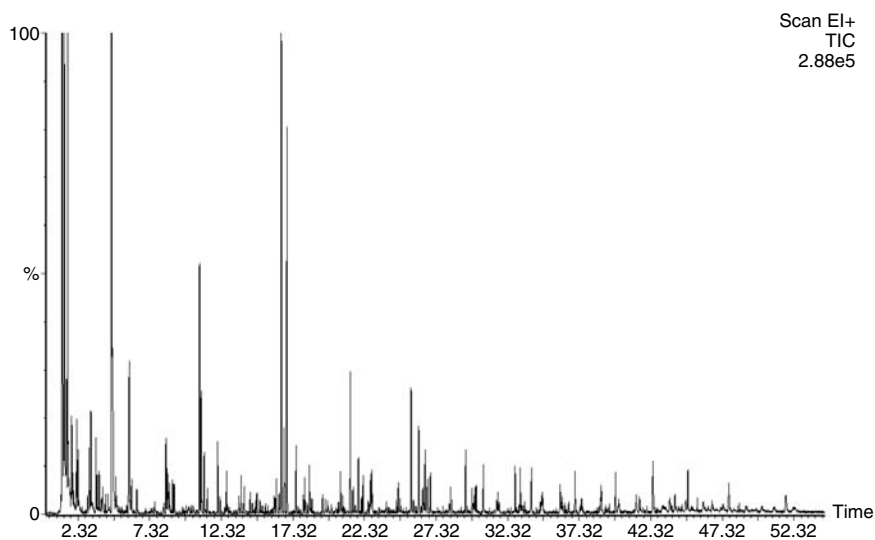
Pyrogram G-25: Chewing gum.



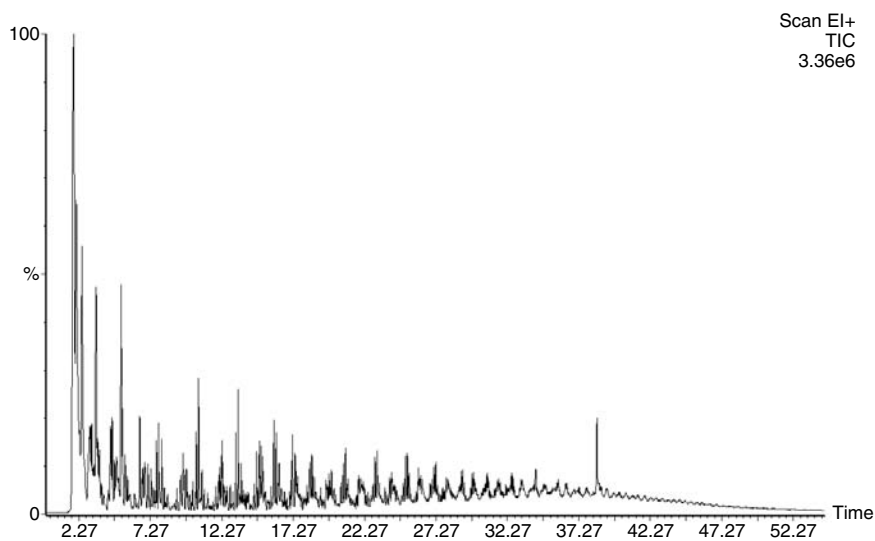
Pyrogram N-8: Nylon 6.



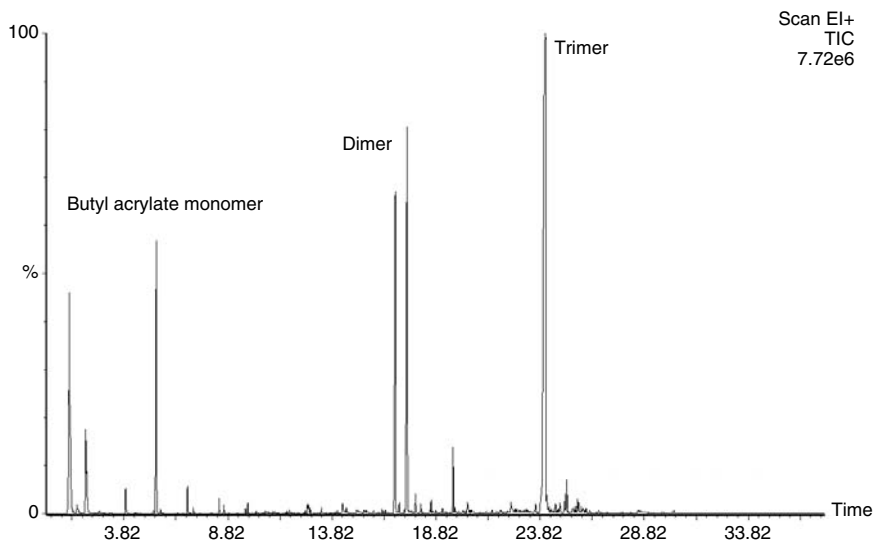
Pyrogram O-13: Ethylene (52%) propylene rubber.



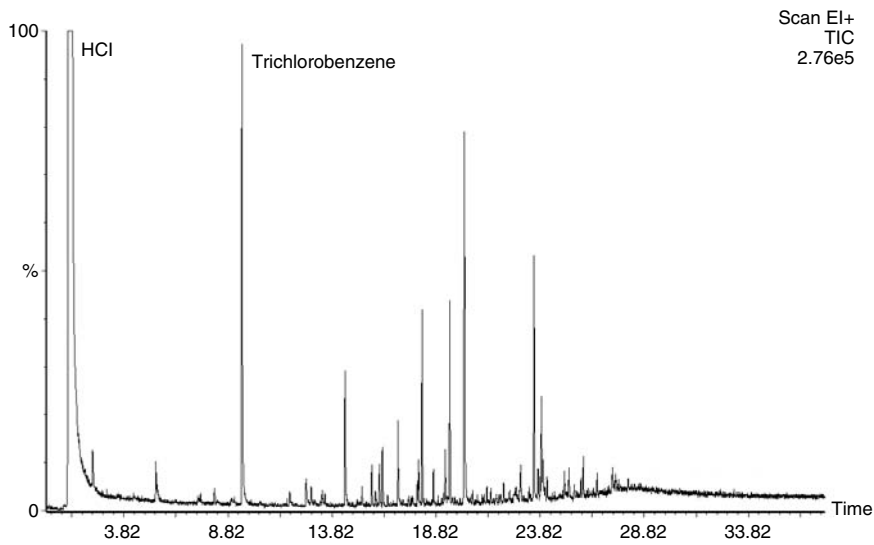
Pyrogram O-12: Polyethylene (25%) propylene.



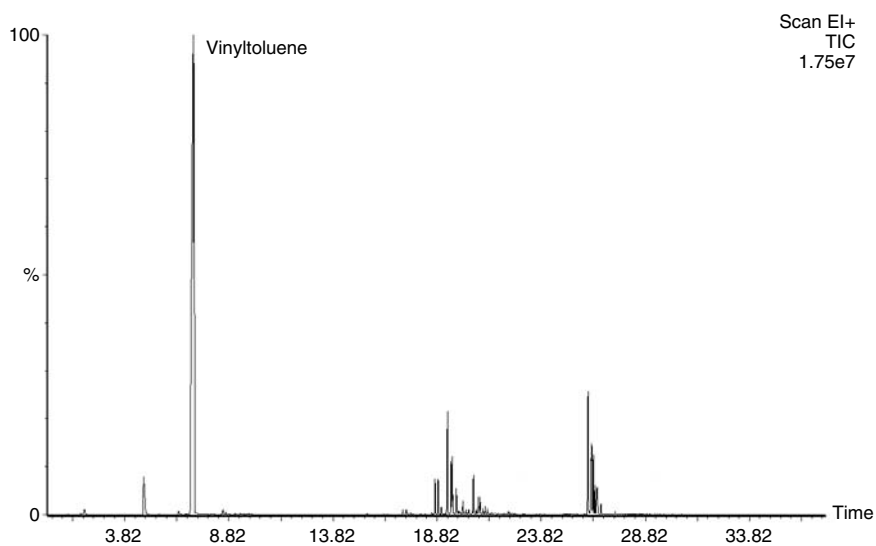
Pyrogram O-13: Ethylene (52%) propylene rubber.



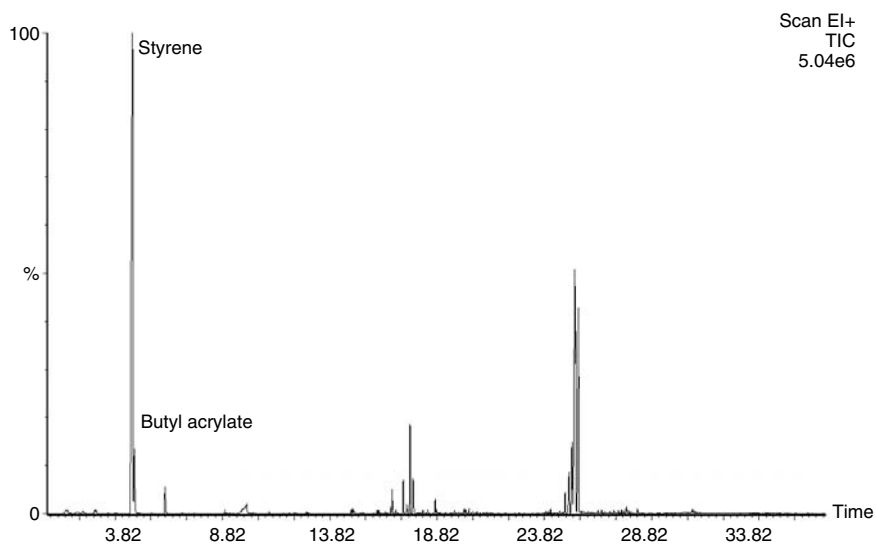
Pyrogram S-8: Polybutyl acrylate.



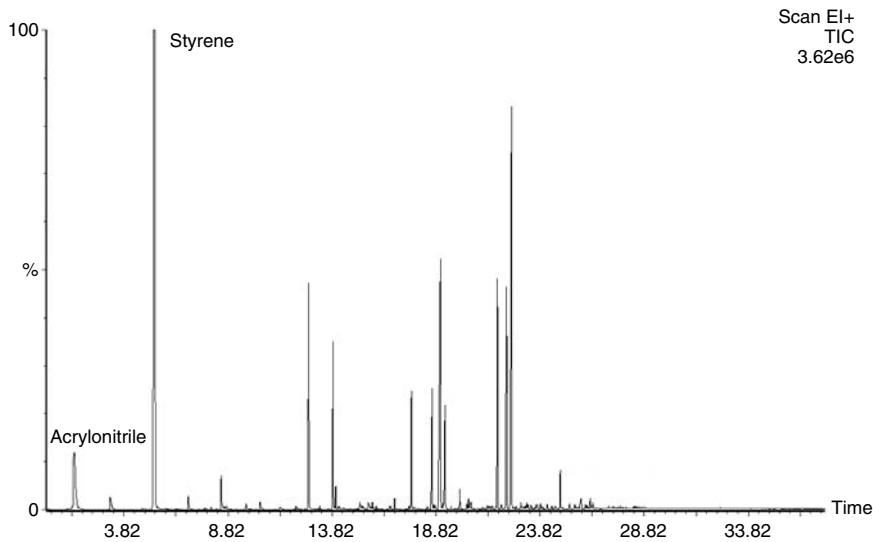
Pyrogram S-9: Polyvinylidene chloride.



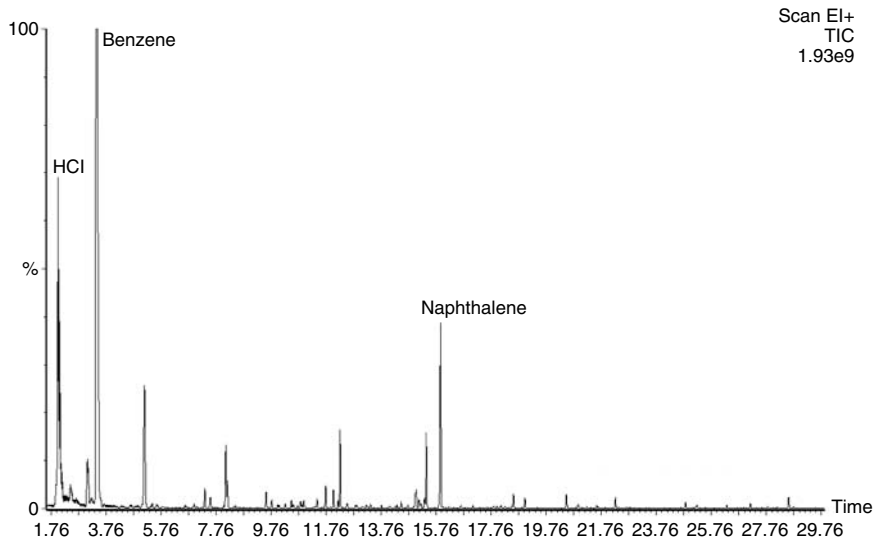
Pyrogram S-10: Polyvinyl toluene.



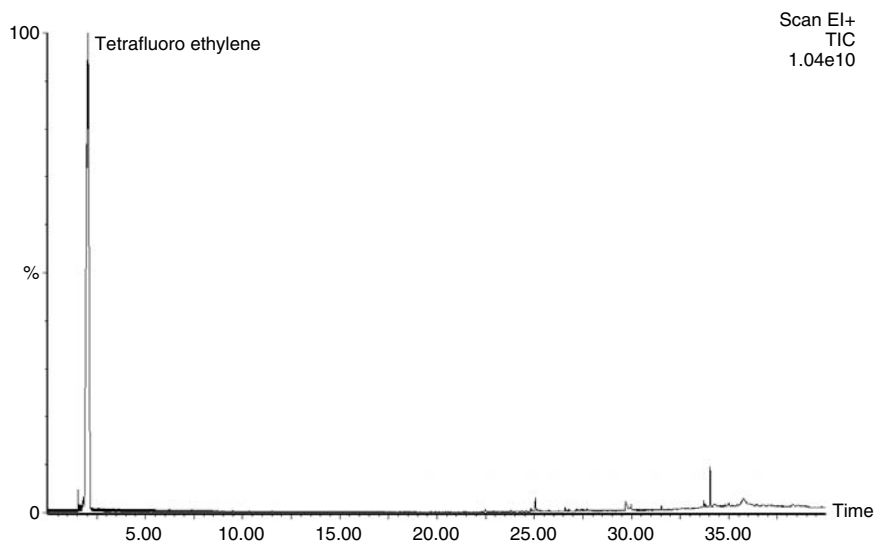
Pyrogram S-11: Polystyrene butyl acrylate.



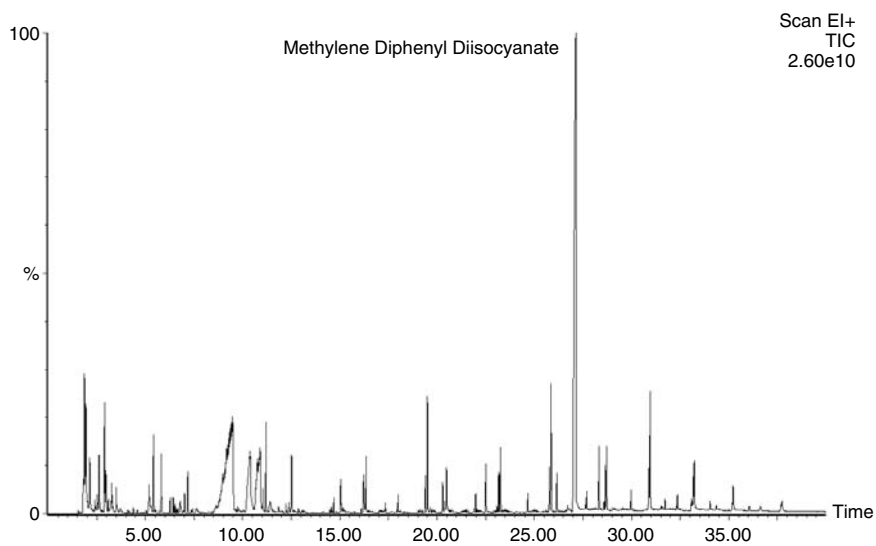
Pyrogram S-12: Polystyrene acrylonitrile.



Pyrogram S-13: Polyvinyl chloride.



Pyrogram S-14: Teflon.



Pyrogram S-15: Polyurethane.

Index

A

Acrylates, 8
Acrylic lacquer, 178
Adhesive, 183
Adipic acid, 92
Aerosols, 135
Airborne particulates, 136
Aliphatic polyesters, 252
Alkyd enamel, 179
Amber, 115
Amino acids, 239
Aminobenzoic acid, 97
Ammonium salt, 242
Aramids, 98
Aroclor, 158
Aromatic polyamides, 98
Aromatic polyester, 88, 251
Aromatic-aliphatic polyamides, 97
Artificial neural network, 57
Atactic, 72
Automotive paint, 177
Autosampler, 43

B

B. anthracis, 214
B. subtilis, 223
Bacillus, 222
Bakelite, 117
Ballpoint pen ink, 196
Baltic amber, 116
Bee pollen, 169
Beeswax, 110
Beta scission, 3
Biodegradation, 252
Biological aerosols, 141
Biological oxygen demand, 147
Biphenol, 88, 251
Bisphenol A, 180, 256
Body filler, vehicle, 187
Body lotion, 192
Branching, poly(ethylene), 66
Branching, polycarbonate, 259
Burmese amber, 119

Burmese lacquer, 194
Butyl rubber, 186

C

Cadinene, 115
Cadmium, 146
Candelilla wax, 110
Canonical variates, 56
Caprolactam, 92
Caprolactone, 87
Carnauba wax, 110
Casein, 126
Catalyst
 Metallocene, 72
 Titanium, 79
 Zeigler-Natta, 77
Cell envelope, 204
Cellulose, 189, 244
Cetyl palmitate, 110
Chemical oxygen demand (COD), 147
Chemotaxonomy, 203
Chitin, 245
Chitosan, 245
Chlorolignin, 148
Coatings, 22
Combustion, 135
Contamination, groundwater, 154
Copal, 116
Cosmetics, 192
Cotton, 14, 189
Crosslinking, 259, 266
Curie-point, 33
Cyclopentanone, 87
Cystine, 125

D

Dammar, 115
Degradation mechanisms, 2
Degradation, enzymatic, 254
Derivatization, 177
Diastereoisomers, 71
Diesel exhaust, 139
Differential thermogravimetry, 145
Dinitriles, 95

Direct insertion probe (DIP), 48
Direct Pyrolysis-MSD, 50
Dissolved organic carbon (DOC), 148
DNA, 220

E

Effluent, pulp mill, 147
End group, 257
Enzymatic degradation, 254
Exhaust, diesel, 139
Exhaust, gasoline, 139

F

Fats, 119, 189
Fiber, cotton, 14
Fiber, polyester, 14
Fibers, 11, 188
Fibroin, 125
Filament pyrolyzer, 32
Forgeries, amber, 117
Fungi, 227
Furnace pyrolyzer, 29

G

Gasoline exhaust, 139
Gelatin, 125
Glutamic acid, 126
Gram positive cell, 204

H

HCl, from PVC, 145
High density poly(ethylene), 69
Homogeneity, 44
Hydrogenation, 65
Hydroxycaproic acid, 256
Hydroxyproline, 125

I

Inductively heated pyrolyzer, 33
Ink, 13
Ink, ballpoint, 196
Ink, printing, 195
Isoalkanes, 67
Isotactic, 72

K

Keratin, 125
Kevlar, 98

L

Lacquer, acrylic, 178
Latex paint, 23
Legionella, 224
Lignosulphonate, 148
Limestone, 164
Linear low density poly(ethylene), 69
Linoleic acid, 190
Lipopolysaccharide (LPS), 204
Lipstick, 192
Liquid crystalline polymer (LCP), 88, 251
Low density poly(ethylene) LDPE, 66

M

Maleic anhydride, 84
Marine sediment, 161
Mechanisms, degradation, 2
Mercury, 146
Metallocene catalyst, 72
Methacrylates, 8, 234
Microstructure, poly(propylene), 71
MOLART project, 106
Monomer reversion, 6
Multi-step pyrolysis, 42
Multivariate statistics, 55

N

Natural materials, 19, 244
Natural poly(styrene), 116
Natural resins, 114, 193
Nomex, 98
Nylon 6, 92
Nylon 6/6, 92

O

Off-line pyrolysis, 41
Oils, 119, 189
Oleic acid, 190
Olive oil, 191
Orlon, 189

P

Paint

- Acrylic, 123
- Architectural, 180
- Automotive, 177
- Industrial, 182
- Latex, 23

Paper, 13

Para-hydroxy benzoic acid, 88

Patina, 166, 251

Peptidoglycan, 204, 206

Phenylalanine, 240

Photocopies, 13

Phthalic anhydride, 84

Pigments, 123

Plastic wrap, 142

Platinum filament, 36

Pollen, 169

Poly(1,3-phenylene isophthalamide), 98

Poly(1,4-phenylene terephthalamide), 98

Poly(1-butene), 4

Poly(3-hydroxybutyrate), 87

Poly(acrylonitrile/butadiene/styrene) ABS, 143

Poly(alkylene terephthalates), 81

Poly(aryl ether sulfones), 266

Poly(butyl methacrylate), 7, 235

Poly(ethylene-1-octene), 70

Poly(ethylene-1-heptene), 70

Poly(ethylene terephthalate) PET, 81, 189, 237

Poly(ethylene), low density, 66

Poly(ethylene-1-butene), 70

Poly(ethylene-propylene), 77

Poly(hydroxyalkanoate), 253

Poly(lactic acid), 87

Poly(laurel methacrylate), 230

Poly(methyl methacrylate), PMMA, 234

Poly(propylene), 71

Poly(styrene), natural, 116

Poly(vinyl chloride), 5

Poly(vinylidene chloride), 142

Polyamides, 89

Polyaromatic hydrocarbons (PAH), 160

Polycarbonate, 256

Polychlorinated biphenyls (PCB), 158

Polychlorinated dibenzodioxins, 145

Polyester fiber, 14

Polyester resin, 188

Polyester, aliphatic, 252

Polyester, aromatic, 251

Polyesters, 81, 237

Polylactams, 92

Polylactones, 84

Polysulfones, 266

Principal component analysis, 56

Printing ink, 195

Programmed pyrolysis, 40

Protein, 20, 125, 246

Pulp mill, 147

Pyrolysis-FT-IR, 11

Pyrolysis-hydrogenation, 65

Pyrolysis-TOF, 54

Pyrolyzer

Curie-point, 33

Filament, 32

Furnace, 29

Resistively heated, 36

Pyrrolidone, 184

R

Random scission, 2

Refinish lacquer, 178

Reproducibility, 44

Resins, natural, 114

Resistively heated filaments, 36

RNA, 220

Rock eval pyrolysis, 163

Rubber, 185

S*Salmonella*, 226

Sample handling, 44

Scission, random, 2

Sediment, 156

Sewage sludge, 146

Shellac, 194

Short chain branching, 66

Side-group scission, 5

Silk, 12

Siloxanes, 124

Slow pyrolysis, 40

Smoke, 135

Soil, 156

Soil, forest, 170

Spermaceti wax, 110

Spruce needles, 170

Staphylococci, 222

Stearine wax, 110

Stereoregularity, 71

Streptococci, 220

Structure, branching, 69

Succinic anhydride, 119

Sulfonamides, 243

Sulfones, 266

Surface water, 153

Surfactants, 240
Syndiotactic, 72

T

Tactic sequence length, 72
Tail-to-tail orientation, 78
Terephthalic acid, 88, 251
Tetrahydrofuran, 82
Tetramethyl ammonium hydroxide, TMAH, 177,
249
Textiles, 11
Time of flight MS, 54
Triglycerides, 190
Tris (2-chloroethyl) phosphate, 142
Tryptophan, 125
Tyrosine, 240

U

Urethane rubber, 186
UV-curing, 266

V

Varnish, 194
Vegetable oil, 190
Vehicle body filler, 187
Vehicular traffic, 136
Vinyl pyrrolidone, 184

W

Waste plastic, 143
Wastewater, 147
Water, natural organic matter, 153
Waxes, 109
Wood rosin, 194

Chemistry

Analytical pyrolysis allows scientists to use routine laboratory instrumentation for analyzing complex, opaque, or insoluble samples more effectively than other analytical techniques alone. **Applied Pyrolysis Handbook, Second Edition** is a practical guide to the application of pyrolysis techniques to various samples and sample types for a diversity of fields including microbiology, forensic science, industrial research, and environmental analysis.

This second edition incorporates recent technological advances that increase the technique's sensitivity to trace elements, improve its reproducibility, and expand its applicability. The book reviews the types of instrumentation available to perform pyrolysis and offers guidance for interfacing instruments and integrating other analytical techniques, including gas chromatography and mass spectrometry. Fully updated with new sample pyrograms, figures, references, and real-world examples, this edition also highlights new areas of application including surfactants, historical artifacts, and environmental materials.

Features

- Reviews the chemistry behind pyrolysis mechanisms, degradation mechanisms, and essential instrumentation considerations
- Contains detailed analytical data for polymers that can easily be compared with the user's own experimental data and analyses
- Re-examines methods in areas with a long history of analysis by pyrolysis including microorganisms, coatings and adhesives, textiles, synthetic polymers, cosmetics, and forensic evidence
- Highlights new areas of application including surfactants, museum pieces, and environmental materials
- Provides guidance for interpreting data, particularly for product comparison or presenting forensic evidence in trials
- Adds new sample pyrograms for 23 materials including tobacco, automobile paint, and packaging polymers

This book illustrates how the latest advances make pyrolysis a practical, cost-effective, reliable, and flexible alternative for increasingly complex sample analyses. **Applied Pyrolysis Handbook, Second Edition** is an essential one-stop guide for determining if pyrolysis meets application-specific needs as well as performing pyrolysis and handling the data obtained.



CRC Press

Taylor & Francis Group
an informa business

www.taylorandfrancisgroup.com

6000 Broken Sound Parkway, NW
Suite 300, Boca Raton, FL 33487
270 Madison Avenue
New York, NY 10016
2 Park Square, Milton Park
Abingdon, Oxon OX14 4RN, UK

DK3999

ISBN 1-57444-641-X



www.crcpress.com